

Meta-Learning and Synthetic Data for Automated Pretraining and Finetuning



Dissertation zur Erlangung des Doktorgrades der
Technischen Fakultät der Albert-Ludwigs-Universität Freiburg

vorgelegt von

Fabio Ferreira

2025

Dean:

Prof. Dr.-Ing. Frank Balle, *University of Freiburg, Germany*

PhD advisor and first examiner:

Prof. Dr. Frank Hutter, *University of Freiburg, Germany*

Second examiner:

Prof. Dr. Josif Grabocka, *University of Technology Nuremberg, Germany*

Date of defense: June 2, 2025

Abstract

Machine Learning · Automated Machine Learning · Meta-Learning · Deep Learning

The growing number of pretrained models in Machine Learning (ML) presents significant challenges for practitioners. Given a new dataset, they need to determine the most suitable deep learning (DL) pipeline, consisting of the pretrained model and the hyperparameters for finetuning to it. Moreover, as models grow in scale, the increasing reliance on real-world data poses a bottleneck for training and requires leveraging data more effectively.

Addressing the first challenge often involves manual model selection and hyperparameter tuning, demanding expert knowledge or costly trial and error. At the same time, as models grow larger and more and more of the available human-generated data is being used for training, data augmentation and synthetic data become critical elements in today's pipelines to improve effective data use and model performance. Automated machine learning offers a path to address these challenges but is traditionally designed for tabular data and classical ML methods. Extending these techniques to Deep Learning presents a key challenge due to high computational and data-related demands. This dissertation adopts meta-learning to extend automated machine learning to the deep learning domain. Its contributions are structured into two clusters:

In the first cluster, we propose empirical approaches to automate DL pipeline selection for Computer Vision tasks using prior task knowledge to learn zero-shot and few-shot surrogate models. Extending these methods to the language domain, we demonstrate their efficacy in meta-learning for finetuning large language models (LLMs) and their cross-domain applicability. Not only removing the reliance on manual selection, we empirically show that our approach generalizes to unseen datasets to suggest task-specific pipelines that can outperform finetuning large, jack-of-all-trades backbone models.

The second cluster focuses on meta-learning for data augmentation and synthetic data to enhance performance and effectively use data in pretraining and finetuning regimes. We empirically show the underestimated importance of data augmentation when using Self-Supervised Learning in the computer vision domain and, based on that, meta-learn advanced data augmentation strategies that enhance pretraining and finetuning performance. Leveraging synthetic data, we propose a framework to meta-learn neural synthetic data generators as proxies for Reinforcement Learning (RL) environments, enabling efficient and hyperparameter-agnostic agent training. Additionally, we explore using synthetic, randomly sampled data to pretrain a general simulator in an in-context learning fashion that covers multiple RL environments, allowing hyperparameter-agnostic training without real-world interactions.

Overall, this dissertation takes a step toward automated pretraining and customizable finetuning through meta-learning and empirically demonstrates how meta-learning can leverage data augmentation and synthetic data for scalable, domain-adaptable machine learning.

Zusammenfassung

Maschinelles Lernen · Automatisiertes Maschinelles Lernen · Meta-Lernen · Tiefes Lernen ·

Die wachsende Zahl von vortrainierten Modellen im maschinellen Lernen (ML) stellt Praktiker vor große Herausforderungen. Beim Einsatz eines neuen Datensatzes müssen sie die geeigneten Deep-Learning-Pipeline bestimmen, bestehend aus dem vortrainierten Modell und den Hyperparametern für das Finetuning. Stetig wachsende Modelle erhöhen die Abhängigkeit von realen Daten, was einen Engpass für das Training darstellt und eine effektivere Datennutzung erfordert.

Die Modellauswahl und Hyperparameterabstimmung erfolgen oft manuell, was Expertenwissen oder kostenintensive Experimente verlangt. Mit stetig größer werdenden Modellen und da immer mehr der verfügbaren, vom Menschen generierten Daten für das Training verwendet werden, werden Datenaugmentierung und synthetische Daten zu entscheidenden Elementen in den heutigen Pipelines, um die effektive Datennutzung und die Modellleistung zu verbessern. Automatisiertes maschinelles Lernen bietet einen Weg zur Bewältigung dieser Herausforderungen, ist jedoch traditionell für tabellarische Daten und klassische ML-Methoden konzipiert. Die Erweiterung dieser Techniken auf Deep Learning stellt aufgrund der hohen rechnerischen und datenbezogenen Anforderungen eine wesentliche Herausforderung dar. In dieser Dissertation wird Meta-Learning eingesetzt, um automatisiertes maschinelles Lernen auf den Bereich des Deep Learning zu erweitern. Die Beiträge dieser Arbeit sind in zwei Cluster gegliedert:

Im ersten Cluster schlagen wir empirische Ansätze zur Automatisierung der DL-Pipeline-Auswahl für Computer-Vision-Aufgaben vor, indem wir vorheriges Aufgabenwissen zum Erlernen von Zero-Shot- und Few-Shot-Surrogatmodellen nutzen. Außerdem zeigen wie diese Methoden auf den Sprachbereich für die Feinabstimmung großer Sprachmodelle (Large Language Models; LLMs) erweitert werden können. Dabei sind wir nicht mehr auf die manuelle Auswahl angewiesen und zeigen auch empirisch, dass unser Ansatz sich auf ungewohnte Datensätze generalisieren lässt, um aufgabenspezifische Pipelines vorzuschlagen, die die Feinabstimmung großer Backbone-Modelle übertreffen können.

Das zweite Cluster konzentriert sich auf Meta-Lernen für Datenaugmentierung und synthetische Daten, um die Leistung zu verbessern und Daten im Vortraining und Feinabstimmung effektiv zu nutzen. Wir zeigen empirisch die unterschätzte Bedeutung der Datenaugmentierung bei der Verwendung von selbstüberwachtem Lernen im Bereich der Computer Vision und erlernen darauf aufbauend fortgeschrittene Strategien zur Datenaugmentierung, die die Vortraining- und Feinabstimmungsleistung verbessern. Außerdem demonstrieren wir, wie wir Meta-Lernen dafür nutzen können, neuronale synthetische Datengeneratoren als Stellvertreter für Reinforcement Learning (RL)-Umgebungen zu erzeugen, welche ein effizientes und hyperparameter-agnostisches Agententraining ermöglichen. Darüber hinaus untersuchen wir die Verwendung synthetischer, zufällig generierter Daten zum Vortraining eines allgemeinen Simulators, die mehrere RL-Umgebungen abdeckt

und ein hyperparameter-agnostisches Training ohne Interaktionen mit der realen Welt ermöglicht.

Zusammenfassend ist diese Dissertation ein Schritt in Richtung automatisiertes Vortraining und anpassbare Feinabstimmung durch Meta-Lernen und zeigt empirisch, wie Meta-Learning dazu genutzt werden kann, effektive Datenaugmentierung und synthetische Datengenerierung für skalierbares, domänenangepasstes maschinelles Lernen zu erlangen.

Acknowledgments

A PhD journey stands and falls with the people who cultivate supportive and inspiring environments where one can feel comfortable and grow. Many of those who supported me in my career I was fortunate to meet early on.

My path as a researcher began during my fifth semester as a Computer Science undergraduate in 2015, when *Prof. Astrid Laubenheimer*'s Computer Vision course sparked my interest in Machine Learning (ML). The class focused on manually engineering feature extraction kernels, but it was also a time when Deep Learning (DL) was on the rise. Fascinated by the idea that DL could automate kernel learning, I decided to focus my studies entirely on ML and DL. I went on to work as a student researcher in *Prof. Tamim Asfour*'s robotics lab, where I also met and befriended my close friend *Jonas Rothfuss* while collaborating on robotic perception and manipulation. Tamim further enabled me to join *Prof. Jeannette Bohg*'s robotics lab at Stanford, where I had the privilege of meeting and working alongside *Krishnan Srinivasan, Michelle Lee, Margot Vulliez, Peter Zachares, Varun Nambiar, Lin Shao, and Suraj Nair*. I am forever grateful for the opportunities I was given and for these good-hearted people I met during this formative stage of my research journey.

Continuing to be fascinated by empirical and automated deep learning research, I joined *Prof. Frank Hutter*'s ML/ AutoML Lab in Freiburg. Frank is not only a stellar researcher but also an exceptional supervisor who sparked my interest in meta-learning, gave me the absolute freedom to work independently, facilitated collaborations, and enabled me to explore exciting ideas outside of my thesis scope. As a supervisor, he believes in inspiring and supporting his team rather than imposing ideas which is an approach that has proven highly effective and fosters a happy and collaborative team environment. Beyond his role as a supervisor, he is a great, humble, and social human being. The fact that everyone I meet speaks so fondly of him is a testament to the positive impact he has on those around him. All these traits combined make him a truly unique and rare individual in ML research, and I am deeply thankful for his guidance and for the opportunity to have been able to work closely with him.

I also thank my current and former lab colleagues *Arbér, André, Arlind, Sam, Sebastian, Eddie, Katharina, Matthias, Jörg, Matilde, Noor, Raghu, Steven, Stefan, Lennart, Thomas, Johannes, Arjun, Rhea, Heri, Ivo, Danny, Max, Jake, Neeratyoy, Julien, David, Timur, Mahmoud, Noah, Robin, Yash, and Frederic* for the shared experiences and conversations over coffee and at conferences, team retreats and hikes, joint team lunches, and board game nights. I thank the secretaries *Svenja, Morgan, Lina, and Petra* for helping me with the bureaucracy.

Special thanks to *Arbér Zela, Raghu Rajan, Samuel Müller, Arlind Kadra, and Jörg Franke* for all the long walks around the office and deep talks. I am particularly grateful to have found a great friend in *Arbér*, and I genuinely hope that our friendship extends far beyond the PhD journey. I am also grateful for the tennis matches and swims in the Dreisam River with *Raghu, Sam, and Yash Mehta*.

Thanks to all the students I have been grateful to have worked with: *Thomas Nierhoff, Ivo Rapant, Diane Wagner, Ekrem Öztürk, Moreno Schlageter, Andreas Sältinger, Muhammad Ali, Dipti Sengupta, Paweł Bugyi, Kashan Karimudin, Maciej Janowski, Albanot Makolli, and Jeta Bekteshi*. I also want to thank all the people with whom I collaborated and published papers.

Special mention to my dear friends *Jonas Rothfuss, David Betghe, Colin Weitmann, Steffen Huber, Makai Chapman, Daniel Ziegerer, Krishnan Srinivasan, Erica Gawley, James Gawley, Michael Wall, Heinrich Dinkel, Janika Schmidt, Eleni Triantafillou*, and to my Karlsruhe-crew consisting of *Paulina Matuszak, Michael Kuzmin, Xenia Hoffmeister, Helen Meier, and Julia Specht*. I am also deeply grateful to my former partner *Atessa Schilli*, who accompanied my research journey from the very beginning and supported me unconditionally during a significant part of it.

Most importantly, I want to thank my parents, *Elisabeth* and *Florindo*, as well as my sister, *Liana*, my niece, *Amália*, and the rest of my family living in Germany and Portugal for always being there for me: Avó Madalena, Avô Raul, Claudia, Duarte, Valerio, Ausenda, Alberto, and Isabel. Your support, love, and encouragement have been my foundation throughout this journey. By always believing in me, my parents give me the strength to pursue my goals, even in the toughest moments. While my sister and I may have had our quarrels, I learned a great deal about myself through our interactions. My niece's joyful energy has brought light to even the most challenging days. I am forever thankful for your strength, stability, and the role you all played in making this achievement possible.

As a passionate listener of electronic music, I am very grateful to producers and labels such as *CRi, Keinemusik, Afterlife, and Above & Beyond* for crafting immersive tracks that have been my constant companions, fueling creativity and concentration during countless hours of coding and learning. I also thank the invaluable online resources *Google Scholar* and *arXiv* and acknowledge the use of *OpenAI's ChatGPT* as a supplementary tool to assist with brainstorming ideas, suggesting alternative phrasing, refining individual sentences, and generating ideas for structuring the dissertation. I authored and reviewed all final content and decisions to ensure originality and academic rigor.

Contents

I	Introduction	1
1	Motivation	3
1.1	In a Nutshell	6
1.2	Organization of the Dissertation	7
2	Goals of this Dissertation	9
2.1	Key Challenges	9
2.2	Contributions	10
2.3	List of Publications	17
3	Meta-Learning	21
3.1	What is Meta-Learning?	21
3.2	Types of Meta-Learning	21
3.3	Algorithm Selection and CASH	23
4	Data Augmentation and Synthetic Data	25
4.1	Data Augmentation	25
4.2	Synthetic Data Generation	27
II	Meta-Learning for Automated Model Selection and Finetuning	29
5	Zero-Shot AutoML with Pretrained Models	31
5.1	Introduction	32
5.2	Related Work	33
5.3	Zero-Shot AutoML with Pretrained Models	34
5.4	ZAP Meta-Dataset Design	36
5.5	Experiments	37
5.6	Conclusion	40
5.7	Limitations	40
6	Quick-Tune: Quickly Learning Which Pretrained Model to Finetune and How	45
6.1	Introduction	46
6.2	Related Work	47
6.3	Motivation	48
6.4	Quick-Tune: Cost-Efficient Finetuning	48
6.5	Quick-Tune: Meta-Dataset	50
6.6	Experiments and Results	51

6.7 Conclusion	54
7 Quick-Tune-Tool: A Practical Tool and its User Guide for Automatically Finetuning Pretrained Models	61
7.1 Introduction	62
7.2 Background and Related Work	63
7.3 Quick-Tune-Tool: A Practical Tool for Finetuning Pretrained Models	63
7.4 A User Guide for Quick-Tune-Tool	65
7.5 Experiments and Results: Quick-Tune-Tool in Action	65
7.6 Conclusion and Outlook	66
8 Transfer Learning for Finetuning Large Language Models	71
8.1 Introduction	72
8.2 Related Work	73
8.3 Method	73
8.4 Results	75
III Meta-Learning Data Augmentation and Synthetic Data for Enhanced Learning	79
9 On the Importance of Hyperparameters and Data Augmentation for Self-Supervised Learning	81
9.1 Introduction	82
9.2 Background and Related Work	82
9.3 Study on the Importance of Hyperparameters and Data Augmentation	83
9.4 GroupAugment	84
9.5 Conclusion and Limitations	85
10 Beyond Random Augmentations: Pretraining with Hard Views	89
10.1 Introduction	90
10.2 Related Work	92
10.3 Method	92
10.4 Implementation and Evaluation Protocols	94
10.5 Main Results	94
10.6 Empirical Analysis of HVP	96
10.7 Conclusion	98
11 Learning Synthetic Environments and Reward Networks for Reinforcement Learning	103
11.1 Introduction	104
11.2 Related Work	105
11.3 Learning Synthetic Environments	106
11.4 Learning Reward Networks	107
11.5 Experiments with Synthetic Environments	108
11.6 Experiments with Reward Networks	110
11.7 Limitations	112
11.8 Conclusion	112
12 One-shot World Models Using a Transformer Trained on a Synthetic Prior	117
12.1 Introduction	118
12.2 Related Work	119
12.3 Method	120

12.4 Experiments	122
12.5 Conclusion	126
IV Conclusion	129
13 Summary and Discussion	131
14 Takeaways and Outlook	133
Appendices	139
A Appendices for Zero-Shot AutoML with Pretrained Models	139
A.1 Paper Appendix	139
A.2 Statement of Contributions	144
B Appendices for Quick-Tune: Quickly Learning Which Pretrained Model to Finetune and How	151
B.1 Paper Appendix	151
B.2 Statement of Contributions	158
C Appendices for Quick-Tune-Tool: A Practical Tool and its User Guide for Automatically Finetuning Pretrained Models	163
C.1 Paper Appendix	163
C.2 Statement of Contributions	168
D Appendices for Transfer Learning for Finetuning Large Language Models	173
D.1 Paper Appendix	173
D.2 Statement of Contributions	180
E Appendices for Beyond Random Augmentations: Pretraining with Hard Views	185
E.1 Paper Appendix	185
E.2 Statement of Contributions	196
F Appendices for On the Importance of Hyperparameters and Data Augmentation for Self-Supervised Learning	201
F.1 Paper Appendix	201
F.2 Statement of Contributions	210
G Appendices for Learning Synthetic Environments and Reward Networks for Reinforcement Learning	215
G.1 Paper Appendix	215
G.2 Statement of Contributions	240
H Appendices for One-shot World Models Using a Transformer Trained on a Synthetic Prior	245
H.1 Paper Appendix	245
H.2 Statement of Contributions	251
Bibliography	257

Part I

Introduction

Motivation

The field of *Artificial Intelligence (AI)* has achieved transformational progress in various domains over the past years. From Bioinformatics with three-dimensional protein structure prediction (Abramson et al., 2024), capabilities to segment novel objects in videos in real-time (N. Ravi et al., 2024), text-to-image-models (Esser et al., 2024), to foundation models such as *Large Language Models (LLMs)* (Brown et al., 2020; Dubey et al., 2024; Jiang et al., 2024; Radford et al., 2019), and large multimodal models (Achiam et al., 2023; Alayrac et al., 2022; Anil et al., 2023; Radford et al., 2021, 2023). While lacking behind in some areas, such as mathematical reasoning, the scaling of models to billions of parameters has allowed these models to surpass human performance on several benchmarks, including visual reasoning and English understanding, with a quickly growing number of open-source models becoming available (Guo et al., 2025; Kaplan et al., 2020; Maslej et al., 2024b). However, the availability of models comes with a multitude of risks and challenges, such as privacy concerns, explainability, safety and security, or inference in low-resource environments.

A significant challenge that arises from these remarkable advancements and the resulting model abundance is the difficulty of choosing suitable AI systems and finetuning them in practical applications. Not only in the rapidly evolving field of LLMs, but also in fields such as image classification, state-of-the-art pretrained models with incremental improvements are released at a high frequency. For example, at the time of writing, the popular model hub Hugging Face hosts over 500,000 pretrained models, including 340,000 in language processing, ~78,000 in computer vision, and ~14,500 models specifically for image classification (Hugging Face, Inc., 2024). This surge in the number of models exemplifies the *Jevons Paradox* (Wikipedia contributors, 2025), which suggests that increased efficiency lowers costs and, paradoxically, results in even higher demand. In the case of LLMs, this paradox is evident in examples like DeepSeek's R1-Zero model (Guo et al., 2025), an open-source release that achieves on-par performance with open and closed-source alternatives while being trained at a fraction of their cost. As training LLMs becomes cheaper and training pipelines more effective, this trend will likely accelerate further, driving the proliferation of available models.

As illustrated in Figure 1.1 (left), this abundance presents practitioners with a complex question: how to select the most suitable *deep learning (DL) pipeline* (Goodfellow et al., 2016; Krizhevsky et al., 2012; LeCun et al., 1989; Rumelhart et al., 1985), which consists of a pretrained model and its finetuning hyperparameters, for a specific new dataset or task? Considering a practical example, Figure 1.2 visualizes this challenge from a practitioner's standpoint. It shows 700 pretrained image classification models taken from the popular timm library (Wightman, 2019), plotted by accuracy against model size (measured in

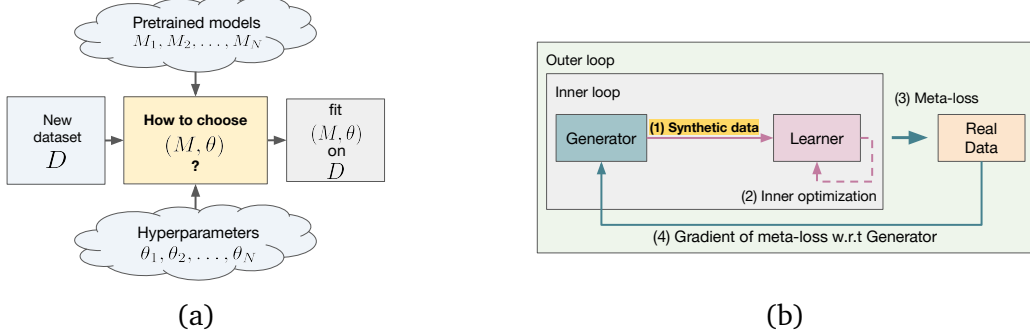


Figure 1.1: (a) The Combined Algorithm and Hyperparameter Optimization (CASH) problem visualized. (b) An exemplary meta-learning framework for learning synthetic data generators (visualization inspired by Such et al. (2020)).

the number of parameters). Even when restricting the choice to models on the Pareto optimal front, practitioners must still select from a subset of 24 models. Additionally considering other fidelities, such as inference time or memory constraints, may further drive the complexity of selecting a DL pipeline to the specific needs of their applications. Lastly, this problem is almost universal: not only in computer vision we see an explosion of pretrained model availability but a similar development can be already observed in the language model domain, where many institutions are competing for the best LLM for coding, conversation, or reasoning.

However, with the recent developments in model scaling, we argue that selecting the best pipeline alone is insufficient without leveraging data effectively. For instance, Hoffmann et al. (2022) has shown that compute-optimal training strategies require scaling the model parameters proportionally with the dataset size to fully realize their potential. However, achieving this assumes often high-quality human data, which is often expensive to obtain or entirely unavailable for certain domains. Meanwhile, the AI Index Report 2024 (Maslej et al., 2024b) indicates that the availability of high-quality language data may soon be depleted, raising concerns about the long-term sustainability of model scaling given this bottleneck.¹ Recently released LLMs such as Llama 3.3 already indicate the increasing reliance on synthetic data, using up to 25M synthetic samples to augment the finetuning corpus (Meta, 2024). We believe this motivates developing strategies to maximize the effectiveness of existing data, such as enhanced data augmentation methods, optimizing existing augmentation strategies, and generating synthetic data to complement real-world data. These challenges emphasize the dual need to navigate the abundance of pretrained models and their finetuning hyperparameters, as well as the effective use of data.

Navigating the Ocean of Deep Learning Pipelines Choosing an appropriate DL pipeline for a new task can be compared to navigating an ocean. Imagine a navigator that needs to

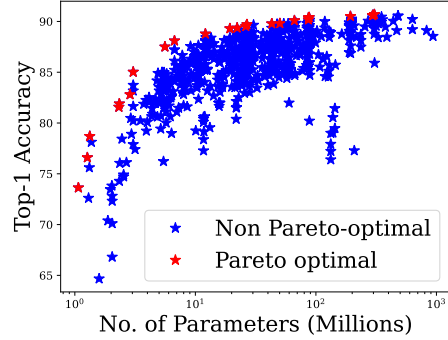


Figure 1.2: Illustrative example of the large set of over 700 pretrained image classification models available from the timm library, with still 24 models on the Pareto front (illustration from the Quick-Tune paper (Arango et al., 2024)).

¹According to Maslej et al. (2024a), high-quality language data is depleted by 2024, and low-quality language data within two decades.

choose the best ship (pretrained model) and adjust its sails (hyperparameters) to reach a new destination (dataset or task to finetune to). Each ship has its own capabilities, size, and speed. Akin to a practitioner, the navigator must not only select an appropriate ship for their journey but also choose an overwhelming number of settings for arriving at the destination, such as the crew size, cargo capacity, rudder, or sail orientation.² Practitioners have to rely on heuristics and intuition or trial-and-error strategies if they have no prior experience. They risk choosing an ill-suited ship, and misselections of such settings may result in the navigator not reaching the destination or reaching it weeks later. While this illustration may seem far-fetched, it emphasizes how challenging the task of making the right decision under uncertainty and a large number of available options. Analogously, choosing an ill-suited DL pipeline can lead to many different problems, such as instability in training, incomplete convergence, under and overfitting of the task and many more. This is aggravated significantly if a practitioner has little or no prior knowledge to make informed decisions. Consequently, it makes sense to find automated and algorithmic solutions to help address this problem and outsource the need for such skills and knowledge to an algorithm.

In Machine Learning (ML), already in the 1970s, this problem was formulated as a search problem by Rice, who introduced the *Algorithm Selection* problem (Rice, 1976). Building on that, the *Combined Algorithm Selection and Hyperparameter Optimization problem (CASH)* (Hutter et al., 2019; Thornton et al., 2013) was introduced, which treats this search as a joint optimization problem in the space of both model (algorithm) and hyperparameters (see Figure 1.1 (right)). This problem can be tackled from various angles, for instance, regression (L. Xu et al., 2008), classification (L. Xu et al., 2012), or clustering-based (Kadioglu et al., 2010). These approaches rely on *meta-learning* (Andrychowicz et al., 2016; Finn et al., 2017; Hospedales et al., 2021; Schmidhuber, 1987; Vanschoren, 2019), i.e. learning from prior experience, to train a *selector* using prior recorded performance data about algorithms on similar problem instances (e.g., datasets), combined with their characteristics, to map new problems to the best algorithm and hyperparameters. Depending on how well the prior data on which the selector was trained resembles future problem instances, the selector is equipped to make well-grounded decisions about which algorithm to apply to new problem instances. To go back to the example, this methodology aims to replace the navigator with one that is capable of meta-learning, i.e. a navigator that exploits past experiences of navigating various ships to different destinations, enabling informed decisions for new journeys. In ML, this approach has mostly been applied to classic ML models that are less complex (e.g., fewer hyperparameters) and less computationally expensive to train compared to Deep Learning models. However, adapting this methodology to DL pipelines introduces new challenges due to the scale and complexity of pretrained models and their hyperparameters. This dissertation aims to bridge this gap by extending the CASH framework to Deep Learning by leveraging meta-learning.

What about the data? Above, we touched on the duality between selecting a DL pipeline and the effective use of data. However, ensuring the effective use of data in machine learning presents several challenges. Returning to the running example, a successful journey depends a lot on the availability of good ships. For instance, the navigator might reinforce parts of a ship to develop specialized ships tailored to different types of journeys: an all-rounder ship capable of handling a variety of conditions or a specialist ship optimized for a specific type of journey (e.g. navigating narrow canals). Analogously, in machine learning, one way to achieve effective use of data is to generate or adapt datasets that are

²for simplicity, this illustration disregards corrections of chosen settings during the journey

appropriate for the task at hand. This can be attained through data augmentation (Chawla et al., 2002; DeVries and Taylor, 2017; Shorten and Khoshgoftaar, 2019; Simard et al., 2003) or synthetic data generation (Goodfellow et al., 2014; J. Ho et al., 2020; Jakobi et al., 1995; Kingma and Welling, 2014; Sankaranarayanan et al., 2018; Tobin et al., 2017; Tremblay et al., 2018), either individually or by mixing them with real data to diversify and expand datasets. These approaches can be an important tool for enhancing robustness (e.g., as measured by a low variance in predictions) and task-specific performance in both pretraining and finetuning DL models (Cubuk et al., 2019; Grill et al., 2020; Shorten and Khoshgoftaar, 2019; Such et al., 2020; Tobin et al., 2017). Despite their potential, data augmentation and synthetic data generation are often treated heuristically, relying on manual adjustments that are time-consuming and may be suboptimal. For example, such strategies remain underexplored in typical pretraining regimes like *Self-Supervised Learning (SSL)* (Grill et al., 2020).

To address this challenge, meta-learning offers a promising solution. For instance, data augmentation can be seen as an input for a meta-learner to help it leverage diverse augmented datasets and inform its decisions. Just like a navigator may leverage prior knowledge from past journeys, meta-learning can use prior experience to inform the development of effective data augmentation strategies. For example, one can think of applying data augmentation on a dataset level to augment the data as input to train a previously described (meta-)selector by varying characteristics of the data and help prepare the selector for rare or unseen scenarios.

It is also viable to treat data augmentation as an optimization hyperparameter since practitioners also often rely on trial and error to identify good configurations. Consequently, incorporating data augmentation as a hyperparameter allows systematic optimization of it, reducing reliance on manual heuristics while improving model robustness. Finally, just as the navigator might innovate entirely new ships by simulating novel scenarios or anticipating challenges, meta-learning can be used to generate data augmentations or synthetic data as an addition or replacement to existing data and tasks. In such cases, synthetic data can be meta-learned and used as training data for subsequent or downstream tasks. This approach is exemplified in Figure 1.1 (right), which illustrates a general meta-learning framework for optimizing synthetic data generators. The framework uses the performance of a learner trained on real data to optimize the synthetic data generator. For instance, this dissertation proposes this framework for Reinforcement Learning and demonstrates how synthetic environments can be learned for efficient subsequent agent training. Synthetic data generation is especially useful when real-world data collection is expensive (e.g., in robotics). Moreover, synthetic data provides a chance to embed desirable properties, such as enhancing learning efficiency, compensating for underrepresented classes, or introducing controlled variability to better prepare models for real-world complexities.

This dissertation explores the use of meta-learning to develop advanced data augmentation strategies and learn synthetic data generators with the goal of enhancing data effectiveness and efficiency during training while also reducing practitioners' reliance on heuristics and trial-and-error. In this dissertation, these efforts are conducted for the automation of DL pipeline and pretraining in SSL with applications in computer vision but also extend to model-based Reinforcement Learning.

1.1 In a Nutshell

This dissertation explores meta-learning to reduce reliance on manual tuning, trial-and-error, and the use of heuristics in Deep Learning by developing solutions for automated pretraining and finetuning. It extends the concepts of *Automated Machine Learning (AutoML)* (Hutter et al., 2019) to Deep Learning and uses meta-learning to enhance data

augmentation methods and generate synthetic data for effective and efficient optimization in Deep Learning. Together, these contributions allow us to address the overarching question of the dissertation:

How can meta-learning and synthetic data advance automated pretraining and finetuning?

For the purposes of this dissertation, *synthetic data* collectively refers to both data augmentation and synthetic generation methods since both seek to artificially expand or alter the data distribution. To emphasize their differences, data augmentation, and synthetic data generation will be distinctly identified when specifically discussed.

In particular, this dissertation includes contributions that individually concern pretraining, finetuning, data augmentation, and synthetic data generation, as well as works that explore the intersection of these themes to advance automation in Deep Learning pipelines.

1.2 Organization of the Dissertation

This dissertation is a *cumulative dissertation*. As such, it consolidates contributions from multiple research publications by the author. Moreover, all publications listed in this dissertation aim to answer an overarching scientific question described in Section 1.1. The dissertation is organized into four parts, arranged by topic rather than chronological order:

- **Part I (Introduction):** the current part, introduces the overarching theme of the dissertation, outlines its primary goals, and provides the relevant background context.
- **Part II (Meta-Learning for Automated Model Selection and Finetuning):** contains the set of publications that cluster contributions on meta-learning for the selection and finetuning of DL pipelines. It encompasses works in the domains of image classification and large language models.
- **Part III (Meta-Learning Data Augmentation and Synthetic Data for Enhanced Learning):** summarizes the second set of publications, which contains contributions focussed on meta-learning data augmentation and synthetic data for better learning.
- **Part IV (Conclusion):** concludes the dissertation with a summarization of the key takeaways, highlights the achievements of this work, and describes potential avenues for future research in the domain of ML and AI.

The background given in Part I is recommended reading if the reader is unfamiliar with meta-learning. Moreover, the publications provided in Parts II and III are self-contained and can be read independently. The primary distinction between these two parts lies in their focus: Part II centers on automating model selection and finetuning in DL pipelines, with data augmentation and synthetic data functioning as secondary components, while Part III addresses directly optimizing data augmentation and synthetic data generation utilizing meta-learning techniques or supporting them to enhance learning. Lastly, the dissertation operates in the following machine learning areas: self-supervised learning, supervised learning, model-based reinforcement learning, in-context learning, automated machine learning, image classification, question-answering, and large language models.

Goals of this Dissertation

As the field of AI grows in scale and complexity, the deployment and finetuning of models become increasingly harder. Practitioners are challenged with the question of how to select and finetune pretrained models for new tasks and how to leverage data effectively to improve training outcomes. This challenge is compounded by the reliance on manual heuristics and the depletion of training data. Addressing these issues requires innovative strategies to automate pipeline selection and finetuning, as well as optimizing data usage. Guided by these challenges, this dissertation seeks to answer the overarching scientific question: *“How can meta-learning and synthetic data advance automated pretraining and finetuning?”* To achieve this, we derived the following research questions that guided our contributions.

2.1 Key Challenges

Challenge 1: Automating Model Selection and Finetuning Amidst a Growing Landscape of Pretrained Models

With the rapid increase in available pretrained models across various domains, identifying an optimal pretrained model and its hyperparameters for finetuning to a new dataset has become increasingly challenging. This task is known as the *Combined Algorithm Selection and Hyperparameter Optimization (CASH)* (Thornton et al., 2013) problem. To illustrate this increase, Hugging Face now hosts over 500,000 pretrained models (of which, for instance, \sim 78,000 are computer vision and \sim 340,000 are language processing models) (Hugging Face, Inc., 2024), making manual selection impractical. Moreover, finetuning involves numerous hyperparameters, and optimizing them is not only time-consuming but often infeasible for practitioners who have to rely on heuristics. Existing meta-learning-based efforts to automate model selection and hyperparameter tuning have primarily focused on traditional Machine Learning (ML) models (Feurer et al., 2019; Kotthoff et al., 2017), do not leverage dataset information, and usually do not consider model selection and hyperparameter optimization as a joint problem. A key challenge lies in adapting these CASH techniques, traditionally used in non-Deep Learning settings, to the vastly more computationally expensive Deep Learning landscape and in effectively using meta-learning to exploit prior training data to execute automated finetuning on new tasks. This includes finding solutions that are scalable and generalizable across domains, such as extending techniques that cover automating finetuning of large language models or image classification.

Challenge 2: Enhancing Learning With Advanced Data Augmentation and Synthetic Data Generation

Building upon the challenge of selecting and finetuning pretrained models in a growing landscape, a central assumption is to develop robust, powerful, and general pretrained models. As models grow larger and much of the available human-generated data is already being used for training, the demand for extensive training datasets continues to increase. In Self-Supervised Learning (SSL), for example, a common approach to extend the pretraining dataset is to rely heavily on data augmentation, making the data augmentation strategy and its hyperparameter settings essential for downstream performance (T. Chen et al., 2020; Grill et al., 2020). However, in SSL, data augmentation remains underexplored due to instability at high augmentation intensities and the cost of identifying effective techniques. The challenge of adopting advanced data augmentation also extends to automated model selection and hyperparameter tuning (Challenge 1), where dataset level augmentation can enable meta-learned model selectors to cope better with variance encountered in datasets at test time. Yet, best practices on how to use data more effectively in these domains are scarce within the scientific community and remain to be explored further. An alternative to data augmentation lies in synthetic data generation. Unlike augmentation, synthetic data can be generated and used more independently of real data, for instance, by sampling synthetic data from distribution priors or by directly (meta-)learning the data. Synthetic data is particularly valuable in domains where collecting real-world data is costly, such as in Reinforcement Learning (RL). For example, in robotics, this is further amplified by the trend toward developing generalist models trained across multiple robot platforms and datasets (A. S. Chen et al., 2021; Physical Intelligence, 2024). Consequently, the need for synthetic datasets and rich simulations allowing minimal real-world interactions is growing. However, creating synthetic data that captures real-world characteristics while balancing diversity and training efficiency remains a significant hurdle (Maslej et al., 2024a). Therefore, we believe a core challenge lies in exploring more ways to leverage data effectively by advancing data augmentation and synthetic data generation. While meta-learning offers a promising avenue for leveraging prior knowledge to inform advanced data augmentation and synthetic data generation, its potential remains underexplored.

Challenge 3: Ensuring Reproducibility and Practical Applicability of Automated Learning Methods

Another challenge we face in machine learning research is ensuring reproducibility and practical applicability (Pineau et al., 2021). Research artifacts are often not made open-source, and datasets or model checkpoints are not released, which results in limited accessibility. Even when research artifacts are made publicly available, they often remain at the research level due to weak incentives for creating reproducible research. Consequently, research methods are challenging to implement without guidance, and high computational demands can pose an additional barrier to replication and adoption. Enabling reproducibility and adopting research findings within and beyond the machine learning community is challenging. It requires more than making code and data available. Lowering the barrier to entry also requires tutorials, tools with standardized interfaces to allow for application across domains, benchmarks for feature comparison, and more.

2.2 Contributions

To address the key challenges identified in the previous section, we formulate a set of research questions that shape the contributions of this cumulative dissertation. We then provide an abstract overview of how the dissertation as a whole addresses these questions.

Since each work within this dissertation is presented as an individual chapter, we also provide individual summaries of those along with how they address the overarching scientific question at the end of this section.

Research Questions

Based on the challenges outlined above, this dissertation seeks to answer the following research questions (RQ) and describes how they address these key challenges:

- **Challenge 1: Automating Model Selection and Finetuning Admidst a Growing Landscape of Pretrained Models**
 - **RQ 1:** Given a set of pretrained models, how can one meta-learn to automatically select the best pretrained model and its hyperparameters to finetune it to a new dataset?
 - **RQ 2:** To what extent can these methods generalize to unseen datasets?
 - **RQ 3:** How do these methods generalize across different learning domains such as vision and language?
- **Challenge 2: Enhancing Learning Through Advanced Data Augmentation and Synthetic Data Generation**
 - **RQ 4:** How does data augmentation impact the effectiveness of model pretraining in Self-Supervised Learning (SSL), and how can meta-learning be leveraged to optimize augmentation strategies?
 - **RQ 5:** How can meta-learning be leveraged to generate synthetic environment models that act as a replacement to Reinforcement Learning (RL) environments and that improve agent training in RL?
 - **RQ 6:** What potential does randomly sampled synthetic data hold for optimizing synthetic environment models, and to what extent can these models be utilized for agent training in RL?
- **Challenge 3: Ensuring Reproducibility and Practical Applicability of Automated Learning Methods**
 - **RQ 7:** What practices and tools can be implemented to ensure that the developed automated learning methods are reproducible, accessible, and practically applicable to the broader machine learning community?

We address research questions 1-3 as well as question 7 in Part II. In particular, we address the first two questions by proposing two model-based and meta-learned methods, *ZAP* and *Quick-Tune*, which provide solutions for supervised learning in computer vision and are detailed in Chapters 5 and 6. Both methods also address the *second research question* by contributing to generalization across unseen datasets in empirical experiments. While *ZAP* incorporates dataset level augmentation to enhance its meta-dataset, *Quick-Tune* further optimizes augmentation strategies and hyperparameters. Addressing the *third research question*, we show the generalization of automated model selection and finetuning to other learning domains through the aid of *Quick-Tune-Tool*, a tool derived from *Quick-Tune* with a standardized interface. We use it to adapt *Quick-Tune* to the domain of Large Language Models, which we discuss in Chapters 7 and 8. The *seventh research question*, which revolves around practices and tools to enable access for the broader machine learning community, is addressed primarily by efforts made in *Quick-Tune-Tool* (Chapter 7) and by

the code releases for all papers in this dissertation except for the work given in Chapter 8 which is the only work without a code release.

With Part III, we turn to data augmentation and synthetic data and address research questions 4-6. We provide empirical insights to the *fourth research question* about the effect of data augmentation in SSL-based pretraining of vision models in Chapter 9. Based on these findings, we introduce *Hard View Pretraining (HVP)* in Chapter 10, where we devise an advanced data augmentation strategy that uses single-task meta-learning. Addressing the *fifth research question*, Chapter 11 introduces *Synthetic Environments*, meta-learned copies of real RL environments that allow efficient agent training through their synthetic dynamics and rewards. In Chapter 12, we explore using randomly sampled synthetic data for training a *One-Shot World Model*, a generalist synthetic environment and hereby address the *sixth question*.

Summary of Contributions

Each chapter of this cumulative dissertation corresponds to a previously peer-reviewed and published work. We now provide a more detailed summary of each work. We explain how these works address the individual research questions and contribute to the overarching scientific question of this dissertation: “*How can meta-learning and synthetic data advance automated pretraining and finetuning?*”

Chapter 5: Zero-Shot AutoML with Pretrained Models

This chapter presents a solution to the central problem of this dissertation: Given a new dataset D , how can a pretrained model be chosen to finetune on D and set its hyperparameters? In this work, we define the combination of a pretrained model and the finetuning hyperparameters as Deep Learning (DL) Pipeline. Our approach, *Zero-shot AutoML with Pretrained Models (ZAP)*, addresses this as a Combined Algorithm Selection and Hyperparameter Optimization (CASH) problem. ZAP involves creating a meta-dataset with performances of various DL pipelines on a broad range of image classification datasets. We also apply data augmentation at the dataset level, for instance, by varying the number of classes or samples to increase the size of the meta-dataset. Using this meta-dataset, we meta-learn a surrogate model that selects the best DL pipeline given meta-features (e.g., image resolution) in a zero-shot setting, i.e., without exploratory evaluations of the target dataset.

Inspired by *Algorithm Selection (AS)* techniques, our zero-shot model selection approach optimizes a ranking objective across datasets, selecting DL pipelines based on both pipeline hyperparameters and dataset meta-features. A key contribution is to frame DL pipeline selection as a classical AS problem and extend it by modeling pipelines as points in a latent space, enabling performance insights from some pipelines to inform predictions for others. To the best of our knowledge, we are the first to adopt AS methods with meta-features beyond classical machine learning algorithms and apply them to pretrained DL models for image classification.

Consequently, we propose two approaches: one tackling ZAP with AS methods and one tackling it by using a neural network selector optimized with a ranking objective over DL pipelines. These approaches were evaluated in the 2019 ChaLearn Automated Deep Learning Challenge, outperforming other participants under budget constraints and anytime performance metrics. Furthermore, we conduct studies on selector performance when trained with a sparse meta-dataset.

How does this work address the overarching scientific question? ZAP addresses the dissertation’s central question by introducing a zero-shot, meta-learned surrogate selection model to automate model selection and hyperparameter tuning for finetuning to image classification datasets. ZAP demonstrates that meta-learned insights from diverse datasets can inform zero-shot model selection and hyperparameter tuning for new datasets. Additionally, it shows that dataset level augmentation effectively enhances selection performance. This aligns with the dissertation’s goals by illustrating how meta-learning, amplified by synthetic data or data augmentation, enables efficient and adaptive automation of model selection and finetuning in computer vision. Lastly, its meta-dataset-based approach is generalizable, extending applicability to other learning domains as well.

Chapter 6: Quick-Tune: Quickly Learning Which Pretrained Model to Finetune and How

In this chapter, we present *Quick-Tune*. Similar to ZAP, Quick-Tune also addresses the problem of automated model selection and finetuning given an unseen dataset (represented by meta-features) and a set of pretrained models (model hub) through the lenses of Combined Algorithm Selection and Hyperparameter Optimization (CASH) and image classification. As such, Quick-Tune builds on ZAP’s foundation but takes a *few-shot*, Bayesian framework-based, and cost-adaptive approach. In contrast to ZAP, which operates in a zero-shot setting (i.e., without updating any meta-model(s)) and uses final performance scores for model selection, Quick-Tune uses partial learning curves as few-shot observations to meta-learn and update its probabilistic predictor (surrogate model) during training, allowing it to predict the performance of pipelines. Additionally, Quick-Tune meta-learns a second model, a cost estimator that estimates the runtime cost of a pipeline. This makes Quick-Tune a multi-fidelity approach, allowing users to specify time budget constraints and adjust the meta-search time to practical limitations. Moreover, Quick-Tune also integrates various finetuning and augmentation strategies into its pipeline search space. Both models, performance predictor and cost estimator, are then used within a Bayesian Optimization framework to form an Expected Improvement-grounded acquisition function, allowing the selection of the next pipeline to maximize expected performance in a cost-sensitive manner. In contrast to ZAP, which approaches the CASH problem in a *zero-shot* way, i.e., without requiring observations from the target dataset, Quick-Tune tackles it with a *few-shot* way. It explores its search space of pipelines by iteratively refitting its performance and cost model based on self-collected observations (shots) from pipeline evaluations during search. All in all, we show that Quick-Tune can outperform both hyperparameter optimization tuning methods and finetuned single large vision models across a large collection of image classification datasets.

How does this work address the overarching scientific question? Quick-Tune, like ZAP, offers an adaptive solution to the central question of how to automatically select and tune pretrained models for image classification using meta-learning. While both leverage meta-learning, Quick-Tune differs by applying a few-shot, Bayesian gray-box optimization based on partial learning curves. This few-shot approach allows not only iterative refinement but also to adhere to time or budget constraints set by practitioners. We also provide empirical evidence that using Quick-Tune can be superior to learning classification heads in combination with large-scale and state-of-the-art feature extractor backbones. Different from ZAP, Quick-Tune does not apply data augmentation on the dataset level but incorporates data augmentation hyperparameters such as the augmentation strategy, operations, and magnitude into its pipeline search space.

Chapter 7: Quick-Tune-Tool: A Practical Tool and its User Guide for Automatically Finetuning Pretrained Models

With *Quick-Tune-Tool (QTT)*, as the name suggests, we aim to make the Quick-Tune algorithm more widely accessible. The main goal of this tool is to provide a standardized interface to facilitate adoption beyond the image classification to domains like image segmentation or large language models (see Chapter 8). QTT further lowers the entry barrier for adopters by providing an architectural overview, a guideline for running Quick-Tune for image classification, and additional example experiments. The tool also supports models from major model hubs like Hugging Face and timm.

How does this work address the overarching scientific question? Open-sourcing research code often falls short of enabling a wide adoption in and beyond the research community. Automating pretraining and finetuning with meta-learning can be complex as it requires leveraging prior training and validation data. By releasing QTT as a user-friendly tool, we aim to advance meta-learning research by making it more efficient and allowing advancements in other domains. Additionally, its interface is designed to accommodate data augmentation in the model search space, further enhancing its flexibility.

Chapter 8: Transfer Learning for Finetuning Large Language Models

In this chapter, we present work that uses Quick-Tune-Tool to explore the applicability of the Quick-Tune algorithm to the language processing domain. More precisely, we investigate whether we can use Quick-Tune to learn to transfer configurations for finetuning Large Language Models (LLM). With this exploratory contribution, we demonstrate the adaptability of meta-learning-based automation beyond image classification. In order to train our meta-models in this case, we created a meta-dataset containing learning curves, meta-features, and cost values. We created it by generating synthetic question-answer (QA) datasets from 30 scientific papers by instructing a Llama-3.1-70B model to extract atomic facts. For each paper, we trained 60 random and default finetuning pipelines and evaluated them using a teacher-student framework, where the teacher (Llama-3.1) model assessed the correctness of answers of the student (finetuned LLM), resulting in a total of 1,800 run recordings. Based on this meta-dataset, we pretrain the performance and cost predictors using the original Quick-Tune logic and search for well-performing finetuning configurations with its acquisition function. Tested on unseen synthetically generated QA datasets, our method outperforms random search, a popular hyperparameter optimization method, and a default finetuning pipeline.

How does this work address the overarching scientific question? This work addresses the overarching scientific question of applying meta-learning to develop methods for automating model selection and finetuning in a learning domain beyond vision: language processing. Additionally, we show how a tool such as Quick-Tune-Tool facilitates this effective transfer. Aligning with the dissertation's emphasis on leveraging synthetic data, we also demonstrate the effective use of synthetic data by generating question-answer datasets to enable meta-learning.

Chapter 9: On the Importance of Hyperparameters and Data Augmentation for Self-Supervised Learning

Coming to Part III, we now turn towards using enhanced data augmentation and synthetic data to achieve more effective pretraining and learning itself. In this chapter, we present a work in computer vision illuminating the underestimated role and importance of hyperparameters and data augmentation in Self-Supervised Learning (SSL), a popular methodology used for pretraining.

We use Bayesian optimization for tuning training (e.g., learning rate) and data augmentation (e.g., image distortion magnitude) hyperparameters using the popular SimSiam SSL approach trained and evaluated on CIFAR-10, CIFAR-100, and a medical dataset. Overall, this work illustrates that optimizing training hyperparameters only leads to marginal improvements, while optimizing data augmentation hyperparameters results in consistent performance improvements (1-2.3%) under the standard linear evaluation protocol. These improvements show empirically that SimSiam’s training hyperparameters are already well-tuned (and also other SSL approaches as reported in 10). Additionally, this study also reports on hyperparameter importance, further highlighting the potential for improvement in data augmentation hyperparameters. As a consequence of these observations, the paper introduces an automated data augmentation method, GroupAugment, that operates on groups of augmentations (e.g., color transformations) and designs sampling strategies over these groups. Automated data augmentation methods have predominantly been investigated in the context of supervised or semi-supervised learning, but their application to SSL remains underexplored (Cubuk et al., 2019, 2020; Lim et al., 2019a,b; S. Müller and Hutter, 2021; Reed et al., 2021). We also report performances of other popular automated data augmentation methods introduced for Supervised Learning when applied to SSL, finding that in the majority of cases, GroupAugment is able to outperform these methods.

How does this work address the overarching scientific question? While many works acknowledge the critical role of data augmentation in SSL, little work identifies the importance of data augmentation hyperparameters and the potential gains achievable through sophisticated data augmentation strategies. This work uncovers that data augmentation is underexplored in SSL. By showing that improved data augmentation yields consistent benefits, this paper sets the stage for the next chapter, which develops a more effective data augmentation strategy in pursuit of automated pretraining techniques.

Chapter 10: Beyond Random Augmentations: Pretraining with Hard Views

The work presented in this chapter builds on the findings made in Chapter 9 that empirically uncovered the underestimated role of data augmentation in discriminative SSL. In this work, we leverage these findings and develop a simple but effective data augmentation strategy, *Hard View Pretraining (HVP)*, generally applicable to discriminative SSL methods. HVP is a learning-free augmentation strategy that extends the widely used random view generation. It exposes the model to challenging samples during pretraining by randomly sampling views and selecting adversarially the ones with the highest loss according to the current training progression during each training step. Compared to standard SSL, our approach introduces a challenging learning scenario in which the model is encouraged to learn more discriminative features by being exposed to harder views. At the beginning of training, the embedding space lacks a defined structure for representing similarity among views. With training progression, HVP refines the concept of similarity through exposure to increasingly harder views. While automated data augmentation has been traditionally investigated in the context of supervised learning, HVP demonstrates its potential in self-supervised settings by automating the selection of challenging augmentations that adapt to the model’s state during training. This simple but effective strategy consistently and significantly improves downstream task performance across four popular SSL methods when trained with ResNets and Vision Transformers (ViT) on ImageNet. Underpinning the effectiveness and scalability of HVP, we achieved a new state-of-the-art result on the ViT-B/16 model architecture. We also show empirically that HVP regularizes models to be more robust to hyperparameter variations when used for downstream tasks.

How does this work address the overarching scientific question? HVP serves as a first step toward automating pretraining by showcasing that challenging and model-state-dependent data augmentation strategies can consistently yield better downstream

task performance. HVP can also be viewed as synthetically generating more diverse and difficult training data by selecting hard views based on their loss, incorporating a notion of difficulty into the augmentation process. Since HVP operates at a meta-level by adversarially selecting hard views based on their loss, it can be interpreted as single-task meta-learning, which directly addresses the overarching scientific question. By exposing models to increasingly challenging scenarios during pretraining, HVP also makes them more robust to hyperparameter variations, thereby simplifying the finetuning process for various vision architectures. This combination of improved augmentation, robustness, and scalability positions HVP as a key advancement toward automated and effective SSL pretraining.

Chapter 11: Learning Synthetic Environments and Reward Networks for Reinforcement Learning

This chapter presents a work that bridges the two central themes of this dissertation: meta-learning and synthetic data. More precisely, we propose using meta-learning in the form of bi-level optimization to learn synthetic neural data generators. We introduce and explore this framework in Reinforcement Learning (RL) since it offers a toy-like environment with reasonable computational costs. The goal of this work is to meta-learn *Synthetic Environments (SEs) and Reward Networks (RNs)* that provide synthetic proxies to target RL environments (defined as Markov Decision Processes). SEs mimic both state dynamics and rewards, while RNs focus solely on modeling rewards of the target (or real) environment. Algorithmically, we use two nested loops: in the inner loop, we train RL agents on the proxy. In the outer loop, we evaluate the agents on the target environment and use their performance to optimize the proxy parameters, which, over time, evolve to resemble more performant compressions of the target environment. We evaluate this approach on a broad range of RL algorithms and classic control environments. Empirically, we show that SEs and RNs are not only able to train agents to solve real environments but can also be trained to be more efficient and robust to agent hyperparameter variations compared to real environments. Our results indicate that synthetic proxies achieve this performance by learning informed representations that guide the agents toward relevant states. Lastly, the SEs are not only robust to hyperparameters but can also transfer to train unseen agent algorithms.

How does this work address the overarching scientific question? In the context of leveraging meta-learning and synthetic data for automated pretraining and finetuning, the works presented in this dissertation so far have primarily used synthetic data and data augmentation as tools to enhance pretraining and finetuning rather than learning them directly. While HVP (Chapter 10) represents a step toward automated data augmentation for pretraining through single-task meta-learning, it does not explicitly optimize the data augmentation itself. Similarly, GroupAugment (Chapter 9) combines existing data augmentation methods with hyperparameter optimization to improve pretraining but does not directly learn augmentations. In contrast, the framework of Synthetic Environments (SEs) takes a step forward by directly learning synthetic data through meta-learning in the context of RL. The emergent properties of SEs and RNs, such as more efficient training, hyperparameter robustness, and agent-agnostic adaptability, contribute to advancing automated and efficient optimization of RL agents. This not only addresses the dissertation’s goal of automated learning but also aligns with the broader trend of developing generalist RL models.

Chapter 12: One-shot World Models Using a Transformer Trained on a Synthetic Prior

In the previous chapter, we introduced a meta-learning framework that directly learns synthetic compressions (SEs and RNs) as proxies for specific RL environments by optimizing them based on agent performance. In this chapter, we propose the *One-Shot World Model (OSWM)*, a transformer-based synthetic environment trained entirely on synthetic data sampled from a prior distribution of untrained, randomly initialized neural networks. These neural networks serve as the prior, with each one mimicking a specific RL environment dimension. In contrast to SEs, OSWM employs in-context learning and a supervised objective without meta-learning to predict the next states and rewards at random cut-off points that match the synthetic trajectories. Unlike SEs, which are tailored to a single target environment, OSWM provides a general proxy capable of representing multiple environments within a single model. After training the OSWM, it acts as a learned simulator for multiple environments, enabling RL agents to train policies purely on the synthetic dynamics it generates. To adapt OSWM to a new target environment, we sample a context of 1,000 transitions from the environment. This context is sufficient for OSWM to infer the dynamics of the target environment and generate synthetic trajectories for training RL agents. Without requiring further interactions with the target environment, OSWM enables agents to achieve competitive performance in simple control environments such as GridWorld, CartPole, a custom control environment, and mediocre performance on Reacher. We also investigate the effect of context sampling and the role of the prior with respect to OSWM’s performance. Our empirical results indicate that with better prior design, OSWM may capture more complex dynamics and scale to more challenging environments.

How does this work address the overarching scientific question? Our work demonstrates how synthetic data and in-context learning can create a general simulator for multiple RL environments and hereby bridges the core themes of meta-learning and synthetic data in this dissertation. Contrary to meta-learned Synthetic Environments, OSWM avoids the computational cost of bi-level optimization by using synthetic priors. However, this comes at the expense of emergent properties such as efficient agent training and hyperparameter robustness. Despite these trade-offs, OSWM underpins the potential of synthetic data approaches for scenarios where real data is expensive, such as in RL and robotics, and contributes to the recent trend of foundation RL models capable of addressing diverse tasks. While RL served as a cost-effective testbed in our work, the methods and insights have applicability beyond RL, offering a foundation for adoption to other domains.

2.3 List of Publications

In this section, we provide an overview of all core publications included in this dissertation, along with additional publications, patents, and achievements by the author. Detailed descriptions of the author contributions are provided in the appendix, with references to their specific sections indicated at the beginning of each chapter.

Core Publications This dissertation integrates the following eight core research papers (sorted in chronological order). All research papers follow the overarching scientific question of “*How can meta-learning and synthetic data advance automated pretraining and finetuning?*”. We also denote code references and presentation types (if awarded).

- **F. Ferreira**, T.Nierhoff, A.Sälinger, F.Hutter (2022). “Learning Synthetic Environments and Reward Networks for Reinforcement Learning”. In: *Proceedings of the International Conference on Learning Representations (ICLR’22)*. Published online:

iclr.cc. ICLR. URL: <https://iclr.cc/virtual/2022/poster/6495>
 Code: https://github.com/automl/learning_environments

- D.Wagner, **F. Ferreira**, D.Stoll, R. T.Schirrmeister, S.Müller, F.Hutter (2022). “On the importance of hyperparameters and data augmentation for self-supervised learning”. In: *Pre-Training Workshop at the International Conference for Machine Learning (ICML)*. ed. by K. Chaudhuri, S. Jegelka, L. Song, C. Szepesvári, G. Niu, and S. Sabato. Vol. 162. Proceedings of Machine Learning Research. PMLR. URL: <https://icml.cc/virtual/2022/20697>
 Code: https://github.com/automl/importance_hp_da_ssl
- E.Öztürk, **F. Ferreira**, H. S.Jomaa, L.Schmidth-Thieme, J.Grabocka, F.Hutter (2022). “Zero-Shot AutoML with Pretrained Models”. In: *Proceedings of the 39th International Conference on Machine Learning (ICML’22)*. Ed. by K. Chaudhuri, S. Jegelka, L. Song, C. Szepesvári, G. Niu, and S. Sabato. Vol. 162. Proceedings of Machine Learning Research. PMLR, pp. 1128–1135. URL: <https://icml.cc/virtual/2022/spotlight/18008>
 Code: <https://github.com/automl/zero-shot-automl-with-pretrained-models>

Note: Awarded with a spotlight presentation at ICML 2022.

- S. P.Arango, **F. Ferreira**, A.Kadra, F.Hutter, J.Grabocka (2024). “Quick-Tune: Quickly Learning Which Pretrained Model to Finetune and How”. In: *Proceedings of the International Conference on Learning Representations (ICLR’24)*. Published online: iclr.cc. ICLR. URL: <https://iclr.cc/virtual/2024/oral/19719>
 Code: <https://github.com/machinelearningnuremberg/quicktune> Note: Awarded with an oral presentation at ICLR 2024.
- **F. Ferreira**, M.Schlageter, R.Rajan, A.Biedenkapp, F.Hutter (2024). “One-shot World Models Using a Transformer Trained on a Synthetic Prior”. In: *NeurIPS 2024 Workshop on Open-World Agents*
 Code: <https://github.com/automl/oswm>
- T.Strangmann, L.Purucker, J. K.H. Franke, I.Rapant, **F. Ferreira**, F.Hutter (2024). “Transfer Learning for Finetuning Large Language Models”. In: *NeurIPS 2024 Workshop on Adaptive Foundation Models*
 Code: see Quick-Tune-Tool code.
- I.Rapant, L.Purucker, **F. Ferreira**, S. P.Arango, A.Kadra, J.Grabocka, F.Hutter (2024). “Quick-Tune-Tool: A Practical Tool and its User Guide for Automatically Finetuning Pretrained Models”. In: *Third International Conference on Automated Machine Learning - Workshop Track*. Ed. by M. Lindauer, K. Eggensperger, R. Garnett, J. Vanschoren, and J. Gardner. URL: <https://openreview.net/forum?id=d0Hapti3Uc>
 Code: <https://github.com/automl/quicktunetool>
- **F. Ferreira**, I.Rapant, J. K.H. Franke, F.Hutter (2025). “Beyond Random Augmentations: Pretraining with Hard Views”. In: *Proceedings of the International Conference on Learning Representations (ICLR’25)*. Published online: iclr.cc. ICLR. URL: <https://openreview.net/forum?id=AK1C55o4r7>
 Code: <https://github.com/automl/pretraining-hard-views/>

Further Publications The following lists additional publications that the author conducted during their doctoral program. While these publications are connected to the ideas presented in this dissertation, they are considered out-of-scope within this dissertation. Additionally, we also list the author’s patents that resulted from their works during the program.

- Z.Liu, A.Pavao, Z.Xu, S.Escalera, **F. Ferreira**, I.Guyon, S.Hong, F.Hutter, R.Ji, J. C. S. J.Junior, G.Li, M.Lindauer, Z.Luo, M.Madadi, T.Nierhoff, K.Niu, C.Pan, D.Stoll, S.Treguer, J.Wang, P.Wang, C.Wu, Y.Xiong, A.Zela, Y.Zhang (2021). “Winning Solutions and Post-Challenge Analyses of the ChaLearn AutoDL Challenge 2019”. In: *IEEE Transactions on Pattern Analysis and Machine Intelligence’21*. Ed. by K. M. Lee. IEEE Computer Society, pp. 3108–3125
- A. E.Baz, I.Ullah, E.Alcobaça, A. C. P. L. F.Carvalho, H.Chen, **F. Ferreira**, H.Gouk, C.Guan, I.Guyon, T.Hospedales, S.Hu, M.Huisman, F.Hutter, Z.Liu, F.Mohr, E.Öztürk, J. N.Rijn, H.Sun, X.Wang, W.Zhu (2021). “Lessons learned from the NeurIPS 2021 MetaDL challenge: Backbone fine-tuning without episodic meta-learning dominates for few-shot learning image classification”. In: *Proceedings of the Neural Information Processing Systems Track on Datasets and Benchmarks*. Ed. by J. Vanschoren and S. Yeung. Curran Associates, pp. 80–96
- R.Rajan, J.Diaz, S.Guttikonda, **F. Ferreira**, A.Biedenkapp, J. O.Hartz, F.Hutter (2023). “MDP Playground: An Analysis and Debug Testbed for Reinforcement Learning”. In: *Journal of Artificial Intelligence Research (JAIR)* 77, pp. 821–890. DOI: 10.1613/jair.1.14314

Patents

- M.Lindauer, A.Zela, D.Stoll, **F. Ferreira**, F.Hutter, T.Nierhoff (Jan. 13, 2022). “Method and device for creating a system for the automated creation of machine learning systems”. U.S. pat. req. US20220012636A1. Robert Bosch GmbH. URL: <https://patents.google.com/patent/US20220012636A1/en>. Published
- T.Nierhoff, **F. Ferreira**, F.Hutter (July 14, 2022). “Device and method to improve reinforcement learning with synthetic environment”. U.S. pat. req. US20220222493A1. Robert Bosch GmbH. URL: <https://patents.google.com/patent/US20220222493A1/en>. Published

Further Achievements We competed with an early version of ZAP in the 2019 ChaLearn AutoDL Challenge, focusing exclusively on the vision track. Our submission achieved performance on par with the competition winner on this track, with an average rank of 1.75, as detailed in the corresponding study (El Baz et al., 2021). Furthermore, ZAP (Öztürk et al., 2022) received a spotlight presentation at ICML 2022³, granted to 20% of submitted papers, while Quick-Tune (Arango et al., 2024) was recognized with an oral presentation at ICLR 2024⁴, a distinction awarded to only 1.2% of submissions.

³<https://icml.cc/virtual/2022/spotlight/18008>

⁴<https://iclr.cc/virtual/2024/oral/19719>

Meta-Learning

3.1 What is Meta-Learning?

Generally, *meta-learning*, or *learning to learn* summarizes any type of learning mechanism that leverages prior experience from tasks (S. Bengio et al., 1997; Hochreiter et al., 2001; Schmidhuber, 1987; Thrun and L. Pratt, 2012; Vilalta and Drissi, 2002). A description of meta-learning can be given by starting from traditional machine learning. In traditional machine learning, we typically train the parameters θ of a *learner* f to maximize a learning cost \mathcal{L} on a specific task $t \in \mathcal{T}$ (or dataset). In contrast, meta-learning can be described as aiming to train a (meta-)learner to generalize across a distribution of tasks $p(\mathcal{T})$. We call this process meta-learning because it is concerned with optimizing the parameters θ of the meta-learner such that it can leverage prior knowledge to tackle new tasks effectively or efficiently. Formally, this can be expressed as

$$\theta^* = \arg \min_{\theta} \mathbb{E}_{t \sim p(\mathcal{T})} \mathcal{L}(f_{\theta}, t),$$

where $p(\mathcal{T})$ represents the distribution of tasks, and \mathcal{L} measures the task-specific cost. Typically, the closer the training tasks sampled from $p(\mathcal{T})$ are to a new task t_{new} , the better the learner f_{θ} can transfer and utilize prior knowledge to tackle T_{new} . Here, we consider the categorization of meta-learning techniques proposed in Vanschoren (2019, Chap. 2), which clusters meta-learning approaches by the meta-data $p(\mathcal{T})$ they leverage: learning from model evaluations, task properties, or prior models.

3.2 Types of Meta-Learning

3.2.1 Learning from Model Evaluations

Meta-learning from model evaluations entails learning from meta-data that consists of recordings from model evaluations. Consider that these recordings are defined by their hyperparameter configurations $h_i \in \mathcal{H}$ (e.g., hyperparameter or pipeline settings). Moreover, assume that we have a performance matrix \mathbb{P} a matrix of scalar evaluations $P_{i,j} = P(h_i, t_j)$ of configuration h_i on task t_j measured by a defined evaluation metric and usually recorded before meta-training time. The goal in this sub-type of meta-learning is to train a meta-learner using \mathbb{P} that predicts configurations $\mathcal{H}_{\text{new}}^*$ for a new task t_{new} . There exist two prominent approaches to this: one is to assume no access to any evaluations on t_{new} , which results in training a meta-learner $f : \mathcal{H} \times \mathcal{T} \rightarrow h_k^*$ that returns a set of best configurations on the meta-training data, independent of t_{new} and to choose the top configurations from this set. On the other hand, if evaluations on t_{new} are permissible, one can transfer configurations using a similarity measure to determine how similar evaluations on t_{new} are to

evaluations on the prior tasks t_j . Suppose evaluations on t_{new} are similar to the ones on t_j . In that case, this knowledge can be exploited to yield the most similar configuration directly. Another family of approaches is to train task-wise surrogate models $s_j(h_i) = P_{i,j}$ used jointly with acquisition function in Bayesian frameworks to suggest a new h_i .

3.2.2 Learning from Task Properties

Meta-learning can also be achieved by learning about the characteristics of a task. These characteristics are descriptive features which we refer to as *meta-features*. Each task t_j is represented by a vector of K such descriptive features, i.e. $\phi_j \in \Phi \subseteq \mathbb{R}^K$. Meta-features provide a straightforward way to quantify task similarity, for instance, by measuring the cosine similarity between the vectors ϕ_i and ϕ_j . This facilitates meta-learning by transferring information from the most similar tasks to a new task t_{new} . A common categorization is to distinguish between learned and not learned meta-features.

Not learned meta-features are typically numerical features extracted directly or indirectly from the dataset. For instance, one can use the number of classes or image resolution (directly) or apply functions like min, max, mean, quartiles, etc., to compute the minimum value of a feature column in tabular data (indirectly). Further processes like normalization, clustering, landmarking, or dimensionality reduction techniques like PCA can be applied. For a more complete introduction and rationale on selecting meta-features, we refer the interested reader to (Vanschoren, 2019, chap. 2.3). The selection of meta-features is well correlated with the performance of a meta-learner. However, choosing a well-performing set of meta-features is challenging and dependent on the application, as reported in studies such as Bilalli et al. (2017).

Because the manual selection of meta-features can be ineffective, studies have investigated whether meta-features can also be learned. This is particularly interesting in the computer vision domain. In contrast to the tabular data domain that consists of low-dimensional data like columns and rows, numerical properties of image or video datasets are often limited in quantity and expressiveness (e.g. pixel values). One approach is to use the performance meta-data or other existing meta-features to learn landmark-like meta-features, i.e. to learn functions $f : \Phi \rightarrow \Phi'$, or $f : \mathcal{P} \times \mathcal{H} \rightarrow \Phi$ (Vanschoren, 2019, Chap. 2.3). More recent approaches take the raw dataset (task) as input and use neural networks to generate meta-features, i.e. $f : \mathcal{T} \rightarrow \Phi$ (Achille et al., 2019; Jomaa et al., 2021) or learn metric spaces for measuring task similarity (Snell et al., 2017).

Once an appropriate set of meta-features has been identified or learned, the relationship between meta-features and performance meta-data can be learned to predict suitable configurations given the meta-features of t_{new} , or more formally: $s : \mathcal{P} \times \Phi \rightarrow \mathcal{H}$. The principle of jointly exploring the relationship between meta-features, performance meta-data, and hyperparameter configurations forms this dissertation's central methodological foundation, which we describe in more detail in Section 3.3 below. A key aspect of this foundation is to leverage transfer learning in neural networks, which we will introduce next.

3.2.3 Learning from Prior Models

Another type of meta-learning revolves around leveraging previously trained machine learning models. Formally, let M denote a pretrained model whose parameters θ have been optimized on one or more tasks $t_j \sim p(\mathcal{T})$, drawn from a distribution over tasks. The general idea is to transfer M to a new task $t_{new} \sim p(\mathcal{T})$, using the knowledge encoded in θ from the source tasks $\{t_j\}$ as a starting point. This process is widely known as *transfer learning* (Y. Bengio et al., 2013; Caruana, 1998; Pan and Q. Yang, 2010; Thrun and L. Pratt, 2012). While this has been explored for different kinds of machine learning models, neural

networks are particularly well-suited due to their model parameters and modular structure. For instance, a standard approach is to replace the final task-dependent layer of a neural network and reuse the remaining pretrained layers as feature extractors, thereby providing a useful initialization that can be finetuned to t_{new} (Y. Bengio, 2011; L. Y. Pratt, 1992; Thrun, 1995; Thrun and Mitchell, 1995).

A body of literature that takes advantage of transfer learning is *few-shot learning*, where the idea is to adapt M to a new task using only a few training examples. Through meta-learning, bootstrapping the initialization such that a common feature representation serves as an inductive bias enables rapid adaptation of the latent representation to t_{new} from only a few examples (Finn et al., 2017; S. Ravi and Larochelle, 2017). Similar ideas have also been realized through memory-augmented neural networks that learn to retrieve and leverage relevant “memories” from previously seen tasks (Santoro et al., 2016). Moreover, another branch of approaches leveraging transfer learning focuses on meta-learning algorithms within neural networks, for instance, by learning optimizers that adapt their own weights or hyperparameters to new tasks (Andrychowicz et al., 2016; Li and Malik, 2017; Schmidhuber, 1992). For other approaches that use meta-learning to leverage prior trained models, we refer the interested reader to (Vanschoren, 2019, Chap. 2.4).

Next, we introduce a framework that allows meta-learning of the relationship between meta-features, performance meta-data, and hyperparameter configurations and adapt it to automate the finetuning of deep learning pipelines by leveraging transfer learning.

3.3 Algorithm Selection and CASH

In the context of Machine Learning, selecting the most appropriate algorithm (e.g., classifiers or regression models) from a discrete set of algorithms without assuming to be able to make observations on the target *task* is known as the *Algorithm Selection* problem (Bischl et al., 2016; Kotthoff et al., 2012; Rice, 1976; Smith-Miles, 2008). Below, we formalize it and extend it to the *Combined Algorithm Selection and Hyperparameter Optimization* (*CASH*) problem (Hutter et al., 2019; Thornton et al., 2013).

Given a set of algorithms \mathcal{A} and tasks $t \in \mathcal{T}$ (also referred to as *problem instance* and often represented by meta-features), along with a cost metric $c : \mathcal{A} \times \mathcal{T} \rightarrow \mathbb{R}$, the goal is to learn a mapping $s : \mathcal{T} \rightarrow \mathcal{A}$ which is often referred to as a *selector* or surrogate model and that minimizes the total cost:

$$s^* = \arg \min_{s: \mathcal{T} \rightarrow \mathcal{A}} \sum_{t \in \mathcal{T}} c(s(t), t). \quad (3.1)$$

Here, the cost metric $c(s(t), t)$ evaluates the performance of algorithm $s(t)$ on task t . Because no individual machine learning model typically achieves the best performance across all tasks, and many machine learning problems require hyperparameter optimization to achieve good performance, it is natural to extend hyperparameter optimization to treat the choice of algorithms as a hyperparameter. The CASH problem integrates hyperparameter optimization with algorithm selection. This extension considers not only the selection of the optimal algorithm for each task but also the tuning of its hyperparameters to minimize the total cost.

To formalize CASH, let \mathcal{H}_i denote the hyperparameter space associated with each algorithm $A_i \in \mathcal{A}$. The combined algorithm and hyperparameter space is given by:

$$S = \bigcup_{i=1}^n \{A_i\} \times \mathcal{H}_i,$$

where each element $(A_i, h_i) \in S$ represents a specific algorithm A_i and a configuration of its hyperparameters $h_i \in \mathcal{H}_i$. The performance of $s(t)$ on task t is now extended to include hyperparameters, expressed as:

$$c((s(t), h_i), t).$$

The objective of CASH is to jointly optimize the choice of algorithm and its hyperparameters to minimize the total cost across all tasks:

$$(s^*, h^*) = \arg \min_{s: \mathcal{T} \rightarrow \mathcal{A}, h_i \in \mathcal{H}_i} \sum_{t \in \mathcal{T}} c((s(t), h_i), t). \quad (3.2)$$

For more details on how to solve Equation 3.2 with mostly applications outside of Deep Learning (DL), we refer the interested reader to Thornton et al. (2013), Hutter et al. (2019), and Feurer et al. (2022).

In this dissertation, we adapt the CASH framework to DL pipelines, where the combined algorithm and hyperparameter tuple correspond to pretrained models M_i and their finetuning hyperparameters h_i , i.e., $x = (M_i, h_i)$ and the cost metric is the loss (e.g., cross-entropy loss in supervised learning). In this setting, a dataset represented by its meta-features $\phi \in \Phi$ is typically split into training, validation, and test splits, i.e., $D^{(tr)}, D^{(val)}, D^{(test)}$. The cost is then defined as:

$$c(x, \phi) = \mathcal{L}(\text{Tune}(x, D^{(tr)}, D^{(val)}), D^{(test)}),$$

where \mathcal{L} measures the loss on the test split after finetuning the pretrained model on the training split.

Analogously to the CASH setting, we aim to optimize the objective given by Equation 3.2 by training the selector or surrogate model on meta-data. In the case of DL pipelines, this meta-data consists of prior recorded performance data about pretrained models M_i when finetuned on similar tasks (identified by meta-features ϕ_i) given a finetuning hyperparameter configuration h_i . Once trained, the surrogate can make informed decisions about which DL pipeline to select for new tasks ϕ_{new} , depending on how well the data on which the surrogate was trained resembles future tasks. In this dissertation, we explore learning both probabilistic surrogates that model uncertainty and non-probabilistic surrogates that predict point estimates to select DL pipelines.

Data Augmentation and Synthetic Data

Data augmentation and synthetic data generation resemble essential methods to systematically expand, modify, or produce entirely new datasets D_t for a given task t . By increasing data diversity, these methods often allow for improving model robustness and mitigate overfitting (Shorten and Khoshgoftaar, 2019). In this chapter, we begin by introducing data augmentation and synthetic data generation in a general and conceptual manner, highlighting their core principles. We then narrow our focus to a subset of approaches that are most relevant to the scope of this thesis.

4.1 Data Augmentation

Data augmentation applies transformations to existing data. Assume \mathcal{F} is a set of sample level transformations. Each transformation $f \in \mathcal{F}$ maps D_t to an augmented dataset \tilde{D}_t . On a sample level, data augmentation transforms each sample $x \in D_t$ independently. In computer vision, these transformations are typically composed of geometric (cropping, flipping, rotating, cut-out, etc.) or appearance (color distortion, blurring, etc.) perturbations (Shorten and Khoshgoftaar, 2019). Formally, this can be described as $\tilde{D}_t = \{f(x) \mid x \in D_t, f \sim p(f \mid \mathcal{F})\}$. Data augmentation can also occur at the dataset level, where a transformation modifies the characteristics of the entire dataset, for instance, changing the number of samples or the resolution of images.

Manual augmentation strategies often rely on domain-specific prior knowledge. To automate the augmentation process, automated data augmentation techniques have been proposed and nowadays resemble important components of modern learning pipelines. In computer vision, for instance, learning-based approaches such as AutoAugment (AA) (Cubuk et al., 2019), Population-based Augmentation (PBA) (D. Ho et al., 2019), or Fast AutoAugment (FAA) (Lim et al., 2019a) aim to learn dataset specific augmentation policies. AA treats augmentation as a sequential decision problem and uses reinforcement learning to solve it, however, at a high computational cost. PBA reduces this cost by learning multiple worker

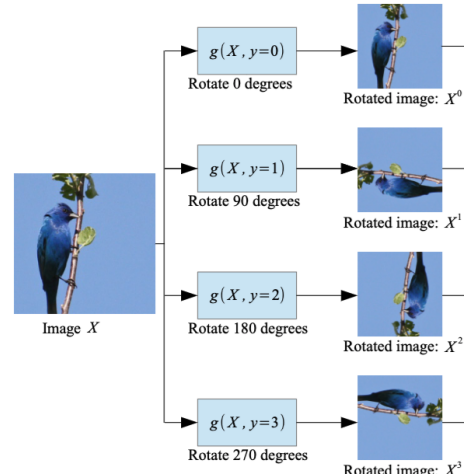


Figure 4.1: Predicting image rotations instead of classes in Self-Supervised Learning (visualization from Giradis et al. (2018)).

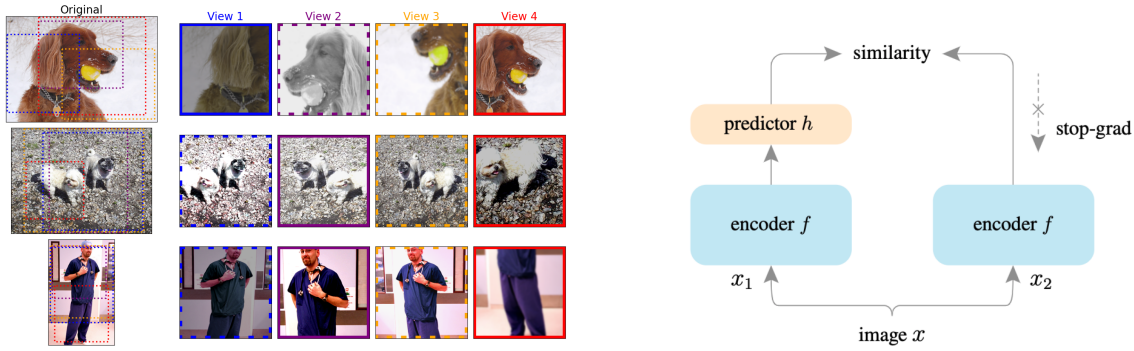


Figure 4.2: **Left:** Example views after applying geometric and appearance transformations (visualization from Ferreira et al. (2025)). **Right:** SimSiam’s architecture asymmetry to facilitate contrastive learning without negative image pairs (visualization from X. Chen and He (2021)).

schedules via evolution-based training. Further reducing the computational cost, FAA employs a strategy that identifies good sub-policies on dataset splits. On the other hand, works exist that learn augmentation networks to generate pixel-level augmentations with an adversarial objective (Antoniou, 2017). However, there also exist pure sampling-based approaches like RandAugment (Cubuk et al., 2020) and TrivialAugment (S. Müller and Hutter, 2021) which are cheaper than the learning-based approaches since they simplify this process further by eliminating the need for any additional learning augmentation policies or generators. Instead, they directly randomly sample the number and magnitude of transformations and show comparable performance to the learning-based approaches.

Data augmentation is particularly essential in self-supervised learning (SSL), where models learn representations without explicitly requiring a labeled dataset by directly extracting a supervision signal from the data. Early SSL approaches formulate and optimize the task of predicting transformations applied to images. For instance, predicting the spatial (pixel) context of image patches (Doersch et al., 2015), reconstructing compressed representations back into pixel-space (Bourlard and Kamp, 1988; Hinton and Zemel, 1993), solving Jigsaw puzzles, where images are divided into patches and shuffled (Noroozi and Favaro, 2016), or classifying randomly sampled rotations applied to images (Giradis et al., 2018) (see Fig. 4.1). By forcing the model to predict or recover the applied transformations, these methods encourage the model to learn semantically meaningful features.

This methodology is also the foundation for the more recent and popular *contrastive SSL* framework (T. Chen et al., 2020) which focuses on learning representations by learning to distinguish between different augmented inputs, referred to as *views* (see Fig. 4.2 left). This framework learns latent representations in which similar image views are located closely, and dissimilar ones distantly. However, for effective learning in this framework, a large pool of negative samples is required to prevent the model from collapsing to trivial solutions (T. Chen et al., 2020). More recent methods, such as BYOL (Grill et al., 2020), SimSiam (X. Chen and He, 2021), DINO (Caron et al., 2021), and iBOT (J. Zhou et al., 2021) eliminate explicit negatives by introducing additional architectural components, such as architectural asymmetry, momentum encoders or averaging schemes, that prevent collapse while relying solely on positive pairs.

More formally, we describe the contrastive learning objective in the example of SimSiam (X. Chen and He, 2021), which is also visualized in Fig. 4.2 (right). Let \mathcal{D} be a set of

images, and \mathcal{F} a set of sample level transformations. Consider a minibatch of M images $\mathbf{x} = \{x_i\}_{i=1}^M$ sampled uniformly from \mathcal{D} . SimSiam draws two random transformations $f_1, f_2 \sim p(f \mid \mathcal{F})$ and applies them to each image in \mathbf{x} , resulting in two augmented sets of views \mathbf{x}^1 and \mathbf{x}^2 . An encoder f_θ and a predictor h_θ then produce embeddings. For the first view, we define

$$\mathbf{e}^1 = f_\theta(\mathbf{x}^1), \quad \mathbf{z}^1 = h_\theta(\mathbf{e}^1),$$

with analogous definitions \mathbf{e}^2 and \mathbf{z}^2 for the second view. SimSiam then minimizes

$$\mathcal{L}(\theta) = \frac{1}{2} \left(D(\mathbf{z}^1, \mathbf{e}^2) + D(\mathbf{z}^2, \mathbf{e}^1) \right), \quad (4.1)$$

where $D(\cdot, \cdot)$ denotes negative cosine similarity. Unlike standard contrastive frameworks, SimSiam does not rely on negative examples. Instead, it avoids trivial solutions (all embeddings collapsing to a constant) by introducing *asymmetry* in its architecture and objective by introducing a small network (predictor) to only one branch and restricting gradient flow on the other. By learning to align these slightly different outputs, SimSiam maintains non-trivial embeddings. A more recent body of literature learns such embeddings through adversarial objectives to automatically select more challenging views (Ferreira et al., 2025; Koçyigit et al., 2023) that aid SSL training or optimize augmentation networks to directly output augmented views given images (Shi et al., 2022; Tamkin et al., 2021; Tian et al., 2020). Collectively, these approaches share the core principle of aligning representations across augmentations of the same input, which enables improved downstream task performance without requiring labeled data.

4.2 Synthetic Data Generation

In contrast to data augmentation, synthetic data generation is concerned with creating entirely new data samples or datasets. One way to employ synthetic data generation is to learn a data-generating model G_ψ trained on one or more existing tasks to produce $D_t = \{x \mid x \sim G_\psi\}$. Many different approaches have been proposed. A popular method is Generative Adversarial Networks (GANs) (Goodfellow et al., 2014). GANs consist of two neural networks, a generator and a discriminator, that are optimized in a joint adversarial learning process. While the generator creates synthetic data samples that mimic the real data, the discrimination distinguishes between real and synthetic samples. Through optimization, the generator’s goal is to effectively fool the discriminator, and the discriminator enhances its ability to detect synthetic samples. Post optimization, the resulting generator can be used as G_ψ to produce new samples independent of the real data-generating process. In addition to GANs, many other generative model techniques exist. For instance, Variational Autoencoders use probabilistic modeling with an encoder that projects data into a latent space and a decoder that reconstructs it, where the generation function G_ψ samples from the latent distribution and decodes it back to the original space. Flow-based models and Diffusion models are complementary techniques to learn G_ψ . They too learn latent spaces from which one can sample synthetic data. Flow-based models do this by learning an invertible mapping from data to latent space through a sequence of transformations. On the other hand, diffusion models learn a reversion function that iteratively denoises random additive noise to arrive at a (synthetic) data sample.

Typically, works using these techniques are incentivized to mimic the real data distribution. However, there exist approaches that use learning objectives that facilitate more efficient learning when training on the produced synthetic data. Particular examples are Generative Teaching Networks (Such et al., 2020) that meta-learn G_ψ to generate synthetic data specifically optimized to accelerate the learning process of a target model:

the inner loop trains the target model on the synthetic data produced by G_ψ , and an outer loop evaluates the target model on a real target task. As illustrated in Figure 1.1 (right), the meta gradients are then backpropagated through the entire learning process to update G_ψ . A related approach is dataset distillation (T. Wang et al., 2018), which backpropagates the validation error gradients directly into the input to generate a synthetic dataset to achieve comparable or better performance than training on the full dataset. In a similar fashion, Maclaurin et al. (2015) optimizes directly for the data by treating it as hyperparameters. Another technique for improving training efficiency is core-set selection (Sener and Savarese, 2018; Tsang et al., 2005). Here, a subset of the original dataset is identified as a proxy dataset which encompasses the most relevant information needed for effective learning. Together, these approaches demonstrate various strategies for generating synthetic datasets, targeting objectives such as efficient learning, reduced dataset size, or the ability to produce large amounts of synthetic data tailored for specific tasks.

A different methodology is to sample data from a user-specified or prior known distribution over data points and labels $q(\mathcal{X}, \mathcal{Y})$, resulting in $D_t = \{x, y \mid x, y \sim q(x, y)\}$ and providing a source of synthetic data that does not depend on the original dataset D_t at all. For example, Prior-Data Fitted Networks (PFNs) (Hollmann et al., 2023; S. Müller et al., 2022) utilize this concept by defining a synthetic prior over supervised learning tasks. These priors encode assumptions about the data-generating process (e.g., the relationships between features or causal structures) and enable the generation of synthetic datasets tailored to the task domain. PFNs repeatedly draw a dataset from the synthetic prior distribution, sample data points and their labels from it, mask one of the labels, and optimize the PFN to predict the masked label given the rest of the data points and labels. By training entirely on synthetic data generated from priors and achieving state-of-the-art performance, PFNs showcase the surprising ability to transfer synthetic pretraining to real-world tasks. Backed by the possibility of generating infinite amounts of synthetic data, PFNs and the synthetic data generation methodology in general offer a powerful framework for scaling up models as training is decoupled from the limitations of real-world datasets.

Part II

Meta-Learning for Automated Model Selection and Finetuning

Zero-Shot AutoML with Pretrained Models

The content of this chapter has been published as:

E. Öztürk, F. Ferreira, H. S. Jomaa, L. Schmidth-Thieme, J. Grabocka, and F. Hutter (2022). “Zero-Shot AutoML with Pretrained Models”. In: *Proceedings of the 39th International Conference on Machine Learning (ICML’22)*. Ed. by K. Chaudhuri, S. Jegelka, L. Song, C. Szepesvári, G. Niu, and S. Sabato. Vol. 162. Proceedings of Machine Learning Research. PMLR, pp. 1128–1135. URL: <https://icml.cc/virtual/2022/spotlight/18008>.

This work represents a core contribution to this dissertation and was published in a peer-reviewed A* conference (CORE2023), with a significant author contribution. The supplementary material and a detailed statement of contributions is provided in Appendix A.

Zero-Shot AutoML with Pretrained Models

Ekrem Öztürk^{*1} **Fabio Ferreira**^{*1} **Hadi S. Jomaa**^{*2} **Lars Schmidt-Thieme**² **Josif Grabocka**¹
Frank Hutter^{1,3}

Abstract

Given a new dataset D and a low compute budget, how should we choose a pre-trained model to fine-tune to D , and set the fine-tuning hyperparameters without risking overfitting, particularly if D is small? Here, we extend automated machine learning (AutoML) to best make these choices. Our domain-independent meta-learning approach learns a zero-shot surrogate model, which, at test time, allows to select the right deep learning (DL) pipeline (including the pre-trained model and fine-tuning hyperparameters) for a new dataset D given only trivial meta-features describing D , such as image resolution or the number of classes. To train this zero-shot model, we collect performance data for many DL pipelines on a large collection of datasets and meta-train on this data to minimize a pairwise ranking objective. We evaluate our approach under the strict time limit of the vision track of the ChaLearn AutoDL challenge benchmark, clearly outperforming all challenge contenders.

1. Introduction

A typical problem in deep learning (DL) applications is to find a good model for a given dataset D in a restrictive time budget. In the case of tabular data, a popular approach for solving this problem is automated machine learning (AutoML), as implemented, e.g., in Auto-sklearn (Feurer et al., 2015a) or Auto-Gluon (Erickson et al., 2020). However, in domains such as computer vision and natural language processing, a better solution, especially under low resource constraints, is typically to fine-tune an existing pre-trained model. This, at first glance, appears to render AutoML unnecessary for those domains. However, as we will demonstrate in this paper, AutoML and pre-trained models can be

combined to yield much stronger performance than either of them alone.

A great advantage of fine-tuning pre-trained models is strong anytime performance: the use of pre-trained models often allows to obtain very strong performance orders of magnitude faster than when training a model from scratch. In many practical applications, this strong anytime performance is crucial, e.g., for DL-based recognition systems in manufacturing, or automated DL (AutoDL) web services. The clock starts ticking as soon as a new dataset is available, and it would be far too costly to train a new model from scratch, let alone optimize its hyperparameters. The recent ChaLearn AutoDL competition (Liu et al., 2021) mimicked these tight time constraints, rewarding performance found in an anytime fashion.

While fine-tuning pre-trained models enjoys strong anytime performance, it also introduces many additional degrees of freedom. Firstly, we need to select a pre-trained network to fine-tune. To obtain good anytime performance, we may even want to start by training a shallow model to obtain good results quickly, and at some point switch to fine-tuning a deeper model. There are many additional degrees of freedom in this fine-tuning phase, concerning learning rates, data augmentation, and regularization techniques. We refer to the combination of a pre-trained model and the fully specified fine-tuning phase, including its hyperparameters, as a *DL pipeline*. Which DL pipeline works best depends heavily on the dataset, for instance, datasets with high-resolution images may favor the use of more downsampling layers than the low-resolution images of the CIFAR dataset (Krizhevsky et al., 2009); likewise, datasets with few images may favor smaller learning rates. We, therefore, require an automated method for selecting the best DL pipeline based on the characteristics of the dataset at hand.

In this paper, we tackle this problem by meta-learning a model across datasets that enables zero-shot DL pipeline selection. Specifically, we create a meta-dataset holding the performance of many DL pipelines on a broad range of datasets. Using this meta-dataset, we then learn a function that selects the right DL pipeline based on the properties of the dataset (e.g., the image resolution and the number of images) in a zero-shot setting. To learn this selection function, we first formulate DL pipeline selection as a classical

^{*}Equal contribution ¹University of Freiburg ²University of Hildesheim ³Bosch Center for Artificial Intelligence. Correspondence to: Fabio Ferreira <ferreira@cs.uni-freiburg.de>.

algorithm selection (AS) problem (Rice, 1976) and then improve upon this formulation by recognizing DL pipelines as points in a geometric space that allows information about the performance of some pipelines to inform performance on others. We then train a deep neural network with a pairwise ranking objective to emphasize the rank of the DL pipeline predicted to perform best in a manner that automatically normalizes across datasets. Note, that we use the *zero-shot* nomenclature not to refer to samples of unseen classes but to express that we cannot even afford a single exploratory evaluation of a pipeline but need to directly select a suitable one in a zero-shot manner.

Our contributions can be summarized as:

- We extend AutoML to best exploit pre-trained models by meta-learning to select the best DL pipeline conditional on dataset meta-features.
- We introduce a large meta-dataset with the performances of 525 DL pipelines across 35 image-classification datasets and 15 augmentations each. With 525*35*15 entries, it is, to our best knowledge, the first DL meta-dataset for image classification of this size, being over 1000 times larger than previous meta-datasets (Triantafillou et al., 2019).
- We go beyond a standard formulation as an algorithm selection problem by formulating the new problem of selecting a DL pipeline as a point in a geometric space to exploit similarities between DL pipelines.
- We introduce a novel zero-shot AutoDL method that addresses this pipeline selection problem with a pairwise ranking loss.
- In the setting of the recent ChaLearn AutoDL challenge (Liu et al., 2021), our zero-shot AutoDL approach dominates all competitors on a broad range of 35 image datasets, as well as in the challenge itself.

To foster reproducibility, we make our PyTorch (Paszke et al., 2019) code, models, and data publicly available under this URL.

2. Related Work

Algorithm selection Assume a set \mathcal{P} of algorithms $\mathcal{A} \in \mathcal{P}$ (e.g., classifiers or neural network hyperparameter configurations), a set of *instances* $i \in \mathcal{I}$ (e.g., dataset features), and a *cost metric* $m : \mathcal{P} \times \mathcal{I} \rightarrow \mathbb{R}$. Specifying the loss of algorithm $\mathcal{A} \in \mathcal{P}$ on instance $i \in \mathcal{I}$ with $m(\mathcal{A}, i)$, the algorithm selection problem (Rice, 1976; Smith-Miles, 2009; Kotthoff et al., 2012; Bischl et al., 2016) is to find a mapping $s : \mathcal{I} \rightarrow \mathcal{P}$ that minimizes the cost metric $\sum_{i \in \mathcal{I}} m(s(i), i)$ across instances \mathcal{I} . Algorithm selection has been applied to achieve state-of-the-art results in many hard combinatorial problems, most prominently Boolean satisfiability

solving (SAT), where SATzilla (Xu et al., 2008) won several competitions by learning to select the best SAT solver on a per-instance basis. There are many methods for solving algorithm selection, based on regression (Xu et al., 2008), k-nearest neighbours (Kadioglu et al., 2011), cost-sensitive classification (Xu et al., 2012), and clustering (Kadioglu et al., 2010; Malitsky et al., 2013). *AutoFolio* (Lindauer et al., 2015) is a state-of-the-art algorithm selection system that combines all of these approaches in one and chooses between them using algorithm configuration (Hutter et al., 2011). We will use AutoFolio as one of our methods for selecting DL pipelines based on dataset meta-features.

Hyperparameter optimization (HPO) HPO plays an integral role in fine-tuning any machine learning algorithm. Beyond simple strategies, such as random search (Bergstra & Bengio, 2012), conventional techniques typically involve fitting (probabilistic) surrogate models of the true response, e.g. Gaussian Process (Rasmussen & Williams, 2006), random forests (Hutter et al., 2011), neural networks (Springenberg et al., 2016), or some hybrid techniques (Snoek et al., 2015), and selecting configurations that optimize pre-defined acquisition functions (Wilson et al., 2018). Recently, approaches started taking into account the dissimilarity between pre-training and downstream domains (Li et al., 2020). HPO multi-fidelity methods further reduce the wall-clock time necessary to arrive at optimal configurations (Li et al., 2017; Falkner et al., 2018; Awad et al., 2021).

Transfer HPO Transfer learning can be used in HPO to leverage knowledge from previous experiments to yield a strong surrogate model with few observations on the target dataset. For example, Wistuba & Grabocka 2021 and Jomaa et al. 2021a both propose a meta-initialization strategy by optimizing a deep kernel Gaussian process surrogate model (Wilson et al., 2016) across meta-train datasets to allow for fast adaptation given a few observations. Similarly, Salinas et al. 2020 learns a Gaussian Copula (Wilson & Ghahramani, 2010) and addresses the heterogeneous scales of the responses across datasets, whereas Perrone et al. 2018 pre-trains a shared layer in a multi-task setting. Transfer HPO is also possible based on meta-features (Vanschoren, 2018), i.e. dataset characteristics which can be either engineered (Feurer et al., 2015b; Wistuba et al., 2016) or learned (Jomaa et al., 2021b) to warm-start HPO.

Zero-shot HPO The conventional setting of zero-shot learning aims to recognize samples whose instances may not have been seen during training (Xian et al., 2018; Verma et al., 2018; Radford et al., 2021). In the setting of zero-shot HPO, in contrast, the focus lies on improving sample efficiency for hyperparameter optimization. Contrary to techniques in previous sections that improve their sample efficiency by increasing the number of trials, zero-shot HPO

has emerged as a more efficient approach that does not require any observations of the response on the target dataset. [Wistuba et al. 2015](#) design a sequential model-free approach that optimizes the ranks of hyperparameter configurations based on their average performance over a collection of datasets. [Winkelmolen et al. 2020](#) propose a Bayesian optimization solution for zero-shot HPO, whereby a surrogate model is fit to the dataset and hyperparameters and optimized by minimizing a ranking meta-loss. We note that both these approaches return a fixed set of hyperparameter configurations without using meta-features, which is undesirable as the AutoDL setting used in this work only allows for running a single model. Related to our work is [\(Tornede et al., 2020\)](#), who also describe datasets and pipelines as joint feature vectors. They use these to assess the learning of zero-shot models with algorithm selection and ranking-based objectives in a benchmark of tabular datasets and shallow base models in a sparse cost-matrix setting. In this paper, we propose a novel zero-shot HPO solution inspired by the success of algorithm selection techniques that learns to select the best DL pipeline based on both parametric choices inside the DL pipeline and dataset meta-features of complex vision datasets, by optimizing a ranking objective jointly across datasets.

AutoDL Competition ChaLearn’s AutoDL Challenge [\(Liu et al., 2021\)](#) evaluated competitors in an anytime setting with strict time limits, leading to the prominent use of pre-trained models by the participants. We focus on the challenge’s image-track and summarize the winning approaches here and give more details in Section 5.3. In the 2019 AutoCV/CV2 competition, the winning approach [\(Baek et al., 2020\)](#) used a ResNet-18 [\(He et al., 2015\)](#) pre-trained on ImageNet [\(Krizhevsky et al., 2012\)](#) with Fast AutoAugment [\(Lim et al.\)](#). All image-track winning solutions used the AutoCV winner code as a skeleton and built their methods on top. Their modifications ranged from switching to a more stable ResNet-9 during training (DeepWisdom), ensembling predictions (DeepBlueAI) to data-adaptive pre-processing (PASA NJU).

Meta-learning Meta-learning [\(Finn et al., 2017\)](#) can be used to solve tasks where the training dataset is small. [Sun et al. 2019](#) meta-learn to transfer large-scale pre-trained DNN weights to solve few-shot learning tasks. [Verma et al. 2019](#) tackle Zero-Shot Learning by meta-learning a generative model for synthesizing examples from unseen classes conditioned on class attributes. [Laadan et al. 2019](#) generate (shallow model) pipelines on diverse datasets and use dataset meta-features to rank the pipelines to create a meta-dataset of pipelines and their performance results.

Despite the abundance of meta-learning methods, and in contrast to the large benchmarks for tabular data [\(Pineda-](#)

[Arango et al., 2021\)](#), few meta-learning benchmarks exist for image datasets. [Zhai et al. 2019](#) introduced a set of 19 vision tasks and evaluated 18 representation learning methods. [Triantafillou et al. 2019](#) also introduced a meta-dataset of 10 few-shot image tasks and a growing set of baselines, currently comprising 11 and 18 evaluations on two different settings. [Dumoulin et al. 2021](#) combines these two benchmarks and compares Big Transfer [\(Kolesnikov et al., 2020\)](#) against the baselines of [Triantafillou et al. 2019](#). As we will show, our DL meta-dataset for image tasks is far larger than all previous meta-learning benchmarks.

3. Zero-Shot AutoML with Pretrained Models

3.1. Notation and Problem Definition

Let $\mathcal{X} := \{x_n\}_{n=1}^N$ denote a set of N distinct deep learning (DL) pipelines. Every DL pipeline $x_n := (M_n, \theta_n)$ comprises a pre-trained model $M_n \in \mathcal{M}$ and fine-tuning hyperparameters $\theta_n \in \Theta$ that are used to fine-tune M_n to a given dataset. Furthermore, let $\mathcal{D} = \{D_i\}_{i=1}^I$ denote a collection of I datasets, where each dataset $D_i \in \mathcal{D}$ is split into disjoint training, validation and testing subsets $D_i := D_i^{(tr)} \cup D_i^{(val)} \cup D_i^{(test)}$. For each dataset, we are given a vector of K descriptive characteristics (a.k.a. meta-features), such as the number of data points and the image resolution, as $\phi_i \in \Phi \subseteq \mathbb{R}^K$ (see Section 4.1 for the full set of meta-features we used in our experiments). We denote by $x_n^{(ft)} := \text{Tune}(x_n, D^{(tr)}, D^{(val)})$ the model resulting from fine-tuning the pre-trained model M_n with hyperparameters θ_n on training data $D^{(tr)}$ using validation data $D^{(val)}$ for early stopping. Then, denoting the loss of a fine-tuned model $x_n^{(ft)}$ on the test split of the same dataset D as $\mathcal{L}(x_n^{(ft)}, D^{(test)})$, the test cost of DL pipeline x_n on D is defined as:

$$C(x_n, D) = \mathcal{L}(\text{Tune}(x_n, D^{(tr)}, D^{(val)}), D^{(test)}). \quad (1)$$

Definition 1. Given a set of N DL pipelines $\mathcal{X} := \{x_n\}_{n=1}^N$ and a collection of I datasets $\mathcal{D} = \{D_i\}_{i=1}^I$ with meta-features ϕ_i for dataset $D_i \in \mathcal{D}$, and a $N \times I$ matrix of costs $C(x_n, D_i)$ representing the cost of pipeline x_n on dataset D_i , the problem of **zero-shot AutoML with pre-trained models (ZAP)** is to find a mapping $f : \Phi \rightarrow \mathcal{X}$ that yields minimal expected cost over \mathcal{D} :

$$\operatorname{argmin}_f \mathbb{E}_{i \sim \{1, \dots, I\}} [C(f(\phi_i), D_i)]. \quad (2)$$

3.2. ZAP via Algorithm Selection (ZAP-AS)

The problem of zero-shot AutoML with pre-trained models from Definition 1 can be directly formulated as an algorithm selection problem: the DL pipelines $\mathcal{X} := \{x_n\}_{n=1}^N$ are the algorithms \mathcal{P} , the datasets $\{D_i\}_{i=1}^I$ are the instances \mathcal{I} , and the test cost $C(x_n, D)$ of DL pipeline x_n on D defines the cost metric $m : \mathcal{P} \times \mathcal{I} \rightarrow \mathbb{R}$. We use the state-of-the-art

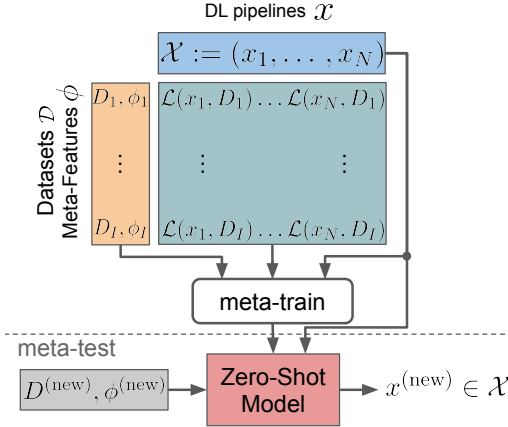


Figure 1. ZAP consists of two stages. In the meta-train stage, the cost matrix on the source tasks is leveraged to learn a joint response surface conditioned on the meta-features and pipelines. During the meta-test stage, ZAP assigns scores to the pipelines of the unseen datasets and the highest-scoring pipeline is selected.

algorithm selection system AutoFolio to learn a selector between our predefined DL pipelines, since it subsumes approaches based on regression, classification, clustering, and cost-sensitive classification, and selects the best one for the data at hand (Lindauer et al., 2015).

While this formulation of zero-shot AutoML with pre-trained models as algorithm selection will turn out to already yield very strong performance, it has one limitation: algorithm selection abstracts away our DL pipelines as uncorrelated algorithms, losing all information about the pre-trained models they are based on, and which hyperparameters are being used for fine-tuning. This information, e.g., allows us to predict the cost of DL pipelines to other DL pipelines with similar settings without ever having run them. Thus, we next introduce a novel approach for exploiting this knowledge.

3.3. ZAP via Zero-Shot HPO (ZAP-HPO)

We now describe a variant of our formulation of zero-shot AutoML that exploits the fact that the DL pipelines between which we select are points in a geometric space, and that we can see the space of DL pipelines we consider as a search space for hyperparameter optimization (HPO), with a categorical value for the choice of pre-trained model and continuous fine-tuning hyperparameters; we can then use concepts from zero-shot HPO to tackle this problem.

We define M as a finite collection of N pre-trained models and represent each instance, M_n , as a one-hot encoded vector, and $\theta_n \in \Theta \subseteq \mathbb{R}^L$ as a vector of continuous variables defining its respective hyperparameters. For instance, Θ can represent the continuous space of learning rates and dropout values of a pre-trained neural network model in $\mathcal{M} \in \{0, 1\}^{|\mathcal{N}|}$. Consequently, the DL pipelines are pro-

jected to the geometric space defined by $\mathcal{X} \subseteq \mathcal{M} \times \Theta$ and can be viewed as a hyperparameter configuration space where pre-trained models are simply categorical variables.

Denote by f_ψ a parametric surrogate with parameters ψ that estimates the test cost observed by fine-tuning the DL pipeline x_j on dataset D_i with meta-features ϕ_i . The surrogate captures the fusion of (i) pipeline hyperparameters (i.e. x represented by the pre-trained model's one-hot-encoding indicator $\mathcal{M} \in \{1, \dots, M\}$ and the fine-tuning hyperparameters $\theta \in \Theta$) with (ii) dataset meta-features ϕ , in order to estimate the cost after fine-tuning. Formally, that is:

$$f(\psi)_{i,j} := f(x_j, \phi_i; \psi) : \mathcal{M} \times \Theta \times \Phi \rightarrow \mathbb{R}_+ \quad (3)$$

A unique aspect of searching for efficient pipelines is that we are concerned with the *relative* cost of the pipelines, to find the best one. As such, we propose to utilize the surrogate model as a proxy function for the rank of configurations, and learn the pairwise cost ranking of pairs of pipelines. In this perspective, pairwise ranking strategies use the relative ordering between pairs of configurations to optimize the probability that the rank of the j -th pipeline is lower than the k -th pipeline on the i -th dataset. Therefore, using given pre-computed cost $C_{i,j} = C(x_j, D_i)$ we define the set of triples $\mathcal{E} := \{(i, j, k) \mid C(x_j, D_i) < C(x_k, D_i)\}$. Every triple (i, j, k) denotes a pair (x_j, x_k) , where the cost of x_j is smaller (better pipeline) than x_k on the i -th dataset. Correspondingly, we want our surrogate to predict $f(\psi)_{i,j}$ to be lower than $f(\psi)_{i,k}$; we thus meta-learn our surrogate with a ranking loss as:

$$\arg \min_{\psi} \sum_{(i,j,k) \in \mathcal{E}} \log \left(\sigma \left(f(\psi)_{i,j} - f(\psi)_{i,k} \right) \right), \quad (4)$$

with $\sigma(\cdot)$ as the sigmoid function which prevents the difference from exploding to negative infinity as we minimize the loss. Equation 4 maximizes the gap between the surrogate scores, by *decreasing the surrogate score for the good DL pipelines with low costs*, while at the same time increasing the surrogate score of bad pipelines with high costs. As a result, the score of the best DL pipeline with the lowest cost will be maximally decreased. Furthermore, Figure 2 presents a visual description of our proposed ranking loss.

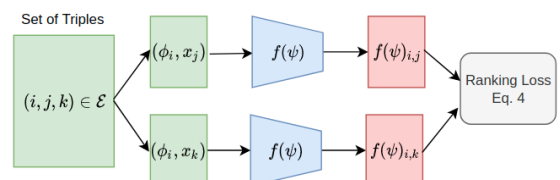


Figure 2. Overview of our pairwise ranking objective

Once we meta-learn the surrogate, we can transfer it to a new dataset $D^{(\text{new})}$ with meta-features $\phi^{(\text{new})}$ in a **zero-shot HPO** mechanism using Equation 5. The full meta-learn and meta-test procedure is depicted in Figure 1.

$$x^{(\text{new})} := \arg \min_{x_n, n \in \{1, \dots, N\}} f(x_n^{(\text{ft})}, \phi^{(\text{new})}; \psi) \quad (5)$$

For an empirical motivation on the benefits of learning surrogates with pairwise ranking losses, we compare to the same surrogate model optimized with a least-squares loss:

$$\arg \min_{\psi} \sum_{i=1}^I \sum_{n=1}^N \left(f(\psi)_{i,n} - C(x_n, D_i) \right)^2 \quad (6)$$

As a sanity check, we also compare the performance of randomly selecting a pipeline. In this experiment, we evaluate the performance of the pipeline having the largest estimated value by the surrogate (Equation 5) across all the I -many source datasets. The results of Figure 3 demonstrate that the surrogate trained with Equation 4 is significantly better than the regression-based variant of Equation 6 in terms of identifying the best pipeline. Further details about the evaluation protocol are found in Section 5.1.

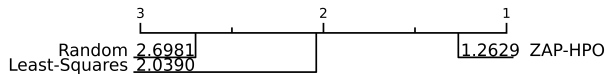


Figure 3. Critical difference diagram comparing loss functions using the Wilcoxon-Holm signed-rank (5% significance level).

4. ZAP Meta-Dataset Design

In this section, we introduce a novel meta-dataset (Pineda-Arango et al., 2021), that will ultimately allow us to perform zero-shot AutoML with pre-trained models (ZAP). The meta-data required for the ZAP problem includes a set of datasets with meta-features, a set of DL pipelines, and the test costs for these pipelines on these datasets. Correspondingly, we describe how we curated a set of 35 image datasets, with 15 augmentations each (4.1); define a space of DL pipelines (4.2); and find strong instantiations in it for each of the datasets, each of which we evaluate on all datasets to obtain a 525×525 matrix of test costs (4.3).

4.1. A Set of Image Datasets for ZAP

The set of datasets should be chosen to be representative of the datasets that will eventually be tackled by the ZAP system building on them. While all our pre-trained networks are pre-trained on ImageNet (Deng et al., 2009), during the fine-tuning stage also smaller and specialized datasets are

to be expected. Consequently, we chose both small and large, as well as diverse datasets that cover a wide range of domains (objects, medical, aerial, drawings, etc.) with varying formats, i.e. colored and black-and-white images and datasets with varying image resolutions or the number of classes. With this preference in mind, we retrieved 35 *core* datasets provided by the TensorFlow (Abadi et al., 2015) Datasets (TFDS) utility library (Google, 2021) and applied a dataset augmentation process (Stoll, 2020) that takes a TFDS core dataset as input and outputs a subset of that differs in the number of classes and the number of train/test samples per class. Note that this dataset augmentation process does not perform augmentations on a sample level. We repeat this subset retrieval 15 times for each dataset, resulting in 525 datasets \mathcal{D} . Further details about the augmentation process are found in Appendix A.2.

To represent a dataset, we use only extremely cheap and readily available dataset-dependent meta-features (Hutter et al., 2020) ϕ : number of training images, number of image channels, image resolution, and number of classes.

4.2. DL Pipeline Design Space for ZAP on Image Data

The DL pipelines we employ should be chosen to be diverse and achieve high performance on the aforementioned datasets since the optimum we can hope for is to choose the best of these pipelines on a per-dataset basis. To obtain strong pipelines, we started from the code base of the winner of the AutoCV competition (Baek et al., 2020), which fine-tuned a pre-trained ResNet-18 model. We then built a highly-parameterized space of DL pipelines around this by exposing a wide range of degrees of freedom. These included fine-tuning hyperparameters, such as learning rate, percentage of frozen parameters, weight decay, and batch size. Additionally, we exposed hyperparameters for the online execution that were previously hard-coded and that control, e.g., the number of samples used or when to evaluate progress with the validation dataset. To span a more powerful space with diverse pipelines, we also added additional architectural, optimization, as well as fine-tuning choices, including:

- A binary choice between an EfficientNet (Tan & Le, 2019) pre-trained on ImageNet (Russakovsky et al., 2015) or the previously-used ResNet-18;
- The proportion of weights frozen when fine-tuning;
- Additional stochastic optimizers (Adam (Kingma & Ba, 2015), AdamW (Loshchilov & Hutter, 2018), Nesterov accelerated gradient (Nesterov, 1983)) and learning rate schedules (plateau, cosine (Loshchilov & Hutter, 2017));
- A choice of using a simple classifier (either a SVM,

random forest or logistic regression) that can be trained and used within the first 90 seconds of run-time in order to improve anytime performance.

Overall, our DL pipeline space \mathcal{X} is comprised of 26 hyperparameters of the types real and integer-valued, categorical, and conditional. A condensed version is presented in Table 6.

Table 1. The search space of our DL pipelines consisting of general DL hyperparameters, training-strategy hyperparameters and fine-tuning strategy hyperparameters. A more detailed version can be found in Appendix A.1.

Name	Type, Scale	Range
Batch size	int, log	[16, 64]
Learning rate	float, log	[10^{-5} , 10^{-1}]
Weight decay	float, log	[10^{-5} , 10^{-2}]
Momentum	float	[0.01, 0.99]
Optimizer	cat	{SGD, Adam, AdamW}
Scheduler	cat	{plateau, cosine}
Architecture	cat	{ResNet18, EffNet-b0, EffNet-b1, EffNet-b2}
Steps per epoch	int, log	[5, 250]
Early epoch	int	[1, 3]
CV ratio	float	[0.05, 0.2]
Max valid count	int, log	[128, 512]
Skip valid thresh.	float	[0.7, 0.95]
Test freq.	int	[1, 3]
Max inner loop	float	[0.1, 0.3]
# init samples	int, log	[128, 512]
Max input size	int	[5, 7]
1 st simple model	cat	{true, false}
Simple model	cat	{SVC, NuSVC, RF, LR}

4.3. Selection and Evaluation of DL Pipelines

With the 525 datasets and our 26-dimensional DL pipeline space at our disposal, we now explain how we generated the DL pipeline candidates that we evaluated on the datasets. Instead of uniformly or randomly sampling the 26-dimensional DL pipeline space, to focus on DL pipelines that are strong at least on one dataset, we ran an optimization process to find a (near-)optimal DL pipeline for one dataset at a time. Specifically, we used the hyperparameter optimization method BOHB (Falkner et al., 2018), which supports high-dimensional and categorical hyperparameter spaces, to find a (near)-optimal instantiation of our DL pipeline space for each dataset. We optimized the anytime Area under the Learning Curve (ALC) score (introduced in the AutoDL challenge (Liu et al., 2021) and described in more detail in Section 5.1) via BOHB, with a budget of five minutes for evaluating one DL pipeline on one dataset. We repeated each of these runs three times and used the mean to handle the substantial noise in these evaluations. This process resulted in one optimized DL pipeline per dataset;

we thus have $N = D = 525$ DL pipelines that comprise the set \mathcal{X} of DL pipelines in our ZAP formulation.

Given this set of 525 DL pipelines \mathcal{X} , and the set of our 525 datasets \mathcal{D} , let us now explain the evaluation procedure. We ran each pipeline $x \in \mathcal{X}$ on each dataset $D \in \mathcal{D}$, computing the ALC score the pipelines reached within 10 minutes, and again computing the mean of three runs to reduce noise. While the AutoDL competition used a budget of 20 minutes, we used a shorter time of 10 minutes here (and 5 minutes for the runs of BOHB above) for two reasons: First, to limit the substantial computational overhead for carrying out these $525 \cdot 525 = 275,625$ evaluations of (DL pipeline, dataset) pairs; still, it required 2,871 GPU days to collect this data. Second, due to the typically monotonically increasing anytime ALC score, performance after 5 and 10 minutes can be expected to be a good proxy for the full 20 minutes.

Finally, we record every pairs’ average-of-three ALC score in the cost matrix $C \in \mathbb{R}^{N \times I}$ (in our case with $N = I = 525$ since we found one DL pipeline per dataset). This cost matrix is visualized in Figure 4. From the cost matrix, we directly see that there are easy datasets (at the top, where all pipelines achieve high scores) and hard ones at the bottom (where only very few pipelines reach high scores). Likewise, there are overall strong pipelines (to the left, with good scores on most datasets) and poor ones (on the right, with good scores on only a few datasets). The most interesting pattern for ZAP is that there exists substantial horizontal and vertical striping, indicating that different datasets are hard for different pipelines. This points to the usefulness of selecting pipelines in a dataset-dependent manner in ZAP.

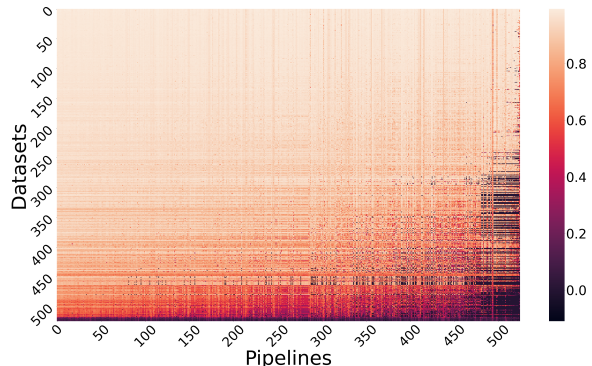


Figure 4. Cost matrix C as a heatmap Color indicates the ALC score (higher is better). We observe that some datasets (dark rows) are more complex and some pipelines (dark columns) generalize worse across datasets systematically than others.

5. Experiments

Our experiments are designed to evaluate the performance of an AutoDL system based on ZAP. We use the anytime

evaluation protocol of the ChaLearn AutoDL Challenge (Liu et al., 2021) and demonstrate that our ZAP methods perform substantially better than the winners of that competition, both in our ZAP evaluation benchmark grounded on our ZAP meta-dataset as well as in the original AutoDL challenge benchmark. We also carry out a range of ablations to better understand the root of our gains.

5.1. Evaluation Protocol

Let us first describe the restrictions of the evaluation protocol under which we evaluate different AutoDL methods (our ZAP approach and various baselines). The main restriction is the anytime learning metric to score participants with the Area under the Learning Curve (ALC): at each time step, an AutoDL system can update its predictions on test data, and in a post hoc evaluation phase, the accuracy of these predictions is averaged over the entire learning curve. A second core aspect of the challenge is the limited time budget of 20 minutes for training models and making predictions on test data. In light of the large training times of conventional deep learning models, this short time window encourages the use of efficient techniques, particularly the use of pre-trained models. The performance measurement starts with the presentation of the training data (and the inputs of the test split), and the AutoDL system can train in increments and interleave test predictions; however, the time for making predictions also counts as part of the run-time budget. Consequently, AutoDL systems need to decide when to make predictions to improve performance.

For a formal description of the metric, as well as an example of a learning curve plot under the competition metric, please see Appendix A.3.

5.2. Benchmarks and Training Protocol

Overall, we evaluate our ZAP methods under two benchmarks: one based on the ZAP meta-dataset which we refer to as *ZAP benchmark* and the original AutoDL benchmark. For the AutoDL benchmark, we submit our ZAP methods trained on the ZAP meta-dataset. The following describes how we train and evaluate our methods on the ZAP benchmark. We evaluate in a “leave-one-core-dataset-out protocol” that avoids any possibility of an information leak across augmented datasets. Specifically, we meta-train our methods on 34 out of the original 35 datasets, plus their augmented versions, and test on the held-out original dataset. We average the resulting performance over 35 outer loop iterations holding out a different core dataset each time. We further apply 5-fold inner cross-validation to optimally identify the best stopping epoch while monitoring validation performance. We evaluate each method (including the baselines) 10 times with different seeds and report averages, standard deviations, boxplots, and statistical tests over these 10 results.

For evaluation under the AutoDL benchmark, we upload our ZAP methods trained on the ZAP meta-dataset as well as the baselines to the submission board, made available to us by the challenge organizers. We report the performances on the five undisclosed final datasets of different domains (objects, aerial, people, medical, handwriting recognition) across 10 submissions. Here, we used the same hyperparameters from the ZAP benchmark.

5.3. Baselines

To assess the performance of our proposed method, we compare it against multiple baselines, which we describe here. Aside from a random selection of one of our 525 carefully designed DL pipelines, and the single best pipeline on average across the datasets, we chose the top-3 winners of the 2019 ChaLearn AutoDL Challenge: DeepWisdom, DeepBlueAI, and PASA NJU.

Given a novel dataset and our 525 selected DL pipelines, **random selection** uniformly samples one of these pipelines and **single-best** picks the one which performs best on average over \mathcal{D} . We average the random selection baseline over three random selections.

Table 2. Summary of winner techniques All contenders use ImageNet pre-trained networks and FAA denotes Fast AutoAugment.

Solution	Augmentation	ML technique
DeepWisdom	FAA	ResNet18/9 Meta-trained solution agents
DeepBlueAI	FAA	ResNet18 Adaptive ensemble learning
PASA NJU	Simple	ResNet18/SeResnext50 Data adaptive preprocessing

The challenge winner baselines build their methods on top of AutoCLINT (Baek et al., 2020), with the following modifications (summarized in Table 2):

- **DeepWisdom** initially caches mini-batches with a pre-trained ResNet-18 model and quickly switches to a pre-trained ResNet-9 by inputting cached batches first. They initialize the networks with ImageNet pre-trained parameters except for the batch normalization and bias layers. After an initial optimization phase, they turn on Fast AutoAugment (Lim et al.).
- **DeepBlueAI** initializes a pre-trained ResNet-18 network and adapts some of the model hyperparameters (image size, steps per epoch, epoch after which starting validating and fusing results, etc.) to the target dataset. They also ensemble the latest n predictions to stabilize them. Later in the procedure, they augment the dataset by Fast AutoAugment for a limited budget.
- **PASA NJU** pre-processes the data with a data-adaptive strategy by first sampling images to analyze. Then

they crop images to a standard shape and apply image flip augmentations. They start the training with a pre-trained ResNet-18 and switch to SeResNext-50 (Hu et al., 2017) when no further improvement is expected on the validation score.

5.4. Results on the ZAP Benchmark

In Figure 5, we depict the performance of our ZAP methods ZAP-AS and ZAP-HPO compared to the winner baselines of the AutoDL challenge. Our algorithm-selection-based ZAP-AS method already outperforms the competition winners, and our geometry-aware ranking-based model, ZAP-HPO, performs even significantly better.

In Table 3, we report the rank of the scores identifying the winners across the two main metrics. Our proposed method wins in both ALC score, i.e., the metric for which it was optimized, but also in terms of the normalized area under the curve (Normalized AUC).

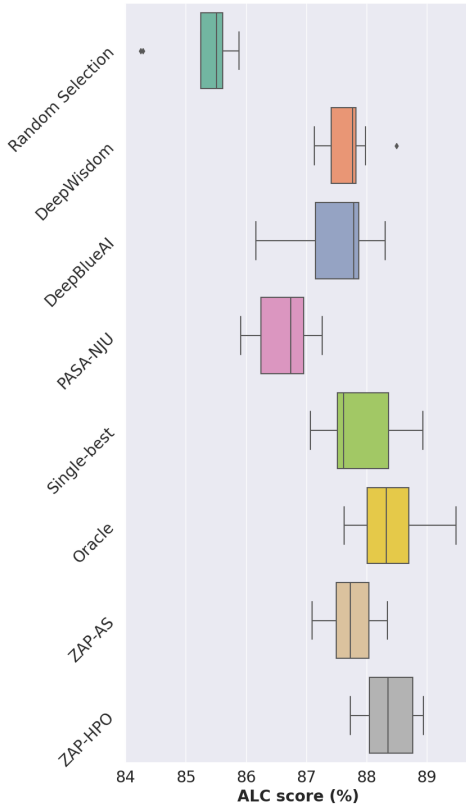


Figure 5. ALC scores of our approach vs. winner baselines over 525 datasets and 10 repetitions. Our ZAP methods clearly improve over the challenge winners (higher is better), by almost 1 point. Our geometry-aware zero-shot HPO version of ZAP with its binary pairwise ranking objective works best.

Table 3. Ranking our approach vs. winner baselines on the ZAP benchmark. We rank the solutions per test dataset and report average ranks over the 525 datasets (averages over 10 repetitions). ZAP clearly performs best (lower is better), both in terms of ALC (which it was optimized for) and also in terms of Normalized AUC.

Solution	Rank (ALC)	Rank(Normalized AUC)
DeepWisdom	2.53 ± 0.06	2.63 ± 0.03
DeepBlueAI	2.64 ± 0.04	2.73 ± 0.03
PASA NJU	2.76 ± 0.03	2.56 ± 0.03
ZAP-HPO	2.07 ± 0.05	2.08 ± 0.03

5.5. Results for a Sparsely-filled Cost Matrix

To further investigate the source of the gains in our model, we propose a more realistic setting, where the cost matrix includes missing values. While algorithm selection methods, such as ZAP-AS, require the dense cost matrix, our geometry-aware rank-based ZAP-HPO method handled missing values gracefully. To evaluate this quantitatively, next to ZAP-AS and ZAP-HPO with the full cost matrix, we also evaluate ZAP-HPO based on cost matrices that only have 75%, 50%, and 25% of the entries (dropped at random) remaining. As Figure 6 shows, ZAP-HPO’s performance loss due to missing entries is quite small, and even with only 25% remaining entries, it still performs similarly to ZAP-AS. We believe that ZAP-HPO’s low sensitivity to missing values stems from the capacity of the model to capture the correlation across the pipelines in the geometric space. It can hereby generalize well and “impute” missing values of the cost matrix. Furthermore, as shown in Table 4, even with missing values in the cost matrix, ZAP-HPO clearly outperforms the winners of the AutoDL competition.

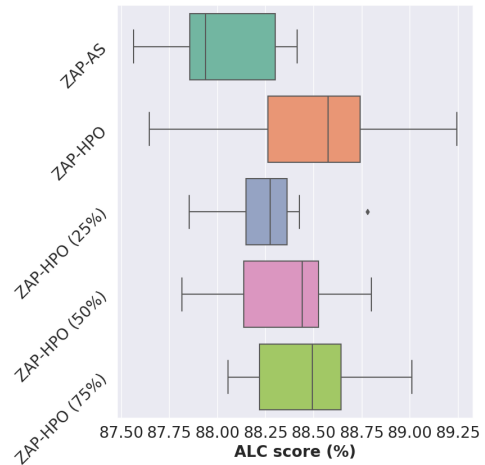


Figure 6. ALC scores of ZAP-HPO when meta-trained on a full (dense) vs. sparse cost matrix over 525 datasets and 10 repetitions. The density of the matrices are denoted as 75%, 50%, and 25%.

Table 4. The ranking of ZAP-HPO when optimized with a sparse cost matrix shows we still outperform the AutoDL challenge winner solutions.

Solution	75% filled	50% filled	25% filled
DeepWisdom	2.52 ± 0.06	2.52 ± 0.05	2.52 ± 0.05
DeepBlueAI	2.64 ± 0.05	2.64 ± 0.04	2.63 ± 0.04
PASA NJU	2.75 ± 0.03	2.75 ± 0.04	2.75 ± 0.04
ZAP-HPO (sparse)	2.09 ± 0.06	2.09 ± 0.05	2.10 ± 0.04

5.6. Results on the AutoDL Benchmark

In Table 5 we report the average rank performances for the AutoDL benchmark on the five undisclosed datasets across 10 submissions. We highlight that, unlike the winner baselines, we did not use the challenge feedback datasets to optimize the base model and zero-shot model hyperparameters for the final submission but reused (only) the ones from the ZAP benchmark. Due to a difference in distributions between these benchmarks, it cannot be taken for granted that our method generalizes to the AutoDL competition datasets. However, as Table 5 shows, ZAP-HPO clearly outperforms the winner baselines on this AutoDL setting. It also clearly outperforms the single-best and random baselines (which have ranks $2.7(\pm 0.1)$ and $3.42(\pm 0.68)$, respectively). In this setting of generalizing out of distribution, the more conservative ZAP-AS method performs even slightly better than ZAP-HPO, with average ranks of $1.81(\pm 0.3)$ vs. $2.16(\pm 0.15)$.

Table 5. Ranking our approach vs. winner baselines on the AutoDL benchmark. We rank the solutions per test dataset and report average ranks over the five AutoDL benchmark final datasets (averages over 10 submissions).

Solution	Rank (ALC)
DeepWisdom	2.46 ± 0.13
DeepBlueAI	2.76 ± 0.08
PASA NJU	2.62 ± 0.11
ZAP-HPO	2.16 ± 0.15

6. Conclusion

In this paper we extend the realm of AutoML to address the common problem of fine-tuning pre-trained Deep Learning (DL) models on new image classification datasets. Concretely, we focus on deciding which pre-trained model to use and how to set the many hyperparameters of the fine-tuning procedure, in a regime where strong anytime performance is essential. We formalize the problem as Zero-shot AutoML with Pre-trained Models (ZAP), which transfers knowledge from a meta-dataset of a number of DL pipelines

evaluated on a set of image datasets. In that context, we open-source the largest meta-dataset of evaluations for fine-tuning DL pipelines with 275K evaluated pipelines on 35 popular image datasets (2871 GPU days of compute). Furthermore, we propose two approaches for tackling ZAP: (i) formulating it as an instance of the algorithm selection (AS) problem and using AS methods, and (ii) a novel zero-shot hyperparameter optimization method trained with a ranking objective. Our methods clearly achieve the new state of the art in terms of anytime Automated Deep Learning (AutoDL) performance and significantly outperform all the solutions of the 2019 ChaLearn AutoDL Challenge.

7. Limitations

As mentioned before, computing the cost matrix is expensive. In particular, when training deep models, early optimization phases are often noisy and the final performance of a model is difficult to predict. Consequently, the accuracy of the cost matrix is directly coupled to the duration of the deep model training. Applying early-stopping methods to reduce the expenses of determining a cost matrix is thus challenging. Another limitation we observed is the sensitivity to the zero shot model’s hyperparameters. For example, we noticed that using a least-squares or a triplet margin objective performed significantly worse than our ZAP-HPO objective. Lastly, it is not clear a-priori which attributes best describe the DL pipelines in order to achieve the best performance and selecting a sub-optimal set may lead to a deterioration of performance.

Acknowledgements

This paper builds on and extends our original submission to the AutoDL challenge, and we are indebted to everyone who helped with that submission; in particular, we would like to thank Danny Stoll for his help on the initial hyperparameter configuration space design and data augmentation as well as Marius Lindauer for his help with AutoFolio. We also thank Dipti Sengupta for her help in reviewing both code and the paper. Moreover, we acknowledge funding by Robert Bosch GmbH, by the Deutsche Forschungsgemeinschaft (DFG, German Research Foundation) under grant number 417962828, by the state of Baden-Württemberg through bwHPC, and the German Research Foundation (DFG) through grant no INST 39/963-1 FUGG, by TAILOR, a project funded by the EU Horizon 2020 research, and innovation programme under GA No 952215, and by European Research Council (ERC) Consolidator Grant “Deep Learning 2.0” (grant no. 101045765). Funded by the European Union. Views and opinions expressed are however those of the author(s) only and do not necessarily reflect those of the European Union or the ERC. Neither the European Union nor the ERC can be held responsible for them.

References

Abadi, M., Agarwal, A., Barham, P., Brevdo, E., et al. TensorFlow: Large-scale machine learning on heterogeneous systems, 2015. URL <https://www.tensorflow.org/>.

Awad, N., Mallik, N., and Hutter, F. DEHB: Evolutionary hyperband for scalable, robust and efficient hyperparameter optimization. In *Proc. of IJCAI'21*, pp. 2147–2153, 2021.

Baek, W., Kim, I., Kim, S., and Lim, S. AutoCLINT: The Winning Method in AutoCV Challenge 2019. volume abs/2005.04373, 2020.

Bergstra, J. and Bengio, Y. Random search for hyperparameter optimization. 13:281–305, 2012.

Bischl, B., Kerschke, P., Kotthoff, L., Lindauer, M., Malitsky, Y., Frechette, A., Hoos, H., Hutter, F., Leyton-Brown, K., Tierney, K., and Vanschoren, J. ASlib: A benchmark library for algorithm selection. 237:41–58, 2016.

Chrzaszcz, P., Loshchilov, I., and Hutter, F. A downsampled variant of imagenet as an alternative to the cifar datasets. *arXiv preprint arXiv:1707.08819*, 2017.

Clanuwat, T., Bober-Irizar, M., Kitamoto, A., Lamb, A., Yamamoto, K., and Ha, D. Deep learning for classical Japanese literature, 2018.

Cohen, G., Afshar, S., Tapson, J., and Schaik, A. V. Emnist: Extending mnist to handwritten letters. *2017 International Joint Conference on Neural Networks (IJCNN)*, 2017. doi: 10.1109/ijcnn.2017.7966217.

Das, N., Reddy, J. M., Sarkar, R., Basu, S., Kundu, M., Nasipuri, M., and Basu, D. K. A statistical-topological feature combination for recognition of handwritten numerals. *Appl. Soft Comput.*, 12(8):2486–2495, August 2012a. ISSN 1568-4946. URL <http://dx.doi.org/10.1016/j.asoc.2012.03.039>.

Das, N., Sarkar, R., Basu, S., Kundu, M., Nasipuri, M., and Basu, D. K. A genetic algorithm based region sampling for selection of local features in handwritten digit recognition application. *Appl. Soft Comput.*, 12(5):1592–1606, May 2012b. URL <http://dx.doi.org/10.1016/j.asoc.2011.11.030>.

Deng, J., Dong, W., Socher, R., Li, L., Li, K., and Fei-Fei, L. ImageNet: A Large-Scale Hierarchical Image Database. In *Proc. of CVPR'09*, pp. 248–255, 2009.

Dumoulin, V., Houlsby, N., Evci, U., Zhai, X., Goroshin, R., Gelly, S., and Larochelle, H. Comparing transfer and meta learning approaches on a unified few-shot classification benchmark. *CoRR*, abs/2104.02638, 2021. URL <https://arxiv.org/abs/2104.02638>.

Elson, J., Douceur, J. J., Howell, J., and Saul, J. Asirra: A captcha that exploits interest-aligned manual image categorization. In *Proceedings of 14th ACM Conference on Computer and Communications Security (CCS)*. Association for Computing Machinery, Inc., October 2007.

Erickson, N., Mueller, J., Shirkov, A., Zhang, H., Larroy, P., Li, M., and Smola, A. Autogluon-tabular: Robust and accurate automl for structured data. *arXiv:2003.06505 [stat.ML]*, 2020.

Falkner, S., Klein, A., and Hutter, F. BOHB: Robust and efficient hyperparameter optimization at scale. In *Proc. of ICML'18*, pp. 1437–1446, 2018.

Feurer, M., Klein, A., Eggensperger, K., Springenberg, J., Blum, M., and Hutter, F. Efficient and robust automated machine learning. In *Proc. of NeurIPS'15*, pp. 2962–2970, 2015a.

Feurer, M., Springenberg, J., and Hutter, F. Initializing Bayesian hyperparameter optimization via meta-learning. In *Proc. of AAAI'15*, pp. 1128–1135, 2015b.

Finn, C., Abbeel, P., and Levine, S. Model-agnostic meta-learning for fast adaptation of deep networks. In Precup, D. and Teh, Y. W. (eds.), *Proceedings of the 34th International Conference on Machine Learning*, volume 70 of *Proceedings of Machine Learning Research*, pp. 1126–1135. PMLR, 06–11 Aug 2017.

Google. TensorFlow Datasets, a collection of ready-to-use datasets. <https://www.tensorflow.org/datasets>, 2021.

He, K., Zhang, X., Ren, S., and Sun, J. Deep residual learning for image recognition. *arXiv:1512.03385 [cs.CV]*, 2015.

Helber, P., Bischke, B., Dengel, A., and Borth, D. Eurosat: A novel dataset and deep learning benchmark for land use and land cover classification, 2017.

Howard, J. Imagenette. URL <https://github.com/fastai/imagenette/>.

Hu, J., Shen, L., and Sun, G. Squeeze-and-excitation networks. *CoRR*, abs/1709.01507, 2017.

Hutter, F., Hoos, H., and Leyton-Brown, K. Sequential model-based optimization for general algorithm configuration. In *Proc. of LION'11*, pp. 507–523, 2011.

Hutter, F., Kotthoff, L., and Vanschoren, J. (eds.). *Meta-Learning*, pp. 35–61. Springer International Publishing, 2020.

Zero-Shot AutoML with Pretrained Models

Jomaa, H. S., Arango, S. P., Schmidt-Thieme, L., and Grabocka, J. Transfer learning for bayesian hpo with end-to-end landmark meta-features. In *Fifth Workshop on Meta-Learning at the Conference on Neural Information Processing Systems*, 2021a.

Jomaa, H. S., Schmidt-Thieme, L., and Grabocka, J. Dataset2vec: Learning dataset meta-features. *Data Mining and Knowledge Discovery*, pp. 964–985, 2021b.

Kadioglu, S., Malitsky, Y., Sellmann, M., and Tierney, K. ISAC - instance-specific algorithm configuration. In *Proc. of ECAI'10*, pp. 751–756, 2010.

Kadioglu, S., Malitsky, Y., Sabharwal, A., Samulowitz, H., and Sellmann, M. Algorithm selection and scheduling. In *Proc. of CP'11*, pp. 454–469, 2011.

Kather, J. N., Weis, C.-A., Bianconi, F., Melchers, S. M., Schad, L. R., Gaiser, T., Marx, A., and Z’ollner, F. G. Multi-class texture analysis in colorectal cancer histology. *Scientific reports*, 6:27988, 2016.

Khosla, A., Jayadevaprakash, N., Yao, B., and Fei-Fei, L. Novel dataset for fine-grained image categorization. In *First Workshop on Fine-Grained Visual Categorization, CVPR'11*, 2011.

Kingma, D. and Ba, J. Adam: A method for stochastic optimization. In *Proc. of ICLR'15*, 2015.

Kolesnikov, A., Beyer, L., Zhai, X., Puigcerver, J., Yung, J., Gelly, S., and Houlsby, N. Big transfer (bit): General visual representation learning. In *Proc. of ECCV'20*, pp. 491–507, 2020.

Kotthoff, L., Gent, I., and Miguel, I. An evaluation of machine learning in algorithm selection for search problems. *25(3):257–270*, 2012.

Krause, J., Stark, M., Deng, J., and Fei-Fei, L. 3d object representations for fine-grained categorization. In *4th International IEEE Workshop on 3D Representation and Recognition (3dRR-13)*, Sydney, Australia, 2013.

Krizhevsky, A., Hinton, G., et al. Learning multiple layers of features from tiny images. 2009.

Krizhevsky, A., Sutskever, I., and Hinton, G. ImageNet classification with deep convolutional neural networks. In *Proc. of NeurIPS'12*, pp. 1097–1105, 2012.

Laadan, D., Vainshtein, R., Curiel, Y., Katz, G., and Rokach, L. Rankml: A meta learning-based approach for pre-ranking machine learning pipelines. *arXiv preprint arXiv:1911.00108*, 2019.

Lake, B. M., Salakhutdinov, R., and Tenenbaum, J. B. Human-level concept learning through probabilistic program induction. *Science*, 350(6266):1332–1338, 2015.

LeCun, Y., Cortes, C., and Burges, C. Mnist handwritten digit database. *ATT Labs [Online]. Available: http://yann.lecun.com/exdb/mnist*, 2, 2010.

Li, H., Chaudhari, P., Yang, H., Lam, M., Ravichandran, A., Bhotika, R., and Soatto, S. Rethinking the hyperparameters for fine-tuning. In *Proc. of ICLR'20*, 2020.

Li, L., Jamieson, K., DeSalvo, G., Rostamizadeh, A., and Talwalkar, A. Hyperband: Bandit-based configuration evaluation for hyperparameter optimization. In *Proc. of ICLR'17*, 2017.

Lim, S., Kim, I., Kim, T., Kim, C., and Kim, S. Fast AutoAugment.

Lindauer, M., Hoos, H., Hutter, F., and Schaub, T. Autofolio: Algorithm configuration for algorithm selection. In *Proc. of Workshops at AAAI'15*, 2015.

Liu, Z., Pavao, A., Xu, Z., Escalera, S., Ferreira, F., Guyon, I., Hong, S., Hutter, F., Ji, R., Junior, J. C. S. J., Li, G., Lindauer, M., et al. Winning solutions and post-challenge analyses of the chalearn autodl challenge 2019. In *TPAMI'21*, pp. 3108–3125, 2021.

Loshchilov, I. and Hutter, F. SGDR: Stochastic gradient descent with warm restarts. In *Proc. of ICLR'17*, 2017.

Loshchilov, I. and Hutter, F. Fixing weight decay regularization in adam. In *Proc. of ICLR'18*, 2018.

Malitsky, Y., Sabharwal, A., Samulowitz, H., and Sellmann, M. Algorithm portfolios based on cost-sensitive hierarchical clustering. In *Proc. of IJCAI'13*, pp. 608–614, 2013.

Moroney, L. Horses or humans dataset, feb 2019a. URL <http://laurencemoroney.com/horses-or-humans-dataset>.

Moroney, L. Rock, paper, scissors dataset, feb 2019b. URL <http://laurencemoroney.com/rock-paper-scissors-dataset>.

Mwebaze, E., Gebru, T., Frome, A., Nsumba, S., and Tusubira, J. icassava 2019fine-grained visual categorization challenge, 2019.

Nene, S. A., Nayar, S. K., Murase, H., et al. Columbia object image library (coil-20). 1996.

Nesterov, Y. A method of solving a convex programming problem with convergence rate $O(1/\sqrt{k})$. *Soviet Mathematics Doklady*, 27:372–376, 1983.

Zero-Shot AutoML with Pretrained Models

Netzer, Y., Wang, T., Coates, A., Bissacco, A., Wu, B., and Ng, A. Y. Reading digits in natural images with unsupervised feature learning. 2011.

Paszke, A., Gross, S., Massa, F., Lerer, A., et al. PyTorch: An imperative style, high-performance deep learning library. In *Proc. of NeurIPS'19*, pp. 8024–8035, 2019.

Perrone, V., Jenatton, R., Seeger, M., and Archambeau, C. Scalable hyperparameter transfer learning. In *Proc. of NeurIPS'18*, pp. 6845–6855, 2018.

Pineda-Arango, S., Jomaa, H. S., Wistuba, M., and Grabocka, J. HPO-B: A large-scale reproducible benchmark for black-box HPO based on openml. volume abs/2106.06257, 2021.

Radford, A., Kim, J. W., Hallacy, C., Ramesh, A., Goh, G., Agarwal, S., Sastry, G., Askell, A., Mishkin, P., Clark, J., et al. Learning transferable visual models from natural language supervision. In *Proc. of ICML'21*, pp. 8748–8763, 2021.

Rajaraman, S., Antani, S. K., Poostchi, M., Silamut, K., Hossain, M. A., Maude, R. J., Jaeger, S., and Thoma, G. R. Pre-trained convolutional neural networks as feature extractors toward improved malaria parasite detection in thin blood smear images. *PeerJ*, 6:e4568, 2018.

Rasmussen, C. and Williams, C. *Gaussian Processes for Machine Learning*. The MIT Press, 2006.

Rice, J. The algorithm selection problem. *Advances in Computers*, 15:65–118, 1976.

Russakovsky, O., Deng, J., Su, H., Krause, J., Satheesh, S., Ma, S., Huang, Z., Karpathy, A., Khosla, A., Bernstein, M., et al. Imagenet large scale visual recognition challenge. *International journal of computer vision*, 115(3): 211–252, 2015.

Salinas, D., Shen, H., and Perrone, V. A quantile-based approach for hyperparameter transfer learning. In *Proc. of ICML'20*, pp. 8438–8448, 2020.

Smith-Miles, K. Cross-disciplinary perspectives on meta-learning for algorithm selection. *ACM Computing Surveys*, 41(1):6:1–6:25, January 2009.

Snoek, J., Rippel, O., Swersky, K., Kiros, R., Satish, N., Sundaram, N., Patwary, M., Prabhat, and Adams, R. Scalable Bayesian optimization using deep neural networks. In *Proc. of ICML'15*, pp. 2171–2180, 2015.

Springenberg, J., Klein, A., Falkner, S., and Hutter, F. Bayesian optimization with robust Bayesian neural networks. In Lee, D., Sugiyama, M., von Luxburg, U., Guyon, I., and Garnett, R. (eds.), *Proc. of NeurIPS'16*, 2016.

Stoll, D. Icgen, 2020. URL <https://github.com/automl/ICGen>.

Sun, Q., Liu, Y., Chua, T.-S., and Schiele, B. Meta-transfer learning for few-shot learning. In *Proc. of CVPR'19*, pp. 403–412, 2019.

Tan, M. and Le, Q. EfficientNet: Rethinking model scaling for convolutional neural networks. In *Proc. of ICML'19*, pp. 6105–6114, 2019.

Team, T. T. Flowers, jan 2019. URL http://download.tensorflow.org/example_images/flower_photos.tgz.

Tornede, A., Wever, M., and Hüllermeier, E. Extreme algorithm selection with dyadic feature representation. In *Proc. of DS'20*, pp. 309–324, 2020.

Triantafillou, E., Zhu, T., Dumoulin, V., Lamblin, P., Xu, K., Goroshin, R., Swersky, C. G. K., Manzagol, P., and Larochelle, H. Meta-dataset: A dataset of datasets for learning to learn from few examples. *CoRR*, abs/1903.03096, 2019.

Vanschoren, J. Meta-learning: A survey. *CoRR*, abs/1810.03548, 2018.

Verma, V. K., Arora, G., Mishra, A., and Rai, P. Generalized zero-shot learning via synthesized examples. In *Proc. of CVPR'18*, pp. 4281–4289, 2018.

Verma, V. K., Brahma, D., and Rai, P. A meta-learning framework for generalized zero-shot learning. In *Proc. of AAAI'19*, pp. 6062–6069, 2019.

Wilson, A. G. and Ghahramani, Z. Copula Processes. In *Proc. of NeurIPS'10*, pp. 2460–2468, 2010.

Wilson, A. G., Hu, Z., Salakhutdinov, R., and Xing, E. P. Deep kernel learning. In *Proc. of AISTATS'16*, pp. 370–378, 2016.

Wilson, J., Hutter, F., and Deisenroth, M. Maximizing acquisition functions for Bayesian optimization. In *Proc. of NeurIPS'18*, pp. 741–749, 2018.

Winkelmolen, F., Ivkin, N., Bozkurt, H. F., and Karnin, Z. S. Practical and sample efficient zero-shot HPO. volume abs/2007.13382, 2020.

Wistuba, M. and Grabocka, J. Few-shot bayesian optimization with deep kernel surrogates. In *Proc. of ICLR'21*, 2021.

Wistuba, M., Schilling, N., and Schmidt-Thieme, L. Sequential Model-free Hyperparameter Tuning. In *Proc. of ICDM '15*, pp. 1033–1038, 2015.

Wistuba, M., Schilling, N., and Schmidt-Thieme, L. Two-stage transfer surrogate model for automatic hyperparameter optimization. In *Proc. of ECML/PKDD'16*, pp. 199–214, 2016.

Xian, Y., Lorenz, T., Schiele, B., and Akata, Z. Feature generating networks for zero-shot learning. In *Proc. of CVPR'18*, pp. 5542–5551, 2018.

Xiao, H., Rasul, K., and Vollgraf, R. Fashion-MNIST: a Novel Image Dataset for Benchmarking Machine Learning Algorithms. *CoRR*, abs/1708.07747, 2017.

Xu, L., Hutter, F., Hoos, H., and Leyton-Brown, K. SATzilla: Portfolio-based algorithm selection for SAT. 32:565–606, 2008.

Xu, L., Hutter, F., Hoos, H., and Leyton-Brown, K. Evaluating component solver contributions to portfolio-based algorithm selectors. In *Proc. of SAT'12*, pp. 228–241, 2012.

Yang, Y. and Newsam, S. Bag-of-visual-words and spatial extensions for land-use classification. In *ACM SIGSPATIAL International Conference on Advances in Geographic Information Systems (ACM GIS)*, 2010.

Zhai, X., Puigcerver, J., Kolesnikov, A., Ruyssen, P., et al. The Visual Task Adaptation Benchmark. *CoRR*, abs/1910.04867, 2019.

Zhu, J., Park, T., Isola, P., and Efros, A. A. Unpaired image-to-image translation using cycle-consistent adversarial networks. *CoRR*, abs/1703.10593, 2017.

Quick-Tune: Quickly Learning Which Pretrained Model to Finetune and How

The content of this chapter has been published as:

S. Pineda Arango, F. Ferreira, A. Kadra, F. Hutter, and J. Grabocka (2024). “Quick-Tune: Quickly Learning Which Pretrained Model to Finetune and How”. In: *Proceedings of the International Conference on Learning Representations (ICLR’24)*. Published online: iclr.cc. ICLR. URL: <https://iclr.cc/virtual/2024/oral/19719>.

The supplementary material and a detailed statement of contributions is provided in Appendix B.

QUICK-TUNE: QUICKLY LEARNING WHICH PRE-TRAINED MODEL TO FINETUNE AND HOW

Sebastian Pineda Arango, Fabio Ferreira, Arlind Kadra, Frank Hutter & Josif Grabocka

Department of Computer Science

University of Freiburg

pineda@cs.uni-freiburg.de

ABSTRACT

With the ever-increasing number of pretrained models, machine learning practitioners are continuously faced with the decision of which pretrained model to use, and how to finetune it for a new dataset. In this paper, we propose a methodology that jointly searches for the optimal pretrained model and the hyperparameters for finetuning it. Our method transfers knowledge about the performance of many pretrained models with multiple hyperparameter configurations on a series of datasets. To this aim, we evaluated over 20k hyperparameter configurations for finetuning 24 pretrained image classification models on 87 datasets to generate a large-scale meta-dataset. We meta-learn a gray-box performance predictor on the learning curves of this meta-dataset and use it for fast hyperparameter optimization on new datasets. We empirically demonstrate that our resulting approach can quickly select an accurate pretrained model for a new dataset together with its optimal hyperparameters. To facilitate reproducibility, we open-source our code and release our meta-dataset.¹.

1 INTRODUCTION

Transfer learning has been a game-changer in the machine learning community, as finetuning pretrained deep models on a new task often requires much fewer data instances and less optimization time than training from scratch (Liu et al., 2021; You et al., 2020). Researchers and practitioners are constantly releasing pretrained models of different scales and types, making them accessible to the public through model hubs (a.k.a. model zoos or model portfolios) (Schürholz et al., 2022; Ramesh & Chaudhari, 2022). This raises a new challenge, as practitioners must select which pretrained model to use and how to set its hyperparameters (You et al., 2021b), but doing so via trial-and-error is time-consuming and suboptimal.

In this paper, we address the resulting problem of quickly identifying the optimal pretrained model for a new dataset and its optimal finetuning hyperparameters. Concretely, we present **Quick-Tune**, a Combined Algorithm Selection and Hyperparameter Optimization (CASH) (Thornton et al., 2013) technique for finetuning, which jointly searches for the optimal model and its hyperparameters in a Bayesian optimization setup. Our technical novelty is based on three primary pillars: *i*) *gray-box hyperparameter optimization (HPO)* for exploring learning curves partially by few epochs and effectively investing more time into the most promising ones, *ii*) *meta-learning* for transferring the information of previous evaluations on related tasks, and *iii*) *cost-awareness* for trading off time and performance when exploring the search space. By utilizing these three pillars, our approach can efficiently uncover top-performing Deep Learning pipelines (i.e., combinations of model and hyperparameters).

In summary, we make the following contributions:

- We present an effective methodology for quickly selecting models from hubs and jointly tuning their hyperparameters.

¹<https://github.com/releaunifreiburg/QuickTune>

- We design an extensive search space that covers common finetuning strategies. In this space, we train and evaluate 20k model and dataset combinations to arrive at a large meta-dataset in order to meta-learn a gray-box performance predictor and benchmark our approach.
- We compare against multiple baselines, such as common finetuning strategies and state-of-the-art HPO methods, and show the efficacy of our approach by outperforming all of the competitor baselines.

2 RELATED WORK

Finetuning Strategies Finetuning resumes the training on a new task from the pretrained weights. Even if the architecture is fixed, the user still needs to specify various details, such as learning rate and weight decay, because they are sensitive to the difference between the downstream and upstream tasks, or distribution shifts (Li et al., 2020; Lee et al., 2022). A common choice is to finetune only the top layers can improve performance, especially when the data is scarce (Yosinski et al., 2014). Nevertheless, recent work proposes to finetune the last layer only for some epochs and subsequently unfreeze the rest of the network (Chen et al., 2019a; Wang et al., 2023), to avoid the distortion of the pretrained information. To reduce overfitting, some techniques introduce different types of regularization that operate activation-wise (Kou et al., 2020; Li et al., 2020; Chen et al., 2019b), parameter-wise (Li et al., 2018), or directly using data from the upstream task while finetuning (You et al., 2020; Zhong et al., 2020). No previous work studies the problem of jointly selecting the model to finetune and its optimal hyperparameters. Moreover, there exists no consensus on what is the best strategy to use or whether many strategies should be considered jointly as part of a search space.

Model Hubs It has been a common practice in the ML community to make large sets of pretrained models publicly available. They are often referred to as model hubs, zoos, or portfolios. In computer vision, in the advent of the success of large language models, a more recent trend is to release all-purpose models (Oquab et al., 2023; Radford et al., 2021; Kirillov et al., 2023) which aim to perform well in a broad range of computer vision tasks. Previous work has argued that a large pretrained model can be sufficient for many tasks and may only need little hyperparameter tuning (Kolesnikov et al., 2020). However, recent studies also show strong evidence that scaling the model size does not lead to a one-model-fits-all solution in computer vision (Abnar et al., 2022). Besides presenting more diversity and flexible model sizes for adapting to variable tasks and hardware, model hubs can be used for regularized finetuning (You et al., 2021a), learning hyper-networks for generating the weights (Schürholt et al., 2022), learning to ensemble different architectures (Shu et al., 2022), ensembling the weights of similar architectures (Wortsman et al., 2022b; Shu et al., 2021; Wortsman et al., 2022a), or selecting a suitable model from the pool (Cui et al., 2018; Bao et al., 2019; Tran et al., 2019a; Nguyen et al., 2020; You et al., 2021b; Bolya et al., 2021). Previous work using model hubs does not analyze the interactions between the used model(s) and the hyperparameters and how to set them efficiently.

HPO, Transfer HPO, and Zero-Shot HPO Several methods for Hyperparameter Optimization (HPO) have been proposed ranging from simple random search (Bergstra & Bengio, 2012a) to fitting surrogate models of true response, such as Gaussian processes (Rasmussen & Williams, 2006), random forests (Hutter et al., 2011), neural networks (Springenberg et al., 2016), hybrid techniques (Snoek et al., 2015), and selecting configurations that optimize predefined acquisition functions (Wilson et al., 2018). There also exist multi-fidelity methods that further reduce the wall-clock time necessary to arrive at optimal configurations (Li et al., 2017; Falkner et al., 2018a; Awad et al., 2021a; Shala et al., 2023a; Kadra et al., 2023). Transfer HPO can leverage knowledge from previous experiments to yield a strong surrogate model with few observations on the target dataset (Wistuba & Grabocka, 2021a; Pineda Arango & Grabocka, 2023; Shala et al., 2023b; Salinas et al., 2020). Methods that use meta-features, i.e., dataset characteristics that can be either engineered (Feurer et al., 2015; Wistuba et al., 2016) or learned (Jomaa et al., 2021), have also been proposed to warm-start HPO. Zero-shot HPO has emerged as an efficient approach that does not require any observations of the response on the target dataset, e.g. approaches that are model-free and use the average performance of hyperparameter configurations over datasets (Wistuba et al., 2015) or approaches that meta-learn surrogate models with a ranking loss (Khazi et al., 2023; Winkelmolen et al., 2020; Öztürk et al., 2022). In contrast to previous work, we propose to not only use the final

performance of configurations but to learn a Gaussian Process-based to predict the performance of partial learning curves as formulated by gray-box HPO approaches (Hutter et al., 2019).

3 MOTIVATION

Before introducing our method, we want to remind the reader about the importance of searching for the optimal pretrained neural network from a pool of models. Our main premise is that *there is no silver bullet model that fits all the finetuning tasks*. To illustrate this fact, we computed the error rates of a group of 24 efficient models (detailed in Section 5.1) from the *timm* library (Wightman, 2019) on all the 26 datasets of the *Extended* split of MetaAlbum (Ullah et al., 2022) (details in Section 5). For every model, we use its best per-dataset hyperparameter configuration found by a comprehensive HPO. Figure 1 shows the ranks of the 24 models for the 26 datasets, demonstrating that there is very little regularity. In particular, there exists no single model that ranks optimally on all datasets, even if we optimize its hyperparameters for each dataset. Since there exists no silver bullet model, and considering that there is a large number of pretrained models available in recent hubs, then *how can we quickly select the best model for a new dataset?*

4 QUICK-TUNE: COST-EFFICIENT FINETUNING

Following our motivation, we aim to find the best pipeline $x = \{m, \lambda\}, x \in \mathcal{X}$, within a search space $\mathcal{X} := \mathcal{M} \times \Lambda$ comprising a model hub $m \in \mathcal{M}$ and a set of hyperparameters $\lambda \in \Lambda$. In this section, we detail how we solve this problem efficiently in order to yield competitive anytime performance.

4.1 QUICK-TUNE

We follow an efficient Bayesian Optimization strategy to search for the optimal pipelines, in a similar style to recent state-of-the-art approaches in HPO (Wistuba & Grabocka, 2021b; Wistuba et al., 2022). At every iteration, our method Quick-Tune fits estimators that predict the performance of pipelines and their cost (for details, see Section 4.2). Then it uses an acquisition function (detailed in Section 4.3) to select the next pipeline to continue finetuning for an incremental number of epochs. Finally, our method evaluates the loss and the runtime cost and adds it to the history. This procedure is repeated until a time budget is reached. We formalize these steps in Algorithm 1, where we use the validation loss as a performance metric. The entire procedure is sped up by starting from a meta-learned surrogate as described in Section 4.4.

Algorithm 1: Quick-Tune Algorithm

Input: Search space of pipelines $x \in \mathcal{X}$, Epoch step Δt
Output: Pipeline with the smallest observed loss

- 1 Select randomly a pipeline $x' \in \mathcal{X}$ and evaluate it for Δt epochs ;
- 2 Initialize the history $\mathcal{H} \leftarrow \{(x', \Delta t, \ell(x', \Delta t), c(x', \Delta t))\}$
- 3 **while** budget **do**
- 4 Update the performance predictor $\hat{\ell}$ from \mathcal{H} using Equation 1;
- 5 Update the cost estimator \hat{c} from \mathcal{H} using Equation 2;
- 6 Select the next pipeline x^* using Equation 3;
- 7 Evaluate the performance $\ell(x^*, \tau(x^*))$ and measure the cost $c(x^*, \tau(x^*))$;
- 8 Update the history $\mathcal{H} \leftarrow \mathcal{H} \cup \{(x^*, \tau(x^*), \ell(x^*, \tau(x^*)), c(x^*, \tau(x^*)))\}$;
- 9 **end**
- 10 **return** $\arg \min_{x \in \mathcal{X}} \{\ell(x, t) \mid (x, t, \ell(x, t), \cdot) \in \mathcal{H}\}$;

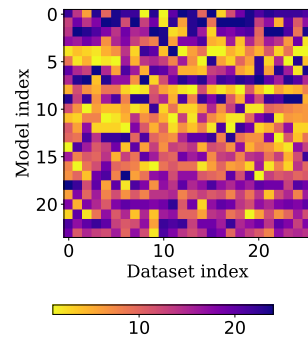


Figure 1: Ranks of model performances across datasets.

4.2 PERFORMANCE AND COST ESTIMATORS

Learning curves record the performance of Deep Learning pipelines at different time steps, such as the validation loss versus the number of epochs. The performance of the pipeline x at step t is denoted as $\ell(x, t)$, and the runtime cost for training the pipeline x until step t is $c(x, t)$. The history of all observed learning curves for n pipelines is denoted as $\mathcal{H} := \{(x_i, t_i, \ell(x_i, t_i), c(x_i, t_i))\}_{i=1}^n$.

Our method learns a probabilistic performance estimator (a.k.a. surrogate) defined as $\hat{\ell}(x, t; \theta)$ and parameterized with θ . We train the surrogate $\hat{\ell}$ to estimate the true performance ℓ from \mathcal{H} as:

$$\theta^* := \arg \min_{\theta} \mathbb{E}_{(x, t, \ell(x, t), \cdot) \sim \mathcal{H}} \left[-\log p(\ell(x, t) | x, t, \hat{\ell}(x, t; \theta)) \right]. \quad (1)$$

Concretely, the surrogate $\hat{\ell}$ is implemented as a deep-kernel Gaussian Process regressor (Wistuba & Grabocka, 2021a). In addition, we train a cost estimator $\hat{c}(x, t; \gamma)$ in the form of a Multilayer Perceptron with parameters γ to predict the ground truth costs as:

$$\gamma^* := \arg \min_{\gamma} \mathbb{E}_{(x, t, \cdot, c(x, t)) \sim \mathcal{H}} \left[c(x, t) - \hat{c}(x, t; \gamma) \right]^2. \quad (2)$$

4.3 COST-SENSITIVE ACQUISITION FUNCTION

We propose a cost-sensitive variant of the Expected Improvement (Jones et al., 1998) (EI) acquisition to select the next pipeline to evaluate within a Bayesian Optimization framework, defined as:

$$x^* := \arg \max_{x \in \mathcal{X}} \frac{\text{EI}(x, \mathcal{H}, \hat{\ell}(x, \tau(x)))}{\hat{c}(x, \tau(x)) - c(x, \tau(x) - \Delta t)} = \arg \max_{x \in \mathcal{X}} \frac{\mathbb{E}_{\hat{\ell}(x, \tau(x))} \left[\max(\ell_{\tau(x)}^{\min} - \hat{\ell}(x, \tau(x)), 0) \right]}{\hat{c}(x, \tau(x)) - c(x, \tau(x) - \Delta t)} \quad (3)$$

The numerator of Equation 3 introduces a mechanism that selects the pipeline x that has the largest likelihood to improve the lowest observed validation error at the next unobserved epoch $\tau(x)$ of pipeline x . The denominator balances out the cost of actually finetuning pipeline x for Δt epochs. $\tau(x)$ is defined for pipeline x as $\tau(x) := \max\{t' | (x, t', \cdot, \cdot) \in \mathcal{H}\} + \Delta t$, where Δt denotes the number of epochs to finetune from the last observed epoch in the history. If the pipeline is not in the history, the query epoch is $\tau(x) = \Delta t$. Simply put, if the validation loss of x is evaluated after every training epoch/step ($\Delta t = 1$) and has been evaluated for k epochs/steps, then $\tau(x) = k + 1$. As a result, we select the configuration with the highest chance of improving the best-measured loss at the next epoch, while trading off the cost of finetuning it. Concretely, the best observed loss is $\ell_{\tau(x)}^{\min} := \min(\{\ell(x, \tau(x)) | (x, \tau(x), \ell(x, \tau(x)), \cdot) \in \mathcal{H}\})$. If no pipeline has been evaluated until $\tau(x)$, i.e. $(x, \tau(x), \cdot, \cdot) \notin \mathcal{H}$, then $\ell_{\tau(x)}^{\min} := \min(\{\ell(x, t) | (x, t, \ell(x, t), \cdot) \in \mathcal{H}, t < \tau(x)\})$.

4.4 META-LEARNING THE PERFORMANCE AND COST ESTIMATORS

A crucial novelty of our paper is to meta-learn BO surrogates from existing pipeline evaluations on other datasets. Assume we have access to a set of curves for the validation errors ℓ and the runtimes c of pipelines over a pool of datasets, for a series of N epochs. We call the collection of such quadruple evaluations a meta-dataset $\mathcal{H}^{(M)} := \bigcup_{x \in \mathcal{X}} \bigcup_{d \in \mathcal{D}} \bigcup_{t \in [1, N]} \{(x, t, \ell(x, t, d), c(x, t, d))\}$, where we explicitly included the dependency of the performance and cost curves to the dataset. To contextualize the predictions on the characteristics of each dataset, we use descriptive features $d \in \mathcal{D}$ to represent each dataset (a.k.a. meta-features).

We meta-learn a probabilistic validation error estimator $\hat{\ell}(x, t, d; \theta)$, and a point-estimate cost predictor $\hat{c}(x, t, d; \gamma)$ from the meta-dataset $\mathcal{H}^{(M)}$ by solving the following objective functions:

$$\theta^{(M)} := \arg \min_{\theta} \mathbb{E}_{(x, t, \ell(x, t, d), c(x, t, d)) \sim \mathcal{H}^{(M)}} \left[-\log p \left(\ell(x, t, d) \mid x, t, d, \hat{\ell}(x, t, d; \theta) \right) \right] \quad (4)$$

$$\gamma^{(M)} := \arg \min_{\gamma} \mathbb{E}_{(x, t, \ell(x, t, d), c(x, t, d)) \sim \mathcal{H}^{(M)}} \left(c(x, t, d) - \hat{c}(x, t, d; \gamma) \right)^2 \quad (5)$$

After meta-learning, we use the learned weights to initialize the performance and cost predictors $\theta \leftarrow \theta^{(M)}$ and $\gamma \leftarrow \gamma^{(M)}$ before running Algorithm 1. As a result, our method starts with a strong prior for the performance of pipelines and their runtime costs, based on the collected history $\mathcal{H}^{(M)}$ from evaluations on prior datasets. We provide details about the meta-learning procedure in Algorithm 2 (Appendix A.3).

5 QUICK-TUNE META-DATASET

5.1 QUICK-TUNE SEARCH SPACE

While our proposed method is agnostic to the application domain, the set of pretrained models and hyperparameter space to choose from, we need to instantiate these choices for our experiments. In this paper, we focus on image classification and base our study on the *timm* library (Wightman, 2019), given its popularity and wide adoption in the community. It contains a large set of hyperparameters and pretrained models on ImageNet (more than 700). Concerning the space of potential finetuning hyperparameters, we select a subset of optimizers and schedulers that are well-known and used by researchers and practitioners. We also include regularization techniques, such as data augmentation and drop-out, since finetuning is typically applied in low data regimes where large architectures easily overfit. Additionally, we modified the framework to include common finetuning strategies, such as methods to select the percentage of layers to finetune (Yosinski et al., 2014), linear probing (Wang et al., 2023), stochastic norm (Kou et al., 2020), Co-Tuning (You et al., 2020), DELTA (Li et al., 2019), BSS (Chen et al., 2019b) and SP-regularization (Li et al., 2018). The last five methods are taken from the *transfer learning library* (Junguang Jiang & Long, 2020). Although we consider these well-known and stable finetuning strategies, we foresee the widespread adoption of new approaches such as LoRA (Hu et al., 2021). They are complementary to our method and can be easily interpreted as an extension of the pipeline search space. We list all the hyperparameters of our search space in Table 1, indicating explicitly the conditional hyperparameters with a "*". For a more detailed description of our search space, including the hyperparameter ranges and dependencies, we point the reader to Table 7 of Appendix B. As we are interested in time efficiency and accuracy, we select the Pareto optimal models from the large set of ca. 700 pretrained architectures in the *timm* library. Specifically, given a model $m \in \mathcal{M}_{\text{Timm}}$ with Top-1 ImageNet accuracy $f_{\text{ImageNet}}(m)$ and $S(m)$ number of parameters, we build our final model hub based on the multi-objective optimization among the predictive accuracy and model size by solving Equation 6. Subsequently, we obtain a set of 24 Pareto-optimal models as shown in Figure 2 and listed in Table 8 of Appendix B.

$$\mathcal{M} = \left\{ m^* \mid m^* \in \arg \max_{m \in \mathcal{M}_{\text{Timm}}} [f_{\text{ImageNet}}(m), -S(m)] \right\} \quad (6)$$

5.2 META-DATASET GENERATION

We created a large meta-dataset of evaluated learning curves based on the aforementioned search space. Overall, we finetuned the 24 Pareto-optimal pretrained models on 86 datasets for different hyperparameter configurations (details in Table 6, Appendix B.1). For every dataset, we sample hyperparameter configurations and models uniformly at random from the search space of Table 7.

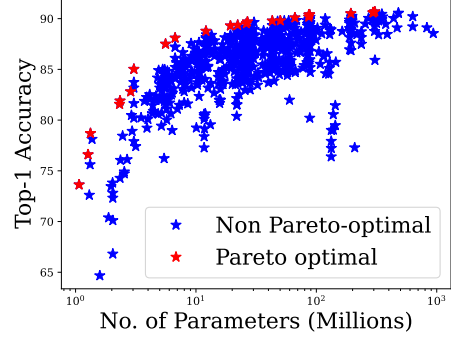


Figure 2: The subset of Pareto optimal pretrained models with respect to the predictive accuracy and model size.

Table 1: Search Space Summary.

Hyperparameter Group	Hyperparameters
Finetuning Strategies	Percentage of the Model to Freeze, Layer Decay, Linear Probing, Stochastic Norm, SP-Regularization, DELTA Regularization, BSS Regularization, Co-Tuning
Regularization Techniques	MixUp, MixUp Probability*, CutMix, Drop-Out, Label Smoothing, Gradient Clipping
Data Augmentation	Data Augmentation Type (Trivial Augment, Random Augment, Auto-Augment), Auto-Augment Policy*, Number of operations*, Magnitude*
Optimization	Optimizer type (SGD, SGD+Momentum, Adam, AdamW, AdamP), Beta-s*, Momentum*, Learning Rate, Warm-up Learning Rate, Weight Decay, Batch Size
Learning Rate Scheduling	Scheduler Type (Cosine, Step, Multi-Step, Plateau), Patience*, Decay Rate*, Decay Epochs*
Model	24 Models on the Pareto front (see Appendix 8)

In our experiments, we use the tasks contained in the Meta-Album benchmark (Ullah et al., 2022) since it contains a diverse set of computer vision datasets. The benchmark is released in three variants with an increasing number of images per dataset: *micro*, *mini*, and *extended*. Concretely, *micro* has computer vision tasks with fewer classes and fewer images per class than *extended*. When generating the learning curves, we limited each run to 50 training epochs. As setting a limit is challenging when considering a pool of models and tasks with different sizes, we decided to constrain the finetuning procedure using a global time limit. The configurations trained on the tasks from *micro*, *mini*, *extended* are finetuned for 1, 4, and 16 hours respectively, using a single NVIDIA GeForce RTX 2080 Ti GPU per finetuning task, amounting to a total compute time of 32 GPU months. We summarize the main characteristics of our generated data in Table 6 in the Appendix.

6 EXPERIMENTS AND RESULTS

6.1 QUICK-TUNE PROTOCOL

While Quick-Tune finds the best-pretrained models and their hyperparameters, it also has hyperparameters of its own: the architecture, the optimizer for the predictors, and the acquisition function. Before running the experiments, we aimed to design a single setup that easily applies to all the tasks. Given that we meta-train the cost and the performance predictor, we split the tasks per Meta-Album version into five folds $\mathcal{D} = \{\mathcal{D}_1, \dots, \mathcal{D}_5\}$ containing an equal number of tasks. When searching for a pipeline on datasets of a given fold \mathcal{D}_i , we consider one of the remaining folds for meta-validation and the remaining ones for meta-training. We used the meta-validation for early stopping when meta-training the predictors.

We tune the hyperparameters of Quick-Tune’s architecture and the learning rate using the *mini* version’s meta-validation folds. For the sake of computational efficiency, we apply the same discovered hyperparameters in the experiments involving the other Meta-Album versions. The chosen setup uses an MLP with 2 hidden layers and 32 neurons per layer, for both predictors. We use the Adam optimizer with a learning rate of 10^{-4} for fitting the estimators during the BO steps. We update their parameters for 100 epochs for every iteration from Algorithm 1. Further details on the set-up are specified in Appendix A.2. The inputs to the cost and performance estimators are the dataset metafeatures (Appendix A.4) and a pipeline encoding that concatenates a categorical embedding of the model m , an embedding of the observed curve $\tau(x)$ and the hyperparameters λ (details in Appendix A.5). Finally, for the acquisition function, we use $\Delta t = 1$ epoch as in previous work (Wistuba et al., 2022), since this allows us to discard bad configurations quickly during finetuning.

Table 2: Performance comparison for Hypothesis 1. Normalized regret, ranks and standard deviations are calculated across all respective Meta-Album (Ullah et al., 2022) subset datasets.

	Normalized Regret			Rank		
	Micro	Mini	Extended	Micro	Mini	Extended
BEiT+Default HP	0.229 ± 0.081	0.281 ± 0.108	0.225 ± 0.059	2.583 ± 0.829	2.611 ± 0.465	3.136 ± 0.215
XCiT+Default HP	0.223 ± 0.075	0.290 ± 0.107	0.199 ± 0.057	2.500 ± 0.751	2.694 ± 0.264	2.522 ± 0.344
DLA+Default HP	0.261 ± 0.074	0.325 ± 0.111	0.219 ± 0.076	3.062 ± 0.770	3.138 ± 0.248	2.977 ± 0.284
Quick-Tune	0.153 ± 0.054	0.139 ± 0.112	0.052 ± 0.031	1.854 ± 1.281	1.555 ± 0.531	1.363 ± 0.376

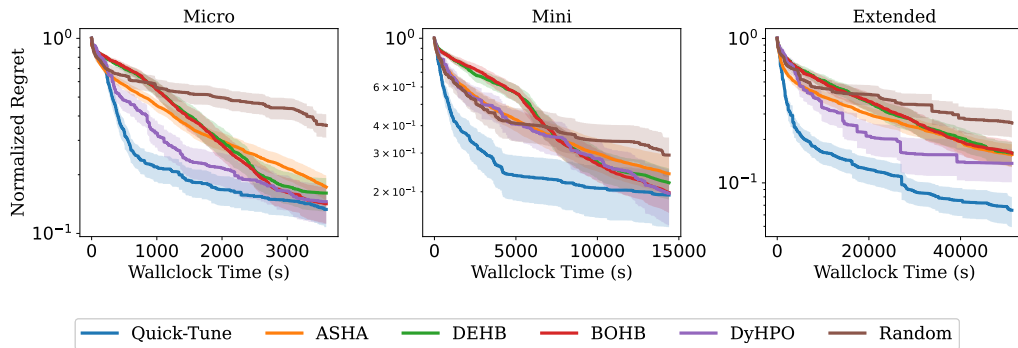


Figure 3: Comparison against state-of-the-art HPO methods.

6.2 RESEARCH HYPOTHESES AND ASSOCIATED EXPERIMENTS

HYPOTHESIS 1: QUICK-TUNE IS BETTER THAN FINETUNING MODELS WITHOUT HYPERPARAMETER OPTIMIZATION.

We argue that ML practitioners need to carefully tune the hyperparameters of pretrained models to obtain state-of-the-art performance. However, due to computational and time limitations, a common choice is to use default hyperparameters. To simulate the simplest practical use case, we select three different models from the subset of Pareto-optimal pretrained models (see Fig. 2), i.e. the largest model with the best accuracy (*beit_large_patch16_512* (Bao et al., 2022); 305M parameters, 90.69% acc.), the middle model with a competitive accuracy (*xcit_small_12_p8_384_dist* (Ali et al., 2021); 26M and 89.52%), as well as the smallest model with the lowest accuracy among the Pareto front models (*dla46x_c* (Yu et al., 2018); 1.3M and 72.61%). On each dataset in Meta-Album (Ullah et al., 2022), we finetune these models with their default hyperparameters and compare their performance against Quick-Tune. The default configuration is specified in Appendix B.2. To measure the performance, we calculate the average normalized regret (Arango et al., 2021), computed as detailed in Appendix A.1. For all Meta-Album datasets in a given category, we use the same finetuning time budget, i.e. 1 (*micro*), 4 (*mini*), and 16 (*extended*) hours. As reported in Table 2, Quick-Tune outperforms the default setups in terms of both normalized regret and rank across all respective subset datasets, demonstrating that HPO tuning is not only important to obtain high performance, but also achievable in low time budget conditions.

HYPOTHESIS 2: QUICK-TUNE OUTPERFORMS STATE-OF-THE-ART HPO OPTIMIZERS.

Gray-box approaches are considered very practical, especially for optimizing expensive architectures. We compare Quick-Tune against four popular gray-box optimizers, ASHA (Li et al., 2018), BOHB (Falkner et al., 2018b), DEHB (Awad et al., 2021b) and DyHPO (Wistuba et al., 2022). We additionally include Random Search (Bergstra & Bengio, 2012b) as a baseline for a sanity check. The normalized regret is computed for the three Meta-album versions on budgets of 1, 4 and 16 hours. The results of Figure 3 show that our proposed method has the best any-time performance compared to the baselines. In an additional experiment, presented in Figure 4, we show that both meta-training and cost-awareness aspects contribute to this goal by ablating each individual component. This

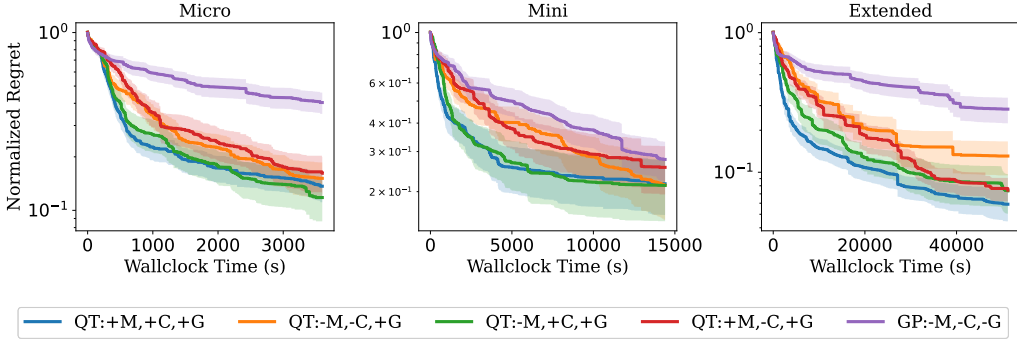


Figure 4: Comparing Quick-Tune with (+) and without (-) (M)eta-learning and (C)ost-Awareness, and (G)ray-box optimization. We also compare against DyHPO (=QT:-M,-C,+G) and a GP.

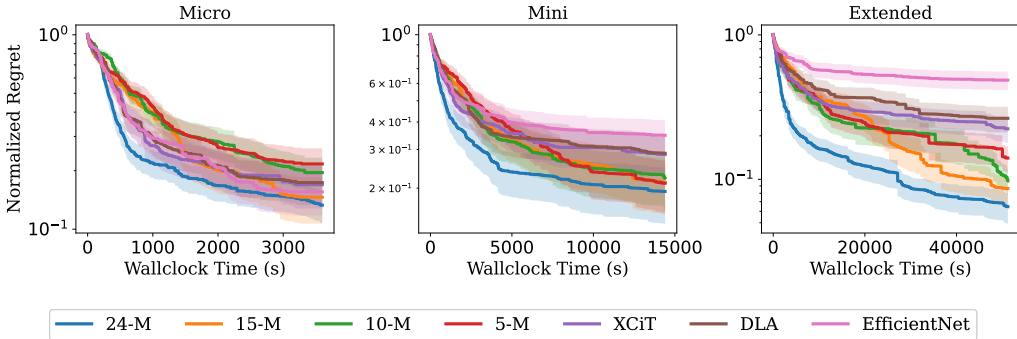


Figure 5: Varying the model hub size.

behavior is consistent among datasets of different sizes and present in all three meta-dataset versions. We attribute the search efficiency to our careful search space design, which includes both large and small models, as well as regularization techniques that reduce overfitting in low-data settings such as in the tasks of the *micro* version. In large datasets, our method finds good configurations even faster compared to the baselines, highlighting the importance of cost-awareness in optimizing hyperparameters for large datasets. We additionally compare against a Gaussian Process (GP) that observes the whole learning curve ($\Delta t = 50$), to highlight the necessity of a gray-box approach. In an additional experiment in Appendix C, we evaluate our method on the well-known Inaturalist (Horn et al., 2021) and Imagenette (Howard, 2019) datasets that are not contained in Meta-Album; there, our method still consistently outperforms the competitor baselines.

HYPOTHESIS 3: CASH ON DIVERSE MODEL HUBS IS BETTER THAN HPO ON A SINGLE MODEL.

A reasonable question is whether we actually need to consider a hub of models at all, or whether perhaps using a single, expressive, and well-tuned architecture is sufficient for most datasets. We hypothesize that the optimal model is dataset-specific because the complexities of datasets vary. Therefore, using a single model for all the datasets is a sub-optimal practice, and it is better to include a diverse model hub. Moreover, using a model hub allows us to explore cheap models first and gain information about the interactions between the hyperparameters. The information can in turn be leveraged by the predictors when considering larger and more accurate models.

To validate our hypothesis, we select *EfficientNet* (Tan & Le, 2019), *XCiT* (Ali et al., 2021) and *DLA* (Yu et al., 2018). These correspond to models with at least 10 evaluated curves in all the datasets and are located on the top, middle, and bottom regions in the Pareto front. Subsequently, we optimize their hyperparameters independently using our Quick-Tune algorithm. We also run Quick-Tune on subsets of 5, 10, and 15 models out of the model hub \mathcal{M} with 24 models. The subset of models was created randomly for every dataset before running BO. We execute the optimization on the three

Table 3: Comparison against efficient-finetuning of a single large model.

	4 Hours			24 Hours		
	Micro	Mini	Extended	Micro	Mini	Extended
Dinov2 + LoRA	0.541 ± 0.093	0.049 ± 0.018	0.055 ± 0.004	0.332 ± 0.095	0.014 ± 0.021	0.004 ± 0.012
Dinov2 + Linear Probing	0.081 ± 0.041	0.067 ± 0.021	0.081 ± 0.012	0.067 ± 0.038	0.017 ± 0.019	0.042 ± 0.011
QuickTune	0.072 ± 0.024	0.039 ± 0.014	0.042 ± 0.016	0.018 ± 0.012	0.012 ± 0.008	0.003 ± 0.008

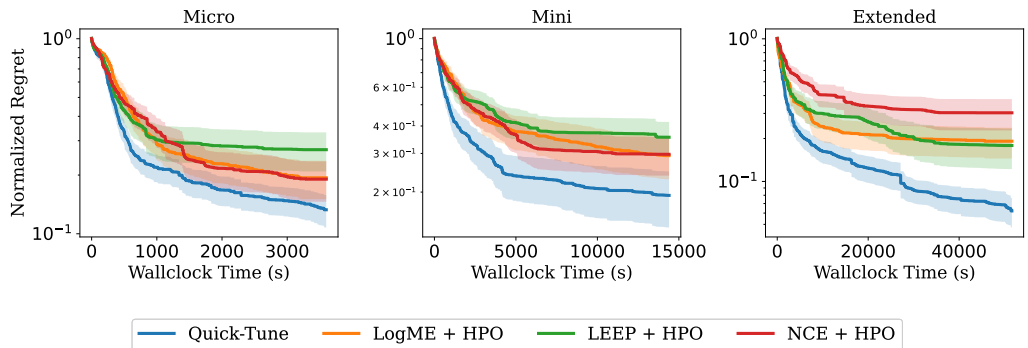


Figure 6: Comparison with a two-stage search for models and hyperparameters.

meta-dataset versions for 1, 2 and 4 hours of total budget. Figure 5 demonstrates that, in general, it is better to have a pool of diverse models such as 24 models (24-M) or 15 models (15-M), than tuning a small set of models or even a unique model. Interestingly, we note the larger the dataset is, the larger the model hub we need.

Quick-Tune vs. Efficient Finetuning of a Single Large Model. Although we propose to use model hubs, practitioners also have the alternative of choosing a large pretrained model from outside or inside the hub. We argue that a large pretrained model still demands HPO (Oquab et al., 2023), and imposes a higher load on computing capabilities. To demonstrate that Quick-Tune still outperforms the aforementioned approach, we compare our method against efficient finetuning approaches of Dinov2 which features 1B parameters by; *i*) finetuning only the last layer of Dino v2, which represents a common practice in the community, and *ii*) finetuning with LoRA (Hu et al., 2021), a parameter-efficient finetuning method. Our results in Table 3 demonstrate that CASH on model hubs via QuickTune attains better results for the different dataset versions.

Quick-Tune vs. Separated Model and Hyperparameter Optimization. We compare Quick-Tune with a two-stage alternative approach where, we first select a model with its default hyperparameters using state-of-the-art model selection methods, such as LogME (You et al., 2021a), LEEP (Nguyen et al., 2020) and NCE (Tran et al., 2019b). Then, we conduct a second search for the optimal hyperparameters of the model selected in the first stage. The results reported in Figure 6 show that Quick-Tune outperforms this two-stage approach, thus highlighting the importance of performing combined HPO and model selection.

7 CONCLUSION

We tackle the practical problem of selecting a model and its hyperparameters given a pool of models. Our method QuickTune leverages gray-box optimization together with meta-learned cost and performance predictors in a Bayesian optimization setup. We demonstrate that QuickTune outperforms common strategies for selecting pretrained models, such as using single models, large feature extractors, or conventional HPO tuning methods. In addition, we present empirical evidence that our method outperforms large-scale and state-of-the-art transformer backbones for computer vision. As a consequence, QuickTune offers a practical and efficient alternative for selecting and tuning pretrained models for image classification.

8 ACKNOWLEDGEMENT

Robert Bosch GmbH is acknowledged for financial support. We also acknowledge funding by the Deutsche Forschungsgemeinschaft (DFG, German Research Foundation) under SFB 1597 (Small-Data), grant number 499552394, the support of the BrainLinks- BrainTools Center of Excellence, and the funding of the Carl Zeiss foundation through the ReScaLe project. This research was also partially supported by the Deutsche Forschungsgemeinschaft (DFG, German Research Foundation) under grant number 417962828, by the state of Baden-Württemberg through bwHPC, and the German Research Foundation (DFG) through grant no INST 39/963-1 FUGG, by TAILOR, a project funded by the EU Horizon 2020 research, and innovation program under GA No 952215, and by European Research Council (ERC) Consolidator Grant “Deep Learning 2.0” (grant no. 101045765). Funded by the European Union. Views and opinions expressed are however those of the authors only and do not necessarily reflect those of the European Union or the ERC. Neither the European Union nor the ERC can be held responsible for them.



REFERENCES

S. Abnar, M. Dehghani, B. Neyshabur, and H. Sedghi. Exploring the limits of large scale pre-training. In *Proc. of ICLR'22*, 2022.

Alaaeldin Ali, Hugo Touvron, Mathilde Caron, Piotr Bojanowski, Matthijs Douze, Armand Joulin, Ivan Laptev, Natalia Neverova, Gabriel Synnaeve, Jakob Verbeek, et al. Xcit: Cross-covariance image transformers. *Advances in neural information processing systems*, 34:20014–20027, 2021.

Sebastian Pineda Arango, Hadi S. Jomaa, Martin Wistuba, and Josif Grabocka. Hpo-b: A large-scale reproducible benchmark for black-box hpo based on openml, 2021.

N. Awad, N. Mallik, and F. Hutter. DEHB: Evolutionary hyperband for scalable, robust and efficient Hyperparameter Optimization. In *Proc. of IJCAI'21*, pp. 2147–2153, 2021a.

Noor H. Awad, Neeratyoy Mallik, and Frank Hutter. DEHB: evolutionary hyperband for scalable, robust and efficient hyperparameter optimization. *CoRR*, abs/2105.09821, 2021b.

Hangbo Bao, Li Dong, Songhao Piao, and Furu Wei. Beit: BERT pre-training of image transformers. In *The Tenth International Conference on Learning Representations, ICLR 2022, Virtual Event, April 25-29, 2022*. OpenReview.net, 2022. URL <https://openreview.net/forum?id=p-BhZSz59o4>.

Y. Bao, Y. Li, S.-L. Huang, L. Zhang, L. Zheng, A. Zamir, and L. J. Guibas. An information-theoretic approach to transferability in task transfer learning. In *2019 IEEE International Conference on Image Processing, ICIP 2019, Taipei, Taiwan, September 22-25, 2019*, pp. 2309–2313. IEEE, 2019.

J. Bergstra and Y. Bengio. Random search for hyper-parameter optimization. 13:281–305, 2012a.

James Bergstra and Yoshua Bengio. Random search for hyper-parameter optimization. *J. Mach. Learn. Res.*, 13:281–305, 2012b.

D. Bolya, R. Mittapalli, and J. Hoffman. Scalable diverse model selection for accessible transfer learning. In *Proc. of NeurIPS'21*, pp. 19301–19312, 2021.

Wei-Yu Chen, Yen-Cheng Liu, Zsolt Kira, Yu-Chiang Frank Wang, and Jia-Bin Huang. A closer look at few-shot classification. *arXiv preprint arXiv:1904.04232*, 2019a.

X. Chen, S. Wang, B. F., M. Long, and J. Wang. Catastrophic forgetting meets negative transfer: Batch spectral shrinkage for safe transfer learning. In *Proc. of NeurIPS'19*, pp. 1906–1916, 2019b.

Y. Cui, Y. Song, C. Sun, A. Howard, and S. J. Belongie. Large scale fine-grained categorization and domain-specific transfer learning. In *Proc. of CVPR'18*, pp. 4109–4118, 2018.

S. Falkner, A. Klein, and F. Hutter. BOHB: Robust and efficient Hyperparameter Optimization at scale. In *Proc. of ICML'18*, pp. 1437–1446, 2018a.

Stefan Falkner, Aaron Klein, and Frank Hutter. BOHB: robust and efficient hyperparameter optimization at scale. In *Proceedings of the 35th International Conference on Machine Learning, ICML 2018, Stockholmsmässan, Stockholm, Sweden, July 10-15, 2018*, pp. 1436–1445, 2018b.

M. Feurer, J. Springenberg, and F. Hutter. Initializing Bayesian Hyperparameter Optimization via meta-learning. In *Proc. of AAAI'15*, pp. 1128–1135, 2015.

Grant Van Horn, Oisin Mac Aodha, and Serge Belongie. inaturalist competition datasets. https://github.com/visipedia/inat_comp, 2021.

Jermey Howard. Imagenette. <https://github.com/fastai/imagenette>, 2019.

Edward J. Hu, Yelong Shen, Phillip Wallis, Zeyuan Allen-Zhu, Yuanzhi Li, Shean Wang, and Weizhu Chen. Lora: Low-rank adaptation of large language models. *CoRR*, abs/2106.09685, 2021. URL <https://arxiv.org/abs/2106.09685>.

F. Hutter, H. Hoos, and K. Leyton-Brown. Sequential model-based optimization for general algorithm configuration. In *Proc. of LION'11*, pp. 507–523, 2011.

F. Hutter, L. Kotthoff, and J. Vanschoren (eds.). *Automated Machine Learning: Methods, Systems, Challenges*. Springer, 2019. Available for free at <http://automl.org/book>.

H. Jomaa, L. Schmidth-Thieme, and J. Grabocka. Dataset2vec: Learning dataset meta-features. *Data Mining and Knowledge Discovery*, 35:964–985, 2021.

Donald R. Jones, Matthias Schonlau, and William J. Welch. Efficient global optimization of expensive black-box functions. *J. of Global Optimization*, 13(4):455–492, dec 1998. ISSN 0925-5001.

Bo Fu Jinguang Jiang, Baixu Chen and Mingsheng Long. Transfer-learning-library. <https://github.com/thuml/Transfer-Learning-Library>, 2020.

Arlind Kadra, Maciej Janowski, Martin Wistuba, and Josif Grabocka. Scaling laws for hyperparameter optimization. In *Thirty-seventh Conference on Neural Information Processing Systems*, 2023. URL <https://openreview.net/forum?id=ghzEUGfRMD>.

A. S. Khazi, S. Pineda Arango, and J. Grabocka. Deep ranking ensembles for hyperparameter optimization. In *The Eleventh International Conference on Learning Representations*, 2023. URL https://openreview.net/forum?id=_ruvo2KCL2x.

A. Kirillov, E. Mintun, N. Ravi, H. Mao, C. Rolland, L. Gustafson, T. Xiao, S. Whitehead, A. C. Berg, W. Lo, P. Dollár, and R. Girshick. Segment anything. *arXiv:2304.02643*, 2023.

A. Kolesnikov, L. Beyer, X. Zhai, J. Puigcerver, J. Yung, S. Gelly, and N. Houlsby. Big transfer (bit): General visual representation learning. In *Proc. of ECCV'20*, pp. 491–507, 2020.

Z. Kou, K. You, M. Long, and J. Wang. Stochastic normalization. In *Proc. of NeurIPS'20*, 2020.

Y. Lee, A. S. Chen, F. Tajwar, A. Kumar, H. Yao, P. Liang, and C. Finn. Surgical fine-tuning improves adaptation to distribution shifts. *CoRR*, abs/2210.11466, 2022. URL <https://doi.org/10.48550/arXiv.2210.11466>.

H. Li, P. Chaudhari, H. Yang, M. Lam, A. Ravichandran, R. Bhotika, and S. Soatto. Rethinking the hyperparameters for fine-tuning. In *Proc. of ICLR'20*, 2020.

L. Li, K. Jamieson, G. DeSalvo, A. Rostamizadeh, and A. Talwalkar. Hyperband: Bandit-based configuration evaluation for Hyperparameter Optimization. In *Proc. of ICLR'17*, 2017.

X. Li, Y. Grandvalet, and F. Davoine. Explicit inductive bias for transfer learning with convolutional networks. In *Proc. of ICML'18*, pp. 2830–2839, 2018.

Xingjian Li, Haoyi Xiong, Hanchao Wang, Yuxuan Rao, Liping Liu, and Jun Huan. Delta: Deep learning transfer using feature map with attention for convolutional networks. In *7th International Conference on Learning Representations, ICLR 2019, New Orleans, LA, USA, May 6-9, 2019*. OpenReview.net, 2019. URL <https://openreview.net/forum?id=rkgbwsAcYm>.

B. Liu, Y. Cai, Y. Guo, and X. Chen. Transtailor: Pruning the pre-trained model for improved transfer learning. In *Proc. of AAAI'21*, pp. 8627–8634, 2021.

C. V. Nguyen, T. Hassner, M. W. Seeger, and Cédric Archambeau. LEEP: A new measure to evaluate transferability of learned representations. In *Proc. of ICML'20*, volume 119, pp. 7294–7305, 2020.

M. Oquab, T. Darcet, T. Moutakanni, H. V. Vo, M. Szafraniec, V. Khalidov, P. Fernandez, D. Haziza, F. Massa, A. El-Nouby, R. Howes, P.-Y. Huang, H. Xu, V. Sharma, S.-W. Li, W. Galuba, M. Rabbat, M. Assran, N. Ballas, G. Synnaeve, I. Misra, H. Jegou, J. Mairal, P. Labatut, A. Joulin, and P. Bojanowski. Dinov2: Learning robust visual features without supervision, 2023.

E. Öztürk, F. Ferreira, H. S. Jomaa, L. Scmidth-Thieme, J. Grabocka, and F. Hutter. Zero-shot automl with pretrained models. In *Proc. of ICML'22*, pp. 1128–1135, 2022.

Sebastian Pineda Arango and Josif Grabocka. Deep pipeline embeddings for automl. In *Proceedings of the 29th ACM SIGKDD Conference on Knowledge Discovery and Data Mining*, KDD '23, pp. 1907–1919, New York, NY, USA, 2023. Association for Computing Machinery. ISBN 9798400701030. doi: 10.1145/3580305.3599303. URL <https://doi.org/10.1145/3580305.3599303>.

A. Radford, J. Wook Kim, C. Hallacy, Aditya Ramesh, G. Goh, S. Agarwal, G. Sastry, A. Askell, P. Mishkin, J. Clark, G. Krueger, and I. Sutskever. Learning transferable visual models from natural language supervision, 2021.

R. Ramesh and P. Chaudhari. Model zoo: A growing brain that learns continually. In *Proc. of ICLR'22*, 2022.

C. Rasmussen and C. Williams. *Gaussian Processes for Machine Learning*. The MIT Press, 2006.

D. Salinas, H. Shen, and V. Perrone. A quantile-based approach for hyperparameter transfer learning. In *Proc. of ICML'20*, pp. 8438–8448, 2020.

David Salinas, Matthias Seeger, Aaron Klein, Valerio Perrone, Martin Wistuba, and Cedric Archambeau. Syne tune: A library for large scale hyperparameter tuning and reproducible research. In *International Conference on Automated Machine Learning, AutoML 2022*, 2022. URL <https://proceedings.mlr.press/v188/salinas22a.html>.

K. Schürholt, B. Knyazev, X. Giró-i Nieto, and D. Borth. Hyper-representations for pre-training and transfer learning. *CoRR*, abs/2207.10951, 2022.

K. Schürholt, D. Taskiran, B. Knyazev, X. Giró-i Nieto, and D. Borth. Model zoos: A dataset of diverse populations of neural network models. In *Thirty-Sixth Conference on Neural Information Processing Systems (NeurIPS) Track on Datasets and Benchmarks*, 2022.

G. Shala, A. Biedenkapp, F. Hutter, and J. Grabocka. Gray-box gaussian processes for automated reinforcement learning. In *ICLR 2023*, 2023a. URL <https://openreview.net/forum?id=rmoMvpTXK7M>.

G. Shala, T. Elsken, F. Hutter, and J. Grabocka. Transfer NAS with meta-learned bayesian surrogates. In *ICLR 2023*, 2023b. URL <https://openreview.net/forum?id=paGvsrl4Ntr>.

Y. Shu, Z. Kou, Z. Cao, J. Wang, and M. Long. Zoo-tuning: Adaptive transfer from A zoo of models. In *Proc. of ICML'21*, volume 139, pp. 9626–9637, 2021.

Y. Shu, Z. Cao, Z. Zhang, J. Wang, and M. Long. Hub-pathway: Transfer learning from A hub of pre-trained models. 2022.

J. Snoek, O. Rippel, K. Swersky, R. Kiros, N. Satish, N. Sundaram, M. Patwary, Prabhat, and R. Adams. Scalable Bayesian optimization using deep neural networks. In *Proc. of ICML'15*, pp. 2171–2180, 2015.

J. Springenberg, A. Klein, S. Falkner, and F. Hutter. Bayesian optimization with robust Bayesian neural networks. In D. Lee, M. Sugiyama, U. von Luxburg, I. Guyon, and R. Garnett (eds.), *Proc. of NeurIPS'16*, 2016.

Mingxing Tan and Quoc V. Le. Efficientnet: Rethinking model scaling for convolutional neural networks. In Kamalika Chaudhuri and Ruslan Salakhutdinov (eds.), *Proceedings of the 36th International Conference on Machine Learning, ICML 2019, 9–15 June 2019, Long Beach, California, USA*, volume 97 of *Proceedings of Machine Learning Research*, pp. 6105–6114. PMLR, 2019. URL [http://proceedings.mlr.press/v97/tan19a.html](https://proceedings.mlr.press/v97/tan19a.html).

C. Thornton, F. Hutter, H. Hoos, and K. Leyton-Brown. Auto-WEKA: combined selection and Hyperparameter Optimization of classification algorithms. In *Proc. of KDD'13*, pp. 847–855, 2013.

A. T. Tran, C. V. Nguyen, and T. Hassner. Transferability and hardness of supervised classification tasks. In *Proc. of ICCV'19*, pp. 1395–1405. IEEE, 2019a.

Anh T Tran, Cuong V Nguyen, and Tal Hassner. Transferability and hardness of supervised classification tasks. In *Proceedings of the IEEE/CVF International Conference on Computer Vision*, pp. 1395–1405, 2019b.

Ihsan Ullah, Dustin Carrion, Sergio Escalera, Isabelle M Guyon, Mike Huisman, Felix Mohr, Jan N van Rijn, Haozhe Sun, Joaquin Vanschoren, and Phan Anh Vu. Meta-album: Multi-domain meta-dataset for few-shot image classification. In *Thirty-sixth Conference on Neural Information Processing Systems Datasets and Benchmarks Track*, 2022. URL <https://meta-album.github.io/>.

H. Wang, T. Yue, X. Ye, Z. He, B. Li, and Y. Li. Revisit finetuning strategy for few-shot learning to transfer the emdeddings. In *The Eleventh International Conference on Learning Representations*, 2023.

Ross Wightman. Pytorch image models. <https://github.com/rwightman/pytorch-image-models>, 2019.

J. Wilson, F. Hutter, and M. Deisenroth. Maximizing acquisition functions for Bayesian optimization. In *Proc. of NeurIPS'18*, pp. 741–749, 2018.

F. Winkelmolen, N. Ivkin, H. Bozkurt, and Z. Karnin. Practical and sample efficient zero-shot HPO. *arXiv:2007.13382 [stat.ML]*, 2020.

M. Wistuba and J. Grabocka. Few-shot bayesian optimization with deep kernel surrogates. In *Proc. of ICLR'21*, 2021a.

M. Wistuba, N. Schilling, and L. Schmidt-Thieme. Sequential Model-free Hyperparameter Tuning. In *Proc. of ICDM '15*, pp. 1033–1038, 2015.

M. Wistuba, N. Schilling, and L. Schmidt-Thieme. Two-stage transfer surrogate model for automatic Hyperparameter Optimization. In *Proc. of ECML/PKDD'16*, pp. 199–214, 2016.

M. Wistuba, A. Kadra, and J. Grabocka. Supervising the multi-fidelity race of hyperparameter configurations. In *Proc. of NeurIPS'22*, 2022.

Martin Wistuba and Josif Grabocka. Few-shot bayesian optimization with deep kernel surrogates. In *9th International Conference on Learning Representations, ICLR 2021, Virtual Event, Austria, May 3-7, 2021*, 2021b.

M. Wortsman, G. Ilharco, S.r Yitzhak Gadre, R. Roelofs, R. Gontijo Lopes, A. S. Morcos, H. Namkoong, A. Farhadi, Y. Carmon, S. Kornblith, and L. Schmidt. Model soups: averaging weights of multiple fine-tuned models improves accuracy without increasing inference time. In *Proc. of ICML'22*, volume 162, pp. 23965–23998, 2022a.

M. Wortsman, G. Ilharco, J. W. Kim, M. Li, S. Kornblith, R. Roelofs, R. G. Lopes, H. Hajishirzi, A. Farhadi, H. Namkoong, and L. Schmidt. Robust fine-tuning of zero-shot models. In *Proc. of CVPR'22*, pp. 7949–7961, 2022b.

J. Yosinski, J. Clune, Y. Bengio, and H. Lipson. How transferable are features in deep neural networks? In *Proc. of NeurIPS'14*, pp. 3320–3328, 2014.

K. You, Z. Kou, M. Long, and J. Wang. Co-tuning for transfer learning. In *Proc. of NeurIPS'20*, pp. 17236–17246, 2020.

K. You, Y. Liu, J. Wang, M. I. Jordan, and M. Long. Ranking and tuning pre-trained models: A new paradigm of exploiting model hubs. *CoRR*, abs/2110.10545, 2021a. URL <https://arxiv.org/abs/2110.10545>.

K. You, Y. Liu, J. Wang, and M. Long. Logme: Practical assessment of pre-trained models for transfer learning. In *Proc. of ICML'21*, pp. 12133–12143, 2021b.

Fisher Yu, Dequan Wang, Evan Shelhamer, and Trevor Darrell. Deep layer aggregation. In *Proceedings of the IEEE conference on computer vision and pattern recognition*, pp. 2403–2412, 2018.

J. Zhong, X. Wang, Z. Kou, J. Wang, and M. Long. Bi-tuning of pre-trained representations. *arXiv preprint arXiv:2011.06182*, 2020.

Quick-Tune-Tool: A Practical Tool and its User Guide for Automatically Finetuning Pretrained Models

The content of this chapter has been published as:

I. Rapant, L. Purucker, F. Ferreira, S. P. Arango, A. Kadra, J. Grabocka, and F. Hutter (2024). “Quick-Tune-Tool: A Practical Tool and its User Guide for Automatically Finetuning Pretrained Models”. In: *Third International Conference on Automated Machine Learning - Workshop Track*. Ed. by M. Lindauer, K. Eggensperger, R. Garnett, J. Vanschoren, and J. Gardner. URL: <https://openreview.net/forum?id=d0Hapti3Uc>.

The supplementary material and a detailed statement of contributions is provided in Appendix C.

Quick-Tune-Tool: A Practical Tool and its User Guide for Automatically Finetuning Pretrained Models

Ivo Rapant¹ Lennart Purucker¹ Fabio Ferreira¹ Sebastian Pineda Arango¹ Arlind Kadra¹
Josif Grabocka² Frank Hutter^{3, 1}

¹University of Freiburg

²University of Technology Nuremberg

³ELLIS Institute Tübingen

Abstract Pretrained models have become essential tools for machine learning practitioners across various domains, including image classification, segmentation, and natural language processing. However, the complexity of selecting the appropriate pretrained model and finetuning strategy remains a significant challenge. In this paper, we present Quick-Tune-Tool, an automated solution to guide practitioners in selecting and finetuning pretrained models. Leveraging the Quick-Tune algorithm, Quick-Tune-Tool abstracts intricate research-level code into a user-friendly tool. Our contributions include the release of Quick-Tune-Tool, a detailed architectural overview, a user guide for image classification, and empirical evaluations. In experiments on four vision datasets, our results underscore the effectiveness and practicality of Quick-Tune-Tool for automating model selection and finetuning.

1 Introduction

Pretrained models are well-performing solutions for many machine learning practitioners for an expanding amount of domains from image classification (Caron et al., 2021), image segmentation (Kirillov et al., 2023), natural language processing (Qiu et al., 2020), time series (Liang et al., 2024), to tabular data (Hollmann et al., 2023). As a result, pretrained models are constantly being published on model hubs such as Hugging Face¹ or in the *timm* library (Wightman, 2019).

A challenge with this practice is that the multitude of pretrained models poses a substantial complexity for machine learning practitioners; prompting hard-to-answer questions such as *which* pretrained model to use and *how*. For instance, a practitioner in the domain of image classification must choose between one of the more than 700 pretrained models in the *timm* library. Afterwards, the practitioner must optimize the model for their application by *also* selecting a finetuning strategy and its hyperparameters, such as the regularization technique or learning rate schedule.

Our overarching goal is to automate the process of *which* pretrained model to use and *how* for *practitioners in any domain*. Therefore, in this paper, we present Quick-Tune-Tool, the first step towards our goal. For this, we adopt the recently proposed Quick-Tune algorithm (Arango et al., 2023) and both abstract and elevate it from research-level code to a practitioner’s tool with a strong focus on usability. We intentionally abstracted and optimized Quick-Tune-Tool for future adaptation to new domains. The first version, presented in this work, is already a user-friendly, broadly accessible, and easy-to-install tool for practitioners in the domain of image classification.

Our contribution. As part of this paper, we: (A) publish the first version of Quick-Tune-Tool², (B) present its architecture and design principles, (C) provide a user-guide to do image classification in 3 lines of code, and (D) perform experiments showing that Quick-Tune-Tool is easy to use and outperforms random search on 4 image classification datasets.

¹<https://huggingface.co/posts>

²<https://github.com/automl/QTTool>

2 Background and Related Work

Finetuning Tools. To leverage pretrained models, the research literature has proposed a large set of methods such as Co-Tuning (You et al., 2020) or SP Regularization (Li et al., 2018) for finetuning. Unfortunately, most of this work does not translate into maintained, easy-to-use code that can be readily applicable in the industry. The development of finetuning tools allows us to close the gap between researchers and practitioners, facilitating the application of the research findings in production use cases. The *Transfer Learning Library* (Jiang et al., 2020) builds a collection of finetuning strategies for computer vision, streamlining testing methods on new datasets. The *PEFT library* (Mangrulkar et al., 2022) encapsulates different state-of-the-art approaches for parameter efficient finetuning such as Adapters or LoRA (Hu et al., 2022), and integrates with Hugging Face Hub. Finally, *TorchTune* (Pytorch, 2024) provides a command line interface for finetuning models natively using the Torch backend while offering a tool that is easy to integrate. However, none of these tools natively offer a way to select the model and hyperparameters to use, thus leaving it to their users to determine which pretrained model to use and how.

AutoML Systems. The diversity of datasets and tasks requires the use of automated machine learning (AutoML) systems to automatically select the best model with the best hyperparameters for a given task without incurring manual trial-and-error. For deep learning, tools such as *AutoKeras* (Jin et al., 2019), *AutoPytorch* (Zimmer et al., 2021), or *NePS* (Stoll et al., 2023) allow users to automatically search for hyperparameter configurations of neural networks; typically tailored to optimizing the architecture or (pre-)training but not finetuning of neural networks. In contrast, *AutoGluon MultiModal* (Tang et al., 2024) offers support for finetuning foundation models for different multimodal tasks, such as Classification, Regression, or Image Segmentation, by evaluating a pre-defined portfolio of hyperparameters and models. Lastly, the AutoML system *ZAP* (Öztürk et al., 2022), addresses the finetuning and hyperparameter search problem by leveraging an algorithm selection perspective to find appropriate finetuning hyperparameters and pretrained models through the abstraction of deep learning pipelines.

QuickTune Method. *QuickTune* (Arango et al., 2023) uses a probabilistic performance predictor $\hat{\ell}_\theta$ and a cost predictor \hat{c}_w to select the pipeline $x \in \mathcal{X}$ to finetune for Δt epochs after resuming from the checkpoint at epoch t (Equation 1). Thus, it balances the Multi-fidelity Expected Improvement (Wistuba et al., 2022) with the actual cost of finetuning. Information from auxiliary tasks is included by meta-learning the parameters θ and w . *QuickTune* selects the pipeline x from a search space \mathcal{X} containing different combinations of hyperparameters and pretrained models. These combinations are fed into the predictors using MLP encoders (Pineda Arango and Grabocka, 2023). Specifically, the authors applied the method on Computer vision tasks from the *Meta-Album* collection (Ullah et al., 2022) using the model Hub contained in *Timm library* (Wightman, 2019). In the search space design, they included different finetuning strategies. However, the method is task-agnostic and can be easily adapted to other data modalities or search spaces.

$$x \in \operatorname{argmax}_{x \in \mathcal{X}} \frac{\text{EI}_{\text{MF}}(x, t + \Delta t, \hat{\ell}_\theta)}{\hat{c}_w(x, t + \Delta t)} \quad (1)$$

Overview. We summarize the position of Quick-Tune-Tool in the area of ML in Appendix A.

3 Quick-Tune-Tool: A Practical Tool For Finetuning Pretrained Models

The architecture of our tool is composed of four main components: QuickTuner, ConfigManager, Optimizer, and the Objective Function. These components work together to provide a comprehensive solution for selecting a finetuning pipeline, i.e. a pretrained model from a Model hub and its finetuning hyperparameters from a search space. We provide an overview of the architecture in Figure 1 and describe each component in detail in the remainder of this section.

In summary, using Quick-Tune-Tool starts by defining the search space and having the ConfigManager generate initial configurations. QuickTuner then employs the Optimizer to suggest configurations based on previous evaluations, e.g. History. Next, the Objective Function evaluates these configurations and returns results of performance metrics. Finally, QuickTuner saves these results, updates the Optimizer, and repeats the cycle until the time budget is exhausted.

QuickTuner. The tuner is the core component that organizes the optimization process by integrating all components, managing environment setup, interacting with the optimizer, invoking the objective function, saving intermediate results, and ensuring experiment continuity.

ConfigManager. The ConfigManager, as the name suggests, manages the configurations and processes them to be input to the optimizer. It takes a configuration space as input, i.e., the pipeline search space over which the optimization is performed. We use ConfigSpace (Lindauer et al., 2019) to define the search space.

Optimizer. The optimizer component can implement various optimization methods. Its main task is to interact with the tuner to suggest the next configuration to evaluate. Currently, we provide the *QuickTune* optimizer (Arango et al., 2023) and additionally, a basic random-search optimizer. To ensure flexibility and extensibility, any optimization method can be easily added, as long as it adheres to the interface requirements of the QuickTuner, e.g. a Bayesian optimization method like BOHB (Falkner et al., 2018), DPL (Kadra et al., 2024) or ifBO (Rakotoarison et al., 2024), or evolutionary based like DEHB (Awad et al., 2021).

Objective Function. The Objective Function is invoked by the tuner during optimization. It can be any function that accepts configuration, budget, and optional task-related information. It returns results as a dictionary or a list of dictionaries. For efficiency, it should manage interrupted training by saving and loading models. Existing training scripts can be adapted to work with Quick-Tune-Tool if they adhere to the interface in Figure 2 and return results as shown in Figure 3.

Quick-Tune-Tool Already Supports Image Classification OOTB. We designed Quick-Tune-Tool to be abstract and provide an interface for fine-tuning in any domain or application. To test this interface in its first version, we implemented support for using Quick-Tune-Tool for image classification. Moreover, we plan to extend it to other domains in the future. In detail, for image classification, Quick-Tune-Tool provides three pretrained optimizers, meta-learned on learning curves from different Meta-Album versions: *micro*, *mini*, and *extended*. Moreover, we

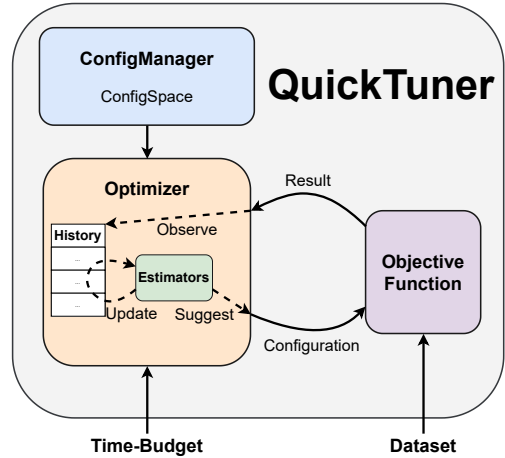


Figure 1: Quick-Tune-Tool Architecture.

```
def objective_function(
    config: dict,
    task_info: dict | None,
) -> dict | list[dict]:
    # 1. setup
    # 2. run objective
    # 3. evaluate model
    # 4. collect results
    return result
```

Figure 2: Objective Function.

```
{
    "config_id": 42,
    "score": 0.99,
    "cost": 123.45,
    "fidelity": 1,
    "status": True,
}
```

Figure 3: Result Dict.

provide a search space (see Table 3 in Appendix) and a connection to a model hub (Table 4). Thus, Quick-Tune-Tool can be applied to solve new image classification problems out-of-the-box.

4 A User Guide for Quick-Tune-Tool

To showcase the proposed Quick-Tune-Tool, we now present its exemplary usage for image classification. Figure 4 shows a basic use of Quick-Tune-Tool with the pretrained optimizer in the *micro* benchmark. The user only has to adapt the path to the custom dataset where the images have to be in PyTorch’s ImageFolder format (Figure 7 in Appendix).

```
from qtt import QuickTuner, get_pretrained_optimizer
from qtt.finetune.cv.classification import finetune_script

task_info, metafeat = extract_task_info_metafeat("path/to/dataset")
optimizer = get_pretrained_optimizer("mtlbtm/micro")
optimizer.setup(128, metafeat) # number of configs
qt = QuickTuner(optimizer, finetune_script)
qt.run(task_info, time_budget=3600)
```

Figure 4: A simple example of using the Quick-Tune-Tool.

1. **Get the Optimizer.** The *get_pretrained_optimizer* method is designed to retrieve an optimizer based on specified parameters. Currently, QuickTuneTool includes three pretrained optimizers, which can be accessed using "mtlbtm/micro", "mtlbtm/mini" and "mtlbtm/extended". This command will load the optimizer along with its associated search space and *ConfigManager*, constructing it for use with QuickTuner.
2. **Create QuickTuner Object With the Finetuning Script.** The finetune script serves as the objective function for QuickTuner. We provide a script for image classification, which takes a configuration as input and manages all aspects of running evaluations, like downloading pretrained weights, saving and loading models, and returning results.
3. **Fit the QuickTuner** The tuner handles the setup and correct flow of the optimization process. We only have to pass the optimizer and an objective function. Optionally, one can specify an output path and the logger verbosity. We start the optimization with *QuickTuner.run()*, we can additionally pass a dictionary with parameters that deviate from default. Depending on the size of the dataset, the fitting can take a few hours. Optionally, we can speed up the training by specifying a time limit and / or fixing the number of evaluations. For example, *qt.fit(..., time_limit=3600)* will stop training after 3600 seconds. Higher limits will generally result in better performance.

We present additional information about the tuning and post-tuning steps in the Appendix.

5 Experiments and Results: Quick-Tune-Tool in Action

We evaluated the performance of our finetuning tool on four widely-used vision datasets: Oxford Flowers 102 (Nilsback and Zisserman, 2008), Stanford Cars (Krause et al., 2013), Imagenette (Howard, 2020), and FGVC-Aircraft (Maji et al., 2013). An in-depth evaluation of the underlying Quick-Tune algorithm can be found in the prior work by Arango et al. (2023).

Quick-Tune-Tool finetuned models on the training sets while top-1 accuracy was measured on the validation sets. We show results using 1 step ($\Delta t = 1$) and 2 step ($\Delta t = 2$), which is the number of epochs evaluated per finetuning step. We select time budgets following prior work (Arango et al., 2023), with 1 and 4 hours for the different optimizers to account for the number of samples in the datasets. Table 1 presents the final top-1 accuracy per dataset, and Figure 5 visualizes the performance over time for all the compared methods. We observe that Quick-Tune-Tool consistently outperforms the RandomOptimizer, with top-1 accuracy improvements ranging from 13% to 23%. In general, Quick-Tune-Tool converges faster to a better solution than random search.

Dataset	Quick-Tune	Random	Time Budget (Hours)	Optimizer
Imagenette	99.6[99.3–99.9]	82.1[60.4–99.9]	1	micro
Oxford Flowers	89.1[84.0–94.2]	74.7[56.0–93.1]	1	micro
Stanford Cars	53.5[34.4–72.7]	40.4[22.2–58.6]	4	mini
FGVC-Aircraft	48.0[35.2–60.8]	25.0[16.2–33.9]	4	mini

Table 1: Top-1 Accuracy Results. Mean over ten seeds with confidence intervals ($\Delta t = 1$).

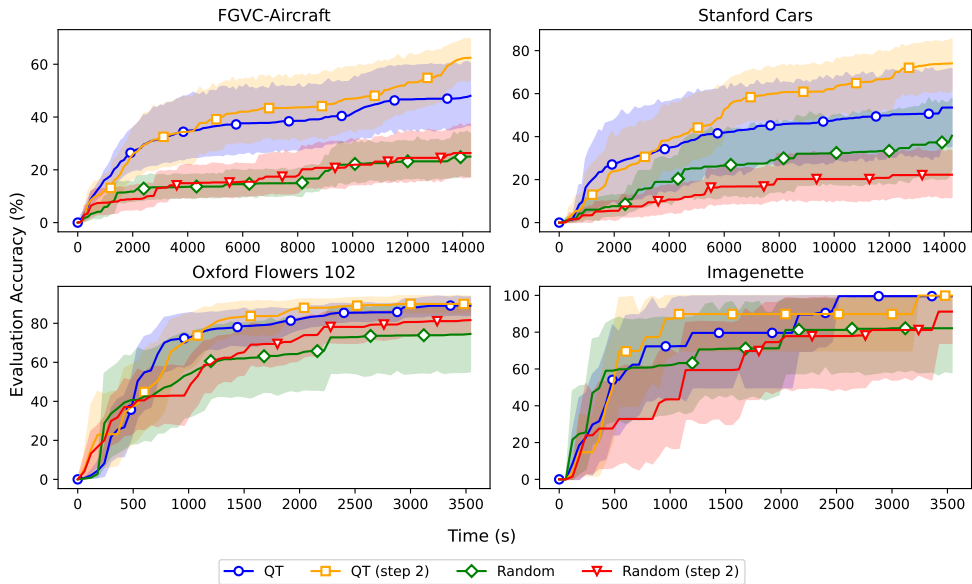


Figure 5: Evaluations on common vision datasets using Quick-Tune-Tool (QT) and Random Search as optimizers. We present results for $\Delta t \in \{1, 2\}$

6 Conclusion and Outlook

In this paper, we introduced Quick-Tune-Tool, a tool that simplifies the automated selection and finetuning of pretrained models. Our tool leverages the Quick-Tune algorithm to offer a user-friendly yet powerful solution for practitioners in image classification. Empirical evaluations on four datasets demonstrate that Quick-Tune-Tool offers a substantial performance improvement in finetuning pretrained models for image classification tasks.

Quick-Tune-Tool is designed with extensibility in mind, allowing for future adaptations to new domains and tasks. Our future work will focus on expanding the tool’s capabilities to support additional data modalities and tasks, incorporating more advanced optimization techniques, and continuous integration of user feedback for further enhancement. By making advanced finetuning accessible and efficient, Quick-Tune-Tool stands to facilitate the wider adoption of pretrained models across diverse application areas.

Broader Impact Statement. We believe that our work does not present notable or new negative broader impacts. Yet, our work initially requires resource-intensive, environmentally costly computation. However, it has the potential for resource savings over time through optimized evaluations. In contrast, we believe that Quick-Tune-Tool provides a positive societal impact by enabling easier access to enhanced image classification tailored to, for example, medical diagnostics or disease detection applications. Furthermore, Quick-Tune-Tool democratizes using and finetuning pretrained models.

Acknowledgements. We acknowledge the financial support of the Hector Foundation. We also acknowledge funding by the European Union (via ERC Consolidator Grant DeepLearning 2.0, grant no. 101045765). Views and opinions expressed are however those of the author(s) only and do not necessarily reflect those of the European Union or the European Research Council. Neither the European Union nor the granting authority can be held responsible for them. Moreover, we acknowledge funding by the Deutsche Forschungsgemeinschaft (DFG, German Research Foundation) under grant number 417962828, by the state of Baden-Württemberg through bwHPC and the German Research Foundation (DFG) through grant INST 35/1597-1 FUGG. We also acknowledge funding by the Deutsche Forschungsgemeinschaft (DFG, German Research Foundation) – Project-ID 499552394 – SFB 1597 and acknowledge Robert Bosch GmbH for financial support.



References

Arango, S. P., Ferreira, F., Kadra, A., Hutter, F., and Grabocka, J. (2023). Quick-tune: Quickly learning which pretrained model to finetune and how. In *The Twelfth International Conference on Learning Representations*.

Awad, N., Mallik, N., and Hutter, F. (2021). DEHB: Evolutionary hyperband for scalable, robust and efficient Hyperparameter Optimization. In *Proc. of IJCAI'21*, pages 2147–2153.

Caron, M., Touvron, H., Misra, I., Jégou, H., Mairal, J., Bojanowski, P., and Joulin, A. (2021). Emerging properties in self-supervised vision transformers. In *Proceedings of the IEEE/CVF international conference on computer vision*, pages 9650–9660.

Cui, Y., Song, Y., Sun, C., Howard, A., and Belongie, S. (2018). Large scale fine-grained categorization and domain-specific transfer learning. In *Proceedings of the IEEE conference on computer vision and pattern recognition*, pages 4109–4118.

Falkner, S., Klein, A., and Hutter, F. (2018). BOHB: Robust and efficient Hyperparameter Optimization at scale. In *Proc. of ICML'18*, pages 1437–1446.

Gardner, J., Pleiss, G., Weinberger, Q., Bindel, D., and Wilson, A. (2018). Gpytorch: Blackbox matrix-matrix gaussian process inference with gpu acceleration. In *Proc. of NeurIPS'18*, pages 7576–7586.

Harris, C., Millman, K., van der Walt, S., Gommers, R., Virtanen, P., Cournapeau, D., Wieser, E., Taylor, J., Berg, S., Smith, N., Kern, R., Picus, M., Hoyer, S., van Kerkwijk, M., Brett, M., Haldane, A., del Río, J., Wiebe, M., Peterson, P., Gérard-Marchant, P., Sheppard, K., Reddy, T., Weckesser, W., Abbasi, H., Gohlke, C., and Oliphant, T. (2020). Array programming with numpy. *Nature*, 585(7825):357–362.

Hollmann, N., Müller, S., Eggensperger, K., and Hutter, F. (2023). TabPFN: A transformer that solves small tabular classification problems in a second. In *Proc. of ICLR'23*.

Howard, J. (2020). imagenette.

Hu, E. J., yelong shen, Wallis, P., Allen-Zhu, Z., Li, Y., Wang, S., Wang, L., and Chen, W. (2022). LoRA: Low-rank adaptation of large language models. In *International Conference on Learning Representations*.

Jiang, J., Chen, B., Fu, B., and Long, M. (2020). Transfer-learning-library. <https://github.com/thuml/Transfer-Learning-Library>.

Jin, H., Song, Q., and Hu, X. (2019). Auto-keras: An efficient neural architecture search system. In Teredesai, A., Kumar, V., Li, Y., Rosales, R., Terzi, E., and Karypis, G., editors, *Proceedings of the 25th ACM SIGKDD International Conference on Knowledge Discovery & Data Mining, KDD 2019, Anchorage, AK, USA, August 4-8, 2019*, pages 1946–1956. ACM.

Kadra, A., Janowski, M., Wistuba, M., and Grabocka, J. (2024). Scaling laws for hyperparameter optimization. *Advances in Neural Information Processing Systems*, 36.

Kirillov, A., Mintun, E., Ravi, N., Mao, H., Rolland, C., Gustafson, L., Xiao, T., Whitehead, S., Berg, A. C., Lo, W.-Y., et al. (2023). Segment anything. In *Proceedings of the IEEE/CVF International Conference on Computer Vision*, pages 4015–4026.

Krause, J., Stark, M., Deng, J., and Fei-Fei, L. (2013). 3d object representations for fine-grained categorization. In *4th International IEEE Workshop on 3D Representation and Recognition (3dRR-13)*.

Li, H., Chaudhari, P., Yang, H., Lam, M., Ravichandran, A., Bhotika, R., and Soatto, S. (2019). Rethinking the hyperparameters for fine-tuning. In *International Conference on Learning Representations*.

Li, X., Grandvalet, Y., and Davoine, F. (2018). Explicit inductive bias for transfer learning with convolutional networks. In Dy, J. G. and Krause, A., editors, *Proceedings of the 35th International Conference on Machine Learning, ICML 2018, Stockholmsmässan, Stockholm, Sweden, July 10-15, 2018*, volume 80 of *Proceedings of Machine Learning Research*, pages 2830–2839. PMLR.

Liang, Y., Wen, H., Nie, Y., Jiang, Y., Jin, M., Song, D., Pan, S., and Wen, Q. (2024). Foundation models for time series analysis: A tutorial and survey. *arXiv preprint arXiv:2403.14735*.

Lindauer, M., Eggensperger, K., Feurer, M., Biedenkapp, A., Marben, J., Müller, P., and Hutter, F. (2019). BOAH: A tool suite for Multi-fidelity Bayesian Optimization & analysis of hyperparameters. *arXiv:1908.06756 [cs.LG]*.

Maji, S., Kannala, J., Rahtu, E., Blaschko, M., and Vedaldi, A. (2013). Fine-grained visual classification of aircraft. Technical report.

Mangrulkar, S., Gugger, S., Debut, L., Belkada, Y., Paul, S., and Bossan, B. (2022). Peft: State-of-the-art parameter-efficient fine-tuning methods. <https://github.com/huggingface/peft>.

McKinney, W. (2010). Data Structures for Statistical Computing in Python. In Stéfan van der Walt and Jarrod Millman, editors, *Proceedings of the 9th Python in Science Conference*, pages 56–61.

Nilsback, M.-E. and Zisserman, A. (2008). Automated flower classification over a large number of classes. In *Proceedings of the Indian Conference on Computer Vision, Graphics and Image Processing*.

Öztürk, E., Ferreira, F., Jomaa, H. S., Scmidtth-Thieme, L., Grabocka, J., and Hutter, F. (2022). Zero-shot automl with pretrained models. In *Proc. of ICML’22*, pages 1128–1135.

Paszke, A., Gross, S., Massa, F., Lerer, A., et al. (2019). PyTorch: An imperative style, high-performance deep learning library. In *Proc. of NeurIPS’19*, pages 8024–8035.

Pineda Arango, S., Ferreira, F., A., K., F., H., and J., G. (2024). Quick-tune: Quickly learning which pretrained model to finetune and how. In *Proc. of ICLR’24*.

Pineda Arango, S. and Grabocka, J. (2023). Deep pipeline embeddings for automl. In *Proceedings of the 29th ACM SIGKDD Conference on Knowledge Discovery and Data Mining*, pages 1907–1919.

Pytorch (2024). Torchtune. <https://github.com/pytorch/torchtune>.

Qiu, X., Sun, T., Xu, Y., Shao, Y., Dai, N., and Huang, X. (2020). Pre-trained models for natural language processing: A survey. *Science China Technological Sciences*, 63(10):1872–1897.

Rakotoarison, H., Adriaensen, S., Mallik, N., Garibov, S., Bergman, E., and Hutter, F. (2024). In-context freeze-thaw bayesian optimization. In *Forty-first International Conference on Machine Learning*.

Stoll, D., Mallik, N., Schrodi, S., Janowski, M., Garibov, S., Abou Chakra, T., Rogalla, D., Bergman, E., Hvarfner, C., Binxin, R., Kober, N., Vallaey, T., and Hutter, F. (2023). Neural Pipeline Search (NePS).

Tang, Z., Fang, H., Zhou, S., Yang, T., Zhong, Z., Hu, T., Kirchhoff, K., and Karypis, G. (2024). Autogluon-multimodal (automm): Supercharging multimodal automl with foundation models. *arXiv preprint arXiv:2404.16233*.

Ullah, I., Carrión, D., Escalera, S., Guyon, I. M., Huisman, M., Mohr, F., van Rijn, J. N., Sun, H., Vanschoren, J., and Vu, P. A. (2022). Meta-album: Multi-domain meta-dataset for few-shot image classification. In *Thirty-sixth Conference on Neural Information Processing Systems Datasets and Benchmarks Track*.

Wightman, R. (2019). Pytorch image models. <https://github.com/rwightman/pytorch-image-models>.

Wistuba, M., Kadra, A., and Grabocka, J. (2022). Supervising the multi-fidelity race of hyperparameter configurations. *Advances in Neural Information Processing Systems*, 35:13470–13484.

You, K., Kou, Z., Long, M., and Wang, J. (2020). Co-tuning for transfer learning. In Larochelle, H., Ranzato, M., Hadsell, R., Balcan, M., and Lin, H., editors, *Advances in Neural Information Processing Systems 33: Annual Conference on Neural Information Processing Systems 2020, NeurIPS 2020, December 6-12, 2020, virtual*.

Zimmer, L., Lindauer, M., and Hutter, F. (2021). Auto-Pytorch: Multi-fidelity metalearning for efficient and robust AutoDL. *TPAMI*, 43:3079–3090.

Transfer Learning for Finetuning Large Language Models

The content of this chapter has been published as:

T. Strangmann, L. Purucker, J. K.H. Franke, I. Rapant, F. Ferreira, and F. Hutter (2024). “Transfer Learning for Finetuning Large Language Models”. In: *NeurIPS 2024 Workshop on Adaptive Foundation Models*.

The supplementary material and a detailed statement of contributions is provided in Appendix D.

Transfer Learning for Finetuning Large Language Models

**Tobias Strangmann¹, Lennart Purucker¹, Jörg K.H. Franke¹, Ivo Rapant¹,
Fabio Ferreira¹, Frank Hutter^{1,2}**

¹University of Freiburg, ²ELLIS Institute Tübingen

Abstract

As the landscape of large language models expands, efficiently finetuning for specific tasks becomes increasingly crucial. At the same time, the landscape of parameter-efficient finetuning methods rapidly expands. Consequently, practitioners face a multitude of complex choices when searching for an optimal finetuning pipeline for large language models. To reduce the complexity for practitioners, we investigate transfer learning for finetuning large language models and aim to transfer knowledge about configurations from related finetuning tasks to a new task. In this work, we transfer learn finetuning by meta-learning performance and cost surrogate models for grey-box meta-optimization from a new meta-dataset. Counter-intuitively, we propose to rely only on transfer learning for new datasets. Thus, we do not use task-specific Bayesian optimization but prioritize knowledge transferred from related tasks over task-specific feedback. We evaluate our method on eight synthetic question-answer datasets and a meta-dataset consisting of 1,800 runs of finetuning Microsoft’s Phi-3. Our transfer learning is superior to zero-shot, default finetuning, and meta-optimization baselines. Our results demonstrate the transferability of finetuning to adapt large language models more effectively.

1 Introduction

The landscape of large language models (LLMs) rapidly expands to a zoo of models (Team, 2024a; Abdin et al., 2024; Liu et al., 2024; DeepSeek-AI et al., 2024; Dubey et al., 2024; Jiang et al., 2023; Mistral AI, 2024; Team, 2024b; Yang et al., 2024), where different models exhibit varying strengths on specific tasks (Wei et al., 2022). At the same time, the landscape of parameter-efficient finetuning methods rapidly expands (Hu et al., 2021; Dettmers et al., 2023; Poth et al., 2023; Hayou et al., 2024).

Consequently, practitioners face a multitude of complex choices for finetuning LLMs. To support practitioners and reduce complexity, we investigate transfer learning of deep-learning pipelines for an LLM and specifications for the finetuning process, including all associated hyperparameters. We aim to transfer knowledge about pipelines from related finetuning tasks to a new task. Thus enabling practitioners to adapt LLMs more effectively to new tasks.

In this work, we transfer learn finetuning by meta-learning performance and cost surrogate models for grey-box meta-optimization from a new meta-dataset. We implement grey-box meta-optimizing by adjusting the Quick-Tune algorithm (Arango et al., 2024). Quick-Tune, was introduced for image classification and supports meta-learning surrogate models. In our version, we propose to rely only on the meta-learned surrogate models trained from scratch. That is, we do not use task-specific Bayesian optimization because *we do not refit the surrogate models* for a new dataset. In other words, our version of Quick-Tune can be understood as a dataset-aware portfolio builder (Xu et al., 2010). While counter-intuitive, we hypothesize that disabling Bayesian optimization leads to better generalization.

We verify the effectiveness of our method for large language models by generating a meta-dataset based on a synthetic question-answer dataset and 1,800 runs of pipelines for finetuning Microsoft’s Phi-3 model (Abdin et al., 2024). Our results show that transfer learning finetuning is superior to random search, DEHB (Awad et al., 2021), and Quick-Tune with Bayesian optimization. Moreover, meta-optimizing finetuning is, as expected, better than zero-shot and default LoRa (Hu et al., 2021).

Our Contributions. To make LLMs more easily adaptable and facilitate future studies, we contribute (1) synthetic datasets that serve a dual purpose: a) to create a meta-dataset for transfer learning and b) as an evaluation framework for LLM models; (2) a version of Quick-Tune for LLM finetuning adapted from the image to language domain; and (3) a novel counter-intuitive yet effective approach to finding the optimal pipeline for finetuning LLMs through transfer learning.

2 Related Work

Synthetic NLP Datasets & Meta-dataset. Question-answer datasets are scarce, with only a few notable examples such as TriviaQA, SQuAD, NaturalQuestions, and PubMedQA (Joshi et al., 2017; Rajpurkar et al., 2016; Kwiatkowski et al., 2019; Jin et al., 2019). Collecting large-scale question-answer datasets is resource-intensive, prompting researchers to explore synthetic generation methods to reduce annotation costs (Yang et al., 2017; Nayak et al., 2024; Lee et al., 2023; Puri et al., 2020; Ovadia et al., 2024). A recent approach by Mecklenburg et al. (2024) utilized *GPT-4* (OpenAI et al., 2024) as an LLM teacher to extract facts from Wikipedia articles and generate question-answer pairs. We use a similar method but apply it to arXiv papers with Llama-3.1-70b (Dubey et al., 2024).

Optimizing Finetuning Many finetuning methods with many hyperparameters exist, cf. (Hu et al., 2021; Dettmers et al., 2023; Li et al., 2023; Hayou et al., 2024; Poth et al., 2023; Liu et al., 2022; Wu et al., 2024). Likewise, many other hyperparameters of the finetuning pipeline exist, such as the choice of optimizer Shazeer and Stern (2018); Loshchilov and Hutter (2019); Franke et al. (2023); Chen et al. (2023). To address the multitude of choices for finetuning, recent work proposed (automated) meta-optimization to determine the optimal combination of finetuning method, optimizer, and hyperparameters. Methods like AutoGluon Multimodal (Tang et al., 2024), AutoPEFT (Zhou et al., 2024), AutoLoRa (Xu et al., 2023), and Quick-Tune (Rapant et al., 2024). However, these methods do not support finetuning LLMs for text generation, which is the focus of our work.

Transfer Learning Finetuning. In general, Quick-Tune (Arango et al., 2024) and its abstraction Quick-Tune-Tool (Rapant et al., 2024), building on earlier frameworks such as Öztürk et al. (2022), focus on transfer learning finetuning pipelines during meta-optimization. However, these prior works are limited to image classification. Our work extends Quick-Tune to finetuning LLMs and proposes a novel algorithmic adjustment. For LLMs, Zhang et al. (2024) introduced a meta-learning-related method for LoRA Hu et al. (2021). This method, however, does not transfer knowledge from related tasks to a new task. Instead, it performs a bi-level optimization for the LoRA rank and weights for one task. In other words, it is comparable to meta-optimizing only the rank of LoRA. In contrast, our work transfers knowledge between tasks via meta-learning. Likewise, all methods we consider can meta-optimize all hyperparameters of a finetuning pipeline.

3 Method

Our method, illustrated in Figure 1, consist of three steps: **A**) create synthetic NLP datasets from scientific papers, **B**) create a meta-dataset by training and evaluating finetuning pipelines; and **C**) transfer learning by pre-training our version of Quick-Tune on our meta-dataset. We then apply pre-trained Quick-Tune to find the optimal finetuning pipeline for new, related NLP tasks. The complete computational resources used for this method are listed in Section E. Limitations of our method can be found in appendix F.

A) Synthetic NLP Datasets. We follow Mecklenburg et al. (2024) to generate synthetic question-answer datasets from scientific papers from arxiv.org. In detail, we crawl papers and convert them to plain text papers with mathematical formulas translated to LaTeX. Next, we use a self-hosted version of *Llama-3.1-70B Instruct* (L3-70B) (AI@Meta, 2024) to extract atomic facts from each chapter of a paper. Then, we generate a set of 12 question-answer pairs for each fact. We add ten to training, one to validation, and one to testing data. Finally, our new question-answer dataset consists of training, validation, and test question-answer pairs for all facts. Appendix A details our prompt templates.

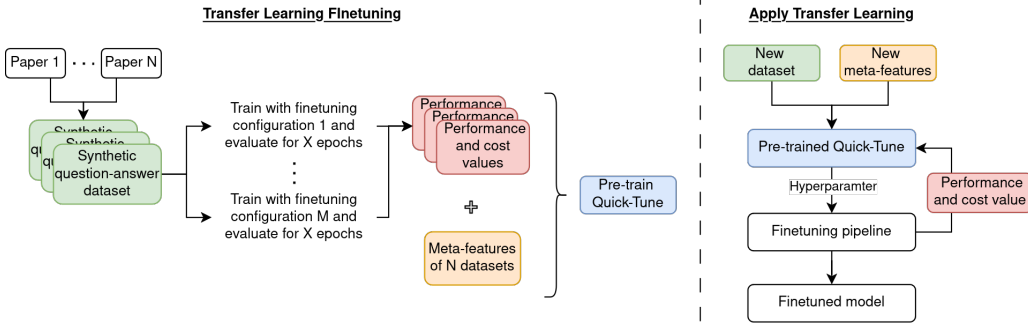


Figure 1: **Method Overview.** We generate new NLP datasets from scientific papers and then create a meta-dataset, which we use for transfer learning to finetune by pre-training Quick-Tune (left). For a new dataset, we compute meta-features and then apply the pre-trained Quick-Tune (right).

B) Our Meta-dataset. We create a meta-dataset by collecting meta-features, performance and cost values for finetuning pipelines on synthetic datasets. Therefore, we create question-answer datasets from 30 papers. Then, for each paper, we train 60 finetuning pipelines with the training and validation question-answer pairs and evaluate them on the test pairs, producing 1,800 runs in total. Finally, we compute meta-features for each paper; see Appendix B for an overview. We visualize an overview of all runs in our meta-dataset in Figure 2.

For each paper, we randomly sample finetuning pipelines from a search space based on hyperparameters for LoRA (Hu et al., 2021), optimizers (AdamW (Loshchilov and Hutter, 2019) or Adam-CPR (Franke et al., 2023)), and the learning rate scheduler. We also include a default finetuning pipeline as a baseline. We detail the search space in Appendix D.

After each epoch, we evaluate the finetuned models in the form of a student with L3-70B as a teacher. Given a finetuned model’s answer to a question, L3-70B evaluates whether the generated answer is correct (0 or 1). Thus, L3-70B assess whether the student model learned to answer new questions about facts in papers after being finetuned on question-answer pairs about these facts.

See Appendix C for the prompt template and an example of this process.

We use four meta-features to characterize each synthetic question-answer dataset: the total number of tokens, average sample length, vocabulary size, and the ratio of question-to-answer lengths.

C) Transfer Learning Finetuning with Quick-Tune. We use the performance metrics and meta-features stored in our meta-dataset to pre-train Quick-Tune, implemented in Quick-Tune-Tool (Rapant et al., 2024). That is, we meta-train the Gaussian Process-based surrogate models of Quick-Tune. This allows Quick-Tune to start with a strong prior for the performance and cost of finetuning pipeline on a new dataset, transferring knowledge across tasks. By default, the surrogate models are continuously refitted during optimization to facilitate Bayesian optimization.

In our version of Quick-Tune, we disable Bayesian optimization by disabling refitting. We hypothesize that disabling Bayesian optimization leads to better generalization by relying more on the knowledge transferred from related tasks than task-specific noise. In other words, while Bayesian optimization exploits the most promising pipeline on validation data, only relying on the prior from transfer learning could lead the meta-optimizer to find better, more general pipelines.

From a broader perspective, our version of Quick-Tune can be understood as a *dataset-aware* portfolio builder. Portfolios (Xu et al., 2010) are known as robust transfer learning methods (Feurer et al., 2022; Salinas and Erickson, 2023).

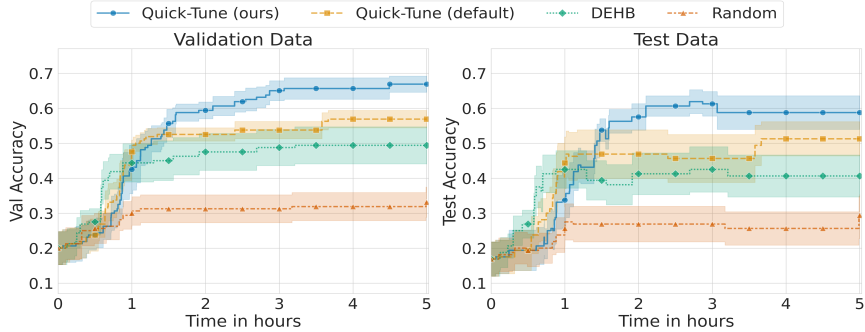


Figure 3: **Optimizer Performance Over Time.** We visualize the average validation (left) and test (right) performance across the eight datasets over time. At each time point, we evaluated the best pipeline found so far. We observe that DEHB and Quick-Tune (default) stagnant after 1 to 1.5 hours, with little progress on test scores afterward. Quick-Tune (ours) only stagnates after 3 hours.

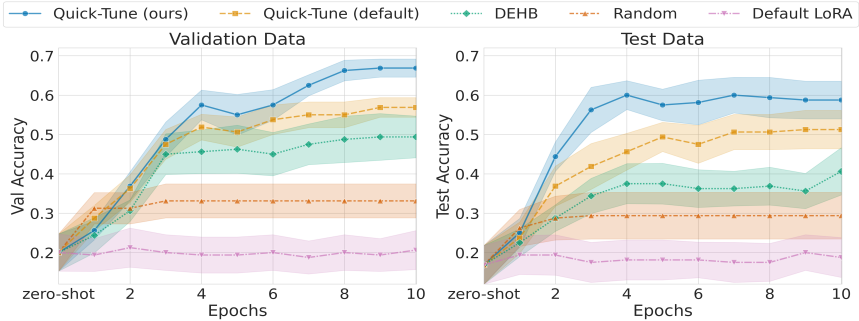


Figure 4: **Final Performance.** We show the validation (left) and test (right) learning curve of the best pipeline returned by the optimizers after 5 hours, averaged across eight datasets. The finetuning pipeline returned by Quick-Tune (ours) performs best.

4 Results

Experimental Setup. We experiment with finetuning Phi 3 Mini Instruct (3.8B parameters) (Abdin et al., 2024) on eight newly generated synthetic question-answer datasets (see Appendix B). We employ random search, DEHB (Awad et al., 2021), default Quick-Tune (Arango et al., 2024), and our version of Quick-Tune to meta-optimize the finetuning pipeline. Furthermore, we evaluate a default finetuning pipeline and zero-shot performance. Each optimizer is given a five-hour time budget. We again use our *Llama-3.1-70B* teacher for evaluation.

HYPOTHESIS: TRANSFER LEARNING LEADS TO BETTER GENERALIZATION.

Figure 3 presents the performance over time of the meta-optimizers for validation and test data. Figure 4 shows the performance of the best pipeline, see Appendix G for configuration details. The error bars in both figures represent the standard error of the mean. Note the initial performance represents the zero-shot performance of Phi 3. We observe that Quick-Tune (default) and DEHB get stuck after 1.5 hours during meta-optimization and fail to find a significantly better finetuning pipeline afterward. In contrast, Quick-Tune (ours), which relies only on transfer learning, further improves test performance. A similar trend manifests when training the best pipeline found by each meta-optimizer. The pipeline found by Quick-Tune (ours) generalizes best to test data.

Conclusion. In this study, we demonstrated that relying only on transfer learning for finetuning yields better performance than alternative methods, challenging conventional approaches and potentially simplifying the process of adapting large language models to specific tasks. In future work, we plan to understand this phenomenon in more detail and to generalize it to a meta-optimization method. Thus allowing us to effectively manage the zoo of and the plethora of methods for adapting large language models to specific tasks.

Acknowledgments

This work was carried out at the HoreKa Cluster, which is funded by the Baden-Württemberg Ministry of Science, Research and the Arts, and the Federal Ministry of Education and Research. The authors would also like to thank the state of Baden-Württemberg for the support provided by the bwHPC and the German Research Foundation (DFG) for funding through INST 35/1597-1 FUGG. We acknowledge funding by the Deutsche Forschungsgemeinschaft (DFG, German Research Foundation) under SFB 1597 (SmallData), grant numbers 499552394 and 417962828. Frank Hutter acknowledges the financial support of the Hector Foundation.

References

Gemma Team. Gemma. 2024a. doi: 10.34740/KAGGLE/M/3301. URL <https://www.kaggle.com/m/3301>.

Marah Abdin, Jyoti Aneja, Hany Awadalla, Ahmed Awadallah et al. Phi-3 technical report: A highly capable language model locally on your phone, 2024. URL <https://arxiv.org/abs/2404.14219>.

Liyuan Liu, Young Jin Kim, Shuohang Wang, Chen Liang et al. Grin: Gradient-informed moe, 2024. URL <https://arxiv.org/abs/2409.12136>.

DeepSeek-AI, Aixin Liu, Bei Feng, Bin Wang et al. Deepseek-v2: A strong, economical, and efficient mixture-of-experts language model, 2024. URL <https://arxiv.org/abs/2405.04434>.

Abhimanyu Dubey, Abhinav Jauhri, Abhinav Pandey, Abhishek Kadian et al. The llama 3 herd of models, 2024. URL <https://arxiv.org/abs/2407.21783>.

Albert Q. Jiang, Alexandre Sablayrolles, Arthur Mensch, Chris Bamford et al. Mistral 7b, 2023. URL <https://arxiv.org/abs/2310.06825>.

Mistral AI. Mistral nemo, 2024. URL <https://mistral.ai/news/mistral-nemo/>. Accessed: 2024-09-24.

Qwen Team. Qwen2.5: A party of foundation models, September 2024b. URL <https://qwenlm.github.io/blog/qwen2.5/>.

An Yang, Baosong Yang, Binyuan Hui, Bo Zheng et al. Qwen2 technical report. *arXiv preprint arXiv:2407.10671*, 2024.

Jason Wei, Yi Tay, Rishi Bommasani, Colin Raffel et al. Emergent abilities of large language models, 2022. URL <https://arxiv.org/abs/2206.07682>.

Edward J. Hu, Yelong Shen, Phillip Wallis, Zeyuan Allen-Zhu et al. Lora: Low-rank adaptation of large language models, 2021. URL <https://arxiv.org/abs/2106.09685>.

Tim Dettmers, Artidoro Pagnoni, Ari Holtzman, and Luke Zettlemoyer. Qlora: Efficient finetuning of quantized llms, 2023. URL <https://arxiv.org/abs/2305.14314>.

Clifton Poth, Hannah Sterz, Indraneil Paul, Sukannya Purkayastha et al. Adapters: A unified library for parameter-efficient and modular transfer learning, 2023. URL <https://arxiv.org/abs/2311.11077>.

Soufiane Hayou, Nikhil Ghosh, and Bin Yu. Lora+: Efficient low rank adaptation of large models, 2024. URL <https://arxiv.org/abs/2402.12354>.

Sebastian Pineda Arango, Fabio Ferreira, Arlind Kadra, Frank Hutter, and Jofis Grabocka. Quick-tune: Quickly learning which pretrained model to finetune and how. In *The Twelfth International Conference on Learning Representations*, 2024. URL <https://openreview.net/forum?id=tqh1zdXIra>.

Lin Xu, Holger Hoos, and Kevin Leyton-Brown. Hydra: Automatically configuring algorithms for portfolio-based selection. In *Proceedings of the AAAI Conference on Artificial Intelligence*, volume 24, pages 210–216, 2010.

Noor Awad, Neeratoy Mallik, and Frank Hutter. Dehb: Evolutionary hyperband for scalable, robust and efficient hyperparameter optimization. *arXiv preprint arXiv:2105.09821*, 2021.

Mandar Joshi, Eunsol Choi, Daniel S. Weld, and Luke Zettlemoyer. Triviaqa: A large scale distantly supervised challenge dataset for reading comprehension, 2017. URL <https://arxiv.org/abs/1705.03551>.

Pranav Rajpurkar, Jian Zhang, Konstantin Lopyrev, and Percy Liang. Squad: 100,000+ questions for machine comprehension of text, 2016. URL <https://arxiv.org/abs/1606.05250>.

Tom Kwiatkowski, Jennimaria Palomaki, Olivia Redfield, Michael Collins et al. Natural questions: a benchmark for question answering research. *Transactions of the Association of Computational Linguistics*, 2019.

Qiao Jin, Bhuwan Dhingra, Zhengping Liu, William W. Cohen, and Xinghua Lu. Pubmedqa: A dataset for biomedical research question answering, 2019. URL <https://arxiv.org/abs/1909.06146>.

Zhilin Yang, Junjie Hu, Ruslan Salakhutdinov, and William W. Cohen. Semi-supervised qa with generative domain-adaptive nets, 2017. URL <https://arxiv.org/abs/1702.02206>.

Nihal V. Nayak, Yiyang Nan, Avi Trost, and Stephen H. Bach. Learning to generate instruction tuning datasets for zero-shot task adaptation, 2024. URL <https://arxiv.org/abs/2402.18334>.

Seongyun Lee, Hyunjae Kim, and Jaewoo Kang. Liquid: A framework for list question answering dataset generation, 2023. URL <https://arxiv.org/abs/2302.01691>.

Raul Puri, Ryan Spring, Mostofa Patwary, Mohammad Shoeybi, and Bryan Catanzaro. Training question answering models from synthetic data, 2020. URL <https://arxiv.org/abs/2002.09599>.

Oded Ovadia, Menachem Brief, Moshik Mishaeli, and Oren Elisha. Fine-tuning or retrieval? comparing knowledge injection in llms, 2024. URL <https://arxiv.org/abs/2312.05934>.

Nick Mecklenburg, Yiyu Lin, Xiaoxiao Li, Daniel Holstein et al. Injecting new knowledge into large language models via supervised fine-tuning, 2024. URL <https://arxiv.org/abs/2404.00213>.

OpenAI, Josh Achiam, Steven Adler, Sandhini Agarwal et al. Gpt-4 technical report, 2024. URL <https://arxiv.org/abs/2303.08774>.

Yixiao Li, Yifan Yu, Chen Liang, Pengcheng He et al. Loftq: Lora-fine-tuning-aware quantization for large language models, 2023. URL <https://arxiv.org/abs/2310.08659>.

Haokun Liu, Derek Tam, Mohammed Muqeeth, Jay Mohta et al. Few-shot parameter-efficient fine-tuning is better and cheaper than in-context learning, 2022. URL <https://arxiv.org/abs/2205.05638>.

Zhengxuan Wu, Aryaman Arora, Zheng Wang, Atticus Geiger et al. Reft: Representation finetuning for language models, 2024. URL <https://arxiv.org/abs/2404.03592>.

Noam Shazeer and Mitchell Stern. Adafactor: Adaptive learning rates with sublinear memory cost, 2018. URL <https://arxiv.org/abs/1804.04235>.

Ilya Loshchilov and Frank Hutter. Decoupled weight decay regularization, 2019. URL <https://arxiv.org/abs/1711.05101>.

Jörg K. H. Franke, Michael Hefenbrock, Gregor Koehler, and Frank Hutter. Constrained parameter regularization, 2023. URL <https://arxiv.org/abs/2311.09058>.

Xiangning Chen, Chen Liang, Da Huang, Esteban Real et al. Symbolic discovery of optimization algorithms, 2023. URL <https://arxiv.org/abs/2302.06675>.

Zhiqiang Tang, Haoyang Fang, Su Zhou, Taojiannan Yang et al. Autogluon-multimodal (automm): Supercharging multimodal automl with foundation models. *arXiv preprint arXiv:2404.16233*, 2024.

Han Zhou, Xingchen Wan, Ivan Vulić, and Anna Korhonen. Autopeft: Automatic configuration search for parameter-efficient fine-tuning, 2024. URL <https://arxiv.org/abs/2301.12132>.

Xilie Xu, Jingfeng Zhang, and Mohan Kankanhalli. Autolora: A parameter-free automated robust fine-tuning framework, 2023. URL <https://arxiv.org/abs/2310.01818>.

Ivo Rapant, Lennart Purucker, Fabio Ferreira, Sebastian Pineda Arango et al. Quick-tune-tool: A practical tool and its user guide for automatically finetuning pretrained models. In *AutoML Conference 2024 (Workshop Track)*, 2024.

E. ÖzTÜRK, F. Ferreira, H. S. Jomaa, L. Scmidtth-Thieme et al. Zero-shot automl with pretrained models. In *Proc. of ICML '22*, pages 1128–1135, 2022.

Ruiyi Zhang, Rushi Qiang, Sai Ashish Somayajula, and Pengtao Xie. Autolora: Automatically tuning matrix ranks in low-rank adaptation based on meta learning. *arXiv preprint arXiv:2403.09113*, 2024.

AI@Meta. Llama 3.1 model card. 2024. URL https://github.com/meta-llama/llama-models/blob/main/models/llama3_1/MODEL_CARD.md.

Matthias Feurer, Katharina Eggensperger, Stefan Falkner, Marius Lindauer, and Frank Hutter. Auto-sklearn 2.0: Hands-free automl via meta-learning. *Journal of Machine Learning Research*, 23(261):1–61, 2022.

David Salinas and Nick Erickson. Tabrepo: A large scale repository of tabular model evaluations and its automl applications. *arXiv preprint arXiv:2311.02971*, 2023.

Tri Dao, Daniel Y. Fu, Stefano Ermon, Atri Rudra, and Christopher Ré. Flashattention: Fast and memory-efficient exact attention with io-awareness, 2022. URL <https://arxiv.org/abs/2205.14135>.

Michael L. Waskom. seaborn: statistical data visualization. *Journal of Open Source Software*, 6(60):3021, 2021. doi: 10.21105/joss.03021. URL <https://doi.org/10.21105/joss.03021>.

Part III

Meta-Learning Data Augmentation and Synthetic Data for Enhanced Learning

On the Importance of Hyperparameters and Data Augmentation for Self-Supervised Learning

The content of this chapter has been published as:

D. Wagner, F. Ferreira, D. Stoll, R. T. Schirrmeister, S. Müller, and F. Hutter (2022). “On the importance of hyperparameters and data augmentation for self-supervised learning”. In: *Pre-Training Workshop at the International Conference for Machine Learning (ICML)*. ed. by K. Chaudhuri, S. Jegelka, L. Song, C. Szepesvári, G. Niu, and S. Sabato. Vol. 162. Proceedings of Machine Learning Research. PMLR. URL: <https://icml.cc/virtual/2022/20697>.

The supplementary material and a detailed statement of contributions is provided in Appendix F.

On the Importance of Hyperparameters and Data Augmentation for Self-Supervised Learning

Diane Wagner¹ Fabio Ferreira¹ Danny Stoll¹ Robin Tibor Schirrmeister¹ Samuel Müller¹ Frank Hutter^{1,2}

Abstract

Self-Supervised Learning (SSL) has become a very active area of Deep Learning research where it is heavily used as a pre-training method for classification and other tasks. However, the rapid pace of advancements in this area comes at a price: training pipelines vary significantly across papers, which presents a potentially crucial confounding factor. Here, we show that, indeed, the choice of hyperparameters and data augmentation strategies can have a dramatic impact on performance. To shed light on these neglected factors and help maximize the power of SSL, we hyperparameterize these components and optimize them with Bayesian optimization, showing improvements across multiple datasets for the SimSiam SSL approach. Realizing the importance of data augmentations for SSL, we also introduce a new automated data augmentation algorithm, *GroupAugment*, which considers groups of augmentations and optimizes the sampling across groups. In contrast to algorithms designed for supervised learning, *GroupAugment* achieved consistently high linear evaluation accuracy across all datasets we considered. Overall, our results indicate the importance and likely underestimated role of data augmentation for SSL.

1. Introduction

Self-supervised learning (SSL) has seen an explosion of research interest in recent years, with significant progress using SSL as a pre-training method for classification (Grill et al., 2020; Chen & He, 2021; Chen et al., 2020a; He et al., 2020; Chen et al., 2020b). A large variety of SSL

¹Department of Computer Science, University of Freiburg, Freiburg, Germany ²Bosch Center for Artificial Intelligence, Germany. Correspondence to: Diane Wagner <wagnerd@cs.uni-freiburg.de>.

First Workshop of Pre-training: Perspectives, Pitfalls, and Paths Forward at ICML 2022, Baltimore, Maryland, USA, PMLR 162, 2022. Copyright 2022 by the author(s).

methods have been developed, for example using different optimization paradigms (van den Oord et al., 2018; Pathak et al., 2016), different objective functions (Giradis et al., 2018; Doersch et al., 2015; Zhang et al., 2016), or different data modalities (Radford et al., 2021).

An aspect of SSL performance that is less researched is the effect of other choices, such as the training hyperparameters or the augmentation strategy. To shed light on these neglected factors, we use Bayesian optimization (Mockus et al., 1978; Shahriari et al., 2016) to search for configurations of the SimSiam SSL algorithm (Chen & He, 2021) on CIFAR-10, CIFAR-100 (Krizhevsky, 2009), and the medical dataset DermaMNIST (Yang et al., 2021a;b). We consider, on the one hand, a search over training hyperparameters and, on the other hand, a search over data augmentation strategies. Among other findings, our results suggest the importance of data augmentation for SSL.

Motivated by the apparent importance of data augmentation for SSL, we then develop a new automated data augmentation algorithm, *GroupAugment*, that covers a more diverse space of augmentation strategies than existing methods and can, e.g., design augmentation strategies that resemble manually-designed SSL augmentation strategies.

In summary, our main contributions are:

- We study the effect of training hyperparameters and augmentation strategies for the SimSiam SSL approach (Section 3). Our results indicate the importance of data augmentation for SSL.
- We introduce the automated data augmentation algorithm *GroupAugment* and demonstrate its high performance for SSL (Section 4).

2. Background and Related Work

Self-Supervised Learning The most cited works in Self-Supervised Learning, such as SimCLR, BYOL, SimSiam, MoCo, or DINO (Grill et al., 2020; Chen & He, 2021; Chen et al., 2020a; He et al., 2020; Chen et al., 2020b) all apply a similar or identical data augmentation protocol (random horizontal flip, color distortion, and nowadays also Gaus-

sian blur and solarization). Most relevant to our work are the findings of Grill et al. (2020) and Chen et al. (2020a), who identify and address the sensitivity to choosing color distortions in their methods. Moreover, Chen et al. (2020a) identified that a sophisticated supervised data augmentation strategy does not perform better than simple cropping with strong color distortion in the self-supervised setting. These observations motivate the contributions regarding data augmentation for SSL, which we will revisit next.

Data Augmentation Algorithms In supervised learning, data augmentation algorithms usually outperform manually selected augmentation strategies: Three algorithms that rely on randomly sampling augmentations from a fixed set of augmentations are TrivialAugment (Müller & Hutter, 2021) and SmartSamplingAugment (Negassi et al., 2022). Other algorithms, such as AutoAugment (Cubuk et al., 2019), RandAugment (Cubuk et al., 2020), and SmartAugment (Negassi et al., 2022) perform a gradient-free search in the space of augmentation policies. It is also possible to apply gradient-based optimization to meta-learn pre-training hyperparameters (Raghu et al., 2021) for ECG data. In Self-Augment (Reed et al., 2021), the authors bootstrap from the correlation between supervised and self-supervised evaluation performance to incorporate a rotation task for generating augmentation policies efficiently. SelfAugment is qualitatively different from the previous approaches in that it does not optimize for general downstream performance but rotation task performance. Additionally, it will likely not include rotations into the selected augmentation policy.

In contrast to these, our approach *GroupAugment* (Section 4) covers a more diverse space of augmentation strategies than existing methods and can, e.g., design augmentation strategies that resemble manually-designed SSL augmentation strategies. It generalizes existing approaches by optimizing group-specific sampling probabilities, the number of group-specific augmentations, and the total number of augmentations applied while imposing no limitations on the set of augmentations such as SelfAugment.

3. Study on the Importance of Hyperparameters and Data Augmentation

We study the following research questions:

- What role does data augmentation play in SSL, and can better data augmentation strategies lead to better performance?
- Which hyperparameters may be notorious for resulting in model collapse when set incorrectly?
- Which hyperparameters are important to optimize in SSL to achieve good performance and outperform baselines?

3.1. Study Design

To answer the presented questions, we conducted the study described below.

Models, Datasets and Hyperparameter Search Spaces

We perform all our experiments on the CIFAR-10, CIFAR-100 and DermaMNIST datasets (Krizhevsky, 2009; Yang et al., 2021a;b) and use the SimSiam (Chen & He, 2021) approach with the ResNet-18 (He et al., 2016) architecture. We optimize a wide range of training pipeline hyperparameters (which we refer to as *Training Hypers*) such as the learning rate, warmup and weight decay, and optimizer, as well as data augmentation hyperparameters (which we refer to as *Augmentations*) involving magnitudes and probabilities of image distortions. Please see Appendix A for more details on our search spaces. We point out that all hyperparameter search spaces of the baselines are chosen identically across all datasets except for the pre-training epochs, where we used 800 for CIFAR-10/100 and 100 for DermaMNIST. Lastly, we report how the train, validation, and test splits were chosen in Appendix B.

Search Algorithm To optimize over the search spaces listed above, we use Bayesian optimization (BO) (Mockus et al., 1978) with expert priors (Hvarfner et al., 2021) as implemented by Stoll et al. (2022). For details on the chosen priors see Appendix B.

Performance Evaluation All reported performance values are based on the standard linear evaluation protocol (Dalal & Triggs, 2005; Grill et al., 2020) from the SSL literature that trains a linear classifier on top of the frozen ResNet backbone weights.

3.2. Results

Hyperparameters vs Data Augmentation Strategy Table 1 shows that (a) optimizing six training hyperparameters (detailed in Table 5 in the appendix) of SimSiam only lead to marginal improvements or even deterioration of performance (due to differences in validation and test split); (b) optimizing the data augmentation strategy lead to consistent significant performance improvements (at least 1%, and up to 2.3% for CIFAR-100). This shows that SimSiam’s training hyperparameters were already very well-tuned.

How to Avoid Collapsing Chen & He (2021) already analyzed which factors, e.g., stop-gradient, can cause collapsing solutions for SimSiam. A collapsing solution is an undesired solution where all the outputs collapse to a constant vector. We continue this study and give insights into which hyperparameters may cause collapsing if chosen suboptimally. While we observed collapsing solutions in some of our experiments on the CIFAR-10 and CIFAR-100 datasets,

Table 1. Mean test accuracy [%] for SimSiam and its tuned variants in the linear evaluation protocol. We report the mean and standard error across five seeds. (†) The original SimSiam result of 91.8% was achieved using early stopping on the test set.

Approach	DermaMNIST	CIFAR-10	CIFAR-100
SimSiam (Chen & He, 2021)	66.2 ± 0.3	$91.6 \pm 0.1^\dagger$	65.6 ± 0.2
SimSiam Tuned Training Hypers	66.5 ± 0.1	91.6 ± 0.1	64.9 ± 0.2
SimSiam Tuned Augmentations	67.2 ± 0.4	92.7 ± 0.1	67.9 ± 0.3

for DermaMNIST, we surprisingly observed no collapsing solutions. We show violin plots in Appendix D giving some insights on which hyperparameters may be responsible for collapsing solutions. For example, Figure 1, an excerpt from Appendix D, indicates that a probability of applying grayscale to CIFAR-100 around 0.5 might cause collapsing solutions.

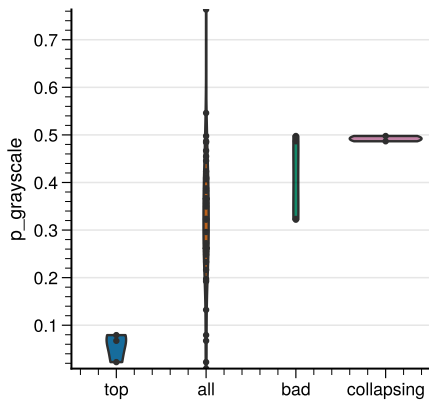


Figure 1. Density estimates for the probability of applying a grayscale augmentation as sampled in our optimization for SimSiam’s augmentation strategy on CIFAR-100. We show density estimates for the best and worst-performing configurations (top and bad), all configurations (all), and configurations leading to collapsing.

Importance of Hyperparameters In the following, we study the importance of individual hyperparameters for achieving good performance. First, we compare the manually designed hyperparameter settings from Chen & He (2021) to the optimized settings found in our study. As Chen & He (2021) do not report results on CIFAR-100 and DermaMNIST, we focus on CIFAR-10 here. For training hyperparameters, we do not observe significant differences in performance (cf. Table 1), and the settings found by (Chen & He, 2021) seem to be quite optimal. For the parameterized data augmentation config space, we observe that the grayscale probability hyperparameter should be set half as high as in the baseline and that the saturation strength from the color jitter needs to be higher than in the baseline. Further, adding solarize seems important, which is also observed by Grill et al. (2020). The hyperparameter

importance study in Table 2 also supports the importance of the above parameters. Additionally, Figure 2 suggests that for the above parameters, good and bad configurations differ, supporting our findings. Moreover, our results also give insights into how individual hyperparameters should be optimally set. As an example, Figure 1 shows how the probability of applying grayscale should be optimally set for the CIFAR-100 dataset. In the best-performing configurations, this probability hyperparameter has been sampled below 0.1 and in bad-performing configurations above 0.3. We show violin plots of all the other individual hyperparameters of the different config spaces and datasets in Appendix D.

Table 2. Hyperparameter importances for the SimSiam data augmentation space for CIFAR-10. We utilized fANOVA (Hutter et al., 2014), which quantifies the contribution of individual hyperparameters to the overall variance in performance. We distinguish between the general importance and the importance of best configurations. Higher importance values denote a higher performance responsibility.

Hyperparameter	Across all	Across best
brightness strength	1	2
contrast strength	2	2
hue strength	8	3
p colorjitter	2	2
p grayscale	16	32
p horizontal flip	8	2
p solarize	30	26
saturation strength	23	7
solarize threshold	5	2

4. GroupAugment

In this section, we introduce *GroupAugment*, an automated data augmentation algorithm that operates on groups of augmentations (such as color or quality transformations) and designs sampling strategies over these groups. Further, we present an empirical study where we find that, in contrast to the data augmentation algorithms designed for supervised learning, GroupAugment robustly outperforms the baseline in all the settings we analyzed.

4.1. Algorithm

Augmentation Sampling Given some groups of data augmentations $\{g_i\}$, GroupAugment uses one global hyperparameter and two sets of group-specific hyperparameters to create a list of augmentation sequences that will be consecutively applied to an image. The global hyperparameter T determines the number of augmentation sequences in that list. The group-specific hyperparameter P_{g_i} determines the probability that augmentation group g_i is chosen to create the following augmentation sequence. N_{g_i} determines the number of augmentations to sample uniformly without replacement to form an augmentation sequence for augmentation group g_i . We provide pseudocode for a GroupAugment policy in Algorithm 1.

Algorithm 1 A GroupAugment policy applied to an image.

```

Input: Image  $I$ , augmentation groups  $\{g_i\}$ ,
        group-specific sampling probabilities  $\{P_{g_i}\}$ ,
        group-specific #augmentations  $\{N_{g_i}\}$ ,
        total #group-samples  $T$ 
Initialize empty list of augmentation sequences  $A$ 
for augmentation sequence  $1, \dots, T$  do
    Sample group  $g$  according to  $\{P_{g_i}\}$ 
    Sample  $N_g$  augmentations from group  $g$ 
    Append augmentations to  $A$ 
end for
Apply sampled augmentation sequences  $A$  to  $I$ 

```

Novelty of Group Sampling While Negassi et al. (2022) explored optimizing the parameters of color and geometric augmentation groups, GroupAugment generalizes this notion to *any* set of augmentation groups and searches over more general spaces of sampling strategies. In our study, we instantiate GroupAugment with five groups: color, geometric, non-rigid, quality, and exotic. See Table 9 in Appendix C for the specific augmentations we used and Table 6 in Appendix A for a detailed description of GroupAugment’s search space.

Search Algorithm To optimize over the resulting search space, we use the same Bayesian optimization (BO) approach with expert priors as above. Further, we normalize the sampled probabilities, as BO samples each group probability individually, and therefore, they do not necessarily add up to 1.

4.2. Comparisons and Results

We compare GroupAugment to several automated data augmentation algorithms. On the one hand, we observe that applying standard automated data augmentation algorithms, e.g., RandAugment, to the self-supervised learning setting worsens the results for most of our analyzed datasets, al-

Table 3. Mean test accuracy for different algorithms in the linear evaluation protocol. We report the mean and standard error across five seeds for methods we ran. For each dataset, we bold the two best accuracies and underline scores that outperform the SimSiam baseline. (†) The original SimSiam result of 91.8% was achieved using early stopping on the test set. (‡) SelfAugment and SelfRandAugment were evaluated using Resnet50 and not Resnet18 as other methods. Reed et al. (2021) report results for multiple instantiations of SelfAugment.

Approach	DermaMNIST	CIFAR-10	CIFAR-100
SimSiam (Chen & He, 2021)	66.2 ± 0.3	$91.6 \pm 0.1^†$	65.6 ± 0.2
SelfRandAugment (Reed et al., 2021)	-	$90.3^‡$	-
SelfAugment (Reed et al., 2021)	-	$87.5 - 92.6^‡$	-
RandAugment (Cubuk et al., 2020)	68.8 ± 0.3	89.9 ± 0.0	59.3 ± 0.5
SmartAugment (Negassi et al., 2022)	67.5 ± 0.1	89.8 ± 0.1	59.8 ± 0.1
TrivialAugment (Müller & Hutter, 2021)	67.7 ± 0.5	89.4 ± 0.1	59.1 ± 0.2
Tuned SimSiam Augmentations (our)	67.2 ± 0.4	92.7 ± 0.1	67.9 ± 0.3
GroupAugment (our)	68.0 ± 0.3	93.0 ± 0.1	66.3 ± 0.4

though those algorithms perform well in the supervised-learning setting (see Table 3). This observation is in line with the finding of Chen et al. (2020a) that a sophisticated supervised data augmentation strategy did not perform better than simple cropping with strong color distortion in the SSL setting. On the other hand, contrary to standard supervised-learning data augmentation algorithms, GroupAugment robustly outperforms the baseline in all the settings we analyzed. We give more details on the experimental settings in Appendix B.

Further, we observe a performance improvement over the baseline when tuning its data augmentation strategy’s magnitudes and application probabilities with the same computational budget we used for the GroupAugment search space. However, as GroupAugment outperforms the tuned SimSiam data augmentation for most of our results, allowing stronger parameterization, we recommend optimizing the data augmentation with GroupAugment, especially for datasets having no intuition about which data augmentation might be helpful.

5. Conclusion and Limitations

While SimCLR and BYOL have analyzed the role of data augmentation, our results show that it is beneficial to analyze it in much greater detail. In summary, we provide evidence for the underestimated role of data augmentation for SSL and present a novel automated data augmentation algorithm, GroupAugment, which outperforms vanilla-SimSiam across all datasets we study.

Limitations We conducted our study on CIFAR-10, CIFAR-100 (Krizhevsky, 2009), and DermaMNIST (Yang et al., 2021a;b). More datasets should be considered to gather more insights and strengthen our experimental con-

clusions. In particular, results on ImageNet (Deng et al., 2009) and more medical datasets are of interest. Further, as automated data augmentation (e.g., our GroupAugment) optimizes the augmentation strategy on a validation set, out-of-distribution test sets can pose a challenge if the validation set is in-distribution.

Acknowledgements

We acknowledge funding by Robert Bosch GmbH, by the Deutsche Forschungsgemeinschaft (DFG, German Research Foundation) under grant number 417962828, by European Research Council (ERC) Consolidator Grant “Deep Learning 2.0” (grant no. 101045765), and by BrainLinks-BrainTools which was funded by the German Research Foundation (DFG, grant no. EXC 1086) and is currently funded by the Federal Ministry of Economics, Science and Arts of Baden Württemberg within the sustainability program for projects of the excellence initiative. Funded by the European Union. Views and opinions expressed are however those of the author(s) only and do not necessarily reflect those of the European Union or the ERC. Neither the European Union nor the ERC can be held responsible for them.



Funded by
the European Union

References

Buslaev, A., Iglovikov, V. I., Khvedchenya, E., Parinov, A., Druzhinin, M., and Kalinin, A. A. Albumentations: Fast and flexible image augmentations. *Information*, 11 (2), 2020. ISSN 2078-2489. doi: 10.3390/info11020125. URL <https://www.mdpi.com/2078-2489/11/2/125>.

Chen, T., Kornblith, S., Norouzi, M., and Hinton, G. A simple framework for contrastive learning of visual representations. In *International conference on machine learning*, pp. 1597–1607. PMLR, 2020a.

Chen, X. and He, K. Exploring simple siamese representation learning. In *Proceedings of the IEEE/CVF Conference on Computer Vision and Pattern Recognition*, pp. 15750–15758, 2021.

Chen, X., Fan, H., Girshick, R., and He, K. Improved baselines with momentum contrastive learning. *arXiv preprint arXiv:2003.04297*, 2020b.

Cubuk, E., Zoph, B., Mane, D., Vasudevan, V., and Le, Q. Autoaugment: Learning augmentation strategies from data. In *Proceedings of the IEEE/CVF Conference on Computer Vision and Pattern Recognition*, pp. 113–123, 2019.

Cubuk, E., Zoph, B., Shlens, J., and Le, Q. Randaugment: Practical automated data augmentation with a reduced search space. In *Proceedings of the IEEE/CVF Conference on Computer Vision and Pattern Recognition Workshops*, pp. 702–703, 2020.

Dalal, N. and Triggs, B. Histograms of oriented gradients for human detection. In *CVPR’05*, volume 1, pp. 886–893 vol. 1, 2005.

Deng, J., Dong, W., Socher, R., Li, L., Li, K., and Fei-Fei, L. ImageNet: A Large-Scale Hierarchical Image Database. In *Proceedings of the International Conference on Computer Vision and Pattern Recognition (CVPR’09)*, pp. 248–255, 2009.

Doersch, C., Gupta, A., and Efros, A. A. Unsupervised visual representation learning by context prediction. In *Proceedings of the 18th International Conference on Computer Vision (ICCV’15)*, pp. 1422–1430, 2015.

Giradis, S., Singh, P., and Komodakis, N. Unsupervised representation learning by predicting image rotations. In *Proceedings of the International Conference on Learning Representations (ICLR’18)*, 2018.

Grill, J.-B., Strub, F., Altché, F., Tallec, C., Richemond, P., Buchatskaya, E., Doersch, C., Avila Pires, B., Guo, Z.,

Gheshlaghi Azar, M., et al. Bootstrap your own latent-a new approach to self-supervised learning. *Advances in Neural Information Processing Systems*, 33:21271–21284, 2020.

He, K., Zhang, X., Ren, S., and Sun, J. Deep residual learning for image recognition. In *Proceedings of the IEEE conference on computer vision and pattern recognition*, pp. 770–778, 2016.

He, K., Fan, H., Wu, Y., Xie, S., and Girshick, R. Momentum contrast for unsupervised visual representation learning. In *Proceedings of the IEEE/CVF conference on computer vision and pattern recognition*, pp. 9729–9738, 2020.

Hutter, F., Hoos, H., and Leyton-Brown, K. An efficient approach for assessing hyperparameter importance. In *International conference on machine learning*, pp. 754–762. PMLR, 2014.

Hvorfner, C., Stoll, D., Souza, A., Lindauer, M., Hutter, F., and Nardi, L. π bo: Augmenting acquisition functions with user beliefs for bayesian optimization. In *Proceedings of the International Conference on Learning Representations (ICLR’21)*, 2021. Published online: iclr.cc.

Krizhevsky, A. Learning multiple layers of features from tiny images. Technical report, University of Toronto, 2009.

Mockus, J., Tiesis, V., and Zilinskas, A. The application of Bayesian methods for seeking the extremum. *Towards Global Optimization*, 2(117-129), 1978.

Müller, S. G. and Hutter, F. Trivialaugment: Tuning-free yet state-of-the-art data augmentation. In *Proceedings of the IEEE/CVF International Conference on Computer Vision (ICCV)*, pp. 774–782, October 2021.

Negassi, M., Wagner, D., and Reiterer, A. Smart(sampling)augment: Optimal and efficient data augmentation for semantic segmentation. *Algorithms*, 15(5), 2022. ISSN 1999-4893. doi: 10.3390/a15050165. URL <https://www.mdpi.com/1999-4893/15/5/165>.

Pathak, D., Krahenbuhl, P., Donahue, J., Darrell, T., and Efros, A. A. Context encoders: Feature learning by inpainting. In *Proceedings of the IEEE conference on computer vision and pattern recognition*, pp. 2536–2544, 2016.

Radford, A., Kim, J. W., Hallacy, C., Ramesh, A., Goh, G., Agarwal, S., Sastry, G., Askell, A., Mishkin, P., Clark, J., et al. Learning transferable visual models from natural language supervision. In *International Conference on Machine Learning*, pp. 8748–8763. PMLR, 2021.

Raghu, A., Lorraine, J., Kornblith, S., McDermott, M., and Duvenaud, D. K. Meta-learning to improve pre-training. *Advances in Neural Information Processing Systems*, 34, 2021.

Reed, C. J., Metzger, S., Srinivas, A., Darrell, T., and Keutzer, K. Selfaugment: Automatic augmentation policies for self-supervised learning. In *Proceedings of the IEEE/CVF Conference on Computer Vision and Pattern Recognition*, pp. 2674–2683, 2021.

Shahriari, B., Swersky, K., Wang, Z., Adams, R., and de Freitas, N. Taking the human out of the loop: A review of Bayesian optimization. *Proceedings of the IEEE*, 104(1): 148–175, 2016.

Stoll, D., Schrodi, S., Janowski, M., Mallik, N., Théophane, V., and Hutter, F. Neural Pipeline Search (NEPS), May 2022. URL <https://github.com/automl/neps>.

van den Oord, A., Li, Y., and Vinyals, O. Representation learning with contrastive predictive coding. *CoRR*, abs/1807.03748, 2018.

Yang, J., Shi, R., and Ni, B. Medmnist classification dcathlon: A lightweight automl benchmark for medical image analysis. In *IEEE 18th International Symposium on Biomedical Imaging (ISBI)*, pp. 191–195, 2021a.

Yang, J., Shi, R., Wei, D., Liu, Z., Zhao, L., Ke, B., Pfister, H., and Ni, B. Medmnist v2: A large-scale lightweight benchmark for 2d and 3d biomedical image classification. *arXiv preprint arXiv:2110.14795*, 2021b.

Zhang, R., Isola, P., and Efros, A. A. Colorful image colorization. In *12th European Conference on Computer Vision (ECCV’16)*, pp. 649–666, 2016.

Beyond Random Augmentations: Pretraining with Hard Views

The content of this chapter has been published as:

F. Ferreira, I. Rapant, J. K.H. Franke, and F. Hutter (2025). “Beyond Random Augmentations: Pretraining with Hard Views”. In: *Proceedings of the International Conference on Learning Representations (ICLR’25)*. Published online: iclr.cc. ICLR. URL: <https://openreview.net/forum?id=AK1C55o4r7>.

The supplementary material and a detailed statement of contributions is provided in Appendix E.

BEYOND RANDOM AUGMENTATIONS: PRETRAINING WITH HARD VIEWS

Fabio Ferreira*
University of Freiburg

Ivo Rapant*
University of Freiburg

Jörg K.H. Franke
University of Freiburg

Frank Hutter
ELLIS Institute Tübingen &
University of Freiburg

ABSTRACT

Self-Supervised Learning (SSL) methods typically rely on random image augmentations, or *views*, to make models invariant to different transformations. We hypothesize that the efficacy of pretraining pipelines based on conventional random view sampling can be enhanced by explicitly selecting views that benefit the learning progress. A simple yet effective approach is to select *hard views* that yield a higher loss. In this paper, we propose *Hard View Pretraining (HVP)*, a learning-free strategy that extends random view generation by exposing models to more challenging samples during SSL pretraining. HVP encompasses the following iterative steps: 1) randomly sample multiple views and forward each view through the pretrained model, 2) create pairs of two views and compute their loss, 3) adversarially select the pair yielding the highest loss according to the current model state, and 4) perform a backward pass with the selected pair. In contrast to existing hard view literature, we are the first to demonstrate hard view pretraining’s effectiveness at scale, particularly training on the full ImageNet-1k dataset, and evaluating across multiple SSL methods, ConvNets, and ViTs. As a result, HVP sets a new state-of-the-art on DINO ViT-B/16, reaching 78.8% linear evaluation accuracy (a 0.6% improvement) and consistent gains of 1% for both 100 and 300 epoch pretraining, with similar improvements across transfer tasks in DINO, SimSiam, iBOT, and SimCLR.

1 INTRODUCTION

Learning effective and generalizable visual representations in Self-Supervised Learning (SSL) has been approached in various ways. Many SSL methods can be broadly categorized into generative and discriminative approaches (Chen et al., 2020a). Generative methods focus on generating image inputs, while discriminative methods, particularly contrastive learning (Hadsell et al., 2006; He et al., 2020), aim at learning latent representations in which similar image views are located closely, and dissimilar ones distantly.

Such views are generated by applying a sequence of (randomly sampled) image transformations and are usually composed of geometric (cropping, rotation, etc.) and appearance (color distortion, blurring, etc.) transformations. Prior work (Chen et al., 2020a; Wu et al., 2020; Purushwalkam & Gupta, 2020; Wagner et al., 2022; Tian et al., 2020b) has identified *random resized crop* (RRC), which randomly crops the image and resizes it back to a fixed size, as well as color distortion as critical transformations for effective representation learning. However, despite this finding and to our best knowledge, little research has gone into identifying more effective ways for generating views to improve performance.

Existing SSL approaches that attempt to control the hardness of views include adversarial (Shi et al., 2022; Tamkin et al., 2021) or cooperative (Hou et al., 2023) techniques. For

*Equal contribution. Correspondence to: ferreira@cs.uni-freiburg.de

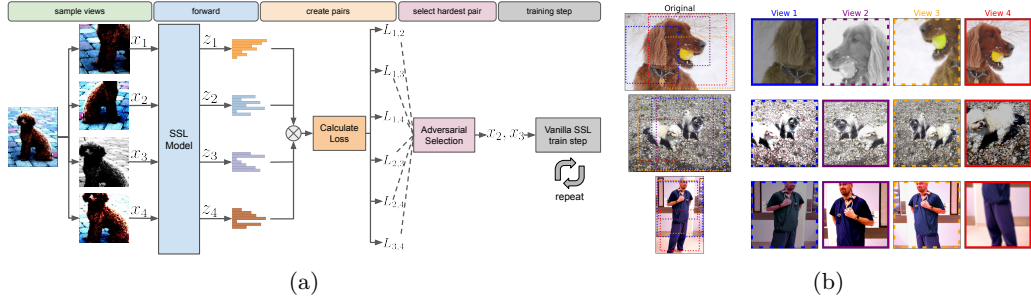


Figure 1: (a) HVP first samples N views, pairs them, and adversarially selects the hardest pair, i.e., the one with the worst loss according to the current model state. (b) Examples (left) and sampled views (right) after transformations. Hard pairs selected by HVP are shown with a solid frame.

instance, Tian et al. (2020b) use mutual information theory to adversarially learn view generators. These methods offer valuable insights into optimizing views but often introduce additional complexity, such as requiring additional models or significant changes to the SSL pipeline, limiting their practicality in state-of-the-art models where resource constraints are already a concern. Similar to what we propose, Koçyigit et al. (2023) introduce a hard view sampling strategy but targeting the acceleration of pretraining. Moreover, their approach requires tuning hyperparameters like learning rate and augmentation magnitude, which can introduce confounding variables. Furthermore, neither Koçyigit et al. (2023) nor Tian et al. (2020b) validate their methods on larger datasets such as ImageNet-1k (Deng et al., 2009), or across larger model architectures, limiting their scalability and applicability.

Building on these observations, we propose *Hard View Pretraining (HVP)*, a fully learning-free, easy-to-integrate approach designed to improve standard pretraining methods without the need for additional model training or complex modifications. Our method leverages the current model state to select challenging samples during pretraining by adversarially sampling pairs of views and selecting the pair that yields the highest loss according to the model’s current state (see Fig. 1a). Unlike previous approaches, HVP requires no hyperparameter tuning and demonstrates scalability to large datasets like ImageNet-1k, offering an efficient and practical solution for improving SSL pretraining. To the best of our knowledge, we are the first to demonstrate the effectiveness of a hard view sampling strategy at scale, particularly on modern architectures like Vision Transformers (ViTs) and training on the full ImageNet dataset. Our approach not only integrates seamlessly with recent state-of-the-art SSL methods but also showcases consistent improvements across both convolutional architectures and ViTs, validating its robustness and scalability.

Overall, our contributions can be summarized as follows:

- We propose *Hard View Pretraining (HVP)*, an easy-to-use method complementing SSL by extending the common random view generation to automatically expose the model to harder samples during pretraining. HVP simply requires the ability to compute sample-wise losses;
- We demonstrate the effectiveness and compatibility of our approach using ImageNet-1k pretraining across four popular SSL methods that cover a diverse range of discriminative objectives such as SimSiam (Chen & He, 2021), DINO (Caron et al., 2021), iBOT (Zhou et al., 2021), and SimCLR (Chen et al., 2020a);
- HVP achieves a new state-of-the-art result on DINO ViT-B/16, improving over the officially reported baseline of 78.2% linear evaluation accuracy by reaching 78.8% (400 epochs). HVP also consistently improves all other baselines by an average of 1% in linear evaluation on ImageNet across 100 and 300 epoch-pretraining runs;
- We show similar improvements on a diverse set of transfer tasks, including finetuning, object detection, and segmentation, and present insights into the underlying mechanisms and robustness of HVP.

We make our PyTorch Paszke et al. (2019) code, models, and all used hyperparameters publicly available under <https://github.com/automl/hvp>.

2 RELATED WORK

2.1 DISCRIMINATIVE SELF-SUPERVISED LEARNING

The core idea behind the discriminative learning framework (Chen et al., 2020a) is to learn image representations by contrasting positive pairs (two views of the same image) against negative pairs (two views of different images) (Hadsell et al., 2006). To work well in practice and to prevent model collapse, contrastive learning methods often require a large number of negative samples (Wu et al., 2018; van den Oord et al., 2018; Chen et al., 2020a; He et al., 2020; Tian et al., 2020a; Chen et al., 2020b) stored in memory banks (Wu et al., 2018; He et al., 2020) or, for instance, in the case of SimCLR, implicitly in large batches (Chen et al., 2020a). Non-contrastive approaches, such as BYOL (Grill et al., 2020), SimSiam (Chen & He, 2021), DINO (Caron et al., 2021) and others (Zbontar et al., 2021; Caron et al., 2020; Ermolov et al., 2021), can only use positive pairs without causing model collapse but rely on other techniques, such as Siamese architectures, whitening of embeddings, clustering, maximizing the entropy of the embeddings, momentum encoders, and more.

2.2 OPTIMIZING FOR HARD VIEWS IN SSL

Due to its performance-improving benefits, the realm of learning task-specific augmentation policies based on data has seen quick development (Cubuk et al., 2019; Ho et al., 2019; Lin et al., 2019; Zhang et al., 2020; Hataya et al., 2020; Hou et al., 2023; Müller & Hutter, 2021). However, these approaches do not include the random resize crop operation in their search spaces, limiting the control of view hardness. Similar to us, Koçyigit et al. (2023) uses the current model state for selecting hard views. However, their approach requires controlling learning hyperparameters, while mostly training on a smaller version of ImageNet and ResNets (He et al., 2016) only. We offer a more complete analysis of hard view pretraining, demonstrating the benefits without potential confounding factors such as hyperparameter adjustments. We also focus on performance rather than pretraining speedups and employ higher budgets (longer pretraining, larger batch sizes) on the full ImageNet dataset and both ResNets and ViTs (Dosovitskiy et al., 2020)). Other works utilize additional networks for view generation, such as Tamkin et al. (2021); Shi et al. (2022); Tian et al. (2020b) (adversarial view generators), Peng et al. (2022) (localization network for semantic awareness), Li et al. (2024) (pretrained generative models to enhance augmentation quality), and Han et al. (2023) (leveraging a pretrained GAN in a SimCLR-only setting). However, unlike HVP, all these methods add non-trivial complexity to the training pipeline by requiring learning auxiliary and adversarial components or are often limited in their applicability across different SSL frameworks (e.g., by requiring negative view pairs).

3 METHOD

3.1 SELF-SUPERVISED LEARNING FRAMEWORK

In this section, we introduce our approach, which is also depicted in Algorithm 1. Many different self-supervised discriminative learning (He et al., 2020) objectives exist, each characterized by variations stemming from design choices, such as by the use of positive and negative samples or asymmetry in the encoder-projector network structure. For simplicity of exposure, we will introduce our approach based on the SimSiam objective (Chen & He, 2021), but we do note that our method can be used with any other discriminative SSL objective that allows the computation of sample-wise losses.

SimSiam works as follows. Assume a given set of images \mathcal{D} , an image augmentation distribution \mathcal{T} , a minibatch of M images $\mathbf{x} = \{x_i\}_{i=1}^M$ sampled uniformly from \mathcal{D} , and two sets of randomly sampled image augmentations A and B sampled from \mathcal{T} . SimSiam applies

A and B to each image in \mathbf{x} resulting in \mathbf{x}^A and \mathbf{x}^B . Both augmented sets of views are subsequently projected into an embedding space with $\mathbf{z}^A = g_\theta(f_\theta(\mathbf{x}^A))$ and $\mathbf{h}^B = f_\theta(\mathbf{x}^B)$ where f_θ represents an encoder (or backbone) and g_θ a projector network. SimSiam then minimizes the following objective:

$$\mathcal{L}(\theta) = \frac{1}{2} (D(\mathbf{z}^A, \mathbf{h}^B) + D(\mathbf{z}^B, \mathbf{h}^A)) \quad (1)$$

where D denotes the negative cosine similarity function. Intuitively, when optimizing θ , the embeddings of the two augmented views are attracted to each other.

3.2 PRETRAINING WITH HARD VIEWS

We now formalize how we expose the model to more challenging views during pretraining. In a nutshell, Hard View Pretraining extends the random view generation by sampling adversarially harder views during pretraining. Instead of having two sets of augmentations A and B , we now sample N sets of augmentations, denoted as $\mathcal{A} = \{A_1, A_2, \dots, A_N\}$. Each set A_i is sampled from the image augmentation distribution \mathcal{T} , and applied to each image in \mathbf{x} , resulting in N augmented sets of views $\mathbf{x}^{A_1}, \mathbf{x}^{A_2}, \dots, \mathbf{x}^{A_N}$. Similarly, we obtain N sets of embeddings $\mathbf{z}^{A_1}, \mathbf{z}^{A_2}, \dots, \mathbf{z}^{A_N}$ and predictions $\mathbf{h}^{A_1}, \mathbf{h}^{A_2}, \dots, \mathbf{h}^{A_N}$ through the encoder and projector networks. We then define a new objective function that seeks to find the pair $(x_i^{A_k}, x_i^{A_l})$ of a given image x_i that yields the highest loss:

$$\begin{aligned} (x_i^{A_k}, x_i^{A_l}) &= \arg \max_{k, l; k \neq l} \mathcal{L}(\theta)_{i, k, l} \\ &= \arg \max_{k, l; k \neq l} \frac{1}{2} (D(z_i^{A_k}, h_i^{A_l}) + D(z_i^{A_l}, h_i^{A_k})), \end{aligned} \quad (2)$$

where $\mathcal{L}(\theta)_{i, k, l}$ simply denotes a sample-wise variant of Eq. 1.

Overall, we first generate N augmented views for each image x_i in the minibatch. Then, we forward these augmented views through the networks and create all combinatorially possible $\binom{N}{2}$ pairs of augmented images. Subsequently, we use Eq. 2 to compute the sample-wise loss for each pair. We then select all pairs that yielded the highest loss to form the new *hard* minibatch of augmented sets $\mathbf{x}^{A_{k*}}$ and $\mathbf{x}^{A_{l*}}$, discard the other pairs and use the hard minibatch for optimization. As shown in Algorithm 1, we repeat this process in each training iteration.

Algorithm 1 Pretraining with Hard Views

- 1: **Input:** Number of views $N \geq 2$, batch size M ,
- 2: augmentation distribution \mathcal{T} , model f
- 3: **for** each x_i in the sampled batch $\{x_i\}_{i=0}^M$ **do**
- 4: Sample N augmentations: $A = \{t_n \sim \mathcal{T}\}_{n=0}^N$
- 5: Create augmented views: $\mathbf{x}_i^A = \{t_n(x_i)\}_{n=0}^N$
- 6: Forward all views through f
- 7: Create all $\binom{N}{2}$ view pairs $\mathbf{x}_i^{A_k} \times \mathbf{x}_i^{A_l}$, $k \neq l$
- 8: Add *hard* pair $(x_i^{A_{k*}}, x_i^{A_{l*}})$ that maximizes Eq. 2 to the new batch with only hard pairs
- 9: Proceed with standard SSL training
- 10: Repeat for all batches
- 11: **return** Pretrained model f

Intuitively, our approach introduces a more challenging learning scenario in which the model is encouraged to learn more discriminative features by being exposed to harder views. In the early stage of training, the embedding space lacks a defined structure for representing similarity among views. As training progresses, our method refines the concept of similarity through exposure to views that, from the perspective of the model, remain challenging given its current state. By limiting the number of sampled views, we upper-bound the difficulty of learning to prevent tasks from becoming too difficult and hindering learning. This ensures a controlled evolution of the embedding space, where the model's perception of difficulty is continuously challenged in tandem with its growing capacity to differentiate views. Consequently, HVP can be seen as a regularization that prevents the model from overfitting to easy views.

While we exemplified the integration of HVP with the SimSiam objective, integrating it into other contrastive methods is as straightforward. The only requirement of HVP is to

be able to compute sample-wise losses (to select the views with the highest loss). In our experiments section and in addition to SimSiam, we study the application of HVP to the objectives of DINO, iBOT, and SimCLR (see also Appendix K.1 for a formal exemplary definition for the integration of HVP into SimCLR).

4 IMPLEMENTATION AND EVALUATION PROTOCOLS

4.1 IMPLEMENTATION

We now describe the technical details of our approach. HVP can be used with any SSL method that allows computing sample-wise losses, and the only two elements in the pipeline we adapt are: 1) the data loader (which now needs to sample N views for each image) and 2) the forward pass (which now invokes a *select* function to identify and return the hard views). The image transformation distribution \mathcal{T} taken from the baselines is left unchanged. Note, for the view selection one could simply resort to random resized crop (RRC) only and apply the rest of the operations after the hard view selection (see Section 6.1 for a study on the influence of appearance on the selection).

All experiments were conducted with $N = 4$ sampled views, yielding $\binom{N}{2} = 6$ pairs to compare, except for DINO which uses 10 views (2 global, 8 local heads) per default. For DINO, we apply HVP to both global and local heads but to remain tractable, we upper-bound the number of total pair comparisons to 128. SimCLR uses positive and negative samples. Following the simplicity of HVP, we do not alter its objective, which naturally leads to selecting hard views that are adversarial to positive and “cooperative” to negative views. For iBOT, we use the original objective as defined by the authors with global views only.

4.2 EVALUATION PROTOCOLS

We now describe the protocols used to evaluate the performance in our main results section. In self-supervised learning, it is common to assess pretraining performance with the linear evaluation protocol by training a linear classifier on top of frozen features or finetuning the features on downstream tasks. Our general procedure is to follow the baseline methods as closely as possible, including hyperparameters and code bases (if reported). It is common to use RRC and horizontal flips during training and report the test accuracy on central crops. Due to the sensitivity of hyperparameters, and as done by Caron et al. (2021), we also report the quality of features with a simple weighted nearest neighbor classifier (k-NN).

5 MAIN RESULTS

Here, we discuss our main results on image classification, object detection, and segmentation tasks. All results are self-reproduced using the original baseline code and hyperparameters (see Appendix Section Afor details).

5.1 EVALUATIONS ON IMAGENET

We report the top-1 validation accuracy on frozen features, as well as the k-NN classifier performance, in Table 1. For DINO, we additionally compare ResNet-50 (He et al., 2016)

Method	Arch.	100 epochs		300 epochs	
		Lin.	k -NN	Lin.	k -NN
DINO	ViT-S/16	73.52	68.80	75.48	72.62
+ HVP	ViT-S/16	74.67	70.72	76.56	73.65
Impr.		+1.15	+1.92	+1.08	+1.03
DINO	RN50	71.93	66.28	75.25	69.53
+ HVP	RN50	72.87	67.33	75.65	70.05
		+0.94	+1.05	+0.40	+0.52
SimSiam	RN50	68.20	57.47	70.35	61.40
+ HVP	RN50	68.98	58.97	70.90	62.97
		+0.78	+1.50	+0.55	+1.57
SimCLR	RN50	63.37	52.83	65.50	55.65
+ HVP	RN50	65.33	54.76	67.30	56.80
		+1.96	+1.93	+1.80	+1.15
iBOT	ViT-S/16	69.55	62.93	72.76	66.92
+ HVP	ViT-S/16	70.27	62.75	73.99	67.16
		+0.73	-0.18	+1.23	+0.24

Table 1: Average top-1 linear and k -NN classification accuracy on the ImageNet validation set for 100 and 300-epoch pretrainings across 3 seeds.

Method	Arch.	CIFAR10		CIFAR100		Flowers102		iNat 21		Food101	
		Lin.	F.T.								
SimSiam	RN50	82.60	95.50	54.20	77.20	34.27	56.40	32.50	60.30	65.70	83.90
+ HVP	RN50	84.40	96.10	57.10	78.20	38.37	58.90	33.90	60.90	67.10	84.70
Impr.		+1.80	+0.60	+2.90	+1.00	+4.10	+2.50	+1.40	+0.60	+1.40	+0.80
DINO	ViT-S/16	94.53	98.53	80.63	87.90	91.10	93.20	46.93	53.97	73.30	87.50
+ HVP	ViT-S/16	95.13	98.65	81.27	88.23	92.07	93.60	49.03	54.16	74.13	87.91
Impr.		+0.60	+0.12	+0.63	+0.33	+0.97	+0.40	+2.10	+0.19	+0.83	+0.41

Table 2: HVP compares favorably against models trained without it when fine-tuned (F.T.) to or linearly evaluated (Lin.) on other datasets (averaged over 3 seeds; 100-ep. preraising).

against the ViT-S/16 (Dosovitskiy et al., 2020) architecture. We point out that both methods, vanilla, and vanilla+HVP always receive the same number of data samples for training. Our method compares favorably against all baselines with an increased performance of approximately 1% on average for 100 and 300 epoch pretraining, showing the benefit of sampling hard views.

Due to limited computing resources, we run the majority of pretrainings in this paper for 100 epochs and 300 epochs (200 epochs for SimCLR) and batch sizes of 512 (100 epoch) or 1024 (200 & 300 epoch trainings), respectively. This choice is in line with a strategy that favors the evaluation of a diverse and larger set of baselines over the evaluation of a less diverse and smaller set and underpins the broad applicability of HVP. We primarily ran our experiments with 8xNVIDIA GeForce RTX 2080 Ti nodes, with which the pretraining and linear evaluation duration ranged from ~ 3.5 to ~ 25 days. While HVP requires roughly 2x the training time of the DINO baseline (see Appendix J for further discussion on the time complexity of HVP), this investment translates directly into improved performance.

Rather than prioritizing efficiency, our focus was on achieving state-of-the-art results, highlighting HVP’s flexibility and robustness across training durations. To showcase this point, we explored the scalability of HVP with larger models and extended training schedules and achieved a new **state-of-the-art result of 78.8% accuracy in linear evaluation, improving over the officially reported baseline of 78.2% on DINO ViT-B/16 (400 epochs)**. For k-NN classification, the same model similarly surpassed the DINO baseline by 0.85%, reaching 76.95% compared to 76.1%. These results demonstrate the scalability of our method to larger models and longer pretraining schedules. We emphasize that HVP is insensitive to the baseline hyperparameters and simply reusing the default ones consistently resulted in improvements in the reported magnitudes across all experiments.

5.2 TRANSFER TO OTHER DATASETS AND TASKS

We now report the transferability of features learned with HVP. For all experiments here, we use our 100-epoch ImageNet pretrained iBOT and DINO ViT-S/16 models, respectively.

5.2.1 LINEAR EVALUATION AND FINETUNING

In Table 2, we apply both the linear evaluation (Lin.) and finetuning (F.T.) protocols to our models across a diverse set of datasets consisting of CIFAR10 (Krizhevsky, 2009), CIFAR100, Flowers102 (Nilsback & Zisserman, 2008), Food101 (Bossard et al., 2014), and iNaturalist 2021 (iNaturalist 2021 competition dataset). Our results show that the improvements achieved by sampling hard views that we observed so far also transfer to other datasets.

Method	Arch.	OD		IS	
		100	300	100	300
iBOT	ViT-S/16	66.13	66.80	63.10	63.63
+ HVP	ViT-S/16	66.50	67.13	63.50	64.23
Impr.		+0.37	+0.33	+0.40	+0.60
DINO	ViT-S/16	65.90	66.60	62.83	63.63
+ HVP	ViT-S/16	66.37	67.00	63.37	64.00
Impr.		+0.47	+0.40	+0.53	+0.37

Table 3: Object Detection (OD) and Instance Segmentation (IS) AP50 performance on COCO for 100/300 epoch pretraining.

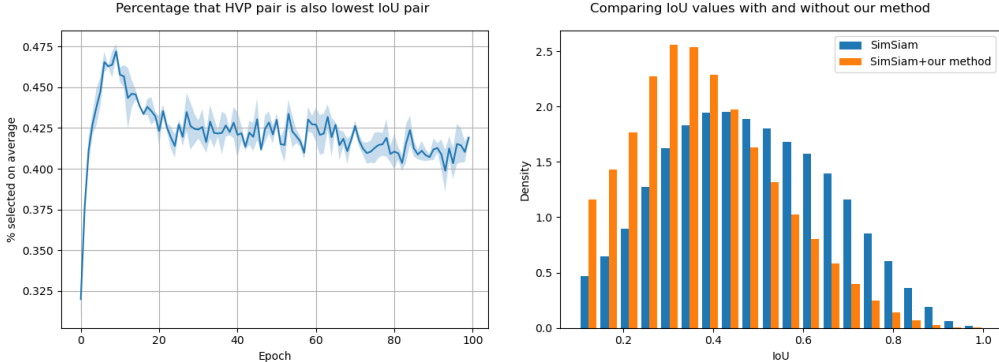


Figure 2: **Left:** In over 40% of the cases, the adversarially selected view pair has also the lowest Intersection over Union throughout SimSiam+HVP pretraining. We attribute the early spike to the random initialization of the embedding. **Right:** HVP (blue) shows a shift to smaller IoU values over standard pretraining (orange). Both results are based on 3 seeds.

5.2.2 OBJECT DETECTION AND INSTANCE SEGMENTATION

For object detection and instance segmentation, we use the COCO (Lin et al., 2014) dataset with Cascade Mask R-CNN (Cai & Vasconcelos, 2019; He et al., 2017). Table 3, where we report the AP50 performance, shows that the features learned with HVP also transfer favorably to these tasks and outperform the iBOT and DINO baseline with a 100-ep. and 300-ep. pretraining. More details and performance results on this task are provided in Appendix H.1.

6 EMPIRICAL ANALYSIS OF HVP

In this section, we discuss studies designed to shed light on the mechanisms underlying HVP. We address the following questions: 1) “Which pattern can be observed that underlies the hard view selection?” and 2) “What are the effects on empowering the adversary?”. For all experiments conducted here, we use our 100-epoch, ImageNet-pretrained SimSiam+HVP models with four sampled views. In Appendix F.1, we also analyze whether we can infer a “manual” augmentation policy from the following observed patterns.

6.1 Q1: WHICH PATTERNS CAN BE OBSERVED WITH HVP?

When visually studying examples and the views selected by HVP in Figures 1b and 5 (in the appendix), we notice that both geometric and appearance characteristics seem to be exploited, for instance, see the brightness difference between the views of the first two rows in Fig. 1b. We also see a generally higher training loss (Fig. 6 in the appendix) indicative of an increased task difficulty.

6.1.1 LOGGING AUGMENTATION DATA

To assess these observations, we logged relevant hyperparameter data during SimSiam training with HVP. The logs include for each view the sampled geometric and appearance parameters from the data augmentation operations (such as the height/width of the crops or the brightness; see Section E in the appendix for more details), as well as the loss and whether the view was selected. As evaluated metrics, we chose the Intersection over Union (IoU), Relative Distance (normalized distance of the center points views), color distortion distance (the Euclidean distance between all four color distortion parameters), and the individual color distortion parameters.

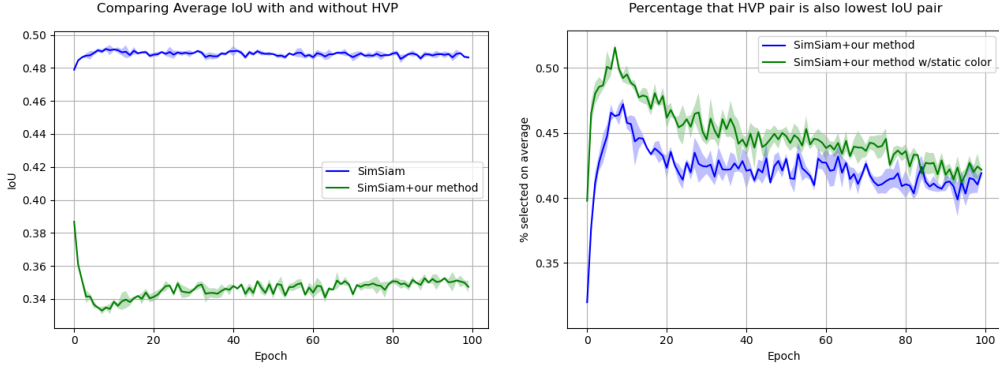


Figure 3: **Left:** The average IoU of view pairs selected by SimSiam+HVP (blue) compared against the default SimSiam training (green). **Right:** Using static color augmentation for all pairs before the selection increases the dependency on the IoU.

6.1.2 IMPORTANCE OF AUGMENTATION METRICS

Given 300k such samples, we then used fANOVA (Hutter et al., 2014) to determine how predictive these metrics are. This resulted in the metric with the highest predictive capacity on the loss being the IoU, explaining 15% of the variance in performance, followed by brightness with 5% (for more details see Fig. 8 in the appendix). The importance of IoU in HVP is further underpinned by the following observation: the fraction of view pairs selected by HVP, which are also the pairs with the lowest IoU among all six pairs ($N=4$), is over 40% (random: $\sim 16.7\%$) during training. Moreover, when using HVP, a shift to smaller IoU values can be observed when comparing against standard pretraining (see Fig. 2).

6.1.3 TAKING A CLOSER LOOK AT THE INTERSECTION OVER UNION

We also examined the IoU value over the course of training in Fig. 3 (left). An observable pattern is that the IoU value with HVP (Fig. 3 (left) in green) is smaller and varies more when compared against training without HVP (blue). We believe this is due to the sample-wise and stateful nature of the adversarial selection as HVP chooses different IoU values between varying samples and model states.

Lastly, we assessed the effect of the color augmentation on the pair selection. For this study, we sampled *one* set of color augmentations (as opposed to one for each view) per iteration and applied it to all views. We apply sampled data augmentations to each view only after identifying the hardest pair. As we show in Fig. 3 (right), the fraction of selected pairs that are also the hardest pairs slightly increases in this case. One possible explanation for this is that it reflects the non-negligible role of color variation between views (as shown previously with the importance analysis), where HVP is given less leverage to increase hardness through a static appearance and instead, depends more on leveraging the IoU. Another key observation is that HVP often chooses view pairs that incorporate zooming in and out or an increased distance between the views (see last row of Fig. 1b).

6.2 Q2: WHAT ARE THE EFFECTS OF STRONG ADVERSARIES?

It is well known that adversarial learning can suffer from algorithmic instability (Xing et al., 2021), e.g. by giving an adversary too much capacity. Here, we further explore the space of adversarial capacity for pretraining with hard views by adapting and varying HVP hyperparameters in order to gain a better understanding of their impact and robustness on discriminative learning. Additionally, we report further results on learning an adversary in Appendix G.1.

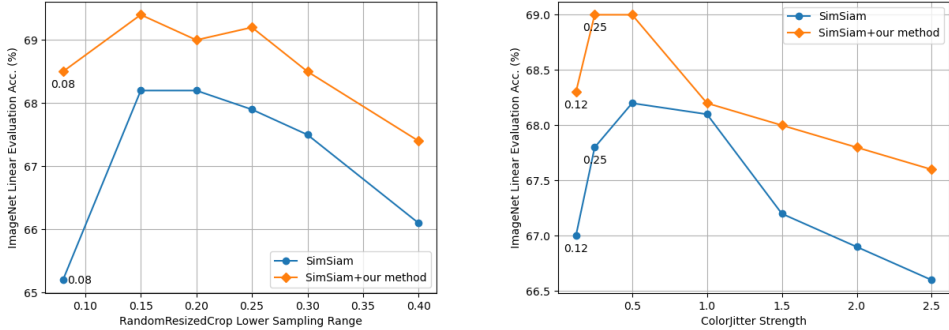


Figure 4: With HVP, SimSiam appears more robust to augmentation hyperparameter variation. We show this for RandomResizedCrop (**left**) and ColorJitter (**right**). For RRC, the values indicate the lower value of the sampling range and for CJ the intensity of the color cues. Results averaged over two seeds and SimSiam defaults are RRC=0.2 and CJ=0.5.

6.2.1 ROBUSTNESS TO AUGMENTATION HYPERPARAMETERS

In assessing the robustness of HVP to augmentation hyperparameters, we conducted an analysis focusing on two primary augmentation operations: RandomResizedCrop (RRC) and ColorJitter (CJ). Our findings depicted in Fig. 4 suggest that HVP enhances the robustness of SSL methods, like SimSiam, against variations in these hyperparameters. Note, when varying one operation, either RRC or CJ, we maintained the other operation at its default configuration. In both settings, we observe less performance degradation with extreme augmentation values and overall smaller degradation rates for HVP. We believe that this robustness stems from hard view pretraining which inadvertently equips the model to handle stronger augmentations.

6.2.2 INCREASING THE NUMBER OF VIEWS

In our initial experiments, we explored variations in the number of sampled views N with SimSiam and HVP. As can be seen in Fig. 7 in the appendix, while $N = 8$ views still outperform the baseline in terms of linear evaluation accuracy, it is slightly worse than using $N = 4$ views (-0.05% for 100 epochs pretraining on linear evaluation). We interpret this result as the existence of a “sweet spot” in setting the number of views, where, in the limit, a higher number of views corresponds to approximating a powerful adversarial learner, capable of choosing very hard and unfavorable learning tasks that lead to model collapse and performance deterioration. We experimented with such an adversarial learner and report results in Appendix G.1.

7 CONCLUSION

We presented HVP, a new data augmentation and learning strategy for Self-Supervised Learning designed to challenge pretrained models with harder samples. This straightforward method allows pushing the effectiveness of the traditional random view generation in SSL. When combined with methods like DINO, SimSiam, iBOT, and SimCLR, HVP consistently showcased improvements of 1% on average in linear evaluation and a diverse set of transfer tasks. HVP achieved a new state-of-the-art result of 78.8% linear evaluation accuracy on DINO ViT-B/16, a 0.6% improvement over the previous baseline. This illustrates the scalability and effectiveness of our approach for larger pretraining settings. With growing models, there is an increasing demand for more data to effectively train them. Synthetic data generation offers a viable solution by enhancing the quantity and diversity of training data. Data augmentation techniques like HVP play a crucial role in this process by creating challenging views, which can serve as synthetic data. All in all, HVP holds promise for scenarios where one seeks to push absolute performance or explore making models less sensitive to hyperparameters, thereby strengthening them for various downstream applications.

REFERENCES

L. Bossard, M. Guillaumin, and L. Van Gool. Food-101 – mining discriminative components with random forests. In *Proc. of ECCV’14*, 2014.

Zhaowei Cai and Nuno Vasconcelos. Cascade r-cnn: High quality object detection and instance segmentation. *IEEE transactions on pattern analysis and machine intelligence*, 43(5):1483–1498, 2019.

M. Caron, I. Misra, J. Mairal, P. Goyal, P. Bojanowski, and A. Joulin. Unsupervised learning of visual features by contrasting cluster assignments. In *Proc. of NeurIPS’20*, 2020.

M. Caron, H. Touvron, I. Misra, H. Jégou, J. Mairal, P. Bojanowski, and A. Joulin. Emerging properties in self-supervised vision transformers. In *Proc. of ICCV’21*, pp. 9630–9640, 2021.

Kai Chen, Jiaqi Wang, Jiangmiao Pang, Yuhang Cao, Yu Xiong, Xiaoxiao Li, Shuyang Sun, Wansen Feng, Ziwei Liu, Jiarui Xu, Zheng Zhang, Dazhi Cheng, Chenchen Zhu, Tianheng Cheng, Qijie Zhao, Buyu Li, Xin Lu, Rui Zhu, Yue Wu, Jifeng Dai, Jingdong Wang, Jianping Shi, Wanli Ouyang, Chen Change Loy, and Dahua Lin. MMDetection: Open mmlab detection toolbox and benchmark. *arXiv preprint arXiv:1906.07155*, 2019.

T. Chen, S. Kornblith, M. Norouzi, and G. E. Hinton. A simple framework for contrastive learning of visual representations. In *Proc. of ICML’20*, pp. 1597–1607, 2020a.

X. Chen and K. He. Exploring simple siamese representation learning. In *Proc. of CVPR’21*, pp. 15750–15758, 2021.

Xinlei Chen, Haoqi Fan, Ross B. Girshick, and Kaiming He. Improved baselines with momentum contrastive learning. *CoRR*, abs/2003.04297, 2020b.

E. Cubuk, B. Zoph, D. Mane, V. Vasudevan, and Q. Le. Autoaugment: Learning augmentation strategies from data. In *Proc. of CVPR’19*, pp. 113–123, 2019.

J. Deng, W. Dong, R. Socher, L. Li, K. Li, and L. Fei-Fei. ImageNet: A Large-Scale Hierarchical Image Database. In *Proc. of CVPR’09*, pp. 248–255, 2009.

A. Dosovitskiy, L. Beyer, A. Kolesnikov, D. Weissenborn, X. Zhai, T. Unterthiner, M. Dehghani, M. Minderer, G. Heigold, S. Gelly, J. Uszkoreit, and N. Houlsby. An image is worth 16x16 words: Transformers for image recognition at scale. *arXiv preprint arXiv:12010.11929*, 2020.

A. Ermolov, A. Siarohin, E. Sangineto, and N. Sebe. Whitening for self-supervised representation learning. In *Proc. of ICML’21*, pp. 3015–3024, 2021.

J. Friedman. Greedy function approximation: A gradient boosting machine. *Annals of Statistics*, pp. 1189–1232, 2001.

J. Grill, F. Strub, F. Altché, C. Tallec, P. H. Richemond, E. Buchatskaya, C. Doersch, B. Ávila Pires, Z. Daniel Guo, M. G. Azar, B. Piot, K. Kavukcuoglu, R. Munos, and M. Valko. Bootstrap your own latent: A new approach to self-supervised learning. In *Proc. of NeurIPS’20*, 2020.

R. Hadsell, S. Chopra, and Y. LeCun. Dimensionality reduction by learning an invariant mapping. In *Proc. of CVPR’06*, pp. 1735–1742, 2006.

L. Han, S. Han, S. Sudalairaj, C. Loh, R. Dangovski, F. Deng, P. Agrawal, D. Metaxas, L. Karlinsky, T.-W. Weng, et al. Constructive assimilation: Boosting contrastive learning performance through view generation strategies. *arXiv preprint arXiv:2304.00601*, 2023.

R. Hataya, J. Zdenek, K. Yoshizoe, and H. Nakayama. Faster autoaugment: Learning augmentation strategies using backpropagation. In *Proc. of ECCV’20*, pp. 1–16, 2020.

K. He, X. Zhang, S. Ren, and J. Sun. Deep residual learning for image recognition. In *Proc. of CVPR’16*, pp. 770–778, 2016.

K. He, G. Gkioxari, P. Dollár, and R. B. Girshick. Mask R-CNN. In *Proc. of ICCV'17*, pp. 2980–2988, 2017.

K. He, H. Fan, Y. Wu, S. Xie, and R. B. Girshick. Momentum contrast for unsupervised visual representation learning. In *Proc. of CVPR'20*, pp. 9726–9735, 2020.

D. Ho, E. Liang, X. Chen, I. Stoica, and P. Abbeel. Population based augmentation: Efficient learning of augmentation policy schedules. In *Proceedings of the 36th International Conference on Machine Learning, ICML 2019, 9-15 June 2019, Long Beach, California, USA*, pp. 2731–2741, 2019.

C. Hou, J. Zhang, and T. Zhou. When to learn what: Model-adaptive data augmentation curriculum. *CoRR*, abs/2309.04747, 2023.

F. Hutter, H. Hoos, and K. Leyton-Brown. An efficient approach for assessing hyperparameter importance. In *Proc. of ICML'14*, pp. 754–762, 2014.

iNaturalist 2021 competition dataset. iNaturalist 2021 competition dataset. https://github.com/visipedia/inat_comp/tree/master/2021, 2021.

M. Jaderberg, K. Simonyan, A. Zisserman, and K. Kavukcuoglu. Spatial transformer networks. In *Proc. of NeurIPS'15*, pp. 2017–2025, 2015.

M. Taha Koçyigit, T. M. Hospedales, and H. Bilen. Accelerating self-supervised learning via efficient training strategies. In *Proc. of WACV*, pp. 5643–5653. IEEE, 2023.

A. Krizhevsky. Learning multiple layers of features from tiny images. Technical report, University of Toronto, 2009.

X. Li, Y. Yang, X. Li, J. Wu, Y. Yu, B. Ghanem, and M. Zhang. Genview: Enhancing view quality with pretrained generative model for self-supervised learning. In *ECCV*, pp. 306–325, 2024.

C. Lin, M. Guo, C. Li, X. Yuan, W. Wu, J. Yan, D. Lin, and W. Ouyang. Online hyperparameter learning for auto-augmentation strategy. In *Proc. of ICCV'19*, pp. 6578–6587, 2019.

T.-Y. Lin, M. Maire, S. Belongie, J. Hays, P. Perona, D. Ramanan, P. Dollár, and C. Zitnick. Microsoft COCO: common objects in context. In *Proc. of ECCV'14*, pp. 740–755, 2014.

I. Loshchilov and F. Hutter. Decoupled weight decay regularization. In *Proc. of ICLR'19*, 2019.

S. Müller and F. Hutter. Trivialaugment: Tuning-free yet state-of-the-art data augmentation. In *Proc. of ICCV'21*, pp. 774–782, 2021.

M.-E. Nilsback and A. Zisserman. Automated flower classification over a large number of classes. In *Proc. of ICVGIP'08*, pp. 722–729, 2008.

A. Paszke, S. Gross, F. Massa, A. Lerer, et al. PyTorch: An imperative style, high-performance deep learning library. In *Proc. of NeurIPS'19*, pp. 8024–8035, 2019.

X. Peng, K. Wang, Z. Zhu, M. Wang, and Y. You. Crafting better contrastive views for siamese representation learning. In *Proc. of CVPR'22*, pp. 16031–16040, 2022.

S. Purushwalkam and A. Gupta. Demystifying contrastive self-supervised learning: Invariances, augmentations and dataset biases. In *Proc. of NeurIPS'20*, 2020.

Y. Shi, N. Siddharth, P. H. S. Torr, and A. R. Kosiorek. Adversarial masking for self-supervised learning. In *Proc. of ICML'22*, volume 162, pp. 20026–20040, 2022.

A. Tamkin, M. Wu, and N. D. Goodman. Viewmaker networks: Learning views for unsupervised representation learning. In *Proc. of ICLR'21*, 2021.

Y. Tian, D. Krishnan, and P. Isola. Contrastive multiview coding. In *Proc. of ECCV'20*, pp. 776–794, 2020a.

Y. Tian, C. Sun, B. Poole, D. Krishnan, C. Schmid, and P. Isola. What makes for good views for contrastive learning? In *Proc. of NeurIPS'20*, 2020b.

A. van den Oord, Y. Li, and O. Vinyals. Representation learning with contrastive predictive coding. *CoRR*, abs/1807.03748, 2018.

D. Wagner, F. Ferreira, D. Stoll, R. T. Schirrmeyer, S. Müller, and F. Hutter. On the importance of hyperparameters and data augmentation for self-supervised learning. In *Pre-Training Workshop at the International Conference for Machine Learning (ICML)*, 2022. URL <https://icml.cc/virtual/2022/20697>.

M. Wu, C. Zhuang, M. Mosse, D. Yamins, and N. D. Goodman. On mutual information in contrastive learning for visual representations. *arXiv:2005.13149 [cs.CV]*, 2020.

Z. Wu, Y. Xiong, S. X. Yu, and D. Lin. Unsupervised feature learning via non-parametric instance-level discrimination. In *Proc. of CVPR'18*, 2018.

Y. Xing, Q. Song, and G. Cheng. On the algorithmic stability of adversarial training. In *Proc. of NeurIPS'21*, pp. 26523–26535, 2021.

Y. You, I. Gitman, and B. Ginsburg. Large batch training of convolutional networks. *arXiv preprint arXiv:1708.03888*, 2017.

J. Zbontar, L. Jing, I. Misra, Y. LeCun, and S. Deny. Barlow twins: Self-supervised learning via redundancy reduction. In *Proc. of ICML'21*, pp. 12310–12320, 2021.

X. Zhang, Q. Wang, J. Zhang, and Z. Zhong. Adversarial AutoAugment. In *Proc. of ICLR'20*, 2020.

J. Zhou, C. Wei, H. Wang, W. Shen, C. Xie, A. L. Yuille, and T. Kong. ibot: Image BERT pre-training with online tokenizer. In *Proc. of ICML'22*, 2021.

Learning Synthetic Environments and Reward Networks for Reinforcement Learning

The content of this chapter has been published as:

F. Ferreira, T. Nierhoff, A. Sälinger, and F. Hutter (2022). “Learning Synthetic Environments and Reward Networks for Reinforcement Learning”. In: *Proceedings of the International Conference on Learning Representations (ICLR’22)*. Published online: iclr.cc. ICLR. URL: <https://iclr.cc/virtual/2022/poster/6495>.

The supplementary material and a detailed statement of contributions is provided in Appendix G.

LEARNING SYNTHETIC ENVIRONMENTS AND REWARD NETWORKS FOR REINFORCEMENT LEARNING

Fabio Ferreira ¹ **Thomas Nierhoff** ¹ **Andreas Sälinger** ¹ **Frank Hutter** ^{1, 2}

¹ University of Freiburg ² Bosch Center for Artificial Intelligence

{ferreira, fh}@cs.uni-freiburg.de

ABSTRACT

We introduce *Synthetic Environments* (SEs) and *Reward Networks* (RNs), represented by neural networks, as proxy environment models for training Reinforcement Learning (RL) agents. We show that an agent, after being trained exclusively on the SE, is able to solve the corresponding real environment. While an SE acts as a full proxy to a real environment by learning about its state dynamics and rewards, an RN is a partial proxy that learns to augment or replace rewards. We use bi-level optimization to evolve SEs and RNs: the inner loop trains the RL agent, and the outer loop trains the parameters of the SE / RN via an evolution strategy. We evaluate our proposed new concept on a broad range of RL algorithms and classic control environments. In a one-to-one comparison, learning an SE proxy requires more interactions with the real environment than training agents only on the real environment. However, once such an SE has been learned, we do not need *any* interactions with the real environment to train new agents. Moreover, the learned SE proxies allow us to train agents with fewer interactions while maintaining the original task performance. Our empirical results suggest that SEs achieve this result by learning informed representations that bias the agents towards relevant states. Moreover, we find that these proxies are robust against hyperparameter variation and can also transfer to unseen agents.

1 INTRODUCTION

Generating synthetic data addresses the question of what data is required to achieve a rich learning experience in machine learning. Next to increasing the amount of available data, synthetic data can enable higher training efficiency that opens up new applications for Neural Architecture Search (Such et al., 2020), may improve algorithm analysis or facilitate custom datasets (Jhang et al., 2020).

In this paper, we consider learning neural synthetic data generators for Reinforcement Learning (RL). We investigate the question of whether we can learn a synthetic Markov Decision Process of a real (target) environment which is capable of producing synthetic data to allow effective and more efficient agent training, that is, to achieve similar or higher performance more quickly compared to when training purely on the real environment. When learning to produce both states and rewards, we refer to these neural network proxies as *synthetic environments* (SEs). Additionally, we investigate the same question for learning reward proxies that do not learn about the state dynamics and which we refer to as a *Reward Networks* (RNs).

We depict our procedure in Figure 1 which resembles a bi-level optimization scheme consisting of an outer and inner loop. The inner loop trains the agent on an SE or RN. Since our method is agnostic to both domain and agent, we can interchangeably adopt standard RL algorithms in the inner loop. In the outer loop, we assess the agent’s performance by evaluating it on the real environment; we then take the collected reward as a score to update the SE’s or RN’s neural parameters used in the inner loop. In this way, the SE/RN is gradually updated such that an agent being trained on it, scores higher on a real environment. For the outer loop we use Evolution Strategies (Rechenberg, 1973; Salimans et al., 2017) with a population of SE/RN parameters.

After discussing related work (Section 2), we make the following contributions:

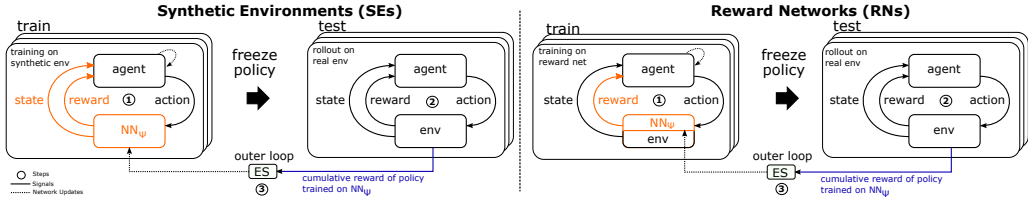


Figure 1: We use an agent-agnostic meta-learning approach to learn neural proxy RL environments (left) and reward networks (right) for a target task. In the inner loop, we train RL agents on the proxy and use the evaluation performance on the target task in the outer loop to evolve the proxy.

- We introduce synthetic environments (Section 3), a novel concept that focuses on the environment instead of agent learning using a bi-level optimization scheme, which is guided purely by the agent performance. This concept goes beyond the usual learning of a one-time internal environment model inside an agent (such as in Dyna (Sutton, 1990)).
- As a sub-problem of SEs, we investigate reward networks (Section 4), contrasting several types of potential-based reward shaping (Ng et al., 1999) variants.
- We show that it is possible to learn SEs (Section 5) and RNs (Section 6) that, when used for agent training, yield agents that successfully solve the Gym tasks (Brockman et al., 2016) CartPole and Acrobot (SEs), as well as Cliff Walking, CartPole, MountainCarContinuous, and HalfCheetah (RNs).
- We show that SEs and RNs are efficient and robust in training agents, require fewer training steps compared to training on the real environment and are able to train unseen agents
- We report empirical evidence showing that SEs and RNs achieve their efficiency gains for training new agents through condensed and informed state and reward representations.

Overall, we find it noteworthy that it is actually possible to learn such proxies, and we believe our research will improve their understanding. Since these learned proxies can train agents quickly and transfer to unseen agents, we believe this work might open up possible avenues of research in RL. Possible future applications include cheap-to-run environments for AutoML (Hutter et al., 2019) or for robotics when training on targets is expensive, as well as agent and task analysis, or efficient RL agent pre-training. Our PyTorch (Paszke et al., 2019) code and models are made available publicly.¹

2 RELATED WORK

Synthetic Environments In the context of RL, learning synthetic environments is related to model-based RL (MBRL) where the dynamics model can be viewed as an SE. In MBRL, one jointly learns both a dynamics model and a policy as in Dyna (Sutton, 1990) or an existing dynamics model is used with planning methods to learn a policy (Silver et al., 2017; Moerland et al., 2020). Our work does not involve planning, nor does it use supervised learning for the dynamics model and it does not mix synthetic and real data during policy learning. Instead, we use purely synthetic data to train agents similar to World Models (Ha & Schmidhuber, 2018) but use the cumulative rewards from the real environment in a bi-level optimization for learning our model jointly with our agent. For a more extensive discussion on the differences between our work and model-based RL, we refer the reader to Appendix D.

Analogous to learning SEs is Procedural Content Generation (Togelius et al., 2011) and Curriculum Learning that concerns automatically selecting (Matiisen et al., 2020) or generating the content of training environments (Volz et al., 2018; Shaker et al., 2016; Wang et al., 2019; Cobbe et al., 2020), with the closest work being Generative Playing Networks (GPNs) (Bontrager & Togelius, 2020). GPNs learn an environment generator that creates increasingly difficult SEs according to what a critic's value function estimates as challenging. While GPNs are a method to generate environment curricula, our approach studies learning an SE for effective and efficient agent training by compressing the relevant information into a single model of the environment. We also use a more generally

¹https://github.com/automl/learning_environments

applicable objective that does not rely on actor-critic formulations but purely on the achieved cumulative reward. Less related areas are methods like domain randomization (Tobin et al., 2017) that generate environments regardless of agent performance or minimax methods that adversarially (instead of cooperatively) generate environments based on the difference between the reward of two competing agents that are trying to solve the generated environment (Dennis et al., 2020).

Related to our work, and inspiring it, are Generative Teaching Networks (Such et al., 2020). While we similarly use a bi-level optimization to learn a synthetic data generator, our approach is different in central aspects: we use Evolution Strategies to avoid the need for explicitly computing Hessians, we do not use noise vectors as input to our SEs, and we target sequential decision-making problems instead of supervised learning.

Reward Networks Reward shaping concerns the question of how to enhance the reward signal to allow agents to be trained more effectively or efficiently. Common learned reward shaping approaches are curiosity or count-based exploration (Pathak et al., 2017; Burda et al., 2019; Singh et al., 2010; Bellemare et al., 2016; Tang et al., 2017). Others achieve reward shaping with prior knowledge through expert demonstrations (Judah et al., 2014; Brys et al., 2015; Ibarz et al., 2018). In contrast to our work, these contributions all apply a single-level optimization. When using a bi-level optimization, the reward shaping function is usually learned in the outer loop while the policy using the learned rewards is optimized in the inner loop. Here, one way is to meta-learn the parameterization of reward functions (Faust et al., 2019; Hu et al., 2020; Jaderberg et al., 2019). Another way is to learn a neural network that resembles the reward function.

While learning full synthetic environments is entirely novel, there exists prior work on learning reward shaping networks. The most related works are (Zheng et al., 2018) for single tasks, (Zou et al., 2019) for entire task distributions, or (Zheng et al., 2020) that additionally take into account the entire lifetime of an agent to learn a “statefulness across episodes”-reward function. Despite the similarities, some noteworthy differences exist. Importantly, the approaches in (Zheng et al., 2018; Zou et al., 2019) are not agent-agnostic, making it less straightforward to exchange agents as in our work. Moreover, the transferability of learned shaped rewards is studied only limitedly (Zheng et al., 2018), not at all (Zou et al., 2019) or only for grid world-like environments (Zheng et al., 2020).

3 LEARNING SYNTHETIC ENVIRONMENTS

Problem Statement Let $(\mathcal{S}, \mathcal{A}, \mathcal{P}, \mathcal{R})$ be a Markov Decision Process (MDP) with the set of states \mathcal{S} , the set of actions \mathcal{A} , the state transition probabilities \mathcal{P} and the immediate rewards \mathcal{R} when transitioning from state $s \in \mathcal{S}$ to the next state $s' \in \mathcal{S}$ through action $a \in \mathcal{A}$. The MDPs we consider are either human-designed environments \mathcal{E}_{real} or learned synthetic environments $\mathcal{E}_{syn, \psi}$ (SE) represented by a neural network with parameters ψ . Interfacing with the environments is identical in both cases, i.e. $s', r = \mathcal{E}(s, a)$. The crucial difference is that for SEs, the state dynamics and rewards are learned. The main objective of an RL agent when acting on an MDP \mathcal{E}_{real} is to find a policy π_θ parameterized by θ that maximizes the cumulative expected reward $F(\theta; \mathcal{E}_{real})$. We consider the following bi-level optimization problem: find the parameters ψ^* , such that the agent policy π_θ parameterized with θ that results from training on $\mathcal{E}_{syn, \psi^*}$ achieves the highest reward on a target environment \mathcal{E}_{real} . Formally that is:

$$\begin{aligned} \psi^* &= \arg \max_{\psi} F(\theta^*(\psi); \mathcal{E}_{real}) \\ \text{s.t. } \theta^*(\psi) &= \arg \max_{\theta} F(\theta; \mathcal{E}_{syn, \psi}). \end{aligned} \tag{1}$$

We use standard RL algorithms for optimizing the agents on the SE in the inner loop. Although gradient-based optimization methods can be applied in the outer loop, we chose Natural Evolution Strategies (Wierstra et al., 2008) (NES) to allow the optimization to be independent of the choice of the agent in the inner loop and to avoid potentially expensive, unstable meta-gradients (Metz et al., 2019). Additional advantages of NES are that it is better suited for long episodes, sparse or delayed rewards, and parallelization (Salimans et al., 2017).

Algorithm We now explain our method. The overall scheme is adopted from (Salimans et al., 2017) and depicted in Algorithm 1. It consists of an Evolutionary Strategy in the outer loop

to learn the SE and an inner loop which trains RL agents. The performances of the trained agents are then used in the outer loop to update the SE. We instantiate the population search distribution as a multivariate Gaussian with mean 0 and a fixed covariance $\sigma^2 I$. The main difference to (Salimans et al., 2017) is that, while they maintain a population over agent parameter vectors, our population consists of SE parameter vectors. Moreover, our approach involves two optimizations (the agent and the SE parameters) instead of one (agent parameters). Our algorithm first stochastically perturbs each population member i which results in ψ_i (Line 5). Then, a new randomly initialized agent is trained on the SE parameterized by ψ_i for n_e episodes (L6). The trained agent with fixed parameters is then tested across 10 episodes on the real environment (L7), yielding the average cumulative reward which we use as a score $F_{\psi,i}$. Finally, we update ψ with a stochastic gradient estimate based on all member scores (L8). We use a parallelized version of the algorithm and an early stopping heuristic to stop in fewer than n_e episodes when progress plateaus (more in Appendix A.1).

4 LEARNING REWARD NETWORKS

Learning both the state dynamics and rewards can be challenging (see Section 7). To reduce computational complexity but still be able to achieve training efficiency, one can therefore reduce the problem formulation to only learn (to augment) the rewards and make use of the real environment for the state dynamics (and original rewards) as illustrated in Figure 1. We reuse the formulation of \mathcal{E}_{syn} and \mathcal{E}_{real} from the problem statement (Eq. 1) and describe learning reward networks as getting the next state and reward $s', r = \mathcal{E}_{real}(s, a)$ and a corresponding synthetic reward $r_{syn} = \mathcal{E}_{rn,\psi}(s, a, s')$ with a (reward) environment represented by a neural network ψ . In the domain of *reward shaping*, r_{syn} is usually added to r to generate an augmented reward $r_{aug} = r + r_{syn}$. A popular approach in reward shaping is potential-based reward shaping (PBRs) (Ng et al., 1999), which defines \mathcal{E}_{rn} as $\mathcal{E}_{rn,\psi}(s, a, s') = \gamma\Phi(s') - \Phi(s)$ with a potential function $\Phi : \mathcal{S} \rightarrow \mathbb{R}$ and a discount factor $\gamma \in (0, 1]$. We adopt PBRs for finding $\mathcal{E}_{rn,\psi}$, represent Φ as a neural network with parameters ψ and use Algorithm 1 to learn ψ . PBRs has the useful property of preserving optimality of policies (Ng et al., 1999) but we also introduce additional variants of $\mathcal{E}_{rn,\psi}$, listed in Table 1, which are motivated by PBRs but are not typically referred to as PBRs as they may not have such guarantees. These variants are motivated by the idea that fewer constraints may enable better reward learning (e.g., in case the difference of potential functions imposes a too strong constraint on the hypothesis space). For simplicity, we refer to the output of Reward Networks (RNs) as r_{aug} .

We now point out the differences between the RN and the SE case. When training on SEs, we use a heuristic for determining the number of required training episodes since both rewards and states are synthetic (see Appendix A.1). In the RN case, the real states allow us to directly observe episode termination, thus such a heuristic is not needed. Another difference to SEs lies in the *EvaluateAgent* function of Algorithm 1: Optimizing SEs for the maximum cumulative reward automatically yielded fast training of agents as a side-product, likely due to efficient synthetic state dynamics. Since we do not learn state dynamics in RNs and motivated by the efficiency gains, we now directly optimize the number of training steps n_{tr} the *TrainAgent* function requires to solve the real environment when being trained on an RN. Additionally, we include the cumulative reward threshold of the real environment C_{sol} and the cumulative reward at the end of training C_{fin} , yielding the final objective $n_{tr} + w_{sol} * \max(0, C_{sol} - C_{fin})$ (to be minimized) where $w_{sol} \in \mathbb{R}_{>0}$ gives

Table 1: Overview of Reward Network variants.

Reward Network	r_{aug}
Additive Potential RN (Ng et al., 1999)	$r + \gamma\Phi(s') - \Phi(s)$
Exclusive Potential RN	$\gamma\Phi(s') - \Phi(s)$
Additive Non-Potential RN	$r + \Phi(s')$
Exclusive Non-Potential RN	$\Phi(s')$

us control over efficiency and effectiveness an RN should achieve. In Appendix B.4, we study the influence of alternative RN optimization objectives.

5 EXPERIMENTS WITH SYNTHETIC ENVIRONMENTS

Experimental Setup So far we have described our proposed method on an abstract level and before we start with individual SE experiments we describe the experimental setup. In our work, we refer to the process of optimizing for suitable SEs with Algorithm 1 as *SE training* and the process of training agents on SEs as *agent training*). For both SE and agent training on the discrete-action-space CartPole-v0 and Acrobot-v1 environments, we use DDQN (van Hasselt et al., 2016). We also address generalization from an algorithmic viewpoint by varying the agent hyperparameters during SE training (Line 6) after each outer loop iteration. Also, we study how robustly found SEs can train agents under varying agent hyperparameters and how well they transfer in training unseen agents. For studying transferability of SEs, we use Dueling DDQN (Wang et al., 2016) and TD3 (Fujimoto & H. Hoof, 2018). TD3 is chosen because it does not solely rely on Q-Learning and is an algorithm of the actor-critic family. Both our tasks employ a discrete action space and to be able to use TD3 we use a Gumbel-Softmax distribution (Jang et al., 2017).

We wrap our algorithm in another outer loop to optimize some of the agent and NES HPs with the multi-fidelity Bayesian optimization method BOHB (Falkner et al., 2018) to identify stable HPs. The optimized HPs are reported in Table 3 in the appendix. We did not optimize some of the HPs that would negatively affect run time (e.g., population size, see Table 4 in the appendix). After identifying the agent and NES HPs, we removed BOHB and used the found HPs for SE training. Once SEs were found, we reverted from specific agent HPs that worked best for training SEs to default agent HPs as reported in Table 5 (appendix) to test out-of-the-box applicability.

Feasibility After introducing the core concept of learning SEs, we now investigate its efficacy of learning SEs for the CartPole and Acrobot tasks. First, we identified stable DDQN and NES hyperparameters. Then, we ran Algorithm 1 with 16 population members for 200 NES outer loop iterations to generate the SEs. We depict the result in Figure 2, which shows the average of the 16 members’ evaluation scores (given by *EvaluateAgent* in Algorithm 1) as a function of the NES outer loop iterations for multiple NES optimization runs (thin lines). The thick solid lines show the average of these. Notice that 50 NES iterations are often sufficient to find SEs that teach agents to solve a task (for more details, we refer the reader to the Appendix Section A).

Performance of SE-trained Agents As we have shown in the last section, learning SEs that can teach agents the CartPole and Acrobot task is feasible with the proposed concept. Now, we investigate how efficient and hyperparameter-sensitive the generated SEs are. For this, we distinguish three different cases: 1) *train: real*, 2) *train: synth., HPs: varied*, and 3) *train: synth., HPs: fixed*. The first is our baseline for which we train agents only on the real environment without any involvement of SEs. The second case denotes SEs for which we randomly sampled agent hyperparameters (HPs) from the ranges in Table 2 before each *TrainAgent* call *during SE training*. Lastly, the third case is similar to the second except that we did not randomly sample agent HPs but rather used the optimized ones reported in Table 3 which we kept *fixed during SE training*.

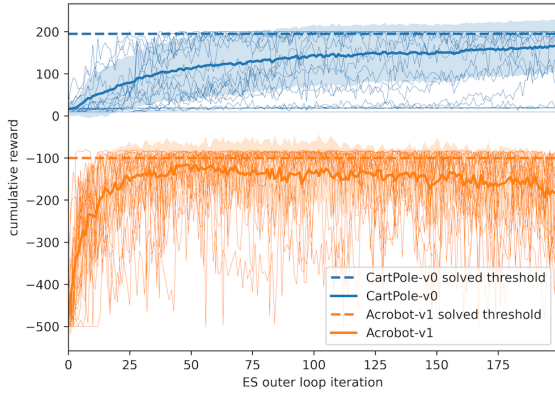


Figure 2: Multiple NES runs of Alg. 1 for CartPole (top) and Acrobot (bottom) which can teach agents the task effectively. Each thin line is the average of 16 worker scores from *EvaluateAgent* of such a run.

Table 2: Agent hyperparameter ranges sampled from for training SEs and agents.

Agent hyperparam.	Value range	log scale
learning rate	$[10^{-3}/3, 10^{-3} * 3]$	✓
batch size	[42, 384]	✓
hidden size	[42, 384]	✓
hidden layer	[1, 3]	x

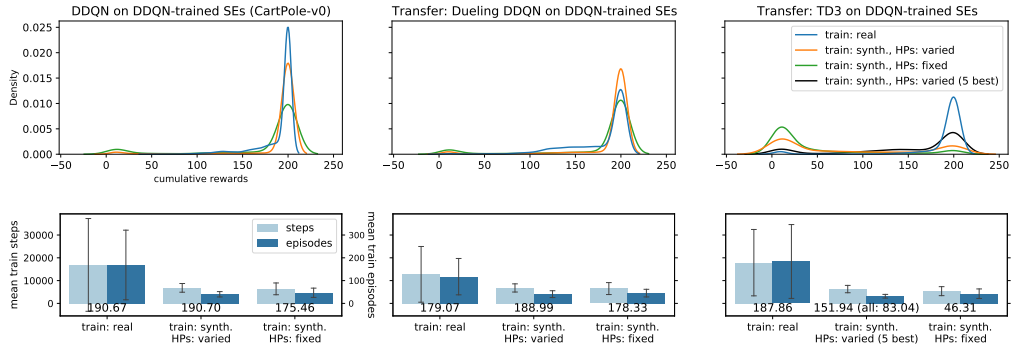


Figure 3: **Top row:** Densities based on each 4000 cumulative test rewards collected by DDQN (left), Dueling DDQN (center), and discrete TD3 (right) agents on CartPole. We show three settings: agents trained on a real environment without any involvement of SEs (blue, baseline), on SEs where the agent HPs were fixed during SE training (green), and on SEs when agent HPs were varied during SE training (orange). After training, the evaluation is always done on the real environment. In all three settings, we randomly sample the agent HPs before agent training. **Bottom row:** Average train steps and episodes corresponding to the densities along with the mean reward (below bars). When training on SEs, we train 30-65% faster compared to training on the real environment.

We first trained 40 SEs for each of the cases 2) and 3); then, we evaluated all approaches with the following procedure: on each SE we trained 10 DDQN agents with randomly sampled HPs according to Table 2. After agent training, we evaluated each agent on the real environment across 10 test episodes, resulting in 4000 evaluations. For our baseline, where no SE is involved, the procedure was identical except that we used 40 *real* environment instantiations instead of SEs to obtain the same number of evaluations. We then used the cumulative rewards from the test episodes for generating the densities in Figure 3 and report the average episodes and training steps required until the heuristic for stopping agent training on SEs/real environment is triggered (Appendix A.1).

Training DDQN agents on DDQN-trained SEs without varying the agent’s HPs (green) during SE training clearly yielded the worst results. We attribute this to overfitting of the SEs to the specific agent HPs.² Instead, when varying the agent HPs (orange) during SE training, we observe that the SEs are consistently able to train agents using $\sim 60\%$ fewer steps (6818 vs. 16887) on average while being more stable than the baseline (fewer train steps / lower episode standard deviations and little mass on density tails). Lastly, the SEs also show little sensitivity to HP variations.

Transferability of SEs In the previous section we evaluated the performance of DDQN-trained SEs in teaching DDQN agents. However, since many environment observations are needed for SE training, it would be beneficial if DDQN-trained SEs are capable of effectively training unseen agents as well. To study this question, we reuse the DDQN-trained SEs from above but now train Dueling DDQN agents on the SEs. From Figure 3 (top and bottom center) we conclude that the transfer to the Dueling DDQN agent succeeds and it facilitates a $\sim 50\%$ faster (6781 vs. 12745 train steps), a more effective (higher reward), and noticeably more stable training (lower std. dev.; smaller tails) on average when compared to the baseline (orange vs. blue). As before, not varying the DDQN agent HPs during SE training reduces transfer performance (green).

We also analyzed the transfer from Q-Learning to a discrete version of TD3 (see Section 3). The result shown in Figure 3 (top right) indicates a limited transferability. We believe this may be due to the different learning dynamics of actor-critics compared to learning with DDQN. However, we also noticed that individual SE models can consistently train TD3 agents successfully while remaining efficient. To show this, we repeated the evaluation procedure from Figure 3 individually for each SE model (see Appendix F.1.1) and selected five SE models that yielded high rewards when training TD3 agents. As a consequence, we can again significantly improve the performance (black curve) with a $\sim 65\%$ speed-up (6287 vs. 17874 train steps; 187 vs. 152 reward) over the baseline.

²We note that even in the "HPs: varied" case we are not evaluating whether SEs extrapolate to new HP ranges but rather how sensitive SEs react to HP variation within known ranges.

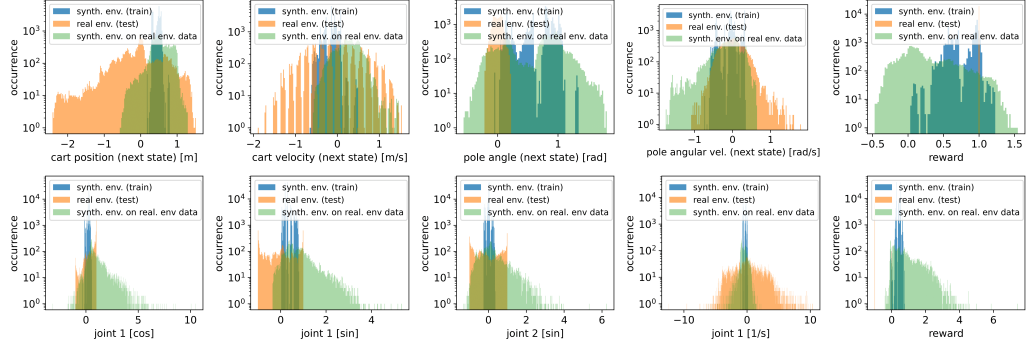


Figure 4: **Top row:** Histograms of next state s' and reward r produced by 10 DDQN agents when trained on a CartPole SE (blue) and afterwards tested for 10 episodes on a real environment (orange). We also show the SE responses when fed with real environment data seen during testing (green). **Bottom row:** The same for Acrobot (subset of state dimensions shown due to brevity).

We executed these experiments with similar results for the Acrobot task (solved with a reward ≥ -100 , see Figure 7 in the appendix). In short, we find that the transfer to Dueling DDQN facilitates a $\sim 38\%$ faster training on average (18376 vs. 29531 steps, mean reward: -111). The discrete TD3 transfer shows a $\sim 82\%$ (14408 vs. 80837 steps, five best models) speed-up but many of the runs also fail (reward: -343) which partly may be due to a sub-optimal hyperparameter selection. Simultaneously, we see that SE-learned policies in the Dueling DDQN transfer case are substantially better on average than those learned on the real environment. All in all, we believe these results are intriguing and showcase the potential of our concept to learn proxy RL environments.

Analyzing SE Behavior In the following, we try to illuminate the inner workings to explain the efficacy of the learned SEs. We exploit CartPole’s and Acrobot’s small state space and visualize an approximation of the state and reward distributions generated by agents trained on SEs and evaluated on real environments. First, we trained 10 DDQN agents on a randomly selected SE with default HPs and logged all (s, a, r, s') tuples. Second, we evaluated the SE-trained DDQN agents on the real environment for 10 test episodes each and again logged the tuples. Lastly, we visualized the histograms of the collected next states and rewards in Figure 4. We observe distribution shifts between the SE and the real environment on both tasks, indicating the agent encounters states and rewards it has rarely seen during training, yet it can solve the task (reward: 199.3 on CartPole and -91.62 on Acrobot). Moreover, some of the synthetic *state* distributions are narrower or wider than their real counterparts, e.g., the real pole angle in CartPole is box-bounded inside ± 0.418 rad but the SEs may benefit from not having such a constraint. The synthetic *reward* distribution is wider than the real one, indicating that the sparse reward distribution becomes dense. The green histograms show the SE responses when fed with real environment data based on the logged state-action the agents have seen during testing. Since the green distributions align better with the blue than the orange ones, we conclude it is more likely the shifts are generated by the SE than the agents itself.

Based on these findings, we hypothesize the SEs produce an informed representation of the target environment by modifying the state distributions to bias agents towards relevant states. These results are likely to explain the efficacy of SEs and can be understood as efficient agent “guiding systems”. We also observed similar patterns with Dueling DDQN and discrete TD3 (see Appendix A.4).

6 EXPERIMENTS WITH REWARD NETWORKS

Experimental Setup To better understand our RN experiments, we first describe similarities and dissimilarities to the experimental setup used for SEs. Similar to SEs, to learn RNs, we first identified stable agent and NES HPs (see Appendix B.3) for each of a total of four environments. Contrary to training SEs, we do not vary the agent HPs *during RN training* as we did not observe improvements in doing so. Now, given these HPs, we then trained multiple RNs for 50 NES outer loop iterations with 16 workers for each environment. For CartPole-v0 we used DDQN for RN training and, similar to SEs, evaluated the transferability of DDQN-trained RNs to train Dueling DDQN agents. For the custom environment Cliff Walking (Sutton & Barto, 2018) (see Appendix B.2 for more details) we used Q-Learning (Watkins, 1989) and show transfer to SARSA (Rummery & Niranjan, 1994). We

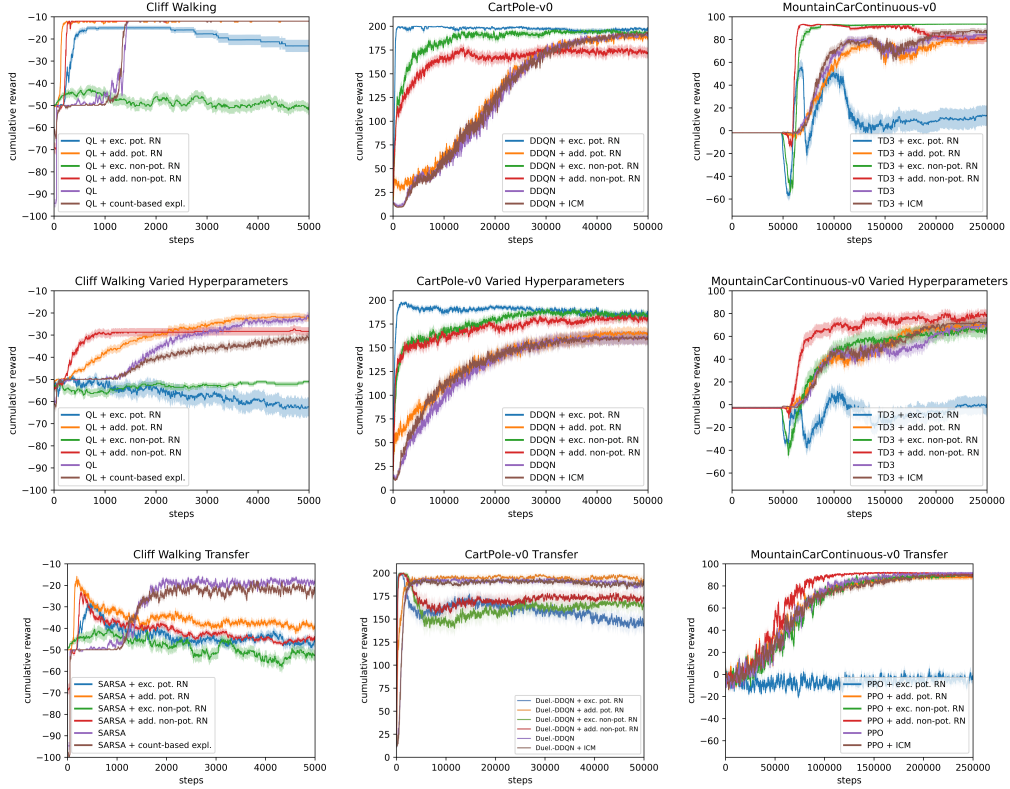


Figure 5: The average cumulative *test* rewards of agents when trained on different RN variants for one episode and evaluated on the real environments for one episode alternatingly. **Top row:** Training and evaluation with the same agent using default agent hyperparameters (HPs). **Center row:** With varied agent HPs. **Bottom row:** Transfer to unseen agents. We show the std. error of the mean and the flat curves in TD3 are due to filling the replay buffer before training.

also include MountainCarContinuous-v0 (Brockman et al., 2016) and HalfCheetah-v3 (Todorov & Tassa, 2012) with TD3 and transfer to PPO (Schulman et al., 2017). With these, we cover a wide range of variation (discrete and continuous state/action spaces, sparse/dense rewards) and computational complexity for training an RN (see Appendix C for details). All RN plots show the average cumulative *test* reward as a function of RN train steps. We alternated episodes of training on the RN and evaluation on the real environment and performed 100 runs ($10 \text{ RNs} \times 10 \text{ agents}$) per curve on each environment except for HalfCheetah where we used 25 runs ($5 \text{ RNs} \times 5 \text{ agents}$).

Baselines For all environments, we compare our approach to multiple baselines, namely the bare agent and the bare agent extended by an Intrinsic Curiosity Module (ICM) (Pathak et al., 2017) that uses the error of predicted action effects as the synthetic reward. Additionally, for Cliff Walking we use count-based exploration (Strehl & Littman, 2008) with a synthetic reward $\frac{\beta}{n(s,a)}$ to encourage exploration of less visited (s,a) -pairs with $\beta \in \mathbb{R}_{\geq 0}$ and $n : \mathcal{S} \times \mathcal{A} \rightarrow \mathbb{N}_0$ a visitation count. For HalfCheetah, we also consider the observation vectors v and v' with the position and velocity of the current and next state that HalfCheetah provides. We use these as input to the RNs with $\Phi(s, v)$ or $\Phi(s', v')$, combine them with the existing variants from Table 1 and tag them with “+ augm.”.

Evaluating the Performance of RN-trained Agents Like in the SE case, we study how efficient and hyperparameter-sensitive the RNs are. Consider the top and middle row of Figure 5 that show how the RNs perform in training *seen* agents (used to optimize the RNs) as well as the performance when we vary the agents’ HPs (i.e., learning rate, discount factor, etc., see Appendix B.3).

For all environments, we see that there always exists an RN variant that offers significant speed-ups compared to the baselines not involving RNs. The variant *additive potential RN* ($r + \gamma\Phi(s') - \Phi(s)$) implementing the original PBRS formulation (Ng et al., 1999) seems to be a good default choice. However, it often does not outperform the baseline, presumably trading reliability and formal guarantees with performance. The variant *additive non-potential RN* ($r + \Phi(s')$) seems to often be the better choice, as it never failed completely and often outperformed the original PBRS variant. We argue that *additive non-potential RN* can be seen as an undiscounted *additive potential RN* ($\gamma = 1$ vs. $\gamma = 0.99$) that may be better in sparse-reward and long-trajectory tasks as in ContinuousMountainCar. In contrast, *exclusive potential RN* ($\gamma\Phi(s') - \Phi(s)$) shows an increased risk of failing and we hypothesize that not involving the real reward may result in a challenging RN optimization. Across all tasks, RNs do not seem to overfit to the HPs (Figure 5, 2nd row). The results and a discussion for HalfCheetah are given in Appendix B.1.

Transferability of RNs In this experiment, we investigate the ability of RNs to train unseen agents. For this, consider the bottom row of Figure 5 (Appendix Figure 9 for HalfCheetah). We used the default agent HPs reported in Appendix B.3 without varying them. The results show that RNs can also train unseen RL agents efficiently. However, for both Cliff Walking and CartPole some RN variants cause a deterioration of the learned policies after initially teaching well-performing policies. While the reason for this is unclear, a workaround is to apply early-stopping since *additive potential RN* and *additive non-potential RN* deliver significant (Cliff W., CartPole) to moderate (MountainCar) speedups or higher final performance (HalfCheetah) even in the agent-transfer scenario.

We noticed that RNs are generally less prone to overfitting than SEs and are overall easier to train. However, the components of the RN variants seem to induce important inductive biases that beg a deeper understanding and may require a more isolated analysis. Nevertheless, we see clear evidence of the benefits of using RNs for efficient RL agent training. All in all, we argue that the RN efficiency, like for SEs, stems from a learned informed representation that biases agents towards helpful states for completing the task quickly. In the same spirit of the qualitative analysis of SEs in Section 5, a similar study for Cliff Walking RNs that supports this hypothesis is in Appendix B.2.

7 LIMITATIONS OF THE APPROACH

As reported in (Salimans et al., 2017), NES methods strongly depend on the number of workers and require a lot of parallel computational resources. We observed this limitation in preliminary SE experiments when we applied our method to more complex environments, such as the HalfCheetah or Humanoid task. Here, 16 workers were insufficient to learn SEs able to solve them. Moreover, non-Markovian states and partial observability may add further complexity to the optimization of SEs and RNs. In contrast to the SE case, in the RN case, scaling our method to more complex tasks was straightforward since learning rewards is intuitively easier than learning complex state dynamics. Nevertheless, the success of learning efficient proxy models also depends significantly on hyperparameter optimization. Lastly, we observed that optimized NES HPs were transferable among different target environments in the RN case but usually not in the SE case.

8 CONCLUSION

We proposed a novel method for learning proxy models outside the current learning schemes. We apply it to learn synthetic environments and reward networks for RL environments. When training agents on SEs without involving the real environment at all, our results on two environments show significant reductions in the number of training steps while maintaining the target task performance. In the RN case, we also noticed similar benefits in three of four environments. Our experiments showed that the proxies produce narrower and shifted states as well as dense reward distributions that resemble informed representations to bias agents towards relevant states. We illustrated that these proxies are robust against hyperparameter variation and can transfer to unseen agents, allowing for various applications (e.g., as agent-agnostic, cheap-to-run environments for AutoML, for agent and task analysis or agent pre-training). Overall, we see our method as a basis for future research on more complex tasks and we believe that our results open an exciting new avenue of research.

ACKNOWLEDGEMENTS

The authors acknowledge funding by Robert Bosch GmbH, by the Deutsche Forschungsgemeinschaft (DFG, German Research Foundation) under grant number 417962828, by the state of Baden-Württemberg through bwHPC and the German Research Foundation (DFG) through grant no INST 39/963-1 FUGG, and by TAILOR, a project funded by the EU Horizon 2020 research and innovation programme under GA No 952215.

ETHICS STATEMENT

As learned data generating processes that teach learners, our proxies may have ethical and societal consequences. On the application side, we see the risk of learning proxies on maliciously re-purposed environments, for example, that allow efficiently learning policies for weapon systems. Ways to control this may include ethically reviewing both environment releases (staging releases) and the used optimization objectives, as well as regulations to enforce their disclosure. In contrast, proxies can also be used for good-natured applications, such as elderly care robotics to help analyze human safety.

Methodologically, we see risks in generating proxies that are purely optimized for efficiency or effectiveness as they may elicit agent policies that achieve the objective by neglecting established societal and moral rules. Effects like these may be reinforced by the design of the target environment. While the latter could be addressed through the democratized design of target environments, the former could be tackled by using multi-objective optimization during proxy learning and by adopting fair-efficient rewards (Jabbari et al., 2017). The flexibility that the proxy optimization allows can also be beneficial to society, for example, by using objectives that enable fuel-saving in (autonomous) vehicles. Moreover, our proxies can have a positive effect on the environment as they target sample inefficiency in RL, e.g., by using them for efficiently pre-training RL agents like in supervised learning and, as addressed in our work, by targeting proxy transferability to exploit invested resources across agent families. In summary, despite the possible negative implications of learning environment proxies, we find that there exist possibilities to successfully address them and that the laid out merits outweigh the potential harms.

REPRODUCIBILITY STATEMENT

In our repository, we include the full code, SE / RN models, hyperparameter configurations, and instructions to reproduce all figures reported in the main paper. All our experiments use random seeds and all results are based on multiple random runs for which standard deviations are reported. Moreover, we dedicate individual experiments to investigate the robustness to variation of randomly sampled hyperparameters in results denoted by *vary HP* in Sections 5 and 6. Additionally, we report the total run-time for SEs and RNs in Sections 5 and 6 and discuss the computational complexity in more detail in Appendix C. Our code can be found here: https://github.com/automl/learning_environments

REFERENCES

- M. G. Bellemare, S. Srinivasan, G. Ostrovski, T. Schaul, D. Saxton, and R. Munos. Unifying count-based exploration and intrinsic motivation. In *Proc. of NeurIPS'16*, pp. 1471–1479, 2016.
- Philip Bontrager and Julian Togelius. Fully differentiable procedural content generation through generative playing networks. *arXiv:2002.05259*, 2020.
- G. Brockman, V. Cheung, L. Pettersson, J. Schneider, J. Schulman, J. Tang, and W. Zaremba. OpenAI Gym. *CoRR*, abs/1606.01540, 2016.
- T. Brys, A. Harutyunyan, H. B. Suay, S. Chernova, M. E. Taylor, and A. Nowé. Reinforcement learning from demonstration through shaping. In *Proc. of IJCAI'15*, 2015.
- Y. Burda, H. Edwards, D. Pathak, A. J. Storkey, T. Darrell, and A. A. Efros. Large-scale study of curiosity-driven learning. In *Proc. of ICLR'19*, 2019.

K. Cobbe, C. Hesse, J. Hilton, and J. Schulman. Leveraging procedural generation to benchmark reinforcement learning. In *Proc. of ICML’20*, pp. 2048–2056, 2020.

M. Dennis, N. Jaques, E. Vinitsky, A. M. Bayen, S. Russell, A. Critch, and S. Levine. Emergent complexity and zero-shot transfer via unsupervised environment design. In *Proc. of NeurIPS’20*, pp. 13049–13061, 2020.

S. Falkner, A. Klein, and F. Hutter. BOHB: Robust and efficient hyperparameter optimization at scale. In *Proc. of ICML’18*, pp. 1437–1446, 2018.

A. Faust, A. Francis, and D. Mehta. Evolving rewards to automate reinforcement learning. In *ICML 2019 Workshop on Automated Machine Learning*, 2019.

S. Fujimoto and D. Meger H. Hoof. Addressing Function Approximation Error in Actor-Critic Methods. In *Proc. of ICML’18*, pp. 1582–1591, 2018.

David Ha and Jürgen Schmidhuber. World models. *arXiv:1803.10122*, 2018.

Y. Hu, W. Wang, H. Jia, Y. Wang, Y. Chen, J. Hao, F. Wu, and C. Fan. Learning to utilize shaping rewards: A new approach of reward shaping. In *Proc. of NeurIPS’20*, 2020.

F. Hutter, L. Kotthoff, and J. Vanschoren (eds.). *Automated Machine Learning: Methods, Systems, Challenges*. Springer, 2019.

B. Ibarz, J. Leike, T. Pohlen, G. Irving, S. Legg, and D. Amodei. Reward learning from human preferences and demonstrations in atari. In *Proc. of NeurIPS’18*, pp. 8022–8034, 2018.

S. Jabbari, M. J., M. Kearns, J. Morgenstern, and A. Roth. Fairness in reinforcement learning. In *Proc. of ICML’18*, pp. 1617–1626, 2017.

M. Jaderberg et al. Human-level performance in 3d multiplayer games with population-based reinforcement learning. *Science*, 364(6443):859–865, 2019.

Eric Jang, Shixiang Gu, and Ben Poole. Categorical reparameterization with gumbel-softmax. In *Proc. of ICLR’17*, 2017.

You-Cyuan Jhang et al. Training a performant object detection ML model on synthetic data using Unity Perception tools. <https://blogs.unity3d.com/2020/09/17/training-a-performant-object-detection-ml-model-on-synthetic-data-using-unity-computer-vision-tools/>, Sep 2020.

K. Judah, A. P. Fern, P. Tadepalli, and R. Goetschalckx. Imitation learning with demonstrations and shaping rewards. In *Proc. of AAAI’14*, pp. 1890–1896, 2014.

T. Mattisen, A. Oliver, T. Cohen, and J. Schulman. Teacher-student curriculum learning. *IEEE Trans. Neural Networks Learn. Syst.*, 31(9):3732–3740, 2020.

Luke Metz, Niru Maheswaranathan, Jeremy Nixon, Daniel Freeman, and Jascha Sohl-Dickstein. Understanding and correcting pathologies in the training of learned optimizers. In *Proc. of ICML’19*, 2019.

T. M. Moerland, J. Broekens, and C. M. Jonker. Model-based reinforcement learning: A survey. *arXiv:2006.16712*, 2020.

A. Y. Ng, D. Harada, and S. J. Russell. Policy invariance under reward transformations: Theory and application to reward shaping. In *Proc. of ICML’99*, pp. 278–287, 1999.

A. Paszke, S. Gross, F. Massa, A. Lerer, J. Bradbury, G. Chanan, T. Killeen, Z. Lin, N. Gimelshein, L. Antiga, A. Desmaison, A. Kopf, E. Yang, Z. DeVito, M. Raison, A. Tejani, S. Chilamkurthy, B. Steiner, L. Fang, J. Bai, and S. Chintala. PyTorch: An imperative style, high-performance deep learning library. In *Proc. of NeurIPS’19*, pp. 8024–8035, 2019.

D. Pathak, P. Agrawal, A. A. Efros, and T. Darrell. Curiosity-driven exploration by self-supervised prediction. In *Proc. of CVPR’17*, pp. 488–489, 2017.

Ingo Rechenberg. *Evolutionsstrategie: Optimierung technischer systeme nach prinzipien der biologischen evolution*. frommann-holzbog, stuttgart, 1973. *PPSN 1973*, 1973.

G. A. Rummery and M. Niranjan. *On-line Q-learning using connectionist systems*, volume 37. University of Cambridge, Department of Engineering Cambridge, UK, 1994.

T. Salimans, J. Ho, X. Chen, and I. Sutskever. Evolution strategies as a scalable alternative to reinforcement learning. *arXiv:1703.03864*, 2017.

J. Schulman, F. Wolski, P. Dhariwal, A. Radford, and O. Klimov. Proximal policy optimization algorithms. *arXiv:1707.06347 [cs.LG]*, 2017.

N. Shaker, J. Togelius, and M. J. Nelson. *Procedural content generation in games*. Springer, 2016.

D. Silver, J. Schrittwieser, K. Simonyan, I Antonoglou, A. Huang, A. Guez, T. Hubert, L. Baker, M. Lai, A. Bolton, et al. Mastering the game of go without human knowledge. *nature*, 550(7676):354–359, 2017.

S. Singh, R. L. Lewis, A. G. Barto, and J. Sorg. Intrinsically motivated reinforcement learning: An evolutionary perspective. *IEEE Transactions on Autonomous Mental Development*, 2(2):70–82, 2010.

A. L. Strehl and M. L. Littman. An analysis of model-based interval estimation for markov decision processes. *Journal of Computer and System Sciences*, 74(8):1309–1331, 2008. ISSN 0022-0000.

Felipe Petroski Such, Aditya Rawal, Joel Lehman, Kenneth O. Stanley, and Jeffrey Clune. Generative teaching networks: Accelerating neural architecture search by learning to generate synthetic training data. In *Proc. of ICML’20*, 2020.

R. S. Sutton. Integrated architectures for learning, planning, and reacting based on approximating dynamic programming. In B. Porter and R. Mooney (eds.), *Machine Learning Proceedings 1990*, pp. 216–224. Morgan Kaufmann, San Francisco (CA), 1990.

Richard S Sutton and Andrew G Barto. *Reinforcement learning: An introduction*. MIT press, 2018.

Richard S Sutton, David McAllester, Satinder Singh, and Yishay Mansour. Policy gradient methods for reinforcement learning with function approximation. In *Proc. of NeurIPS’20*, 2020.

H. Tang, R. Houthooft, D. Foote, A. Stooke, X. Chen, Y. Duan, J. Schulman, F. De Turck, and P. Abbeel. #exploration: A study of count-based exploration for deep reinforcement learning. In *Proc. of NeurIPS’17*, pp. 2753–2762, 2017.

J. Tobin, R. Fong, A. Ray, J. Schneider, W. Zaremba, and P. Abbeel. Domain randomization for transferring deep neural networks from simulation to the real world. In *Proc. of IROS’17*, pp. 23–30, 2017.

E. Todorov and T. Erez and Y. Tassa. Mujoco: A physics engine for model-based control. In *Proc. of IROS’12*, pp. 5026–5033, 2012.

J. Togelius, G. N. Yannakakis, K. O. Stanley, and C. Browne. Search-based procedural content generation: A taxonomy and survey. *IEEE Transactions on Computational Intelligence and AI in Games*, 3(3):172–186, 2011.

Hado van Hasselt, Arthur Guez, and David Silver. Deep reinforcement learning with double q-learning. In *Proc. of AAAI’16*, pp. 2094–2100, 2016.

V. Volz, J. Schrum, J. Liu, S. M. Lucas, A. Smith, and S. Risi. Evolving mario levels in the latent space of a deep convolutional generative adversarial network. In *Proceedings of the Genetic and Evolutionary Computation Conference*, pp. 221–228, 2018.

Rui Wang, Joel Lehman, Jeff Clune, and Kenneth O Stanley. Paired open-ended trailblazer (poet): Endlessly generating increasingly complex and diverse learning environments and their solutions. *arXiv:1901.01753*, 2019.

One-shot World Models Using a Transformer Trained on a Synthetic Prior

The content of this chapter has been published as:

F. Ferreira, M. Schlageter, R. Rajan, A. Biedenkapp, and F. Hutter (2024). “One-shot World Models Using a Transformer Trained on a Synthetic Prior”. In: *NeurIPS 2024 Workshop on Open-World Agents*.

The supplementary material and a detailed statement of contributions is provided in Appendix H.

One-shot World Models Using a Transformer Trained on a Synthetic Prior

Fabio Ferreira*
University of Freiburg

Moreno Schlageter*
University of Freiburg

Raghу Rajan
University of Freiburg

André Biedenkapp
University of Freiburg

Frank Hutter
ELLIS Institute Tübingen
University of Freiburg

Abstract

A World Model is a compressed spatial and temporal representation of a real world environment that allows one to train an agent or execute planning methods. However, world models are typically trained on observations from the real world environment, and they usually do not enable learning policies for other real environments. We propose *One-Shot World Model* (OSWM), a transformer world model that is learned in an in-context learning fashion from purely synthetic data sampled from a prior distribution. Our prior is composed of multiple randomly initialized neural networks, where each network models the dynamics of each state and reward dimension of a desired target environment. We adopt the supervised learning procedure of Prior-Fitted Networks by masking next-state and reward at random context positions and query OSWM to make probabilistic predictions based on the remaining transition context. During inference time, OSWM is able to quickly adapt to the dynamics of a simple grid world, as well as the CartPole gym and a custom control environment by providing 1k transition steps as context and is then able to successfully train environment-solving agent policies. However, transferring to more complex environments remains a challenge, currently. Despite these limitations, we see this work as an important stepping-stone in the pursuit of learning world models purely from synthetic data.

1 Introduction

World models have emerged as a powerful approach for creating compressed spatial and temporal representations of real-world environments, enabling efficient agent training and planning in reinforcement learning (RL) tasks [Ha and Schmidhuber, 2018, Kaiser et al., 2019, Hafner et al., 2023, Wu et al., 2022]. These models have shown significant promise in improving sample efficiency and performance across various RL domains. For instance, SimPLe [Kaiser et al., 2019] demonstrated strong results on Atari games by using a learned dynamics model to generate simulated data. More recently, transformer-based world models have pushed the boundaries of sample efficiency and performance. TWM [Robine et al., 2023] utilized a Transformer-XL architecture to surpass other methods on the Atari 100k benchmark [Kaiser et al., 2019], while IRIS [Micheli et al., 2023] and STORM [Zhang et al., 2023] achieved human-level performance using GPT-style transformers. However, these approaches typically require training on observations from the target environment, which can be time-consuming and impractical in many real-world scenarios. Moreover, traditional world models often lack the ability to generalize across different environments, limiting their applicability in diverse

*Equal contribution. Correspondence to: ferreira@cs.uni-freiburg.de

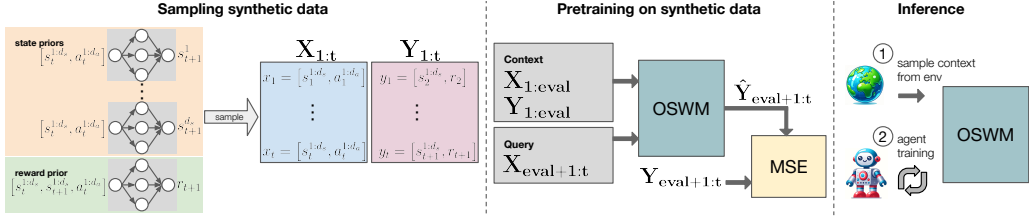


Figure 1: OSWM is trained on synthetic data sampled from a prior distribution of randomly initialized, untrained neural networks that mimic RL environments (left). Given a sequence of synthetic interactions, OSWM is optimized by predicting future dynamics at random cut-offs (center). RL agents can then be trained on OSWM to solve simple real environments given a context.

RL tasks. The challenge of transferring learned dynamics efficiently to new environments remains a significant hurdle in the field of model-based RL.

To address these challenges, we explore the potential of training world models with in-context learning using purely synthetic data. We propose the One-Shot World Model (OSWM), a transformer-based approach that learns a world model from a synthetic prior distribution. Our method draws inspiration from Prior-Fitted Networks [Müller et al., 2022] and leverages in-context learning to adapt to new environments with minimal real-world interactions. By training on a diverse synthetic prior, OSWM aims to capture a wide range of environment dynamics, potentially enabling rapid adaptation to various RL tasks. We release our code under <https://github.com/automl/oswm> and our contributions can be summarized as follows:

- We explore training world models with synthetic data sampled from a synthetic prior distribution based on randomly initialized and untrained neural networks, using in-context learning to predict future dynamics and rewards given previous state and action sequences.
- We demonstrate that our model, One-Shot World Model (OSWM), is capable of adapting to the dynamics of unseen environments in a one-shot manner by only providing 1,000 randomly sampled transitions as context.
- Although OSWM adaptability is still limited to very simple environments, we show that training world models on such a synthetic prior surprisingly allows for the training of RL agents that solve the GridWorld, CartPole gym and a custom control environment.
- We investigate OSWM’s limitations and analyze learned reward functions, as well as strategies for prior construction and the relevance of context sampling, providing insights for future improvements in this direction.

2 Related Work

World Models and Model-Based Reinforcement Learning Classical RL often suffers from sample inefficiency, as it requires many interactions with the environment. Model-Based Reinforcement Learning (MBRL) mitigates this by learning environment dynamics, allowing agents to train using simulated data. For example, Ha and Schmidhuber [2018] proposed World Models, which use generative neural networks to encode compact spatial-temporal representations, optimizing RL efficiency. MuZero [Schrittwieser et al., 2020] advanced MBRL by learning both environment dynamics and reward functions, which proved highly effective across board games. Dreamer [Hafner et al., 2020, 2021, 2023] applied learned world models across diverse domains, including real-world robotics [Wu et al., 2022]. More recently, TD-MPC2 [Hansen et al., 2024] demonstrated scalability and robustness in continuous control tasks. Transformer-based models have also become prominent, with TransDreamer [Chen et al., 2022] or TWM [Robine et al., 2023] that excelled in sample efficiency on Atari 100k. Other Transformer-based approaches such as IRIS [Micheli et al., 2023] or STORM [Zhang et al., 2023] achieved over 100% human performance on Atari 100k with GPT-style training. However, Most if not all methods are trained on the target environment and utilize the attention mechanism to attend to previous parts of the roll-out.

Despite these successes, transferring learned dynamics across environments remains a significant hurdle in the field of MBRL. Augmented World Models [Ball et al., 2021] tackle environmental

dynamics changes by learning a world model from offline data. During training, they provide predicted dynamics and possible changes as latent context, helping agents generalize to new variations. Similarly, Evans et al. [2022] uses transformers or RNNs to encode environment parameterization into a latent space, enabling a world model robust to variations like friction or object mass changes.

Synthetic Data and Priors and RL Synthetic data plays a crucial role in RL, particularly in methods that transfer knowledge from simulation to real environments, known as *sim2real*. Domain randomization [Tobin et al., 2017, Rajan et al., 2023], which varies simulation settings like lighting and object shapes, enhances generalization and improves the transfer from simulation to the real world. Pretraining with synthetic data has also gained prominence. For example, Wang et al. [2024] pretrains the Decision Transformer using synthetic Markov chain data, outperforming pretraining with natural text (e.g., DPT trained on Wikipedia [Lee et al., 2023]) in both performance and sample efficiency. Other techniques include training on synthetic reward distributions to allow zero-shot transfer to new tasks [Frans et al., 2024], while TDM [Schubert et al., 2023] demonstrates strong few-shot and zero-shot generalization across procedural control environments. UniSim [Yang et al., 2023] uses internet-scale data to train realistic robotic control models, enabling more efficient RL training. A meta-learning approach trains Synthetic Environments [Ferreira et al., 2021] for RL that serve as proxies for a target environment, providing only synthetic environment dynamics. These synthetic dynamics allow RL agents to significantly reduce the number of interactions needed during training. Lastly, Prior Fitted Networks (PFNs) [Müller et al., 2022] utilize synthetic priors for supervised learning, with its adaptation to tabular data, TabPFN [Hollmann et al., 2023], achieving state-of-the-art results while significantly speeding up inference.

Unlike previous approaches that depend on real-world observations or extensive training in target environments, we introduce a new approach that trains a transformer world model entirely on synthetic data sampled from a prior distribution which is based much further away from reality as it based on randomly initialized neural networks. Using the Prior-Fitted Networks paradigm, OSWM employs in-context learning to adapt to new environments with just a simple context sequence.

3 Method

Let $x_t = [s_t^{1:d_s}, a_t^{1:d_a}]$ denote the concatenated state-action vector (or *input*) at time step t , where $s_t^{1:d_s}$ represents the state and $a_t^{1:d_a}$ represents the action, with d_s and d_a being the dimensionalities of the state and action, respectively. Similarly, let $y_t = [s_{t+1}^{1:d_s}, r_{t+1}]$ represent the next state and reward vector (or *target*). The sequences of these vectors, $\{x_1, \dots, x_T\}$ and $\{y_1, \dots, y_T\}$, are summarized as $X_{1:T}$ and $Y_{1:T}$, respectively. To ensure consistent input sizes across varying environments, padding is applied: $x_t = [s_t^1, \dots, s_t^{d_s}, pad_s, a_t^1, \dots, a_t^{d_a}, pad_a]$, where pad_s and pad_a are zero vectors used to match the maximum state and action dimensions across environments. The same padding scheme is applied to y_t . The OSWM is trained on synthetic batches $(X_{1:T}, Y_{1:T})$ sampled from a prior distribution P_{RL} . At randomly sampled cut-off positions, the synthetic batches are divided into context and target data and the model is trained to predict the target data given the context, which we visualized in Fig. 1 (center).

At inference, OSWM adapts to a new environment using a few context samples $(X_{1:T-1}, Y_{1:T-1})$ collected from the real environment, i.e. the target environment (see Fig. 1). This context consist of state-action transitions and their corresponding rewards, which provide information about the dynamics of the real environment. To ensure sufficient coverage of the target environment, multiple transitions are collected, often spanning several episodes. We typically collect 1,000 transitions from random rollouts, though the collection process can be performed using any policy, ranging from random to expert-driven actions. We analyze the role of context generation on the predictive performance of the model in Section 4.3.

Once the context is collected, OSWM predicts the next state and reward (s_{t+1}, r_{t+1}) given the current state-action pair (s_t, a_t) and the prior context. The OSWM acts as a learned simulator, enabling RL agents to interact with predicted dynamics and learning by standard RL algorithms. Note, that the OSWM is initialized by sampling an initial state from the real environment at inference time. Both inputs $X_{1:T}$ and targets $Y_{1:T}$ are normalized to zero mean and unit variance. OSWM predicts in this normalized space, and the predictions are projected back to the original value space using the

mean and variance of the context data. Finally, we assume that the termination condition of the target environment is known, but we note that it could also be learned.

3.1 Training the One-Shot World Model (OSWM)

The OSWM is trained on synthetic data sampled from a prior distribution P_{RL} (see Section 4.2), which is constructed to simulate the dynamics of various environments. The goal is to optimize the model for predicting the dynamics of unseen target environments based on initial interactions used by in-context learning. We describe the entire training procedure in Algorithm 1.

At first, the model weights θ are initialized randomly. During each training step, a batch of $(X_{1:T}, Y_{1:T}) \sim \mathcal{P}_{RL}$ is sampled, with each batch containing input and target sequences. A context size $eval$ is sampled from the interval $[k, T - 1]$, where k is the minimum context size used for the prediction (see Appendix C for more details about the sampling). The model is provided with $X_{1:eval}$ and $Y_{1:eval}$ to predict future targets $\hat{Y}_{eval+1:T}$ based on the remaining inputs $X_{eval+1:T}$. The training loss is computed using the mean-squared error (MSE) between the predicted and actual future transitions: $L = MSE(\hat{Y}_{eval+1:T}, Y_{eval+1:T})$.

Algorithm 1 Training the OSWM with the synthetic prior

Initialize θ	▷ Initialize OSWM’s parameters
while not finished do	
$X_{1:T}, Y_{1:T} \sim \mathcal{P}_{RL}$	▷ Sample batch from RL prior
$eval \sim \mathcal{U}(k, T - 1)$	▷ Sample $eval$ size
$\hat{Y}_{eval_pos+1:T} \leftarrow \mathcal{M}_\theta(X_{1:eval}, Y_{1:eval}, X_{eval+1:T})$	▷ Predict dynamics with OSWM
$L \leftarrow MSE(\hat{Y}_{eval+1:T}, Y_{eval+1:T})$	▷ Calculate loss
$\theta \leftarrow \theta - \alpha \nabla_\theta L$	▷ Update parameters
end while	
return \mathcal{M}_θ	

3.2 Prior for Training OSWM

One of the core contributions of this method is the design of a prior that aims to mimic the properties of RL environments while incorporating stochasticity for diverse dynamics. The prior consists of two components: a neural network-based (NN) prior and a physics-based momentum prior. These two priors are combined, with the states produced by both the NN and momentum priors concatenated as input to the NN prior for further updates. This split allows the model to capture both complex, neural network-generated behaviors and simple, physics-driven interactions, like pendulum motion or velocity-position relations. In Figure 1 (left), we illustrate the mechanics of the NN prior, and below we describe both priors in more detail.

Neural Network Prior The NN prior generates dynamics using randomly initialized neural networks. Each state dimension s_t^i is produced by a separate neural network f_{θ^i} , which is randomly-initialized and untrained and takes as input the entire previous state $s_{t-1} = [s_{t-1}^1, \dots, s_{t-1}^{d_s}]$ and action $a_t = [a_{t-1}^1, \dots, a_t^{d_a}]$. The next state is computed as $s_t^i = f_{\theta^i}(s_{t-1}, a_{t-1})$. The networks consist of three linear layers, with random activations (ReLU, tanh, or sigmoid) after the first two layers, and a residual connection that aggregates the outputs of the first and second layers. This structure allows for complex dependencies between state dimensions and actions. To introduce variability, each NN-based state dimension is initialized with a random scale and offset. When the individual NN prior networks are reset, which occurs periodically after a pre-defined fixed interval, their initial state values s_0 are sampled from $\mathcal{U}(0, 1)$, and then scaled and offset according to the prior configuration (see Table 6 for the prior hyperparameters in the appendix), ensuring stochastic behavior across environments. This method allows the model to capture rich and diverse dynamics by introducing different dependencies between states and actions across dimensions.

Momentum Prior The momentum prior models physical interactions through two components: velocity and positional updates. Velocity is updated based on the action and gravity ($v_{t+1} = v_t + a_t \cdot \Delta t - g \cdot \Delta t$), while position is updated using the current velocity ($p_{t+1} = p_t + v_{t+1} \cdot \Delta t$). In

this model, velocity v_t and position p_t are influenced by factors such as gravity and the current action, and the position updates rely on velocity. The initial position is sampled from $[0, 2\pi]$, and the initial velocity is sampled from $\mathcal{U}(-3, 3)$. This setup enables the model to simulate both linear and angular motion. Angular dynamics can incorporate gravity, and they are represented internally in radians, though the output can be sine, cosine, or radian values. The momentum prior values are concatenated with the NN prior values and fed into the NN prior networks for the subsequent transitions.

Rewards and Invariance The reward function follows a similar structure to the NN prior used for state dynamics but with different inputs, including the new state, action, and the previous state. This reflects how rewards in real RL environments are based on state transitions and action costs, such as penalizing high action magnitudes. The reward at time step t can be expressed as: $r_{t+1} = g(s_{t+1}, a_t, s_t)$ where g represents the reward model that takes the new state s_{t+1} , the action a_t , and, optionally, the previous state s_t as inputs. To maintain flexibility, the reward is replaced by a constant reward of 1 with a probability of 0.5, a common approach in tasks like CartPole, where extending the episode is rewarded, or MountainCar, where faster completion is incentivized. To prevent the model from overfitting to the order of state-action dimensions, we shuffle both states and actions and apply identical permutations to X_1 and Y_1 .

4 Experiments

We first test the model’s performance on various environments with the goal to provide an overview of the capabilities and limitations. We then describe how different prior components affect the predictions of OSWM, explore the impact of various context generation methods, and analyze learned reward functions.

4.1 Results for Agent Training

We evaluate the performance of OSWM by training an RL agent using the PPO algorithm [Schulman et al., 2017], as implemented in stable-baselines 3 [Raffin et al., 2021]. We chose PPO because it can handle both discrete and continuous action spaces, making it well suited for the variety of environments in this study. We selected environments that provide a mix of discrete and continuous state and action spaces, allowing us to assess OSWM’s performance across different types of RL challenges. The selected environments include two custom environments, GridWorld and SimpleEnv (see Appendix D for details), as well as CartPole-v0, MountainCar-v0, Pendulum-v1, and Reacher-v4 from the classic control gym suite.

In GridWorld, the agent navigates a discrete, 8x8 grid to reach a target location, receiving a positive reward for reaching the target and small penalties for each step, and the environment is considered solved when the agent consistently reaches the target efficiently. SimpleEnv involves moving a point along a 1D continuous line toward the center, with rewards negatively proportional to the distance from the center. CartPole-v0 is solved with an average reward of 195, MountainCar-v0 with an average reward of -110, Pendulum-v1 maximizes the reward when balancing the pendulum upright, and Reacher-v4 is solved with an average reward of around -3.75.

We trained agents for 50k steps in all environments, except MountainCar-v0, where training was extended to 200k steps with actions repeated five times to enhance exploration. All PPO hyperparameters were kept in their default settings. In all experiments, unless stated otherwise, OSWM was provided with 1k context steps collected from the real environment using random actions.

4.1.1 Quantitative Evaluation of Agent Performance

In Table 1, we compare the average performance of 100 test episodes for three agents: OSWM-PPO, PPO, and a Random Baseline. OSWM-PPO is trained purely on the dynamics predicted by OSWM using 1k context steps from the real environment, while PPO is trained only on the real environment, and the Random Baseline selects actions randomly. Since OSWM’s synthetic rewards may not be indicative of the current agent’s performance on the real environment, we evaluate each agent periodically after 100 training steps. Moreover, as discussed below in Section 4.1.2, training the agent too long on OSWM can result in performance degradation. Therefore, we apply an early stopping heuristic that takes the best agent training checkpoint. We do this on a per-seed-basis and compute the mean over multiple seeds.

Environment	OSWM-PPO	PPO	Random Baseline
GridWorld	5.2 ± 0.0	5.2 ± 0.0	-14.2 ± 0.3
CartPole-v0	196.5 ± 4.2	200.0 ± 0.0	21.3 ± 3.9
SimpleEnv	-4.7 ± 5.2	-0.8 ± 0.1	-256.2 ± 16.6
MountainCar-v0	-200.0 ± 0.0	-110.5 ± 2.1	-200.0 ± 0.0
Pendulum-v1	-1185.4 ± 31.2	-268.9 ± 22.2	-1230.3 ± 8.6
Reacher-v4	-10.2 ± 0.9	-4.6 ± 0.3	-42.8 ± 0.3

Table 1: Average performances over 3 seeds on 100 test episodes of 3 different agents (higher values are better). OSWM-PPO is a PPO agent trained only on the OSWM, PPO is a PPO agent trained on the real environment and the random baseline is an agent taking random actions. All agents are evaluated on the real environment, and we apply an early stopping heuristic for each seed before we compute the mean.

In GridWorld, OSWM-PPO matches PPO with a reward of 5.2, outperforming the random baseline (-14.2) and demonstrating robustness in simple environments. In CartPole-v0, OSWM-PPO achieves 196.5, close to PPO’s 200 (random baseline: 21.3). Also in SimpleEnv, OSWM-PPO reaches -4.7, performing well compared to PPO (-0.8) and significantly better than the random baseline (-256.2). These results are particularly surprising, as they show that pretraining on synthetic dynamics generated by random, untrained neural networks can still lead to strong performance in certain tasks, even without direct training on real environment data.

In more complex environments like MountainCar-v0 and Pendulum-v1, OSWM-PPO struggles to match PPO, with larger gaps in rewards, indicating that the approach here is less effective. However, for Reacher-v4, OSWM-PPO shows noticeable improvement, coming closer to PPO performance and performing far better than the random baseline. In MountainCar-v0, the model appears inferior at interpolating behavior in unseen states or areas of the environment, as the random context covers only a small part of this task. In contrast, Pendulum-v1 should benefit from better exploration through random actions, as the initial state covers all pendulum rotations, and the random actions provide a wide range of velocities. Despite this, OSWM does not provide sufficiently accurate dynamics to support effective training, suggesting that Pendulum-v1 requires more precise control and dynamic predictions than OSWM can currently offer. This may be due to the inherent difficulty posed by these environments, including sparse rewards and continuous action spaces, which likely require more sophisticated priors to improve performance.

4.1.2 Performance Progression Across Training Steps

To better understand the progression of agent training when training on OSWM, we report the learning curves in Figure 2. Here, we depict the mean evaluation rewards over training steps for three PPO agents using OSWM, with the best and worst performances highlighted.² Performance is measured on the real environment over 10 test episodes.

In the GridWorld environment (left), agents quickly solve the task after minimal interaction, with only one agent showing slightly suboptimal behavior after about 15,000 steps. This demonstrates the robustness of OSWM in simple environments.

For CartPole-v0 (center), agents show strong early performance, with the mean curve stabilizing after a brief drop. The best-performing agent continues to improve, while the worst-performing agent experiences a notable drop-off later in training. This phenomenon, where initial improvements are followed by a decline, can be attributed to gaps in the OSWM’s understanding of certain environment dynamics. For instance, OSWM might model the dynamics accurately at higher angular velocities but struggle at lower velocities, failing to account for subtle drifts that are not captured. As a result, the agent may receive overconfident reward signals, leading to poor performance when these unmodeled drifts become significant in the real environment.

In SimpleEnv (right), agents exhibit a sharp initial increase in performance, followed by a plateau or decline. The worst-performing agent’s reward nearly returns to its initial level, highlighting variability in training outcomes. This suggests that while OSWM supports learning, the one-shot prediction

²We point out that the mean curves in Fig. 2 do not use the early stopping heuristic and therefore, do not correspond to the mean values of Tab. 1 where we take the mean over early stopped agents.

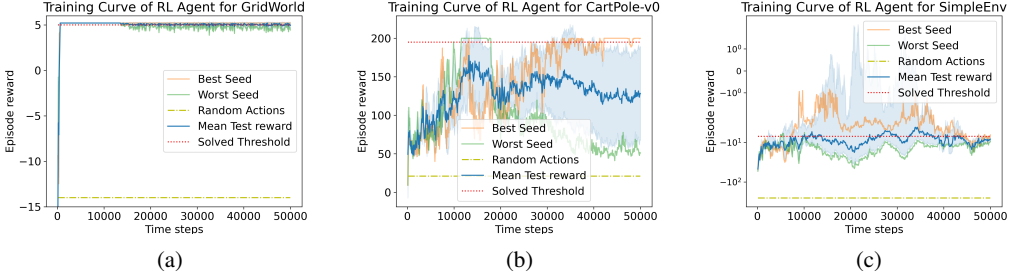


Figure 2: Evaluation scores for RL agent training on the OSWM for GridWorld, CartPole-v0, and SimpleEnv. Blue shows the mean over 3 runs, with the standard deviation in light blue. Orange and green depict the best and worst-performing agents, respectively.

approach can introduce variability in performance, particularly in continuous environments where fine control is crucial.

4.2 Studying the Prior

In this section, we analyze the behavior of the Neural Network (NN) prior used in OSWM, which generates diverse dynamics through randomly initialized neural networks. To understand the state dynamics produced by the NN prior, we sample batches of data, reflecting what OSWM encounters during training. For each prior dimension (e.g., the agent’s position in GridWorld), we calculate the minimum and maximum values and divide them into 100 equal bins, visualizing the distribution for each dimension. The histograms in Fig. 3 show three distinct types of distributions produced by the NN prior. Some prior dimensions exhibit highly peaked distributions, as shown in Fig. 3a, where most values fall within a narrow range. For other dimensions, we observe wider and smooth distributions with a more even spread of values, as seen in Fig. 3b. Finally, some prior dimensions follow multimodal distributions, with two or more distinct peaks, as depicted in Fig. 3c. This pattern of three distinct distribution types is commonly observed across various dimensions.

The variation in distribution types suggests that the NN prior can capture both simple and more complex, multimodal scenarios. However, as shown in Table 2 (left), using only the NN prior impacts OSWM-PPO performance in environments like CartPole-v0, where momentum is key for modeling the pole’s angular dynamics. In contrast, GridWorld and SimpleEnv, which do not entail momentum, perform similarly to when both the NN and momentum priors are used (see Table 1). MountainCar-v0, Reacher-v4, and Pendulum-v1 were unsolvable before, and as expected, removing complexity from the prior does not make them solvable. This highlights that while the NN prior’s multimodality supports diverse behaviors, it is insufficient for tasks that rely on accurate momentum-based dynamics. The distributions of the momentum prior are reported in Appendix A. The right column of Table 2 on improved context generation is analyzed further in Section 4.3.

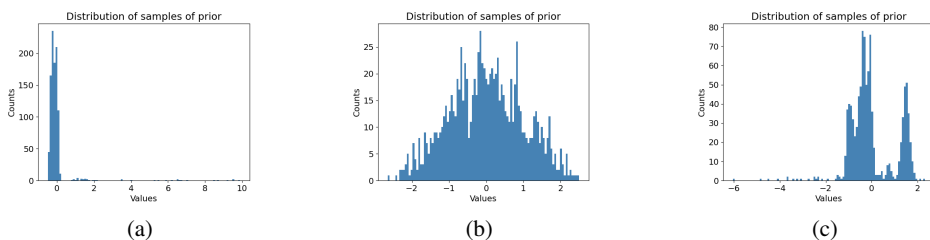


Figure 3: Typical distribution patterns generated by the NN prior: (a) highly peaked, (b) wide or smoother, and (c) multi-modal distributions.

4.3 Studying the Context Sampling

Context is crucial for the predictive performance of OSWM. This section explores how different context sampling methods affect the model’s predictions. Assessing the role of sampling strategies

Environment	NN Prior Only	Improved Context
GridWorld	5.2 ± 0.0	3.9 ± 1.9
CartPole-v0	191.7 ± 11.2	108.0 ± 34.6
SimpleEnv	-1.3 ± 0.3	-2.5 ± 0.8
MountainCar-v0	-200.0 ± 0.0	-200.0 ± 0.0
Pendulum-v1	-1217.4 ± 40.9	-1245.0 ± 25.1
Reacher-v4	-10.0 ± 0.6	-

Table 2: Average performances when the OSWM is trained with the NN prior only (left; with randomly sampled context), as well as when a more sophisticated context sampling strategy is adopted (with NN+momentum prior). Higher values are better.

requires multiple agent trainings in OSWM and evaluations across multiple test episodes and environments. Since this is computationally expensive, we make use of a proxy dataset to evaluate the effectiveness of various sampling strategies more efficiently. The details of the generation of the proxy set are provided in Appendix B, but a high-level overview is given here.

The proxy set is created from transitions collected in the real environment using a PPO agent trained to perform at the expert level. First, the PPO agent is used to generate 5000 expert transitions across multiple episodes. From this, 500 transitions are sampled for each of three settings: 0% randomness (expert actions only), 50% randomness (half expert, half random) and 100% randomness (random actions only). This total of 1500 transitions spans expert behavior to exploratory actions and the proxy. The intuition behind mixing random and expert transitions is to cover states that are not typically encountered by an expert agent alone and thus, the proxy set can capture a wider range of environment dynamics. We then tested five different context sampling strategies: *random* (actions sampled uniformly), *repeat* (random actions repeated for three steps), *expert* (policy solving the environment), *p-expert* (mixing PPO expert and random actions 50/50), and *mixture* (first third random, second third *p-expert*, final third PPO expert).

For evaluation, OSWM is provided with 1000 context steps from each strategy, and the proxy set is used to assess their impact on model predictions (Table 3 in the appendix) by computing the mean squared error (MSE) between predicted dynamics and true targets from the proxy set. Based on the proxy loss, the best strategy is selected for each environment and evaluated in Table 2 (right). In complex tasks like MountainCar-v0 and Pendulum-v1 (using *mixture*), even with improved context, these environments remain unsolved. For Reacher-v4 (*random*), simple random sampling proves best, reflecting that basic methods can sometimes capture the necessary dynamics. In SimpleEnv (*p-expert*), the improved context sampling enhances performance. GridWorld (*mixture*) sees minimal variation, with random sampling generally being sufficient to capture its simpler dynamics. Overall, *p-expert* and *mixture* often yield the best results, while *repeat* and *expert* strategies are less effective. *Random* proves to be a reliable default, offering solid performance across many environments.

4.4 Studying the Reward Function

Visualizing the reward function across environments reveals the dynamics learned by OSWM and their differences from the real environment. Figure 4 shows the reward analysis, with each plot

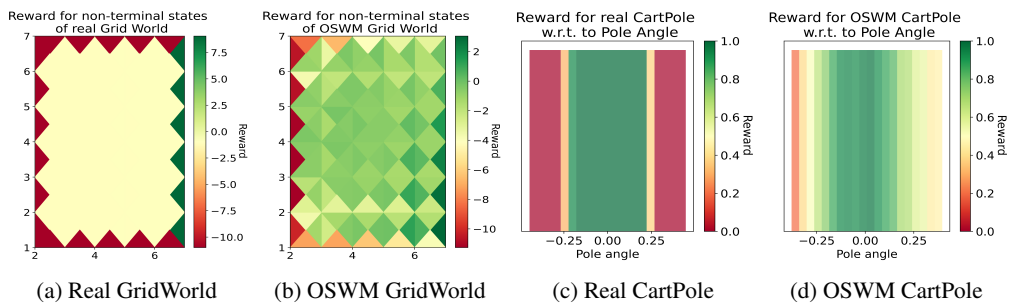


Figure 4: Reward distributions for the real and OSWM GridWorld and CartPole environments.

generated based on the rewards predicted by OSWM given a random seed and a randomly sampled context.

In the **GridWorld** environment, each triangle corresponds to an action, which means that for every state (x, y) we represent four possible actions. OSWM smooths the reward function, making it easier for agents to be guided toward a goal state. Nevertheless, some inaccuracies appear in the reward distribution, for instance, in areas like the bottom-right corner, where states are rewarding instead of penalizing. We hypothesize that this may stem from a combination of undersampled states in the context as well as the inherent smoothness induced by the synthetic prior training.

For **CartPole**, the reward distribution predicted by OSWM is smoother than in the real environment, and we argue that this makes it easier for the agent to keep the pole upright. However, this smoothness can result in certain states near instability receiving rewards when they should be penalized.

We report the results for **Pendulum** and further details in Appendix E. The original Pendulum reward function is already dense and OSWM mostly mimics the original reward function. However, OSWM seems to provide higher rewards for safe states, for instance, where the pendulum is almost upright. In some of the originally penalizing states, OSWM rewards the agent, which may negatively affect the model’s ability to capture nuanced control at the edges of the pendulum’s range of motion. This could potentially explain the weaker performance on Pendulum.

Our results suggest that the smooth reward distributions produced by OSWM may be a reflection of the multifaceted prior dimensions analyzed in Section 4.2. The mixture of distribution types, ranging from peaked to smooth distributions, is mirrored in the learned smooth-reward function. Despite some imprecision in certain states, this smoothness helps the agent efficiently grasp the environment’s dynamics, particularly in sparse reward environments where the combination of a smooth synthetic prior and in-context learning proves to be well-suited. These observations are consistent across multiple seeds, and no specific seeds were cherry-picked for the results presented here.

5 Conclusion

We introduced One-Shot World Model (OSWM), a world model trained purely on synthetic data sampled from a prior distribution based on randomly initialized, untrained neural networks by leveraging In-context Learning. Despite the simplicity of the prior, OSWM achieved promising results as it is able to train RL agents to solve tasks like GridWorld and control tasks such as CartPole-v0, demonstrating the potential of synthetic pretraining in Model-Based Reinforcement Learning. Although the model still struggles with more complex environments like Pendulum-v1 and MountainCar-v0, our empirical analysis suggests that improving the priors and refining context sampling are key to enhancing performance. Our results highlight the potential of synthetic pretraining in RL, suggesting that with further optimization, this approach could be a key step towards foundation world models, capable of tackling increasingly complex tasks. With further optimization of the prior, synthetic pretraining could enable the development of more generalizable foundation world models, offering a scalable solution for RL training, especially when evaluating real-world environments is costly and challenging.

Acknowledgments and Disclosure of Funding

Frank Hutter acknowledges the financial support of the Hector Foundation. We also acknowledge funding by the European Union (via ERC Consolidator Grant DeepLearning 2.0, grant no. 101045765). Views and opinions expressed are however those of the author(s) only and do not necessarily reflect those of the European Union or the European Research Council. Neither the European Union nor the granting authority can be held responsible for them. Moreover, we acknowledge funding by the Deutsche Forschungsgemeinschaft (DFG, German Research Foundation) under grant number 417962828.



References

Philip J. Ball, Cong Lu, Jack Parker-Holder, and Stephen Roberts. Augmented world models facilitate zero-shot dynamics generalization from a single offline environment, 2021. URL <https://arxiv.org/abs/2104.05632>.

Chang Chen, Yi-Fu Wu, Jaesik Yoon, and Sungjin Ahn. Transdreamer: Reinforcement learning with transformer world models, 2022. URL <https://arxiv.org/abs/2202.09481>.

Ben Evans, Abitha Thankaraj, and Lerrel Pinto. Context is everything: Implicit identification for dynamics adaptation, 2022. URL <https://arxiv.org/abs/2203.05549>.

F. Ferreira, T. Nierhoff, A. Sälinger, and F. Hutter. Learning synthetic environments and reward networks for reinforcement learning. In *Proc. of ICLR’21*, 2021. URL <https://iclr.cc/virtual/2022/poster/6495>.

Kevin Frans, Seohong Park, Pieter Abbeel, and Sergey Levine. Unsupervised zero-shot reinforcement learning via functional reward encodings, 2024. URL <https://arxiv.org/abs/2402.17135>.

David Ha and Jürgen Schmidhuber. World models. *CoRR*, abs/1803.10122, 2018. URL <http://dblp.uni-trier.de/db/journals/corr/corr1803.html#abs-1803-10122>.

D. Hafner, T. P. Lillicrap, J. Ba, and M. Norouzi. Dream to control: Learning behaviors by latent imagination. In *Proc. of ICLR’20*, 2020.

D. Hafner, T. P. Lillicrap, M. Norouzi, and J. Ba. Mastering atari with discrete world models. In *Proc. of ICLR’21*, 2021.

D. Hafner, J. Pasukonis, J. Ba, and T. P. Lillicrap. Mastering diverse domains through world models. *arXiv:2301.04104 [cs.AI]*, 2023.

N. Hansen, H. Su, and X. Wang. TD-MPC2: scalable, robust world models for continuous control. In *Proc. of ICLR’24*, 2024.

N. Hollmann, S. Müller, K. Eggensperger, and F. Hutter. TabPFN: A transformer that solves small tabular classification problems in a second. In *Proc. of ICLR’23*, 2023.

L. Kaiser, M. Babaeizadeh, P. Milos, B. Osinski, R. H. Campbell, K. Czechowski, D. Erhan, C. Finn, P. Kozakowski, S. Levine, A. Mohiuddin, R. Sepassi, G. Tucker, and H. Michalewski. Model-based reinforcement learning for atari, 2019. URL <https://arxiv.org/abs/1903.00374>.

Jonathan N. Lee, Annie Xie, Aldo Pacchiano, Yash Chandak, Chelsea Finn, Ofir Nachum, and Emma Brunskill. Supervised pretraining can learn in-context reinforcement learning, 2023. URL <https://arxiv.org/abs/2306.14892>.

Vincent Micheli, Eloi Alonso, and François Fleuret. Transformers are sample-efficient world models, 2023. URL <https://arxiv.org/abs/2209.00588>.

S. Müller, N. Hollmann, S. Arango, J. Grabocka, and F. Hutter. Transformers can do Bayesian inference. In *Proc. of ICLR’22*, 2022.

Antonin Raffin, Ashley Hill, Adam Gleave, Anssi Kanervisto, Maximilian Ernestus, and Noah Dormann. Stable-baselines3: Reliable reinforcement learning implementations. *Journal of Machine Learning Research*, 22(268):1–8, 2021. URL <http://jmlr.org/papers/v22/20-1364.html>.

Raghu Rajan, Jessica Lizeth Borja Diaz, Suresh Guttikonda, Fabio Ferreira, André Biedenkapp, Jan Ole von Hartz, and Frank Hutter. Mdp playground: An analysis and debug testbed for reinforcement learning. *Journal of Artificial Intelligence Research (JAIR)*, 77:821–890, 2023. doi: 10.1613/jair.1.14314.

Jan Robine, Marc Höftmann, Tobias Uelwer, and Stefan Harmeling. Transformer-based world models are happy with 100k interactions, 2023. URL <https://arxiv.org/abs/2303.07109>.

J. Schrittwieser, I. Antonoglou, T. Hubert, K. Simonyan, L. Sifre, S. Schmitt, A. Guez, E. Lockhart, D. Hassabis, T. Graepel, T. P. Lillicrap, and D. Silver. Mastering atari, go, chess and shogi by planning with a learned model. *Nat.*, 588(7839):604–609, 2020. doi: 10.1038/S41586-020-03051-4. URL <https://doi.org/10.1038/s41586-020-03051-4>.

Ingmar Schubert, Jingwei Zhang, Jake Bruce, Sarah Bechtle, Emilio Parisotto, Martin Riedmiller, Jost Tobias Springenberg, Arunkumar Byravan, Leonard Hasenclever, and Nicolas Heess. A generalist dynamics model for control, 2023. URL <https://arxiv.org/abs/2305.10912>.

John Schulman, Filip Wolski, Prafulla Dhariwal, Alec Radford, and Oleg Klimov. Proximal policy optimization algorithms, 2017. URL <https://arxiv.org/abs/1707.06347>.

Josh Tobin, Rachel Fong, Alex Ray, Jonas Schneider, Wojciech Zaremba, and Pieter Abbeel. Domain randomization for transferring deep neural networks from simulation to the real world, 2017. URL <https://arxiv.org/abs/1703.06907>.

Zecheng Wang, Che Wang, Zixuan Dong, and Keith Ross. Pre-training with synthetic data helps offline reinforcement learning, 2024. URL <https://arxiv.org/abs/2310.00771>.

Philipp Wu, Alejandro Escontrela, Danijar Hafner, Pieter Abbeel, and Ken Goldberg. Daydreamer: World models for physical robot learning. In Karen Liu, Dana Kulic, and Jeffrey Ichnowski, editors, *Conference on Robot Learning, CoRL 2022, 14-18 December 2022, Auckland, New Zealand*, volume 205 of *Proceedings of Machine Learning Research*, pages 2226–2240. PMLR, 2022. URL <https://proceedings.mlr.press/v205/wu23c.html>.

Mengjiao Yang, Yilun Du, Kamyar Ghasemipour, Jonathan Tompson, Dale Schuurmans, and Pieter Abbeel. Learning interactive real-world simulators. *arXiv preprint arXiv:2310.06114*, 2023.

Weipu Zhang, Gang Wang, Jian Sun, Yetian Yuan, and Gao Huang. Storm: Efficient stochastic transformer based world models for reinforcement learning, 2023. URL <https://arxiv.org/abs/2310.09615>.

Part IV

Conclusion

Summary and Discussion

In this chapter, we will now summarize the contributions presented in this dissertation. In Part I, we outlined the broader context and motivation for the dissertation topic and derived three key challenges this work sought to answer:

- Challenge 1:** Automating Model Selection and Finetuning Amidst a Growing Landscape of Pretrained Models
- Challenge 2:** Enhancing Learning With Advanced Data Augmentation and Synthetic Data Generation
- Challenge 3:** Ensuring Reproducibility and Practical Applicability of Automated Learning Methods

From this, we identified the overarching scientific question "*How can meta-learning and synthetic data advance automated pretraining and finetuning?*". We addressed the first two challenges in the two core parts of this dissertation:

- Part II:** Meta-Learning for Automated Model Selection and Finetuning
- Part III:** Meta-Learning Data Augmentation and Synthetic Data for Enhanced Learning

The third challenge was a recurring theme throughout the dissertation since the majority of the papers integrated replicable experiments, open-sourcing of code, and transparent reporting for reproduction. In particular, Quick-Tune-Tool directly addressed this challenge by offering a tool to facilitate reproducible experimentation.

Addressing the first key challenge in Part II, the associated works focus on leveraging meta-learning to automate the selection and hyperparameter optimization of Deep Learning (DL) pipelines for finetuning given a set of candidate pretrained models. The primary emphasis of these works lies in the automation of finetuning computer vision models, and both data augmentation and synthetic data play a secondary role. The core works to highlight in this part are ZAP (Chapter 5) and Quick-Tune (Chapter 6), which propose to address the key challenge by meta-learning zero-shot and few-shot surrogate models based on prior finetuning data. These works' central novelty and contribution showcase how the classic perspective of algorithm selection can be adopted and elegantly extended to provide effective solutions for the deep learning era, allowing the incorporation of hyperparameters such as data augmentation or finetuning strategies. While ZAP employs dataset level augmentation to enrich its performance matrix, showing how data augmentation can be utilized in the input space to aid meta-learning, Quick-Tune exploits data augmentation in its search space. Importantly, the Quick-Tune results empirically illustrate that a suitable model's customization can compete with or outperform the finetuning of large-scale backbones. This underscores the effectiveness of the broader approach to automating DL pipeline selection and customization as a viable strategy for optimizing deep learning

models. The remaining works (Chapter 7 and Chapter 8) in this part mainly show the utility of developing Quick-Tune-Tool to facilitate wider adoption of Quick-Tune and how it can be transferred to automating the finetuning of large language models (LLMs). Like ZAP’s dataset augmentation in the input space, Chapter 8 shows how generating synthetic Q&A datasets similarly serves as an input-level augmentation strategy for aiding meta-learned LLM finetuning.

In Part III, we address the second key challenge of exploring new ways to leverage data effectively through the help of advanced data augmentation and synthetic data generation. In contrast to the contributions of the previous part, data augmentation and synthetic data are key components of the works in this part. Starting with data augmentation in Self-Supervised Learning (SSL) for computer vision models, the study presented in Chapter 9 provides empirical evidence that data augmentation plays an underestimated role in impacting model performance. No significant improvements were attainable when optimizing training hyperparameters, but significant improvements were achieved when optimizing data augmentation hyperparameters. This finding further motivated the development of the novel data augmentation strategy of Hard View Pretraining (HVP) presented in Chapter 10. HVP leverages meta-learning to select challenging views based on the model’s current performance by extending the random view generation common in SSL. Despite its simplicity, pretraining with HVP results in improved hyperparameter robustness and downstream task performance across architectures, datasets, and SSL methods. HVP also achieves a new state-of-the-art result on the ViT-B/16 transformer architecture and demonstrates the potential of meta-learned data augmentation strategies. Building on this foundation, the work in Chapter 11 uses meta-learning to optimize not just data augmentation but the data generation process itself. This work demonstrates the strength of adopting meta-learning for optimizing the effective use of data: the meta-learned synthetic proxies exhibit valuable properties, such as facilitating agent training with significantly fewer training steps and greater robustness to agent hyperparameter variations. However, meta-learning synthetic environments is computationally expensive, even in the relatively controlled domain of RL. To address this, the work presented in Chapter 12 investigates reducing the costs by replacing meta-learning with randomly sampled synthetic data. The approach samples the data from network-based prior distributions that mimic the dynamics of multiple RL environments, allowing the learned proxy to support agent training across diverse target environments. By achieving a proxy environment that generalizes to multiple targets, we further reduce computational demands and take a step toward foundational world models trained entirely on synthetic data.

Takeaways and Outlook

This dissertation has explored how meta-learning and synthetic data can advance automated pretraining and finetuning. The works throughout this dissertation encompass a broad range of tasks, including image classification and large language model finetuning, pretraining with self-supervised learning (SSL), and world model learning for reinforcement learning (RL). Together, the contributions in this dissertation illustrate that meta-learning can inform strategies for selecting pretrained models and tuning their hyperparameters, automated data augmentation, and synthetic data generation. By integrating insights from diverse domains, this dissertation presents novel approaches that go a step towards more automated, adaptive, and generalizable machine learning workflows.

Meta-Learning for Automated Model Selection and Finetuning

With ZAP, we took initial steps toward adapting the principles of Combined Algorithm Selection and Hyperparameter Optimization (CASH) to modern deep learning pipelines. Crucially, ZAP demonstrated that when combined with meta-features, suitable augmentations, and a large-scale meta-dataset, such AutoML methods can be applied effectively in the deep learning domain to automate finetuning. ZAP introduced a zero-shot approach, where no exploratory evaluations on the target dataset were required for the DL pipeline selection. ZAP’s dataset level augmentation strategy revealed how expanding and diversifying a meta-dataset allows the selection process to accommodate test-time variation and handle missing values. We believe this robustness likely arises from the model’s capacity to capture correlations across pipelines in a geometric space, generalizing beyond observed conditions. Building on ZAP, Quick-Tune proposed a few-shot setting and leveraged partial learning curves to meta-learn probabilistic surrogate models. This integration allowed Quick-Tune to iteratively select pipelines through Bayesian optimization under practical user time and resource constraints.

Together, ZAP and Quick-Tune have established a foundation for automated finetuning in the deep learning era. We believe these works established a baseline by showing that tailored model selection and hyperparameter tuning can outperform finetuning large, general-purpose billion-parameter models like DINOv2, especially when the target tasks differ substantially from the models’ original pretraining domains. A pivotal design decision was the integration of finetuning and data augmentation strategies in Quick-Tune’s search space, aligning with ongoing developments in machine learning practices. The ability of methods like ZAP and Quick-Tune to explore vast search spaces and their compatibility with newly emerging methods like parameter-efficient finetuning (PEFT) (Lialin et al., 2023; L. Xu et al., 2023) such as LoRA (E. J. Hu et al., 2021) gives them a competitive edge.

Notably, ZAP and Quick-Tune illustrate how CASH can be adopted for a quickly growing space of LLMs. For example, they allow generalizing to LLMs' post-pretraining phase that encompasses a multitude of adaptations such as finetuning, PEFT, adapters, prefix tuning, and chain-of-thought (Wei et al., 2022) design. As PEFT and other technologies become more widespread, automated methods such as ZAP and Quick-Tune may become increasingly relevant as the importance of systematically exploring configuration spaces grows. These methods likewise introduce a potentially large number of additional hyperparameters that require systematic exploration. For instance, to just name a few: low-rank dimension, adapter size, chain-of-thought styles, or number of LLM agents in multi-agent settings. Lastly, as large-scale model training requires large-scale data pipelines, more and more "support models" are being developed, such as for sample deduplication detection, RLHF rewards, high-quality prompts and responses selection, or even for curriculum learning (Y. Bengio et al., 2009; Meta, 2024) (e.g., when and how to mix real with synthetic data). By unifying domain knowledge with large-scale hyperparameter search and model selection, automated methods like ZAP or Quick-Tune can play a pivotal role in future LLM research and development.

However, not all design decisions during the development of ZAP and Quick-Tune were fruitful. For instance, attempts to improve performance by integrating learned meta-features (Achille et al., 2019) in both ZAP and Quick-Tune have so far underperformed simpler, static meta-features, which remain insufficiently understood and beg future investigation. Furthermore, while we have shown the applicability of Quick-Tune to the language processing domain for finetuning LLMs, we found that empirical search performance is better when no iterative refinement of the surrogate models is executed. We hypothesize this is due to overfitting to a meta-dataset that is too small, hinting at the disadvantage of few-shot and Bayesian Optimization in contrast to zero-shot approaches. However, more experiments with larger meta-datasets are required to validate this hypothesis and to understand this phenomenon better. Apart from that, a range of open questions and refinements still exists. For instance, meta-hyperparameters of our approaches, such as the computational budget allocated for evaluating candidate configurations, can significantly influence performance and achievable speed-ups over black-box methods. How to encode hyperparameters and architectures remains an underexplored factor, as a default practice is to rely on categorical embeddings (Feurer et al., 2015) mostly. Future work could also extend these approaches to the domain of large *multimodal* models, and leveraging multi-GPU and distributed computation setups could further broaden their impact and reveal how they respond to automated optimization. Moreover, recent work (Liu et al., 2024) proposed using LLMs as surrogate models. This poses an intriguing alternative for the performance and cost prediction of DL pipelines that can extend to multi-objective optimization. Building on this, one could also use LLMs to directly output the kernel function in Bayesian Optimization for pipeline cost and performance prediction. Addressing these points will help move from promising baselines and initial successes toward more mature and widely deployable automated finetuning solutions in deep learning.

Meta-Learning Data Augmentation and Synthetic Data for Enhanced Learning

Beyond addressing CASH in the deep learning context, this dissertation underscores the importance of viewing data augmentation and synthetic data as central, meta-learned elements rather than peripheral components of learning pipelines. Our studies illustrate empirically that carefully leveraging data augmentation and synthetic data can yield significant performance improvements in supervised, self-supervised, and reinforcement learning. For instance, in self-supervised learning, we investigated the role of data augmentation.

We showed that even simple, learning-free automated data augmentation techniques like Hard View Pretraining (HVP) proved sufficient to challenge existing discriminative pretraining pipelines and to improve robustness and downstream performance. This empirically shows that advancements in automated data augmentation do not need to rely on parametric or complex architectural changes but can be achieved by effectively leveraging state-dependent augmentation strategies. However, we also noticed that some early design decisions were less successful. For example, training a network to generate augmented views resulted in unstable training, as the network generated either very hard or static views, resulting in repeated model collapse. This shows how challenging it can be to design augmentation strategies that adapt to the learning state without destabilizing a given training process. Going forward, future work could use the HVP objective to learn the parameters of parameterized distributions of data augmentation operations instead of learning the view generation itself. This may not only make the task more computationally affordable than learning entire view generators as is common in the literature but also allow for an interpretation of the required augmentations at any given learning state. Moreover, the HVP paradigm can be applied wherever random augmentations sampling is used, not just in pretraining but also during finetuning. Similarly, future work could also extend selecting hard augmentations to multimodal model training such as CLIP (Radford et al., 2021). Lastly, HVP’s principles could also be adapted for LLM training. In the supervised finetuning phase of LLMs, for example, one could automatically select high-loss samples from each training batch where the model’s predictions diverge most from ground-truth labels.

With Synthetic Environments (SEs), we turned our attention to the possibility of meta-learning synthetic data itself. SEs allowed agent training without continuous reliance on real-world interactions while drastically reducing the environment interactions needed and increasing agent hyperparameter robustness. Due to their efficiency, agent hyperparameter robustness, and agent algorithm agnosticism, such environment proxies could aid automated reinforcement learning (AutoRL) (Parker-Holder et al., 2022) by enabling the pretraining of general agents or facilitating efficient development cycles for new RL algorithms. Developing analytical tools based on SEs can also facilitate inverse reinforcement learning, providing deeper insights into environment dynamics and task structures. These tools aid human understanding and analysis of complex RL tasks from optimization and parametric perspectives.

The SE framework could also be applicable in the LLM context: current LLM reward models (RMs) often optimize proxy objectives (e.g. human preferences or outcome and rule-based rewards (Uesato et al., 2022), i.e. they optimize “what responses are preferred by humans?” instead of “how to solve tasks?”) that lead to LLMs exploiting shortcuts (e.g. poor readability and language mixing) or complex multi-stage training that requires post-rejection sampling to generate synthetic datasets with strong samples for finetuning (Guo et al., 2025). This is because coming up with RMs that facilitate open-ended problem-solving is very challenging. Learned environments and RMs may present an interesting step towards aligning better with open-ended problem-solving capabilities that is worth exploring. The SE framework may offer a pathway to address this by meta-learning task-aligned reward functions through bi-level optimization. For instance, inspired by SEs’ ability to meta-learn synthetic environment dynamics and rewards, one could replace the traditional RL agent in the SE framework with an LLM agent in a language task environment (e.g., constrained code generation or math-solving) and meta-learn RMs that elicit task solving behaviors. Moreover, RMs’ potential-based reward shaping could ground these rewards in verifiable outcomes (e.g., code executability or answer consistency) and avoid reliance on brittle human judgments or mitigate exploiting reward shortcuts.

In the context of world models, the large-scale world model Genie 2 (Parker-Holder et al., 2024) was represented recently which is a first step toward foundational world models that may enable generalist capabilities for open-ended agent learning (R. Wang et al., 2019). As architectures and data scale, it may become relevant to incorporate insights from approaches like SEs that exploit algorithmic properties such as agent agnosticism, hyperparameter robustness, and training efficiency. For instance, agents could be trained using Genie 2’s pixel space, while SEs operate in the latent embedding space to model the underlying dynamics and actions. The SEs could be meta-learned by adjusting their dynamics predictions based on the agent’s performance on a target task. Combining such latent-space modeling with Genie 2 may provide a pathway to integrating meta-learning approaches like SEs with AutoRL and foundation world models.

Motivated by world models that model multiple tasks or target environments, we introduced the One-Shot World Model (OSWM). OSWM leverages randomly sampled data from mixed prior distributions and in-context learning to pretrain a world model that approximates the dynamics of multiple simple control environments. A key insight is that the complexity and diversity of the prior distribution correlate positively with the performance of the learned agent policy, emphasizing the importance of designing sophisticated priors. While still very limited, OSWM demonstrates what may be possible by advancing our understanding of how prior distributions should be modeled. With well-designed priors tailored to target tasks, agents and robots could be pretrained in simulation before deployment, potentially reducing risks such as failure modes that damage robots and reducing costs by requiring less real-world data. This approach offers a path toward safer and more efficient pretraining strategies for real-world applications.

All in all, this dissertation has contributed to the development of individual components and solutions that advance the vision of fully automated, meta-learned machine learning systems for pretraining and finetuning. By combining the automated model selection and hyperparameter optimization capabilities of ZAP, Quick-Tune, and Quick-Tune-Tool jointly with the data augmentation and synthetic data strategies provided by HVP, GroupAugment, SEs, and OSWM, future research can develop unified systems that integrate components like these and further automate key elements of the machine learning pipelines. As computational resources grow, these components could be meta-learned jointly to unlock synergies beyond isolated automation. Such systems would tailor solutions to specific tasks and domains by dynamically selecting high-performing configurations, adjusting data strategies, and integrating synthetic environments. The modularity of this dissertation’s contributions allows for refining components individually or combining them to enhance their performance and address the evolving complexities of modern AI applications. Lastly, the contributions in this dissertation interface with data in a manner that imposes no strong assumptions about its representation, ensuring that these methods can seamlessly extend to new model architectures, including LLMs and future model architectures. This broad applicability positions our meta-learned solutions as versatile candidates for future machine learning deployment and research.

Appendices

Appendices for Zero-Shot AutoML with Pretrained Models

A.1 Paper Appendix

A. Appendix

A.1. Search Space of DL Pipelines

We list the search space of the DL pipelines clustered into two groups. The first group are general DL hyperparameters including the architecture and fine-tuning strategy. The second group defines the early stopping, validation and test strategies during the 20 minutes of training, including set sizes and evaluation timings.

Table 6. The search space of our DL pipelines clustered into two groups. The first group are general DL hyperparameters including the architecture and fine-tuning strategy. The second group defines the early stopping, validation and test strategies during the 20 minutes of training, including set sizes and evaluation timings.

Name	Type, Scale	Range
Batch size	int, log	[16, 64]
Learning rate	float, log	[10^{-5} , 10^{-1}]
Min learn. rate	float, log	[10^{-8} , 10^{-5}]
Weight decay	float, log	[10^{-5} , 10^{-2}]
Momentum	float	[0.01, 0.99]
Optimizer	cat	{SGD, Adam, AdamW}
Nesterov	cat	{true, false}
Amsgrad	cat	{true, false}
Scheduler	cat	{plateau, cosine}
Freeze portion	cat	{0.0, 0.1, ..., 0.5}
Warm-up mult.	cat	{1.0, 1.5, ..., 3.0}
Warm-up epoch	int	[3, 6]
Architecture	cat	{ResNet18, EffNet-b0, EffNet-b1, EffNet-b2}
Steps per epoch	int, log	[5, 250]
Early epoch	int	[1, 3]
CV ratio	float	[0.05, 0.2]
Max valid count	int, log	[128, 512]
Skip valid thresh.	float	[0.7, 0.95]
Test freq.	int	[1, 3]
Test freq. max	int	[60, 120]
Test freq. step	int	[2, 10]
Max inner loop	float	[0.1, 0.3]
# init samples	int, log	[128, 512]
Max input size	int	[5, 7]
1 st simple model	cat	{true, false}
Simple model	cat	{SVC, NuSVC, RF, LR}

A.2. Dataset Augmentation

In the following Table 7 we list all TFDS datasets we used for creating our 525 datasets with their respective domains. For each dataset $\mathcal{D}_{original}$ we create 15 subsets by sampling number of classes from range [2, 100] and min/max number of samples per class from range [20, 10^5] such that $\mathcal{D}_i \subseteq \mathcal{D}_{original}, \forall i \in \{1, \dots, 15\}$ (Figure 7). Remark that there is no procedure on sample level, meaning that subsets inherit image resolutions and channels from the original dataset as given in the Tables 8 and 9. Figure 8 contains the number of sample and class distributions of these subsets along with the AutoDL Challenge benchmark datasets.

A.3. AutoDL: Area Under the Learning Curve (ALC) Metric

In the 2019 ChaLearn AutoDL challenge and also in all our experiments, the main performance metric is the Area under the Learning Curve (ALC). Formally, we test the currently trained model on a test set p_i at time t_i by calculating a scalar score,

Table 7. Domains of the original datasets

Domain	Datasets
Objects	Cifar100 (Krizhevsky et al., 2009), Cifar10, Horses or Humans (Moroney, 2019a), CycleGAN Horse2zebra (Zhu et al., 2017), CycleGAN Facades, CycleGAN Apples2orange, Imagenette (Howard), Coil100 (Nene et al., 1996), Stanford Dogs (Khosla et al., 2011), Rock, Paper and Scissors (Moroney, 2019b), TF Flowers (Team, 2019), Cassava (Mwebaze et al., 2019), Fashion MNIST (Xiao et al., 2017), Cars196 (Krause et al., 2013), Cats vs Dogs (Elson et al., 2007), ImageNet Resized 32x32 (Chrabaszcz et al., 2017)
Characters	Cmaterdb Devanagari (Das et al., 2012a;b), Cmaterdb Bangla, MNIST (LeCun et al., 2010), KMNIST (Clanuwat et al., 2018), EMNIST Byclass (Cohen et al., 2017), EMNIST MNIST, Cmaterdb Telugu, EMNIST Balanced, Omniglot (Lake et al., 2015), SVHN Cropped (Netzer et al., 2011)
Medical	Colorectal Histology (Kather et al., 2016), Malaria (Rajaraman et al., 2018)
Aerial	Uc Merced (Yang & Newsam, 2010), CycleGAN Maps, Eurosat RGB (Helber et al., 2017)
Drawings/Pictures	CycleGAN Vangogh2photo, CycleGAN Ukiyoe2photo

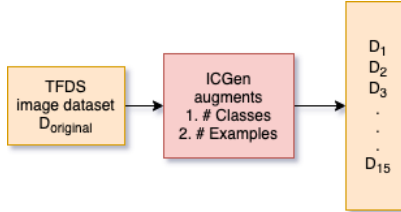


Figure 7. Dataset augmentation flow

the Normalized Area Under ROC Curve (AUC):

$$s_i = 2 * AUC(\vec{p}_i) - 1 \quad (7)$$

We then convert this score to a time-sensitive step function

$$s(t) = step_fn(\vec{s}) \quad (8)$$

and we also transform the time non-linearly between $[0, 1]$ such that the performance on the first minute is weighted roughly the same as the last 10 minutes of the budget:

$$\tilde{t}(t) = \frac{\log(1 + t/t_0)}{\log(1 + T/t_0)} \quad (9)$$

where $T = 1200$ is the total default training budget and $t_0 = 60$ is the default reference time.

Finally, we measure the ALC by:

$$ALC = \int_0^1 s(t) d\tilde{t}(t) \quad (10)$$

For more details on the metric, we refer the reader to (Liu et al., 2021). We depict an example of an ALC plot in Figure 9.

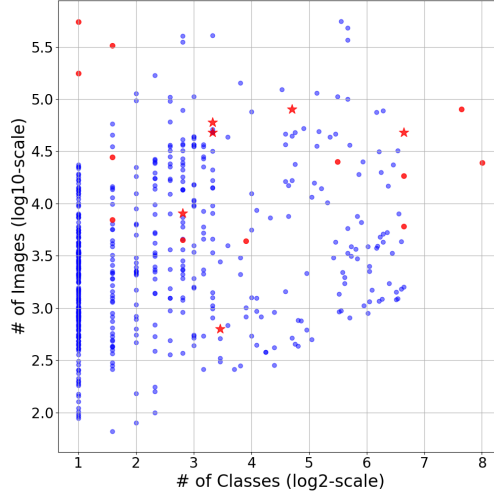


Figure 8. **Distribution of the meta-features** where each point corresponds to a dataset. Blue points come from our meta-dataset, whilst red ones are the datasets provided by AutoDL challenge. Star and point markers are public AutoDL datasets and private AutoDL datasets (from feedback and final phases), respectively.

A.4. Hardware Setup

Due to the anytime performance measurements of the AutoDL challenge’s training and evaluation protocol and the resulting importance on wall clock time, we ensured that all experiments in this work were run on machines with the same hardware setup. The specification of our machines is the following: AMD EPYC 7502 32-Core Processor, NVIDIA GeForce RTX 2080 Ti, 500GB RAM, CUDA version 11.5, Ubuntu 20.04.3 LTS.

Statement of Contributions

Ekrem Öztürk: Methodology, Software (extending the AutoDL 2019 challenge submission base code from Fabio with more datasets), Validation (running all ZAP-AS experiments after the challenge deadline starting June 2020 and also the ZAP-HPO rebuttal experiments), Investigation, Data Curation, Writing: Original Draft, Writing: Review and Editing, Visualization

Fabio Ferreira: Conceptualization, Methodology, Software (providing the base code for the AutoDL challenge 2019 submission), Validation (and running all ZAP-AS experiments up to the challenge deadline on March 14 2020), Investigation,

Table 8. **Resolution Distribution** of datasets

Resolution	# of Datasets
28×28	90
32×32	105
64×64	15
105×105	15
128×128	15
150×150	15
256×256	90
300×300	30
600×600	15
Varying	135

Table 9. Image channels distribution of datasets

Channel	# of Datasets
B&W	90
RGB	435

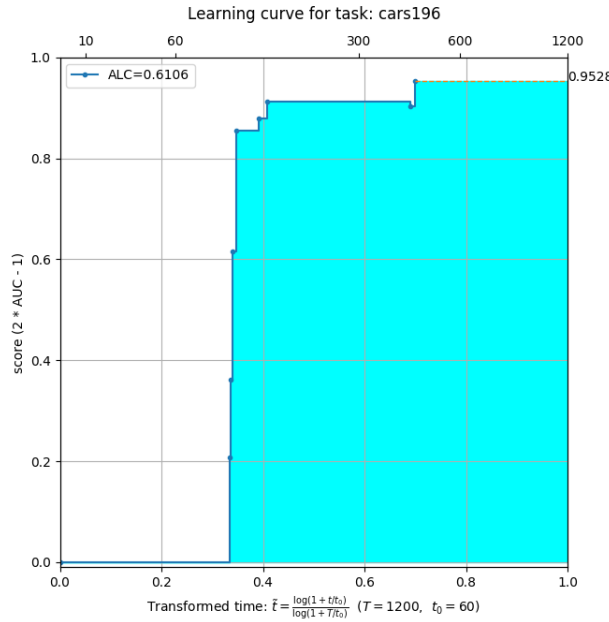


Figure 9. **Learning curve of a task** is the step function of normalized AUC (NAUC) scores received during the 20 minutes and the light blue area underneath is the area under the learning curve(ALC). Every dark blue point (steps) corresponds to a set of predictions made and y-axis to its NAUC score. When the procedure stops early, the final NAUC is interpolated to the end with a horizontal line. Top x-axis is the time limited to 1200 seconds and the bottom axis is the transformed version between [0, 1]. Visualization clearly shows that the first 60 seconds contributes to more than 20% of the total score and has the same weight as the last 600 seconds. Remark that total budget $T = 1200$ and reference time constant $t_0 = 60$ here, the same values as in our experiments.

A.2 Statement of Contributions

Statement of Contributions for the following publication:

Title	Zero-shot AutoML with Pretrained Models
Link to Publication, DOI	https://proceedings.mlr.press/v162/ozturk22a
Authors	Ekrem Öztürk*, Fabio Ferreira*, Hadi Jomaa*, Lars Schmidt-Thieme, Josif Grabocka and Frank Hutter (*: joint first author)
Publication Status	Accepted and published
Publisher, Date	Proceedings of the 39th International Conference on Machine Learning (ICML), 2022
Peer-Review-Process	Yes
Rank	Ranked A* by the CORE2023 ranking

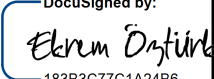
Paper Summary

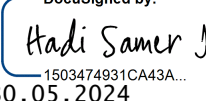
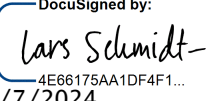
The paper "Zero-Shot AutoML with Pretrained Models" introduces an innovative approach to Automated Machine Learning (AutoML) that leverages pretrained models and meta-learning to select and tune deep learning pipelines without requiring any exploratory evaluations on new datasets. It enables efficient model and hyperparameter selection under resource constraints and contributes to the fields of meta-learning and AutoML. The key contributions of the paper are:

1. The study extends traditional automated machine learning approaches by using meta-learning to learn a selector that chooses the right pretrained model and finetuning hyperparameters (referred to as a "deep learning pipeline") for unseen image classification datasets conditioned only on the dataset meta-features ("zero-shot").
2. The paper provides a large-scale meta-dataset comprising evaluations of 525 deep learning pipelines across 525 popular image classification datasets. This dataset is used for meta-learning the selector and is one of the largest of its kind at the time of the paper publication.
3. The paper introduces a novel methodology for zero-shot AutoML, beginning with the development of a powerful meta-selector known as "ZAP-AS". This meta-selector leverages the algorithm selection system "AutoFolio", which incorporates techniques from regression, classification, clustering, and cost-sensitive classification. ZAP-AS operates independently of geometric spaces, focusing instead on algorithmic selection without exploiting correlated spatial information about deep learning pipelines. Subsequently, the paper presents "ZAP-HPO", which approaches the pipeline selection by formulating it as an algorithm selection problem within a geometric space. In contrast to ZAP-AS, this method utilizes a ranking objective for pipelines.
4. The proposed approach was evaluated in the ChaLearn AutoDL challenge under tight computational constraints and demonstrated superior performance, significantly outperforming all competition entries and baselines.

Contributions Listing

Name	Contributions	Signature
Fabio Ferreira	<p>As the core developer and main contributor of the AutoML Freiburg Lab's submission to the AutoDL challenge 2019 [1], Fabio laid the foundation of the project by providing all project code to Ekrem, who extended and scaled up the idea to more datasets, better augmentation methods and tuned ZAP-AS models. The code from Fabio included the meta-dataset collection/curation, meta-dataset augmentation, Hyperparameter Optimization (HPO) scripts for generating the meta-dataset, training logic for ZAP-AS with AutoFolio, cluster submissions and experiment execution;</p> <p>Supported Ekrem on the code-level through code reviews and small code changes (e.g., meta-dataset augmentation).</p> <p>Proposed and defined the DL pipeline hyperparameter search space (jointly with Frank), as well as the meta-dataset design including the meta-dataset augmentations present in the paper;</p> <p>Co-led the project's methodology and overall strategic direction (jointly with Frank);</p> <p>Ran initial ZAP-AS model experiments and tuned its early versions on a smaller version of the meta-dataset for the challenge submission; analyzed the effect of simple and complex meta-features on the performance of ZAP-AS; the analysis of how simple and complex meta-features impact the performance of ZAP-AS/ZAP-HPO was incorporated into the final evaluations and conclusions presented in the paper;</p>	<p>DocuSigned by:</p>  <p>CA7363FD31BF45C... 29.05.2024</p>

	<p>Owned, led and wrote the majority of the paper, including contributions to all parts of the paper and creating figures 1 and 2; led and contributed significantly to the rebuttal process;</p> <p>Supervised Ekrem Öztürk.</p> <p>[1] Zhengying Liu, Adrien Pavao, Zhen Xu, Sergio Escalera, Fabio Ferreira, et al., <i>Winning solutions and post-challenge analyses of the chalearn autodl challenge 2019</i>. IEEE Transactions on Pattern Analysis and Machine Intelligence, 43(9):3108–3125, 2021.</p>	
Ekrem Öztürk	<p>Owned and led the extension of the AutoDL competition code from Fabio, which included adding more datasets to the meta-dataset, running the HPO with larger budgets for the DL pipelines that resulted in the large-scale meta-dataset (present in paper), finetuned the ZAP-AS models, and implemented all baseline methods;</p> <p>Executed all ZAP-AS meta-trainings on the extended meta-dataset and some ZAP-HPO experiments for the rebuttal;</p> <p>Supported with writing, editing, reviewing and rebutting all parts of the paper, but the parts of the paper he had the major contributions were: ZAP Meta-Dataset Design (Section 4), Experiments (Section 5), and Figures 4-6.</p>	<p>DocuSigned by:</p>  <p>Ekrem Öztürk 183B3C77C1A24B6... 30/05/2024</p>

Hadi Jomaa	<p>Owned and led the implementation and training of ZAP-HPO, including defining its hyperparameter configuration space;</p> <p>Ran the ZAP-HPO experiments for the initial paper submission (Ekrem executed the experiments for the rebuttal);</p> <p>Supported with writing, editing, and reviewing all parts of the paper, but the parts of the paper he had the major contributions were: Related Work (Section 2), ZAP via Zero-Shot HPO (ZAP-HPO) (Section 3.3), Experiments (Section 5), and Figure 3.</p>	<p>DocuSigned by:</p>  <p>Hadi Samer Jomaa 1503474931CA43A... 30.05.2024</p>
Lars Schmidt-Thieme	<p>Helped with reviewing, rebutting and editing the paper;</p> <p>Supervision of Hadi Jomaa.</p>	<p>DocuSigned by:</p>  <p>Lars Schmidt-Thieme 4E66175AA1DF4F1... 6/7/2024</p>
Josif Grabocka	<p>Proposed the idea of using a ranking surrogate objective;</p> <p>Helped conceptualize the problem;</p> <p>Co-led writing the paper, including contributions to all parts of the paper;</p> <p>Helped with reviewing, rebutting and editing the paper.</p>	<p>DocuSigned by:</p>  <p>Josif Grabocka 257E43784D71473... 6/8/2024</p>
Frank Hutter	<p>Proposed the original idea for tackling the problem specification of the AutoDL challenge with a meta-learned algorithm selection surrogate model based on deep learning pipeline meta-training data;</p> <p>Helped conceptualize the problem;</p> <p>Co-led writing the paper, including contributions to all parts of the paper;</p>	<p>DocuSigned by:</p>  <p>Frank Hutter 3CDF1E88127C47F... 6/28/2024</p>

	<p>Helped with reviewing, rebutting and editing the paper.</p> <p>Supervised the project and Fabio Ferreira.</p>	
--	--	--

Appendices for Quick-Tune: Quickly Learning Which Pretrained Model to Finetune and How

B.1 Paper Appendix

A ALGORITHMIC DETAILS

A.1 NORMALIZED REGRET

Given an observed performance y , the normalized regret is computed per datasets as follows:

$$y_{\text{norm}} = \frac{y_{\text{max}} - y}{y_{\text{max}} - y_{\text{min}}} \quad (7)$$

where $y_{\text{max}}, y_{\text{min}}$ in Equation 7 are respectively the maximum and minimum performances in the meta-dataset.

A.2 ADDITIONAL SET-UP DETAILS

The categorical encoder of the model is a linear layer with 4 output neurons, while the learning curve embedding is generated from a convolutional neural network with two layers. For the rest of the hyperparameters of the deep-kernel Gaussian process surrogate and the acquisition function, we followed the settings described in the respective publication (Wistuba et al., 2022) and always used the setup suggested from the authors unless specified otherwise. We use the Synetune library (Salinas et al., 2022) for the implementation of the baselines.

A.3 META-TRAINING ALGORITHMS

We present the procedure for meta-training the cost and loss predictors in Algorithm 2. Initially, we sample random batches after choosing a dataset randomly within our meta-dataset, and then we update the parameters of each predictor so that it minimizes their respective losses. The same strategy is used when updating during BO but with fewer iterations. We meta-train for 10000 iterations using the Adam Optimizer with a learning rate of 0.0001.

Algorithm 2: Meta-training Algorithm

Input: Metadata with precomputed losses and cost $\mathcal{H}^{(M)}$ with datasets $\mathcal{D} = \{d_1, \dots, d_N\}$, learning rate μ , Epochs E

Output: Meta-learned parameters θ, γ

```

1 Random initialize parameters  $\theta, \gamma$  for loss predictor  $\hat{\ell}(\cdot)$  and cost predictor  $\hat{c}(\cdot)$ ;
2 for  $i \in \{1 \dots E\}$  do
3   Sample dataset index  $i \sim U[1, |\mathcal{D}|]$  and its metafeatures  $d_i$ ;
4   Define the subset of history associated to  $d_i$ :  $\mathcal{H}_i \subset \mathcal{H}^{(M)} : \{(x, t, \ell(x, t, d_i), c(x, t, d_i))\}$  ;
5   Compute  $\delta\theta = -\nabla_{\theta} \sum_{(x, t, \ell(x, t, d_i), \cdot) \sim \mathcal{H}_i} \left[ \log p(\ell(x, t, d_i) | x, t, d, \hat{\ell}(x, t, d_i; \theta)) \right]$  ;
6   Compute  $\delta\gamma = \nabla_{\gamma} \sum_{(x, t, \cdot, c(x, t, d_i)) \sim \mathcal{H}_i} \left[ c(x, t, d_i) - \hat{c}(x, t, d_i; \gamma) \right]^2$  ;
7   Update parameters  $\theta = \theta - \mu \cdot \delta\theta, \gamma = \gamma - \mu \cdot \delta\gamma$ 
8 end
9  $\theta^{(M)} \leftarrow \theta, \gamma^{(M)} \leftarrow \gamma$ ;
10 return  $\theta^{(M)}, \gamma^{(M)}$ 

```

A.4 META-FEATURES

Similar to previous work (Öztürk et al., 2022), we use descriptive meta-features of the dataset: number of samples, image resolution, number of channels, and number of classes. Any other technique for embedding datasets is compatible and orthogonal with our approach.

A.5 PIPELINE ENCODING

Our pipeline encoding is the concatenation of the hyperparameters λ_i , the embedding of the model name $\mathcal{E}_{\text{model}}(m_i)$, and the embedding of the learning curves. Given the performance curve $\tau(x_i, t)$,

we obtain the respective embedding $\mathcal{E}_{\text{perf}}(\tau(x_i, t))$ using a 2-layer convolutional networks following a similar setup from previous work (Wistuba et al., 2022). For obtaining the model embedding, we transform the model names into one-hot-encoding and feed this representation into a linear layer (Pineda Arango & Grabocka, 2023). The pipeline encoding is finally defined as:

$$\text{Pipeline Encodig}(x_i) = [\lambda_i, \mathcal{E}_{\text{model}}(m_i), \mathcal{E}_{\text{perf}}(\tau(x, t))] \quad (8)$$

The parameters of the encoders $\mathcal{E}_{\text{model}}(\cdot)$, $\mathcal{E}_{\text{perf}}(\cdot)$ are jointly updated during meta-training and while fitting the predictors during BO.

B META-DATASET DETAILS

B.1 META-DATASET COMPOSITION DETAILS

While generating the meta-dataset, we take into account the dependencies of the conditional hyperparameters. Every triple (model, dataset, hyperparameter configuration) resulted in a finetuning optimization run that produced a validation error and cost curves. A few of the combinations are infeasible to evaluate due to the model size, thus some triples can have fewer evaluations. For instance, some pipelines failed due to the GPU requirements demanded by the number of parameters of the model and the number of classes of the datasets. In that case, we decreased the batch size iteratively, halving the value, until it fits to the GPU. In some cases, this strategy was not enough, thus some models have more evaluations than others. In Table 4, we present the list of datasets per set and indicate the heavy datasets with a (*), i.e. with a lot of classes or a lot of samples in the extended version. The majority of the datasets are present in all three versions of Meta-Album, except the underlined ones, which are not present in the extended version. The OpenML IDs associated to the datasets are listed in Table 5. Table 6 provides descriptive statistics regarding the generated meta-dataset for every corresponding Meta-Album version.

Table 4: Datasets per Set in Meta-Album

Set	Dataset Names
0	BCT, BRD*, CRS, FLW, <u>MD_MIX</u> , PLK*, PLT_VIL*, RESISC, SPT, TEX
1	ACT_40, APL, DOG, INS_2*, <u>MD_5_BIS</u> , <u>MED_LF</u> , PLT_NET*, PNU, RSICB, TEX_DTD
2	ACT_410, AWA*, BTS*, FNG, INS*, <u>MD_6</u> , PLT_DOC, PRT, RSD*, TEX_ALOT*

Table 5: OpenML IDs for Datasets per Split and Version

Version	Set 0	Set 1	Set 2
Micro	44241, 44238, 44239, 44242,	44313, 44248, 44249, 44314,	44275, 44276, 44272, 44273,
	44237, 44246, 44245, 44244,	44312, 44315, 44251, 44250,	44278, 44277, 44279, 44274,
	44240, 44243	44247, 44252	44271, 44280
Mini	44285, 44282, 44283, 44286,	44298, 44292, 44293, 44299,	44305, 44306, 44302, 44303,
	44281, 44290, 44289, 44288,	44297, 44300, 44295, 44294,	44308, 44307, 44309, 44304,
	44284, 44287	44291, 44296	44301, 44310
Extended	44320, 44317, 44318, 44321,	44331, 44326, 44327, 44332,	44338, 44340, 44335, 44336,
	44316, 44324, 44323, 44322,	44330, 44333, 44329, 44328,	44342, 44341, 44343, 44337,
	44319	44325	44334

Table 6: Quick-Tune Composition

Meta-Dataset	Number of Tasks	Number of Curves	Total Epochs	Total Run Time
Micro	30	8.712	371.538	2.076 GPU Hours
Mini	30	6.731	266.384	6.049 GPU Hours
Extended	26	4.665	105.722	15.866 GPU Hours

B.2 HYPERPARAMETER SEARCH SPACE

Table 7: Detailed Search Space for Curve Generation. Bold font indicates the default configuration.

Hyperparameter Group	Name	Options	Conditional
Fine-Tuning Strategies	Percentage to freeze	0 , 0.2, 0.4, 0.6, 0.8, 1	-
	Layer Decay	None , 0.65, 0.75	-
	Linear Probing	True, False	-
	Stochastic Norm	True, False	-
	SP-Regularization	0 , 0.0001, 0.001, 0.01, 0.1	-
	DELTA Regularization	0 , 0.0001, 0.001, 0.01, 0.1	-
	BSS Regularization	0 , 0.0001, 0.001, 0.01, 0.1	-
Regularization Techniques	Co-Tuning	0 , 0.5, 1, 2, 4	-
	MixUp	0 , 0.2, 0.4, 1, 2, 4, 8	-
	MixUp Probability	0 , 0.25, 0.5, 0.75, 1	-
	CutMix	0 , 0.1, 0.25, 0.5, 1, 2, 4	-
	DropOut	0 , 0.1, 0.2, 0.3, 0.4	-
	Label Smoothing	0 , 0.05, 0.1	-
Data Augmentation	Gradient Clipping	None , 1, 10	-
	Data Augmentation	None , trivial_augment, random_augment, auto_augment	-
	Auto Augment	None, v0, original	-
	Number of Operations	2, 3	Data Augmentation (Random Augment)
Optimizer Related	Magnitude	9, 17	Data Augmentation (Random Augment)
	Optimizer Type	SGD , SGD+Momentum, Adam, AdamW, Adamp	-
	Betas	(0.9, 0.999), (0, 0.99), (0.9, 0.99), (0, 0.999)	Scheduler Type (Adam, Adamw, Adamp)
	Learning Rate	0.1 , 0.01, 0.005, 0.001, 0.0005, 0.0001, 0.00005, 0.00001	-
	Warm-Up Learning Rate	0 , 0.000001, 0.00001	-
	Weight Decay	0 , 0.00001, 0.0001, 0.001, 0.01, 0.1	-
	Batch Size	2, 4, 8, 16, 32, 64, 128 , 256, 512	-
Scheduler Related	Momeutm	0 , 0.8, 0.9, 0.95, 0.99	Optimizer Type (SGD+Momentum)
	Scheduler Type	None, Cosine , Step, Multistep, Plateau	-
	Patience	2, 5	Scheduler Type (Plateau)
	Decay Rate	0.1, 0.5	Scheduler Type (Step, Multistep)
Model	Decay Epochs	10, 20	Scheduler Type (Step, Multistep)
	Model	See Table 8	

Table 7 shows the complete search space of hyperparameters. During the curve generation, we sample uniformly among these discrete values. Some hyperparameters are conditional, i.e. their are only

present when another hyperparameter gets a specific set of values. Thus, we also list explicitly which are the conditions for such hyperparameters.

We report the hyperparameters for the default configuration in Experiment 1 by using a bold font in Table 7.

B.3 MODEL HUB

We list all the models on the Pareto Front from Timm’s library as provided on version *0.7.0dev0*. Moreover, we report their size (number of parameters) and the top-1 accuracy in ImageNet.

Table 8: Models on the pareto front

Model Name	No. of Param.	Top-1 Acc.
beit_large_patch16_512	305.67	90.691
voilo_d5_512	296.09	90.610
voilo_d5_448	295.91	90.584
voilo_d4_448	193.41	90.507
swinv2_base_window12to24_192to384_22kft1k	87.92	90.401
beit_base_patch16_384	86.74	90.371
voilo_d3_448	86.63	90.168
tf_efficientnet_b7_ns	66.35	90.093
convnext_small_384_in22ft1k	50.22	89.803
tf_efficientnet_b6_ns	43.04	89.784
voilo_d1_384	26.78	89.698
xcit_small_12_p8_384_dist	26.21	89.515
deit3_small_patch16_384_in21ft1k	22.21	89.367
tf_efficientnet_b4_ns	19.34	89.303
xcit_tiny_24_p8_384_dist	12.11	88.778
xcit_tiny_12_p8_384_dist	6.71	88.101
edgenext_small	5.59	87.504
xcit.nano_12_p8_384_dist	3.05	85.025
mobilevitv2_075	2.87	82.806
edgenext_x_small	2.34	81.897
mobilevit_xs	2.32	81.574
edgenext_xx_small	1.33	78.698
mobilevit_xxs	1.27	76.602
dla46x_c	1.07	73.632

C ADDITIONAL EXPERIMENT: QUICK-TUNE ON DATASETS OUTSIDE META-ALBUM

Meta-album contains a broad set of datasets, ranging from small-size datasets with 20 samples per class and 20 classes, to more than 700 classes with up to 1000 samples per class. Moreover, it offers a diverse set of domains that foster a strong benchmarking of image classification methods. To further verify the generalization outside the curated datasets present in Meta-Album, we run experiments on two well-known datasets that are not present in Meta-Album. Initially, we run Quick-Tune on Imagenette (Howard, 2019) by using a time budget of 4 hours. Additionally, we run Quick-Tune it on Inaturalist (Horn et al., 2021) with a time budget of 16 hours. Finally, we transfer the estimators meta-learned on the *mini* and *extended* splits respectively. We compare the results to the same gray-box HPO baselines as Hypothesis 2. The selection of the budget and the transferred estimators is based on the similarity of each dataset size to the corresponding Meta-Album super-set.

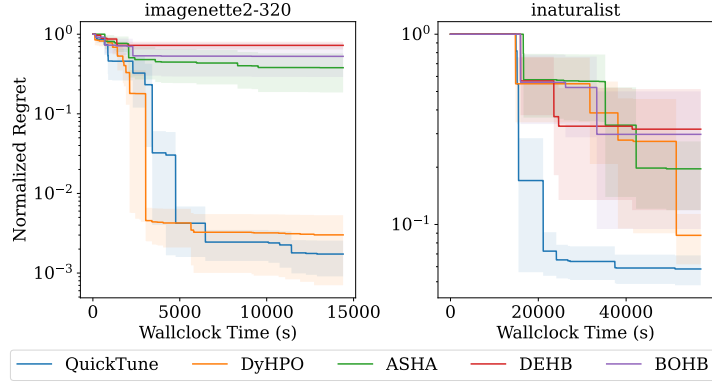


Figure 7: Evaluation of Quick-Tune on Datasets outside Meta-Album.

D DETAILS ON DINOV2 EXPERIMENT

D.1 FINETUNING LAST LAYER IN DINOV2

A common practice is to use large feature extractors as the backbone and just train a linear output layer. We argue that selecting the model from a pool and optimizing its hyperparameters jointly is a more effective approach. Firstly, large backbones are often all-purpose models that may be inferior to model hubs when downstream tasks deviate largely from the backbone pretraining and may require non-trivial finetuning hyperparameter adaptations. As such, individual large models may violate the diversity property observed in our third hypothesis above. Secondly, due to their large number of parameters, they are expensive to optimize.

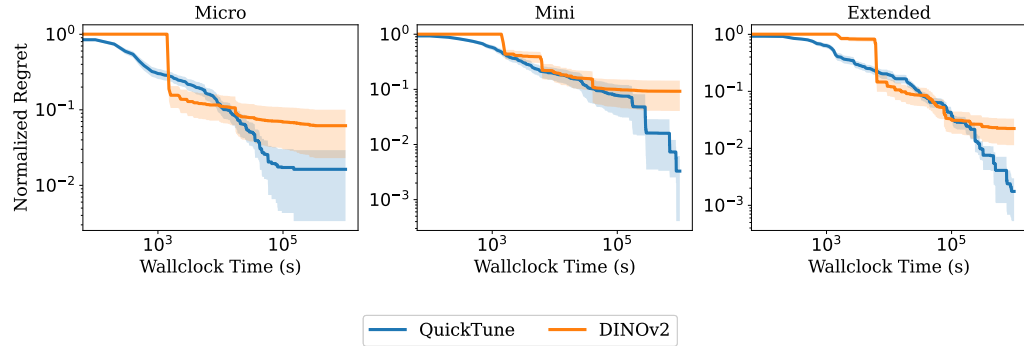


Figure 8: Results for finetuning the last layer of DINOV2. We relax the efficiency conditions by allowing a bigger time budget but still limited to 1 GPU.

To verify that selecting a model from a model hub with Quick-Tune is a more effective approach than using an all-purpose model, we compare to DINOV2 (Oquab et al., 2023). According to the method’s linear evaluation protocol, the procedure to classify downstream tasks with pretrained DINOV2 involves performing a small grid search over a subset of its finetuning hyperparameters (104 configurations in total including learning rate, number of feature extraction layers, etc.). We adopt this grid search in our comparison, evaluating all the hyperparameter configurations on the grid. For each meta-album version, we then compare the normalized regret against the wall-clock time between DINOV2 and Quick-Tune. For the experiment, we increase Quick-Tune’s budget to match DINOV2’s budget requirements since the evaluation of the full grid of DINOV2 requires more time than our previous experiments. In Figure 8, we present the results of our comparison, where, our method manages to outperform DINOV2 in all the considered benchmarks, highlighting the benefits of our designed search space.

While performing our comparison, a small minority of the DINOv2 runs failed due to GPU memory limitations, and for a few runs, we had to minimally adjust the DINOv2 default hyperparameter configurations "*n_last_blocks*" to adapt to our GPU memory limitation. Tables 9, 10, 11 depict for which of the datasets we ran with the default hyperparameter configurations according to (Oquab et al., 2023) and which we adapted due to the single-GPU constraint (RTX2080). Runs indicated with "*" failed due to GPU memory limitations and for runs indicated by "*n_last_blocks* = 1" we ran with the default hyperparameters except for the "*n_last_blocks*" argument that had to be changed from 4 to 1 to fit on the GPU.

Table 9: Subset Micro

Dataset	Linear Eval. Hyp.
micro_set0_BCT	DINOv2 default
micro_set0_BRD	DINOv2 default
micro_set0_CRS	DINOv2 default
micro_set0_FLW	DINOv2 default
micro_set0_MD_MIX	DINOv2 default
micro_set0_PLK	DINOv2 default
micro_set0_PLT_VIL	DINOv2 default
micro_set0_RESISC	DINOv2 default
micro_set0_SPT	DINOv2 default
micro_set0_TEX	DINOv2 default
micro_set1_ACT_40	DINOv2 default
micro_set1_APL	DINOv2 default
micro_set1_DOG	DINOv2 default
micro_set1_INS_2	DINOv2 default
micro_set1_MD_5_BIS	DINOv2 default
micro_set1_MED_LF	DINOv2 default
micro_set1_PLT_NET	DINOv2 default
micro_set1_PNU	DINOv2 default
micro_set1_RSICB	DINOv2 default
micro_set1_TEX_DTD	DINOv2 default
micro_set2_ACT_410	DINOv2 default
micro_set2_AWA	DINOv2 default
micro_set2_BTS	DINOv2 default
micro_set2_FNG	DINOv2 default
micro_set2_INS	DINOv2 default
micro_set2_MD_6	DINOv2 default
micro_set2_PLT_DOC	DINOv2 default
micro_set2_PRT	DINOv2 default
micro_set2_RSD	DINOv2 default
micro_set2_TEX_ALOT	DINOv2 default

Table 10: Subset Mini

Dataset	Linear Eval. Hyp.
mini_set0_BCT	DINOv2 default
mini_set0_BRD	<i>n_last_blocks</i> =1
mini_set0_CRS	<i>n_last_blocks</i> =1
mini_set0_FLW	DINOv2 default
mini_set0_MD_MIX	<i>n_last_blocks</i> =1
mini_set0_PLK	DINOv2 default
mini_set0_PLT_VIL	DINOv2 default
mini_set0_RESISC	DINOv2 default
mini_set0_SPT	DINOv2 default
mini_set0_TEX	DINOv2 default
mini_set1_ACT_40	DINOv2 default
mini_set1_APL	DINOv2 default
mini_set1_DOG	<i>n_last_blocks</i> =1
mini_set1_INS_2	<i>n_last_blocks</i> =1
mini_set1_MD_5_BIS	<i>n_last_blocks</i> =1
mini_set1_MED_LF	DINOv2 default
mini_set1_PLT_NET	DINOv2 default
mini_set1_PNU	DINOv2 default
mini_set1_RSICB	DINOv2 default
mini_set1_TEX_DTD	DINOv2 default
mini_set2_ACT_410	DINOv2 default
mini_set2_AWA	DINOv2 default
mini_set2_BTS	DINOv2 default
mini_set2_FNG	DINOv2 default
mini_set2_INS	<i>n_last_blocks</i> =1
mini_set2_MD_6	<i>n_last_blocks</i> =1
mini_set2_PLT_DOC	DINOv2 default
mini_set2_PRT	DINOv2 default
mini_set2_RSD	DINOv2 default
mini_set2_TEX_ALOT	<i>n_last_blocks</i> =1

Table 11: Subset Extended

Dataset	Linear Eval. Hyp.
extended_set0_BCT	<i>n_last_blocks</i> =1
extended_set0_CRS	<i>n_last_blocks</i> =1
extended_set0_FLW	<i>n_last_blocks</i> =1
extended_set0_RESISC	<i>n_last_blocks</i> =1
extended_set0_SPT	<i>n_last_blocks</i> =1
extended_set0_TEX	<i>n_last_blocks</i> =1
extended_set1_ACT_40	DINOv2 default
extended_set1_APL	<i>n_last_blocks</i> =1
extended_set1_DOG	<i>n_last_blocks</i> =1
extended_set2_ACT_410	DINOv2 default
extended_set2_PLT_DOC	DINOv2 default
extended_set0_BRD	*
extended_set0_PLK	*
extended_set0_PLT_VIL	*
extended_set1_INS_2	*
extended_set1_MED_LF	<i>n_last_blocks</i> =1
extended_set1_PLT_NET	*
extended_set1_PNU	<i>n_last_blocks</i> =1
extended_set1_RSICB	*
extended_set1_TEX_DTD	<i>n_last_blocks</i> =1
extended_set2_AWA	*
extended_set2_BTS	*
extended_set2_FNG	<i>n_last_blocks</i> =1
extended_set2_PRT	<i>n_last_blocks</i> =1
extended_set2_RSD	*
extended_set2_TEX_ALOT	<i>n_last_blocks</i> =1
extended_set2_INS	*

D.2 DINOv2 EFFICIENT FINETUNING WITH LoRA

As an alternative, instead of the infeasible full finetuning, we finetune DINOv2 with LoRA [2], which is a state-of-the-art method for finetuning transformer models (such as DINOv2). LoRA demands ca. 1% of the parameters of the full finetuning strategy and fits into our GPU restrictions for most of the datasets. Furthermore, LoRA is reported to achieve similar or better performance compared to full finetuning [2].

We stress that even with LoRA, the large DINOv2 model (1B params) exceeds our GPU memory capacity in some datasets. Thus, we present the results of the experiments in Table 3 with the datasets that DINOv2 were successfully trained, namely: 30 datasets for micro, 20 datasets for mini, and 4 datasets for extended. We report results for 4 Hours (4H) and 24 Hours (24H) of total budget where QuickTune outperforms both alternatives of finetuning DINOv2.

B.2 Statement of Contributions

Statement of Contributions for the following publication:

Title	Quick-Tune: Quickly Learning Which Pretrained Model to Finetune and How
Link to Publication, DOI	https://openreview.net/forum?id=tqh1zdXIra
Authors	Sebastian Pineda Arango, Fabio Ferreira, Arlind Kadra, Frank Hutter and Josif Grabocka
Publication Status	Accepted and published
Publisher, Date	The Twelfth International Conference on Learning Representations (ICLR), 2024
Peer-Review-Process	Yes
Rank	Ranked A* by the CORE2023 ranking

Paper Summary

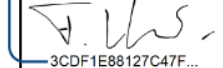
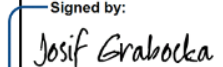
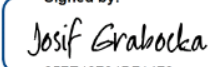
This paper introduces QuickTune, a method to select a model and its hyperparameters (a.k.a. pipelines) for finetuning efficiently. To this end, this work applies in a novel way multifidelity, cost-awareness, and meta-learning. It contains the following contributions:

1. We present an effective methodology for quickly selecting models from hubs and jointly tuning their hyperparameters.
2. We design an extensive search space that covers common finetuning strategies. In this space, we train and evaluate 20k models and dataset combinations to arrive at a large meta-dataset to meta-learn a gray-box performance predictor and benchmark our approach.
3. We compare against multiple baselines, such as common finetuning strategies and state-of-the-art HPO methods, and show the efficacy of our approach by outperforming all of the competitor baselines.

Contributions Listing

Name	Contributions	Signature and Date
Sebastian Pineda Arango	<p>Co-led the conceptualization of the idea; Owned and was responsible for implementing the proposed method.</p> <p>Created the repository with the final version of the code.</p> <p>Had a key role in data curation of Meta-album datasets (together with Fabio) and loading, integrating finetuning strategies such as Co-tuning, Stoch-norm, SP-Regularization, Layer freezing (together with Fabio), and others. Defined the search space and config space (together with Fabio and Arlind). Integrated the architectures to finetune (together with Fabio). Generated the meta-dataset. Performed failure analysis (together with Arlind).</p> <p>Created the initial draft of all sections. Co-led writing the majority of the paper including contributions to all parts of the paper. Created the visualizations of the final paper version. Contributed significantly to the rebuttal process (together with Arlind).</p>	<p>DocuSigned by:</p> <p><i>Sebastian Pineda Arango</i></p> <p>FC1C0379C4234BB...</p> <p>7/1/2024</p>

Fabio Ferreira	<p>Co-led the conceptualization of the idea;</p> <p>Owned and was responsible for implementing the execution pipeline for creating the meta-dataset on the cluster infrastructure and provided initial templates for running pipelines on the cluster.</p> <p>Had a key role in data curation (together with Sebastian), config space definition (together with Sebastian and Arlind), coding for the DINO experiments (section “Hypothesis 4”), implementing architectures and developing finetuning strategies (both together with Sebastian).</p> <p>Co-led writing the paper including contributions to all parts of the paper but the parts of the paper he had the major contributions were:</p> <p>The Related Work (together with Josif and Frank), Quick-Tune Meta-Dataset (together with Sebastian), Experiments “Hypothesis 4”, he also helped with the vision and introduction of the paper.</p>	<p>DocuSigned by:</p>  <p>CA7363FD31BF45C...</p> <p>7/10/2024</p>
Arlind Kadra	<p>Co-led the conceptualization of the idea;</p> <p>Owned and was responsible for the HPO baseline experiments (section “Hypothesis 2”), including code development and experiment execution (together with Sebastian). Helped with the config space definition (together with Sebastian and Fabio); Provided the code for the core component of the proposed method (DyHPO algorithm). Performed failure analysis (together with Sebastian).</p> <p>Co-led writing the paper including contributions to all parts of the paper but the parts of the paper he had the major contributions were:</p> <p>Experiments and Supplementary sections;</p> <p>Contributed to the rebuttal process (together with Sebastian).</p>	<p>DocuSigned by:</p>  <p>655FFB067F26476...</p> <p>7/4/2024</p>

Frank Hutter	Helped with reviewing and editing the paper; Helped conceptualize the problem; Co-led supervision of the project.	<p>Signed by:</p>  <p>3CDF1E88127C47F...</p> <p>7/10/2024</p>
Josif Grabocka	Co-led writing the paper including contributions to all parts of the paper but the parts of the paper he had the major contributions were: Introduction and Method; Helped with reviewing and editing the paper; Helped conceptualize the problem; Co-led supervision of the project.	<p>Signed by:</p>  <p>257E43784D71473...</p> <p>7/10/2024</p> <p>Signed by:</p>  <p>257E43784D71473...</p>

Appendices for Quick-Tune-Tool: A Practical Tool and its User Guide for Automatically Finetuning Pretrained Models

C.1 Paper Appendix

A Supplementary Materials

Feature/Aspect	HPO Tools	Finetuning Tools	AutoML Systems
Primary Focus	Optimizing hyperparameters	Adapting pretrained models to new tasks	Automating the entire ML pipeline
User Input Required	High (defining model architecture, hyper-params)	Moderate (selecting pretrained model, data)	Low (minimal input required, fully automated)
Automation Level	Partial (automates hyperparameter search)	Partial (automates training on new data)	Full (data processing, model selection, tuning)
Use Case	Improve model performance by tuning hyperparameters	Adapt models to new tasks with small datasets	End-to-end automation for building ML models
Tools & Libraries	Optuna Hyperopt Ray Tune SMAC3 NePS	Hugging Face (Transformers, PEFT) torchtune TensorFlow Hub	AutoGluon Google AutoML H2O.ai AutoKeras Microsoft Azure AutoML
Customization	High	Moderate	Low
Expertise Required	High	Moderate	Low to Moderate
Outcome	Optimized hyperparameters for better performance	Fine-tuned model specific to the new task	Fully trained and optimized ML model
Target Audience	Data Scientists, ML Engineers, Researchers	Data Scientists, ML Engineers, Researchers	Non-experts, Business Analysts, Data Scientists

Table 2: Comparison of HPO Tools, Finetuning Tools, and AutoML Systems

Positioning Quick-Tune-Tool: Bridging Finetuning and AutoML. Hyperparameter optimization (HPO) tools, finetuning tools, and AutoML systems are crucial in machine learning, each with specific purposes but common objectives. They differ in focus, automation level, and user expertise required, but all aim to improve model performance. We provide our interpretation of this complex landscape in Table 2. Within this area, Quick-Tune-Tool represents a hybrid approach that integrates finetuning principles with HPO techniques and aims to offer accessible usability.

Quick-Tune-Tool differs from conventional HPO tools, e.g., Optuna or Ray Tune, as it supports and leverages meta-learning on top of traditional optimizes. Furthermore, Quick-Tune-Tool integrates libraries of pretrained models (such as the Timm library). Finally, Quick-Tune-Tool can integrate conventional HPO tools into its pipeline to utilize different optimization methods, which clearly differentiates Quick-Tune-Tool from HPO tools.

Quick-Tune-Tool is similar to AutoML systems as it offers a curated finetuning script and a predefined search space. Thus, Quick-Tune-Tool also enables an easy-to-use interface for finetuning which aims to be accessible for non-experts.

In summary, we believe that Quick-Tune-Tool is currently positioned on the transition of a finetuning tool towards an AutoML system.

Additional QuickTuner Notes. The tuner supports basic logging and monitoring to track the progress of the tuning process. After Quick-Tune-Tool terminated, the user will find the finetuned models and the intermediate results in an experiment folder.

Post-Tuning Notes. Once the fitting is done, we can access the evaluation results by calling the `statistics()` function. This provides an overview (see Figure 6) of the evaluated configurations, their scores, and additional information. Subsequently, we can either fully finetune the best configurations using the `finetune()` function or assess the performance of each trained model on new data, e.g. that was not used during training, with the `leaderboard(path_to_test_data)` function.

Resources used. Our experiments utilized an internal cluster equipped with NVIDIA GeForce RTX 2080 Ti GPUs, requiring one GPU per experiment. We conducted four experiments with four different settings and ten seeds each, totaling 400 GPU-hours.

config	score	fidelity	model	...
10	0.987	2	beit_large_patch16_512	...
0	0.948	4	swinv2_base_window12to24_192to384	...
9	0.803	36	edgenext_x_small	...
114	0.673	19	edgenext_xx_small	...
1	0.554	12	mobilevit_xs	...
...				

Figure 6: Evaluation results.

Search Space. A subset of the hyperparameters (see Figure 3 and 4) defined in the search space, that was used for the image classification experiments. For a complete list, please refer to the original Quick-Tune paper (Pineda Arango et al., 2024).

Hyperparameter Group	Name	Options
Fine-Tuning Strategies	Percentage to freeze	0, 0.2, 0.4, 0.6, 0.8, 1
	Layer Decay	None, 0.65, 0.75
	Linear Probing	True, False
	Stochastic Norm	True, False
Regularization Techniques	MixUp	0, 0.2, 0.4, 1, 2, 4, 8
	MixUp Probability	0, 0.25, 0.5, 0.75, 1
	CutMix	0, 0.1, 0.25, 0.5, 1, 2, 4
	DropOut	0, 0.1, 0.2, 0.3, 0.4
Data Augmentation	Data Augmentation	None, Trivial-Augment, Random-Augment, Auto-Augment
	Auto Augment	None, v0, original
Optimizer Related	Type	SGD, SGD+Momentum, Adam, AdamW, AdamP
	Learning Rate	0.1, 0.01, 0.005, 0.001, 0.0005, 0.0001, 0.00005, 0.00001
	Batch Size	2, 4, 8, 16, 32, 64, 128, 256, 512
Model	Model	See Table 4

Table 3: Search space for image classification.

Libraries Used. The Quick-Tune-Tool is built on top of the popular deep learning library PyTorch (Paszke et al., 2019), benefiting from its large and active open-source community. This foundation allows the use of GPyTorch (Gardner et al., 2018) for GPU-accelerated Gaussian Processes in the optimization process and easy integration with Hugging Face’s model hub for pretrained models. The framework employs Pandas (McKinney, 2010) and NumPy (Harris et al., 2020) for data handling and loading, providing efficient data manipulation capabilities.

Datasets. In our experiments, we chose three datasets with a large dissimilarity concerning Imagenet, the dataset used for pretraining the models. Following previous work (Li et al., 2019), we select the datasets using Earth’s Moving Distance as similarity metric (Cui et al., 2018): FGVC-Aircraft, Stanford Cars and Oxford 102 Flower. Additionally, we include Imagenette, a dataset more similar to Imagenet. We report a brief description of the datasets in Table 5.

Model Name	No. of Param. (M)	Top-1 Acc.
beit_large_patch16_512	305.67	90.691
volo_d5_512	296.09	90.610
volo_d5_448	295.91	90.584
volo_d4_448	193.41	90.507
swinv2_base_window12to24_192to384_22kft1k	87.92	90.401
beit_base_patch16_384	86.74	90.371
volo_d3_448	86.63	90.168
tf_efficientnet_b7_ns	66.35	90.093
convnext_small_384_in22ft1k	50.22	89.803
tf_efficientnet_b6_ns	43.04	89.784
volo_d1_384	26.78	89.698
xcit_small_12_p8_384_dist	26.21	89.515
deit3_small_patch16_384_in21ft1k	22.21	89.367
tf_efficientnet_b4_ns	19.34	89.303
xcit_tiny_24_p8_384_dist	12.11	88.778
xcit_tiny_12_p8_384_dist	6.71	88.101
edgenext_small	5.59	87.504
xcit.nano.12.p8.384.dist	3.05	85.025
mobilevitv2_075	2.87	82.806
edgenext_x_small	2.34	81.897
mobilevit_xs	2.32	81.574
edgenext_xx_small	1.33	78.698
mobilevit_xxs	1.27	76.602
dla46x_c	1.07	73.632

Table 4: Vision models in search space.

Dataset Name	# Samples	# Classes	Image Resolution
Oxford 102 Flower	2040	102	500 - 1168
FGVC-Aircraft	10,200	102	430 - 1188
Stanford Cars	16,185	196	57 - 3744
Imagenette	13,394	10	320

Table 5: Vision Datasets used for Evaluation.

Image-Folder. The images of the custom datasets have to be arranged in a certain way to be compatible with PyTorch ImageFolder-format, see Figure 7.

```
root/train/
|-- a
|   |-- xyz.jpg
|   |-- abc.jpg
|   |-- ...
|-- ...

root/val/
|-- a
|   |-- efg.jpg
|   |-- opq.jpg
|   |-- ...
|-- ...
```

Figure 7: ImageFolder format

C.2 Statement of Contributions

Statement of Contributions for the following publication:

Title	Quick-Tune-Tool: A Practical Tool and its User Guide for Automatically Finetuning Pretrained Models
Link to Publication, DOI	https://openreview.net/forum?id=d0Hapti3Uc
Authors	Ivo Rapant, Lennart Purucker, Fabio Ferreira, Sebastian Pineda Arango, Arlind Kadra, Josif Grabocka, and Frank Hutter
Publication Status	Accepted at the AutoML Conference 2024 (Workshop Track)
Publisher, Date	Proceedings of the third International Conference on Automated Machine Learning (AutoML), 2024
Peer-Review-Process	Yes
Rank	not ranked by CORE2023

Paper Summary

This paper introduces Quick-Tune-Tool, a tool that simplifies the selection and finetuning of pretrained models, with a focus on image classification tasks. The tool is built on the QuickTune algorithm [1], which abstracts research-level code into an accessible, user-friendly interface designed for machine learning practitioners. Given the growing complexity and variety of pretrained models available, Quick-Tune-Tool aims to help users determine the most suitable pretrained model and optimize its finetuning strategy without extensive trial-and-error.

The contributions of this paper include the release of Quick-Tune-Tool, offering a detailed architectural overview of its design, a user guide for image classification, and empirical evaluations. It was evaluated on four commonly used image classification datasets: Oxford Flowers 102, Stanford Cars, Imagenette, and FGVC-Aircraft. The experiments demonstrate that Quick-Tune-Tool not only simplifies the finetuning process, but also consistently outperforms random search baselines in terms of top-1 accuracy and speed of convergence.

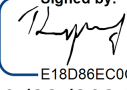
With its straightforward adaptability, Quick-Tune-Tool is positioned as a practical solution for automating finetuning workflows, providing significant value to practitioners working on image classification tasks. The tool's architecture has been designed with future adaptability in mind, allowing for off-the-shelf adaptation to other domains. The key contributions of the paper are:

1. The paper introduces *Quick-Tune-Tool*, which abstracts the QuickTune algorithm [1] into a user-friendly tool designed to automate model selection and finetuning for image classification tasks.
2. It provides a detailed architectural overview of *Quick-Tune-Tool*, explaining its components and functionality, alongside a comprehensive user guide that enables users to implement the tool with just a few lines of code. It allows easy adaptation to other domains.
3. The authors conduct empirical evaluations on four widely-used image classification datasets – Oxford Flowers 102, Stanford Cars, Imagenette, and FGVC-Aircraft,

demonstrating the tool's effectiveness in outperforming random search in both accuracy and convergence speed.

[1] Arango, S. P., Ferreira, F., Kadra, A., Hutter, F., & Grabocka, J. (2024). *Quick-Tune: Quickly Learning Which Pretrained Model to Finetune and How*. In The Twelfth International Conference on Learning Representations (ICLR 2024). Paper: <https://openreview.net/forum?id=tqh1zdXra>

Contributions Listing

Name	Contributions	Signature
Ivo Rapant	<p>Owned and led the development of <i>Quick-Tune-Tool</i> and handled all core implementations;</p> <p>Owned, led, and implemented all experiments conducted;</p> <p>Contributed to shaping the project's vision and methodology in collaboration with the supervisory team;</p> <p>Owned and led the writing of the paper, as well as reviewing and rebutting it.</p>	<p>Signed by:  E18D86EC0C94416... 10/22/2024</p>
Lennart Purucker	<p>Co-supervised the project alongside Fabio;</p> <p>Contributed to shaping the project's vision and methodology in collaboration with the supervisory team;</p> <p>Contributed substantially to writing, reviewing, and rebutting the paper, including positioning it within the broader research context;</p> <p>Helped design the API and provided input on the use cases of the tool;</p> <p>Co-led supervision during the later phases of the project.</p>	<p>Signiert von:  6A52A22B8876416... 22.10.2024</p>

Fabio Ferreira	<p>Initiated the project with Frank and supervised Ivo in the first third of the project; later co-supervised with Lennart;</p> <p>Contributed to defining the API and tool use cases (initially with Ivo, then jointly with Lennart);</p> <p>Provided input on shaping the vision of the tool;</p> <p>Supported in writing the paper and addressed questions related to the DINOv2 experiments.</p> <p>Contributed to shaping the project's vision and methodology;</p> <p>Helped in writing, reviewing, and rebutting the paper.</p>	 CA7363FD31BF45C... 22.10.2024
Sebastian Pineda Arango	<p>Co-supervised the project alongside Lennart and Fabio;</p> <p>Supported Ivo with the original QuickTune code (of which Sebastian is the core author) and debugging the method;</p> <p>Contributed to steering the project;</p> <p>Helped in writing, reviewing, and rebutting the paper; provided input on related work;</p>	 FC1C0379C4234BB... 10/23/2024
Arlind Kadra	<p>Helped steer the project and provided advice on baselines;</p> <p>Helped in writing, reviewing, and rebutting the paper.</p>	 655FFB067F26476... 10/24/2024

Josif Grabocka	<p>Helped in writing, reviewing, and rebutting the paper;</p> <p>Supervised Sebastian and Arlind.</p>	<p>Signed by:  257E43784D71473...</p> <p>10/24/2024</p>
Frank Hutter	<p>Proposed the initial idea to develop a tool based on the QuickTune paper [1];</p> <p>Proposed the tool's adaptation to domains like image segmentation or large language models; and overall contributed to shaping the project's vision and methodology;</p> <p>Helped in writing, reviewing, and rebutting the paper;</p> <p>Supervised the project and supervised Ivo, Lennart, and Fabio.</p>	<p>Signed by:  3CDF1E88127C47F...</p> <p>25/10/2024</p>

Appendices for Transfer Learning for Finetuning Large Language Models

D.1 Paper Appendix

Matthias Feurer, Katharina Eggensperger, Stefan Falkner, Marius Lindauer, and Frank Hutter. Auto-sklearn 2.0: Hands-free automl via meta-learning. *Journal of Machine Learning Research*, 23(261):1–61, 2022.

David Salinas and Nick Erickson. Tabrepo: A large scale repository of tabular model evaluations and its automl applications. *arXiv preprint arXiv:2311.02971*, 2023.

Tri Dao, Daniel Y. Fu, Stefano Ermon, Atri Rudra, and Christopher Ré. Flashattention: Fast and memory-efficient exact attention with io-awareness, 2022. URL <https://arxiv.org/abs/2205.14135>.

Michael L. Waskom. seaborn: statistical data visualization. *Journal of Open Source Software*, 6(60):3021, 2021. doi: 10.21105/joss.03021. URL <https://doi.org/10.21105/joss.03021>.

Appendix

A Prompt Templates To Generate Our Synthetic NLP Dataset

We follow the prompt (Facts generation) to extract atomic facts out of unlabeled text. Our self-hosted version of L3-70B extracts as many as possible facts out of reprocessed approximately 2k token long text fragments. For each fact, we generate 12 question-answers pairs by using Q & A generation prompt, skipping facts that are too general or insufficiently specific to the article's topic (generated by Key topic generation). We aim to generate as many questions and answers as possible that explicitly relate to the fact, then paraphrase them to achieve the required 12 pairs.

Facts generation prompt (Mecklenburg et al., 2024)

System: "You are an AI assistant who knows about current artificial intelligence. Be precise but concise in your answer."

User: "Please break down the following snippet from an article about {key_topic} into atomic facts.\nGoal 1: The atomic facts should be as simple as possible, if it's a compound sentence, break down one more time.\nGoal 2: For clarity, avoid using pronouns like 'it', 'he', 'she', 'this', 'that' etc., and instead use the full names or titles.\nGoal 3: Output in the format: 1 факт_1\n\n{passage}\n\n1."

Q & A generation prompt (Mecklenburg et al., 2024)

System: "You are an AI assistant who knows about factual information about the paper with the title: {paper title}. Be precise but concise in your answer."

User: "Write 12 pairs of questions and answers probing the facts and statistics the given fact {fact} about {key_topic}.\nConsider first generating questions and answers that are very relevant and explicit to the fact, then paraphrase those questions and answers to reach the desired 12 Q&A pairs. If the fact is too broad or not specific enough to theme, you may reply with only with 'SKIP' and be done.\nEXAMPLE:\nFACT: 14 million viewers tuned in to the opening game of the series.\n1. Q: How many viewers watched the first game? A: 14 million people watched the first game of the series.\n\nEXAMPLE:\nFACT: The rose is red.\nSKIP\n\nFACT: fact['fact']\n1."

Key topic generation prompt

System: "You are given a summary of the scientific paper. Return the key topic of this paper an nothing else"

User: {paper summary}

Atomic fact example

"Masked Image Modeling (MIM) is a learning framework that derives visual representations from unlabeled image data."

Q & A example

Question: "What does Masked Image Modeling (MIM) derive from unlabeled image data?"

Answer: "Masked Image Modeling (MIM) derives visual representations from unlabeled image data."

B Synthetic Datasets Details

We list our meta-features from our meta-dataset in Table 1 and the meta-dataset used for our experiments in Table 2.

Table 1: Meta-features trainings dataset

Dataset	token size	sample length	ratio q/a length	vocab size
2407.15849v1	46913	137.63	1.43	1530
2407.15847v1	82307	144.92	1.55	2570
2407.15845v1	75410	145.55	1.51	2330
2407.15843v1	117247	139.03	1.72	3840
2407.15839v1	59966	146.83	1.57	1900
2407.15837v1	83873	139.39	2.08	2720
2406.18451v2	91480	161.24	1.4	2520
2407.15835v1	87863	134.18	1.66	2940
2407.15831v1	3874	157.48	1.19	120
2405.04657v3	65048	144.11	1.3	2070
2407.15820v1	73764	164.01	1.51	1980
2402.16822v2	131833	141.71	1.57	4190
2401.00009v3	87762	131.66	2.42	2740
2407.15815v1	69078	142.61	1.41	2210
2407.15814v1	76705	149.07	1.55	2540
2403.20262v2	93673	131.59	1.91	2930
2407.13044v2	27154	129.01	1.8	920
2307.15220v3	146050	142.7	1.55	4840
2407.15786v1	109720	143.94	1.8	3410
2407.15784v1	44928	151.83	1.44	1460
2405.17814v4	88773	144.15	1.65	2720
2407.15771v1	84305	139.16	1.67	2680
2407.15762v1	133882	139.16	1.62	4030
2407.15748v1	136205	140.48	1.57	4260
2407.15739v1	94869	145.1	1.74	2990
2407.15738v1	143443	137.99	1.52	4570
2407.15734v1	144566	131.11	1.57	5010
2407.04856v2	147437	141.79	1.48	4600
2402.07370v2	64881	134.8	1.57	2100
2403.07805v3	87032	140.16	1.8	2810

Table 2: Meta-features HPO comparison

Dataset	token size	sample length	ratio q/a length	vocab size
2407.15723v1	54923	139.66	1.67	1840
2407.15720v1	157268	147.32	1.49	4740
2407.15719v1	86733	148.17	1.41	2570
2407.15708v1	45482	139.93	1.70	1390
2407.15656v1	124420	145.04	1.72	3900
2407.15617v1	82637	142.93	1.57	2580
2407.15600v1	89996	139.59	1.49	2970
2401.04152v2	42769	147.14	1.53	1280

C LLM Model Evaluation Details

For the evaluation, we continue to use our in-house hosted L3-70B model implemented with llama.cpp, leveraging it for both performance and resource efficiency. We make a small adjustment to our configuration, setting llama.cpp to process 128 parallel sequences and limiting the context size to 500 tokens, which is sufficient for our evaluation needs. To ensure efficient processing, we limit the maximum number of new tokens to 50 for each generated answer. Given that a comprehensive evaluation of the entire validation and test datasets would be time-prohibitive, we opted to select 20 random, fixed validation and test indices per paper (dataset) for this study.

Based on Mecklenburg et al. (2024) we use Evaluation prompt to generate our evaluation score.

Resulting to either a positive (Positive evaluation response) or negative (Negative evaluation response) result.

Evaluation prompt (based on Mecklenburg et al. (2024))

System: "You are a high school teacher grading student's responses for questions about {key_topic}. These responses are either correct or incorrect."

User: "Please evaluate the correctness of a sentence in answering the question: "{question}".\nThe correct answer is: "{sample_answer}"\nThe student response is: "{gen_answer}".\nYour grading is binary. Give 0 if the sentence is incorrect, give 1 if the sentence is correct, based on the given correct answer and the question.\n"Please note that your output is either 0 or 1, with the corresponding justification as python dict in the following format and nothing else:\n r"{'rating': <rating>, 'justification': <justification>}"

Positive evaluation response

Question: what does imitation learning (il) rely on to learn?

Generated answer: imitation learning (il) relies on expert demonstrations to learn.

Sample answer: il learns from expert guidance.

Decision: 'rating': 1, 'justification': 'The student response is correct because it conveys the same meaning as the correct answer, which is that imitation learning relies on some form of expert input, whether it is called "guidance" or "demonstrations".'

Negative evaluation response

Question: do agents and equipped functions work together in taskgen?

Generated answer: yes, they work together as part of the hybrid approach.

Sample answer: no, agents and equipped functions operate independently.

Decision: 'rating': 0, 'justification': 'The student response is incorrect because it states that agents and equipped functions work together, whereas the correct answer is that they operate independently.'

D Search Space Details

We employ AdamW and AdamCPR optimizers (Table 3) as well cosine schedulers (Table 4) with varying warmup steps (as a percentage of training set length) and decay factors. LoRA configurations (Table 5) include different ranks, alpha values, and dropout rates, with target modules being either query, key, and value; only the output layer; or all linear layers.

While we train 10 epochs, the batch size is fixed at 32, with gradient accumulation steps of 2, 4, or 8 to achieve mini-batch sizes of 64, 128, or 256. We utilize the Hugging Face tokenizer's chat template for Phi 3 Instruct to maintain consistency with the model's original template during training. An additional configuration option is the return_assistant_mask, which generates an attention mask excluding "user" and "system" segments, focusing the model's learning on "assistant" responses.

Fixed settings across all configurations include:

- `torch.nn.CrossEntropyLoss` as the loss function
- Gradient clip value of 1.0
- `torch.bfloat16` precision
- Flash Attention 2 (Dao et al., 2022)
- Left-side padding (due to Flash Attention requirements)

To ensure all samples in the train set are used, we augment the dataset with random samples to make it divisible by the product of batch size and gradient accumulation steps. The number of additional samples (asc) is calculated as:

$$asc = (\lceil ltrain/bg \rceil * bg) - ltrain \quad (1)$$

where bg is the product of batch size and gradient accumulation steps, and $ltrain$ is the length of the train dataset.

Default values used for "Default LoRA" in Figure 4 are marked in bold in Tables 3, 4, and 5. A gradient accumulation step of 2 was used.

Table 3: Optimizer configuration space

optimizer	parameter	
	AdamW	AdamCPR
learning_rate	1e-6 , 1e-5.5, 1e-5, 1e-4.5, 1e-4, 1e-3.5, 1e-3	
weight_decay	1e-0.5, 1e-1, 1e-1.5, 1e-2 , 1e-3, 1e-4	_____
kappa_init_method	_____	warm_start
kappa_init_param	_____	warmup_steps x (1,2,4)

Table 4: Scheduler hyperparameter

	parameter
schedule	cosine
warmup_steps %	10 , 20, 30, 40, 50
decay_factor	0, 0.1, 0.01

Table 5: Lora configuration space

With $q = \text{query}$, $k = \text{key}$, $v = \text{value}$, $o = \text{output}$.
 $\text{all-linear} = q, k, v$.

	parameter
target_modules	[q, k, v], o, all-linear
rank	8 , 16, 32, 64
alpha	16 , 32
dropout	0 , 0.1

E Experiments Compute Resources

It took 900 compute hours to run all 1800 configurations for our meta-dataset and 170 compute hours for the experiments on a single NVIDIA A100 GPU.

Each run for the meta-dataset and experiments was allocated 8 CPU cores and 16 GB RAM.

Concurrently, we utilized two NVIDIA A6000 GPUs in parallel to run our self-hosted L3-70B model.

F Limitations Of Our Method

Although our method shows promising results compared to alternative methods, our meta-features are not based on an importance analysis. Furthermore, the evaluation does not take into account whether the model to be fine-tuned might start hallucinating during training and add further invented facts to the correct answer. Furthermore, at the current state we have too little data to understand why we achieve better performance when we only do transfer learning without Bayesian optimization. Another limitation is that we do not know how our finetuning generalizes with real tasks, i.e. not with synthetic data and without a teacher model.

G Results Configuration Details

The best pipeline configurations found by the individual optimizers, listed below. Resulting configurations by Quick-Tune (ours), Quick-Tune (default), DEHB, and random optimizer in Table 6, 7, 8, and 9.

Table 6: Quick-Tune (Ours) Found Configurations

With batch size = batch size 32 and gradient accumulation step [2, 4, 8].

Dataset	batch size	decay factor	fidelity	kappa init param	lora alpha	lora dropout	lora layer	lora rank	lr	warmup steps %	optimizer	return assistant mask	weight decay
2407.15723v1	64	1.0	4	nan	16	0.0	all-linear	64	1e-3	10	AdamW	False	1e-0.5
2407.15720v1	64	0.01	7	4.0	32	0.0	o	32	1e-3	10	AdamCPR	False	1e-0.5
2407.15719v1	64	1.0	8	nan	16	0.0	all-linear	64	1e-3	10	AdamW	False	1e-0.5
2407.15708v1	64	0.01	4	4.0	32	0.0	o	32	1e-3	10	AdamCPR	False	1e-0.5
407.15656v1	64	0.1	9	nan	32	0.0	o	16	1e-3	10	AdamW	False	1e-0.5
2407.15617v1	64	1.0	8	nan	16	0.0	all-linear	64	1e-3	10	AdamW	False	1e-0.5
2407.15600v1	128	0.01	8	nan	16	0.1	o	64	1e-3	10	AdamW	True	1e-3
2401.04152v2	64	0.01	4	4.0	32	0.0	o	32	1e-3	10	AdamCPR	False	1e-0.5

Table 7: Quick-Tune (Default) Found Configurations

With batch size = batch size 32 and gradient accumulation step [2, 4, 8].

Dataset	batch size	decay factor	fidelity	kappa init param	lora alpha	lora dropout	lora layer	lora rank	lr	warmup steps %	optimizer	return assistant mask	weight decay
2407.15723v1	64	0.01	2	1.0	32	0.1	all-linear	8	1e-3	10	AdamCPR	True	1e-2
2407.15720v1	64	0.01	5	4.0	32	0.0	o	32	1e-3	10	AdamCPR	False	1e-0.5
2407.15719v1	64	0.01	3	4.0	32	0.0	o	32	1e-3	10	AdamCPR	False	1e-0.5
2407.15708v1	64	0.01	2	4.0	32	0.0	o	32	1e-3	10	AdamCPR	False	1e-0.5
2407.15656v1	128	0.01	2	nan	16	0.1	o	64	1e-3	10	AdamW	True	1e-3
2407.15617v1	64	0.01	4	4.0	32	0.0	o	32	1e-3	10	AdamCPR	False	1e-0.5
2407.15600v1	128	0.01	1	4.0	16	0.1	all-linear	16	1e-4.5	30	AdamCPR	False	1e-4
2401.04152v2	64	0.01	2	4.0	32	0.0	o	32	1e-3	10	AdamCPR	False	1e-0.5

Table 8: DEHB Found Configurations

With batch size = batch size 32 and gradient accumulation step [2, 4, 8].

Dataset	batch size	decay factor	fidelity	kappa init param	lora alpha	lora dropout	lora layer	lora rank	lr	warmup steps %	optimizer	return assistant mask	weight decay
2407.15723v1	128	1.0	3	nan	32	0.0	o	16	1e-3	10	AdamW	True	1e-0.5
2407.15720v1	64	1.0	10	2.0	32	0.0	o	32	1e-3	10	AdamCPR	True	1e-0.5
2407.15719v1	256	1.0	3	4.0	16	0.0	o	16	1e-3.5	10	AdamCPR	True	1e-0.5
2407.15708v1	128	0.1	1	2.0	32	0.0	o	32	1e-06	30	AdamCPR	True	1e-0.5
2407.15656v1	64	0.01	10	nan	16	0.0	all-linear	16	1e-3	30	AdamW	False	1e-1.5
2407.15617v1	128	0.1	10	nan	32	0.1	o	32	1e-3	10	AdamW	True	1e-0.5
2407.15600v1	64	0.1	3	4.0	16	0.0	all-linear	16	1e-06	20	AdamCPR	False	1e-1.5
2401.04152v2	128	1.0	3	2.0	16	0.0	all-linear	32	1e-3	20	AdamCPR	True	1e-2

Table 9: Random Found Configurations

With batch size = batch size 32 and gradient accumulation step [2, 4, 8].

Dataset	batch size	decay factor	fidelity	kappa init param	lora alpha	lora dropout	lora layer	lora rank	lr	warmup steps %	optimizer	return assistant mask	weight decay
2407.15723v1	256	0.10	1	4.0	16	0.1	o	16	1e-5	10	AdamCPR	True	1e-4
2407.15720v1	64	0.01	1	NaN	16	0.0	o	16	1e-3.5	40	AdamW	False	1e-3
2407.15719v1	64	1.00	1	NaN	32	0.0	o	64	1e-3	20	AdamW	True	1e-1.5
2407.15708v1	256	0.01	1	4.0	16	0.0	qkv	32	1e-5	40	AdamCPR	True	1e-0.5
2407.15656v1	128	0.01	3	2.0	32	0.1	o	64	1e-3	10	AdamCPR	False	1e-2
2407.15617v1	64	0.01	1	NaN	32	0.1	all-linear	32	1e-3	10	AdamW	True	1e-1.5
2407.15600v1	64	0.10	1	4.0	32	0.0	qkv	16	1e-3.5	50	AdamCPR	False	1e-4
2401.04152v2	64	0.01	1	NaN	16	0.1	o	64	1e-3	10	AdamW	True	1e-2

D.2 Statement of Contributions

Statement of Contributions for the following publication:

Title	Transfer Learning for Finetuning Large Language Models
Link to Publication, DOI	https://openreview.net/forum?id=gDeW6B8WCh https://arxiv.org/abs/2411.01195
Authors	Tobias Strangmann, Lennart Purucker, Jörg K.H. Franke, Ivo Rapant, Fabio Ferreira, Frank Hutter
Publication Status	Submitted to NeurIPS 2024 Workshop on Adaptive Foundation Models
Publisher, Date	-
Peer-Review-Process	yes
Rank	not ranked by CORE2023 (workshop)

Paper Summary

This paper presents a new approach to finetuning large language models (LLMs) using transfer learning. The paper focuses on transferring knowledge about previous configurations from related finetuning tasks to new tasks. The authors introduce an adapted version of the Quick-Tune algorithm [1], originally developed for image classification tasks, and apply it as a meta-learner for the finetuning of LLMs. Central to this approach is a meta-dataset consisting of 1,800 finetuning runs of Microsoft's Phi-3 model on a board set of different hyperparameter configurations and using two optimizers, AdamW and the recently proposed AdamCPR [2]. The meta-dataset is used to optimize Quick-Tune as the meta-learner. This optimization enables the transfer of knowledge from previously optimized tasks to new ones, allowing for more efficient and effective finetuning across different domains.

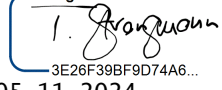
The experiments, conducted on eight synthetic question-answer datasets, demonstrate that the adapted Quick-Tune method outperforms default finetuning approaches and other optimization baselines in terms of accuracy and efficiency. Empirical results further reveal that not refitting the performance and cost surrogate models leads to better generalization and performance across tasks, with the authors hypothesizing that avoiding task-specific refitting enhances overall transferability. The key contributions of the paper are:

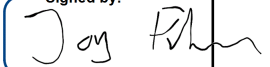
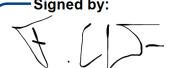
1. Introduction of *Quick-Tune* as a meta-learner to transfer knowledge from related tasks for finetuning large language models (LLMs).
2. Creation of a meta-dataset consisting of 1,800 finetuning runs of Microsoft's Phi-3 model to optimize the meta-learner and improve generalization across tasks.
3. Experimental results demonstrate that the adapted *Quick-Tune* approach outperforms default finetuning methods and other optimization baselines across eight synthetic question-answer datasets.

[1] Arango, S. P., Ferreira, F., Kadra, A., Hutter, F., & Grabocka, J. (2024). *Quick-Tune: Quickly Learning Which Pretrained Model to Finetune and How*. In The Twelfth International Conference on Learning Representations (ICLR 2024). Paper: <https://openreview.net/forum?id=tqh1zdXra>

[2] Franke J.K.H., Hefenbrock, M., Koehler, G., & Hutter, F. (2024). Improving Deep Learning Optimization through Constrained Parameter Regularization. In The Thirty-Eighth Annual Conference on Neural Information Processing Systems (NeurIPS 2024). Paper: <https://arxiv.org/abs/2311.09058>

Contributions Listing

Name	Contributions	Signature
Tobias Strangmann	<p>Owned and led the development of the adaptation of <i>Quick-Tune</i> to LLMs and handled all core implementations;</p> <p>Owned, led, and implemented all experiments conducted;</p> <p>Owned and led the writing of the paper, as well as reviewing and rebutting it.</p>	<p>Signiert von:</p>  <p>3E26F39BF9D74A6... 05.11.2024</p>
Lennart Purucker	<p>Co-supervised the project alongside Jörg and Fabio;</p> <p>Contributed to writing and reviewing the paper and identifying key research questions;</p> <p>Framed the research and experiments with a topic-wise focus on hyperparameter optimization (HPO), finetuning, and transfer learning.</p> <p>Contributed to shaping the project's vision and methodology in collaboration with the supervisory team;</p> <p>Provided input on shaping the vision of the project.</p>	<p>Signiert von:</p>  <p>6A52A22B8876416... 05.11.2024</p>

Jörg K.H. Franke	<p>Proposed the project vision for more efficient LLM finetuning by transfer learning;</p> <p>Supervised Tobias throughout the project;</p> <p>Designed the synthetic data generation and experiments for LLM tuning;</p> <p>Contributed to framing the paper with a focus on LLM tuning and how to adapt Quick-Tune for LLMs;</p>	<p>Signed by:</p>  <p>DC6598DF2302491... 05/11/2024</p>
Ivo Rapant	<p>Acted as the Quick-Tune code expert and supported Tobias with coding-related questions;</p> <p>Ran additional experiments involving Quick-Tune;</p>	<p>Signed by:</p>  <p>E18D86EC0C94416... 11/6/2024</p>
Fabio Ferreira	<p>Co-supervised the project alongside Jörg and Lennart;</p> <p>Contributed to framing the paper and supported with Quick-Tune-related questions;</p> <p>Contributed to writing the paper and reviewing, as well as identifying key research questions;</p> <p>Provided input on shaping the vision of the project.</p>	<p>DocuSigned by:</p>  <p>CA7363FD31BF45C... 05.11.2024</p>
Frank Hutter	<p>Proposed Quick-Tune's adaptation to other domains; and overall contributed to shaping the project's vision and methodology;</p> <p>Helped conceptualize the problem;</p> <p>Supported in reviewing, and editing the paper;</p> <p>Supervised Lennart, Jörg, and Fabio.</p>	<p>Signed by:</p>  <p>3CDF1E88127C47F... 06/11/2024</p>

Appendices for Beyond Random Augmentations: Pretraining with Hard Views

E.1 Paper Appendix

APPENDIX

A REPRODUCIBILITY STATEMENT

We provide complete code, environment installation instructions, hyperparameter settings and model checkpoints here: <https://anonymous.4open.science/r/pretraining-hard-views/>. For transparency, we outline all hyperparameters, data splits, and evaluation protocols in detail in Section I. Most experiments were run across multiple seeds, and we report average results to account for variability. Information regarding the required computational resources is discussed in Section J below.

B EXAMPLES SAMPLED BY HVP

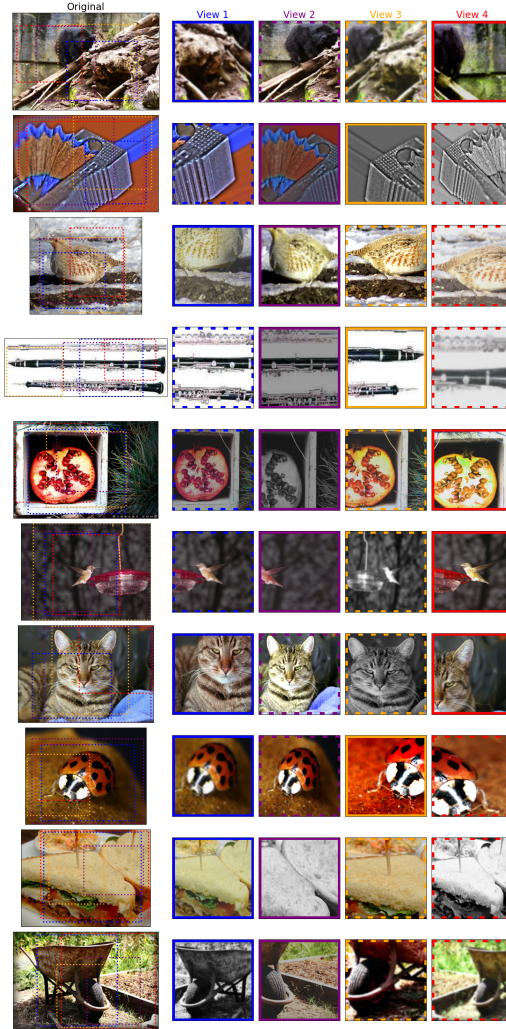


Figure 5: We depict row-wise ten example images from the ImageNet train set along with their sampled views with a finished, 100-epoch trained SimSiam ResNet50 model. Left: original image with the overlaid randomly sampled crops (colored dashed rectangles). Right: All views after applying resizing and appearance augmentations. The pair that is selected adversarially by HVP is highlighted in solid lines, eg. View 1 and View 4 in the first row.

C TRAINING LOSS

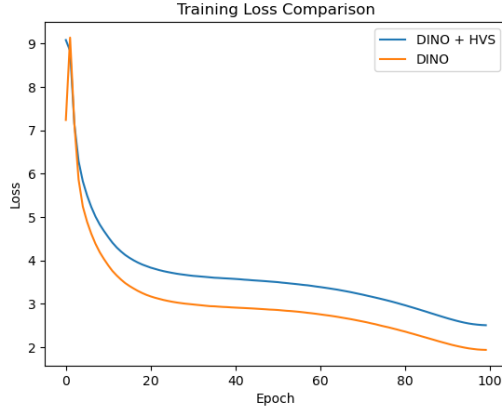


Figure 6: The training loss over 100 epochs. Comparing the DINO vanilla method with DINO + HVP. The spike and drop in the loss curve of DINO is caused by freezing the last layer in the first epoch which was proposed by the authors as a strategy to enhance downstream performance. For HVP we can only see a drop and no spike. We believe this is because HVP exposes the model to hard views from the beginning of training (i.e. the loss is immediately maximized).

D EFFECT OF MORE VIEWS ON LINEAR EVALUATION PERFORMANCE

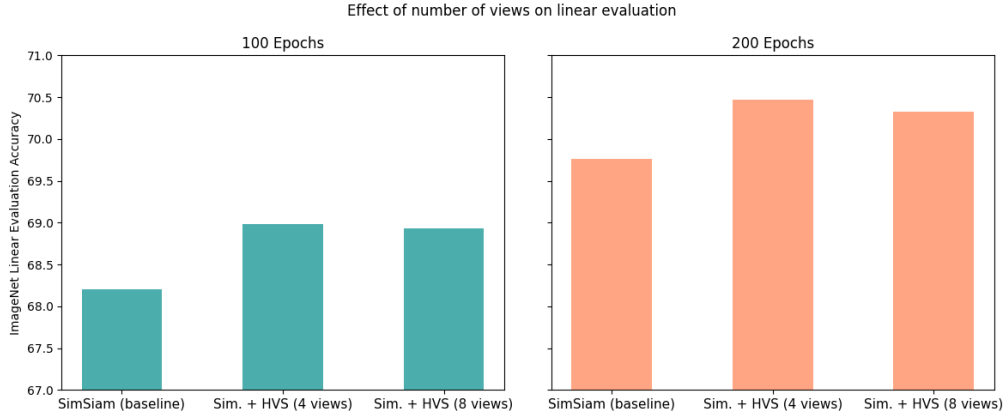


Figure 7: Setting the number of views too high can result in performance deterioration. This shows that diminishing returns exist, likely because the adversary becomes too strong, resulting in a too hard learning task.

E ASSESSING THE IMPORTANCE OF METRICS WITH fANOVA

To assess the importance of various metrics on the training loss, we apply fANOVA Hutter et al. (2014) on data that we logged during training with HVP. We used 300k samples that contain the following sampled parameters from the geometric and appearance data augmentation operations for each view: all random resized crop parameters (height and width of the original image, coordinates of crop corners and height and width of the crop), all Colorjitter (color distortion) strengths (brightness, contrast, saturation, hue), grayscale on/off, Gaussian blurring on/off, horizontal flip on/off, loss, and if the crop was selected or

IoU Policy Type	SimSiam	DINO
Baseline (B)	68.20	73.50
B+range(0.3-0.35)	-0.80	-1.47
B+range(0.3-0.35)+alt.	+0.10	-0.45
B+range(0.4-0.6)	+0.55	-0.40
B+range(0.4-0.6)+alt.	+0.25	-0.20
B+range(0.1-0.8)	-33.95	-1.50
B+range(1.0-0.1)	+0.07	-

Table 4: Top-1 lin. eval. accuracies for the manual IoU policy.

not. The metrics we chose are Intersection over Union (IoU), Relative Distance (sample-wise normalized distance of the center points of crop pairs), color distortion distance (the Euclidean distance between all four color distortion operation parameters, i.e. brightness, contrast, saturation, hue), and the individual color distortion parameters of the Colorjitter operation. As can be seen in Fig. 8, the metric with the highest predictive capacity on the loss is the IoU with an importance of 15.2% followed by brightness with 5.1%. The relative distance has an importance of 3.3%, the Colorjitter distance 2.3%, the contrast 1.6%, the saturation 1.4%, hue 0.6%, and all parameters jointly 1.7%.

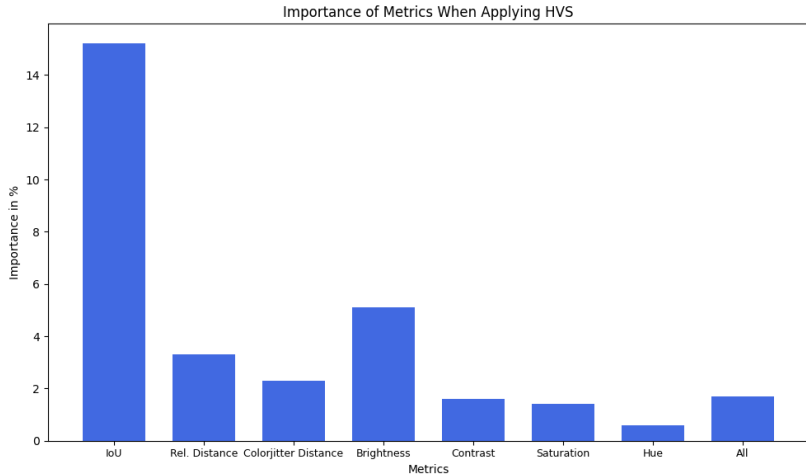


Figure 8: Application of fANOVA Hutter et al. (2014) on logged training data to determine metrics with high predictive capacity on the training loss.

F ADDITIONAL EMPIRICAL ANALYSIS

F.1 CAN A MANUAL AUGM. POLICY BE DERIVED?

Since harder pretraining tasks seem beneficial according to observations made in Q1, a natural question arises: can we mimic the adversarial selection with a manually scripted augmentation policy? Such a policy would replace HVP and lower the computational cost. Since the IoU plays an important role, below, we study several ways to construct a simple manual augmentation policy based on IoU.

F.1.1 DERIVING AN AUGMENTATION POLICY

We implemented the following rejection sampling algorithm in the augmentation pipeline: we linearly approximate the IoU values from Fig. 3 (left; in blue) with start and end values of 0.30 and 0.35 (ignoring the dip in the early phase). For each iteration, we then check if the pairs exceed the IoU value and if so, we reject the pair and re-sample a new pair. This ensures that only pairs are sampled that entail a minimum task difficulty (by means

of a small enough IoU). We varied different hyperparameters, e.g., IoU start/end ranges, inverse schedules, and alternating between the IoU schedule and the standard augmentation. Training both SimSiam and DINO models for 100 epochs yielded performance drops or insignificant improvements (see Table 4). These results indicate that using a manual policy based on metrics in pixel space such as the IoU is non-trivial. Additionally, these results show that transferring such a policy from SimSiam to DINO does not work well, possibly due to additional variations in the augmentation pipeline such as multi-crop. In contrast, we believe that HVP is effective and transfers well since it 1) operates on a similarity level of latent embeddings that may be decorrelated from the pixel space and 2) has access to the current model state.

F.1.2 ASSESSING THE DIFFICULTY OF PREDICTING THE PAIR SELECTED BY HVP

We further validate the previous result and assess an upper limit on the performance for predicting the hardest pair. By fitting a gradient boosting classification tree Friedman (2001), we predict the selected view pair conditioned on all SimSiam hyperparameter log data from Q1 except for the flag that indicates whether a view was selected. As training and test data, we used the logs from two seeds (each 300k samples) and the logs from a third seed, respectively. We also tuned hyperparameters on train/valid splits and applied a 5-fold CV. However, the resulting average test performance in all scenarios never exceeded 40%, indicating that it is indeed challenging to predict the hardness of views based on parameter-level data. This further supports our hypothesis that deriving a policy for controlling and increasing hardness based on geometric and appearance parameters is non-trivial and that such a policy must function on a per-sample basis and have access to the current model state as in HVP.

G LEARNING VIEW GENERATION

G.1 ADVERSARIAL LEARNER

In this experiment, we explore adversarially learning a network to output the transformation matrix for view generation. We use Spatial Transformer Network (STN) Jaderberg et al. (2015) to allow generating views by producing 6D transformation matrices (allowing translating, rotating, shearing, scaling, affine transformations, and combinations thereof) in a differentiable way since most common augmentations are not off-the-shelf differentiable. We optimize the STN jointly with the DINO objective and a ViT-tiny. We train it alongside the actual pretrained network using the same (inverted) objective. For our experiments, we use DINO with multi-crop, i.e. 2 global and 8 local heads. As STN we use a small CNN followed by a linear layer for outputting the 10×6 transformation matrices. In this scenario, we use a ViT-tiny/16 with a 300 epoch pretraining on CIFAR10 with a batch size of 256. All other hyperparameters are identical to the ones reported in the DINO paper.

Figure 9 visualizes the procedure. The STN takes the raw image input and generates a number of transformation matrices that are applied to transform the image input into views. These views are then passed to the DINO training pipeline. Both networks are trained jointly with the same loss function. DINO is trained with its original contrastive objective, where the STN is trained by inverting the gradient after the DINO during backpropagation.

The STN, without using auxiliary losses, starts zooming in and generating single-color views. To counteract this behavior, we experimented with different penalties on the transformation matrices produced by the STN. For instance, in order to limit the zooming pattern, we can use the determinants of the sub-matrices of the transformation matrix to penalize based on the area calculated and apply a regression loss (e.g. MSE). We refer to this type of penalty as *Theta Crops Penalty* (TCP). Additionally, we also restrict its parameters to stay within a sphere with different parameters for local and global crops. Next to determinant-based penalty losses, we also experimented with other penalty functions such as the weighted MSE between the identity and the current transformation matrix or penalties based on histograms of the input image and generated views after applying the transformation. To avoid strong uni-dimensional scaling behavior, we also implemented restricting scaling in a symmetric

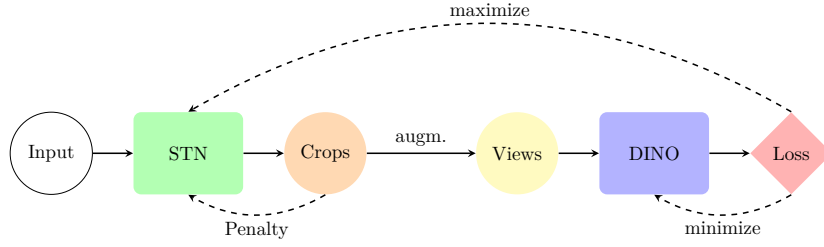


Figure 9: Illustration of adversarial learning with a Spatial Transformer Network (STN) jointly with contrastive learning (here: DINO).

way (i.e. applied to both x and y dimensions) and refer to this as *scale-sym..*. We report our best results in Table 5 which are all TCP-based. As can be seen, no setting is able to outperform the baseline. Our best score was achieved with translation-scale-symmetric which is very similar to random cropping. When removing the symmetries in scaling, the performance drops further. Removing a constraint adds one transformation parameter and therefore one dimension. This can be seen as giving more capacity to the adversarial learner which in turn can make the task significantly harder. Similarly, when adding rotation, the performance drops further and in part drastically. This is on the one hand due to the penalties not being fully able to restrict the output of the STN. On the other, the task of extracting useful information from two differently rotated crops is even harder, and learning spatial invariance becomes too challenging. All in all, we experienced two modes: either the STN is too restricted, leading to *static output* (i.e. independent of image content, the STN would produce constant transformation matrices) or the STN has too much freedom, resulting in extremely difficult tasks. See Fig. 10 for an example of the former behavior.



Figure 10: Example for static output behavior of the STN.

Mode	Penalty	Lin.	F.T.
baseline	-	86.1	92.7
translation-scale-sym.	TCP	83.7	90.3
translation-scale	TCP	82.8	89.7
rotation-translation	TCP	56.7	-
rotation-translation-scale	TCP	31.7	-
rotation-translation-scale-sym.	TCP	77.6	-
affine	TCP	78.3	83.5

Table 5: **Linear evaluation and finetuning classification performance on CIFAR10.** Top-1 accuracy on the validation set of CIFAR10 for our best results reported with different STN transformation modes.

G.2 COOPERATIVE LEARNER

To investigate the effect of a *cooperative*, i.e. easy pair selection, we conducted a small experiment. Instead of selecting the pair yielding the worst loss, we inverted the objective and selected the pair with the best loss. As expected, this led to model collapses with a linear eval. performance of 0.1%. This result is in line with previous findings that highlight the importance of strong augmentations in CL.

H ADDITIONAL RESULTS

H.1 OBJECT DETECTION AND INSTANCE SEGMENTATION

Here we provide more detailed results on object detection and instance segmentation, shown in Tab. 6 and Tab. 7 respectively. We followed iBOT’s default configurations which employed Cascade Mask R-CNN as the task layer.

Method	Arch.	Object Detection			Instance Segmentation		
		AP ^b	AP ^b ₅₀	AP ^b ₇₅	AP ^m	AP ^m ₅₀	AP ^m ₇₅
iBOT	ViT-S/16	47.00	66.13	50.63	40.67	63.10	43.37
+ HVP	ViT-S/16	47.27	66.50	50.90	40.90	63.50	43.83
Improvement		+0.27	+0.37	+0.27	+0.23	+0.40	+0.47
DINO	ViT-S/16	46.50	65.90	50.30	40.43	62.83	43.27
+ HVP	ViT-S/16	47.07	66.37	50.63	40.80	63.37	43.87
Improvement		+0.57	+0.47	+0.33	+0.37	+0.53	+0.60

Table 6: Additional object detection and instance segmentation results on the COCO dataset. The ViT-S/16 models were pretrained for 100 epochs.

Method	Arch.	Object Detection			Instance Segmentation		
		AP ^b	AP ^b ₅₀	AP ^b ₇₅	AP ^m	AP ^m ₅₀	AP ^m ₇₅
iBOT	ViT-S/16	47.60	66.80	51.33	41.10	63.63	44.07
+ HVP	ViT-S/16	48.03	67.13	51.73	41.50	64.23	44.40
Improvement		+0.43	+0.33	+0.40	+0.40	+0.60	+0.33
DINO	ViT-S/16	47.27	66.60	51.00	41.00	63.63	44.03
+ HVP	ViT-S/16	47.50	67.00	51.33	41.17	64.00	44.13
Improvement		+0.23	+0.40	+0.33	+0.17	+0.37	+0.10

Table 7: Additional object detection and instance segmentation results on the COCO dataset. The ViT-S/16 models were pretrained for 300 epochs.

I HYPERPARAMETERS

I.1 EVALUATIONS ON IMAGENET

I.1.1 DINO

For DINO, we report the ViT pretraining hyperparameters in Table 8 (ViT-S) and Table 9 (ViT-B) which are the original ones as reported by the authors. Note, for HVP we limit the total number of comparisons to 128 across all heads. Linear evaluation is executed for 100 epochs and we use a learning rate of 0.00075, SGD optimizer (AdamW Loshchilov & Hutter (2019) during pretraining), a batch size of 1024, a momentum of 0.9, and no weight decay (as reported by the authors).

Hyperparameter	Value	Hyperparameter	Value
architecture	vit-small	epochs:	100
img-size	224	warmup-epochs:	10
patch-size	16	freeze-last-layer:	1
out-dim	65536	lr:	0.0005
norm-last-layer	true	min-lr:	1.0e-06
momentum-teacher	0.996	optimizer:	AdamW
use-bn-in-head	false	weight-decay:	0.04
teacher-temp	0.04	weight-decay-end:	0.4
warmup-teacher-temp	0.04	global-crops-scale:	0.4, 1.0
warmup-teacher-temp-epochs	0	global-crops-size:	224
fp16	true	local-crops-number:	8
batch-size	512	local-crops-scale	0.05, 0.4
clip-grad	3.0	local-crops-size:	96
drop-path-rate	0.1		

Table 8: Pretraining ImageNet hyperparameters for the runs with DINO ViT-S/16. For 300 epochs, we use a batch size of 1024.

Hyperparameter	Value	Hyperparameter	Value
architecture	vit-base	epochs:	400
img-size	224	warmup-epochs:	10
patch-size	16	freeze-last-layer:	3
out-dim	65536	lr:	0.00075
norm-last-layer	true	min-lr:	2.0e-06
momentum-teacher	0.996	optimizer:	AdamW
use-bn-in-head	false	weight-decay:	0.04
teacher-temp	0.07	weight-decay-end:	0.4
warmup-teacher-temp	0.04	global-crops-scale:	0.25, 1.0
warmup-teacher-temp-epochs	50	global-crops-size:	224
fp16	false	local-crops-number:	10
batch-size	1024	local-crops-scale:	0.05, 0.25
clip-grad	0.3	local-crops-size:	96
drop-path-rate	0.1		

Table 9: Pretraining ImageNet hyperparameters for the runs with DINO ViT-B/16.

I.1.2 SIMSiam

In Table 10, we report the ResNet-50 pretraining hyperparameters. Linear evaluation is executed for 90 epochs (as reported by the SimSiam authors) and we use a learning rate of 0.1, LARS optimizer You et al. (2017), a batch size of 4096, and no weight decay.

I.1.3 SIMCLR

We report the ResNet-50 pretraining hyperparameters for SimCLR in Table 11. Linear evaluation is executed for 90 epochs with a learning rate of 0.1, SGD optimizer, batch size of 4096, and no weight decay.

I.2 TRANSFER TO OTHER DATASETS AND TASKS

For linear evaluation on the transfer datasets, we simply used the same hyperparameters for linear evaluation on ImageNet (DINO and SimSiam respectively). For finetuning DINO ViT-S/16, we used the hyperparameters reported in Table 12 and for SimSiam ResNet-50 we used the hyperparameters in Table 13

Hyperparameter	Value
architecture	resnet50
batch-size	512
blur-prob	0.5
crops-scale	0.2, 1.0
crop-size	224
feature-dimension	2048
epochs	100
fix-pred-lr	true
lr	0.05
momentum	0.9
predictor-dimension	512
weight-decay	0.0001
optimizer	SGD

Table 10: Pretraining ImageNet hyperparameters for the runs with SimSiam. For 300 epochs, we use a batch size of 1024.

Hyperparameter	Value
architecture	resnet50
proj-hidden-dim	2048
out-dim	128
use-bn-in-head	true
batch-size	4096
optim	LARS
lr	0.3
sqrt-lr	false
momentum	0.9
weight-decay	1e-4
epochs	100
warmup-epochs	10
zero-init-residual	true

Table 11

Hyperparameter	CIFAR10	CIFAR100	Flowers102	iNat 21	Food101
lr	7.5e-6	7.5e-6	5e-5	5e-5	5e-5
weight-decay	0.05	0.05	0.05	0.05	0.05
optimizer	AdamW	AdamW	AdamW	AdamW	AdamW
epochs	300	300	300	100	100
batch-size	512	512	512	512	512

Table 12: Finetuning hyperparameters for DINO ViT-S/16.

Hyperparameter	CIFAR10	CIFAR100	Flowers102	iNat 21	Food101
lr	7.5e-6	5e-6	5e-4	7e-5	5e-6
weight-decay	0.05	0.05	0.05	0.05	0.05
optimizer	AdamW	AdamW	AdamW	AdamW	AdamW
epochs	300	300	300	100	100
batch-size	512	512	512	512	512

Table 13: Finetuning hyperparameters for SimSiam and ResNet-50.

I.3 OBJECT DETECTION AND INSTANCE SEGMENTATION

Our experiments utilized Open MMLab’s detection library Chen et al. (2019) for object detection and instance segmentation on COCO Lin et al. (2014). We followed iBOT’s default configuration.

Obj. Det. & Inst. Segm. on COCO	
Hyperparameter	Value
epochs	12
batch-size	32
lr	0.02

Table 14: Hyperparameters object detection and instance segmentation on COCO.

J COMPUTATIONAL OVERHEAD OF HVP

The additional forward passes that HVP introduces for the selection phase increase the time complexity of the individual baseline methods. Several possible approaches exist to mitigate this overhead, one of which is to alternate between the vanilla and HVP training step. We measured the overhead factors for different alternating frequencies (i.e., after how many training steps we use the hard views from HVP; we refer to this as *step*) for SimSiam, DINO, and iBOT which we report in Table 15. Below, we propose additional ways that may allow using hard views more efficiently.

Step	SimSiam (RN50)	DINO (ViT-S/16)	DINO (RN50)	iBOT (ViT-S/16)
1 (HVP)	x1.64	x2.21	x2.01	x2.13
2	x1.38	x1.61	x1.56	x1.57
3	x1.32	x1.43	x1.42	x1.38
4	x1.29	x1.34	x1.35	x1.29

Table 15: Slowdown factors for HVP and the alternating training method, where *step* refers to the interval at which HVP is applied during training (i.e., step=1 refers to full HVP and step=3 indicates that HVP is approx. used 33% of the training time). Measurements are averages across 3 seeds.

As an alternative to the alternating training, we also experimented with a 50% image resolution reduction for the selection phase but observed that the final performance was negatively affected by it or that baseline performance could not be improved.

The details of hardware and software used for this analysis are: one single compute node with 8 NVIDIA RTX 2080 Ti, AMD EPYC 7502 (32-Core Processor), 512GB RAM, Ubuntu 22.04.3 LTS, PyTorch 2.0.1, CUDA 11.8. For DINO’s 2 global and 8 local views (default), applying HVP with nviews=2 sampled for each original view results in 4 global and 16 local views. Since considering all combinations would yield over 77k unique comparisons ($\binom{4}{2} \times \binom{16}{8}$), to remain tractable, we limit the number of total comparisons to 64. For training experiments that exceed the limit of 8x RTX 2080 Ti, we apply gradient accumulation.

While technically there can be a memory overhead with HVP, with the number of sampled views chosen in this paper, the backward pass of the methods that compute gradients only for the selected view pair still consumes more memory than the selection part of HVP (even for 8 sampled views in SimSiam). Note, that selection and the backward computation are never executed at the same time but sequentially.

We emphasize that further ways exist to optimize HVP’s efficiency which remain to be explored. For instance:

- using embeddings of views from “earlier” layers in the networks or
- using 4/8 bit low-precision for the view selection or
- using one GPU just for creating embeddings and selecting the hardest views while the remaining GPUs are used for learning or
- other approaches to derive manual augmentation policies or
- bypassing forwarding of similar pairs.

K HARD VIEW PRETRAINING OBJECTIVES

K.1 SIMCLR

In this section, we are going to introduce the application of HVP with the SimCLR objective. Assume a given set of images \mathcal{D} , an image augmentation distribution \mathcal{T} , a minibatch of M images $\mathbf{x} = \{\mathbf{x}_i\}_{i=1}^M$ sampled uniformly from \mathcal{D} , and two sets of randomly sampled image augmentations $A = \{t_i \sim \mathcal{T}\}_{i=1}^M$ and B sampled from \mathcal{T} . We apply A and B to each image in \mathbf{x} resulting in \mathbf{x}^A and \mathbf{x}^B . Both augmented sets of views are subsequently projected into an embedding space with $\mathbf{z}^A = g_\theta(f_\theta(\mathbf{x}^A))$ and $\mathbf{z}^B = g_\theta(f_\theta(\mathbf{x}^B))$ where f_θ represents an encoder (or backbone) and g_θ a projector network. Contrastive learning algorithms then minimize the following objective function:

$$\mathcal{L}(\mathcal{T}, \mathbf{x}; \theta) = -\log \frac{\exp(\text{sim}(\mathbf{z}_i^A, \mathbf{z}_i^B)/\tau)}{\sum_{i \neq j} \exp(\text{sim}(\mathbf{z}_i^A, \mathbf{z}_j^B)/\tau)} \quad (3)$$

where τ denotes a temperature parameter and sim a similarity function that is often chosen as cosine similarity. Intuitively, when optimizing θ , embeddings of two augmented views of the same image are attracted to each other while embeddings of different images are pushed further away from each other.

To further enhance the training process, we introduce a modification to the loss function where instead of having two sets of augmentations A and B , we now have “ N ” sets of augmentations, denoted as $\mathcal{A} = \{A_1, A_2, \dots, A_N\}$. Each set A_i is sampled from the image augmentation distribution \mathcal{T} , and applied to each image in \mathbf{x} , resulting in “ N ” augmented sets of views $\mathbf{x}^{A_1}, \mathbf{x}^{A_2}, \dots, \mathbf{x}^{A_N}$.

Similarly, we obtain N sets of embeddings $\mathbf{z}^{A_1}, \mathbf{z}^{A_2}, \dots, \mathbf{z}^{A_N}$ through the encoder and projector networks defined as:

$$\mathbf{z}^{A_i} = g_\theta(f_\theta(\mathbf{x}^{A_i})), \quad i = 1, 2, \dots, N$$

We then define a new objective function that seeks to find the pair of augmented images that yield the highest loss. The modified loss function is defined as:

$$\mathcal{L}_{\max}(\mathcal{T}, \mathbf{x}; \theta) = \max_{k, l: k \neq l} \mathcal{L}(\mathcal{T}, \mathbf{x}; \theta)_{kl}$$

where

$$\mathcal{L}(\mathcal{T}, \mathbf{x}; \theta)_{kl} = -\log \frac{\exp(\text{sim}(\mathbf{z}_k^{A_k}, \mathbf{z}_l^{A_l})/\tau)}{\sum_{i \neq j} \exp(\text{sim}(\mathbf{z}_i^{A_k}, \mathbf{z}_j^{A_l})/\tau)}$$

and $k, l \in \{1, 2, \dots, N\}$ and $i, j \in \{1, 2, \dots, M\}$.

For each iteration, we evaluate all possible view pairs and contrast each view against every other example in the mini-batch. Intuitively, the pair that yields the highest loss is selected, which is the pair that at the same time minimizes the numerator and maximizes the denominator in the above equation. In other words, the hardest pair is the one, that has the lowest similarity with another augmented view of itself and the lowest dissimilarity with all other examples.

E.2 Statement of Contributions

Statement of Contributions for the following publication:

Title	Beyond Random Augmentations: Pretraining with Hard Views
Link to Publication, DOI	https://arxiv.org/abs/2310.03940 https://openreview.net/forum?id=AK1C55o4r7
Authors	Fabio Ferreira*, Ivo Rapant*, Jörg Franke, and Frank Hutter (*: joint first author)
Publication Status	Accepted and published
Publisher, Date	Proceedings of the Thirteenth International Conference on Learning Representations (ICLR), 2025
Peer-Review-Process	Yes
Rank	Ranked A* by the CORE2023 ranking

Paper Summary

Many Self-Supervised Learning (SSL) methods aim for a model invariance to different image augmentations known as *views*. The paper "Beyond Random Augmentations: Pretraining with Hard Views" introduces Hard View Pretraining (HVP), an approach to Self-Supervised Learning (SSL) that extends the conventional random view sampling by explicitly selecting views that benefit the learning process. By exposing the model to harder, more challenging samples during SSL pretraining, the model achieves higher downstream task performance. The key contributions of the paper are:

1. Proposing to use HVP that automatically exposes the model to harder samples (views) during pretraining. It only requires the computability of sample-wise losses and is easily integrated into existing SSL pipelines.
2. The study demonstrates the effectiveness and compatibility using ImageNet-1k across four popular SSL methods (DINO, iBOT, SimSiam, SimCLR), achieving linear evaluation accuracy improvements of 1% on average.
3. The paper shows that HVP-pretrained models also yield performance improvements on a diverse set of transfer tasks, including finetuning, object detection, and segmentation.
4. The study also presents insights into the underlying mechanisms and robustness of HVP.

Contributions Listing

Name	Contributions	Signature
Fabio Ferreira	<p>Proposed the original idea of adversarially learning a view network to output hard views to challenge a model during SSL pretraining. Fabio implemented an initial version of this idea with DINO and SimSiam. Ivo investigated and enhanced this idea further in the scope of his student project that Fabio supervised. Ultimately, the idea was dismissed due to computational instability. To understand the adversary network's behavior better, Ivo proposed forwarding multiple randomly sampled views and selecting those with the highest loss for the backward pass, which improved downstream task performance. Fabio encouraged further development of this method in Ivo's master thesis for other SSL methods and transfer tasks, leading to the present paper;</p> <p>Provided base code for training DINO and SimSiam on ImageNet on the cluster infrastructure; implemented transfer tasks for linear evaluation and finetuning (Table 2) and baselines (BarlowTwins; not in the paper); proposed and investigated methods to make HVP more efficient (jointly with Ivo)</p> <p>Owned and led the project's methodology and overall strategic direction, including the methods used in the empirical analysis Section;</p> <p>Co-carried out approximately 50% of all the experiments (Ivo carried out the other approx. 50%);</p> <p>Owned, led and wrote the majority of the paper, including contributions to all parts of the paper; led and contributed significantly to the rebuttal process;</p>	<p>DocuSigned by:</p>  <p>CA7363FD31BF45C... 22.01.2025</p>

	<p>Supported Ivo on the code-level through code reviews and small code changes.</p> <p>Supervised Ivo Rapant.</p>	
Ivo Rapant	<p>Proposed the idea of forwarding multiple random views and selecting the hardest for the backward pass;</p> <p>Developed further the DINO and SimSiam base code from Fabio; implemented HVP, implemented baselines (iBOT, SimCLR), proposed and investigated methods to make HVP more efficient (jointly with Fabio);</p> <p>Carried out the empirical analysis of HVP, as well as the object detection and instance segmentation transfer task experiments;</p> <p>Co-carried out approximately 50% of all the experiments (Fabio carried out the other approx. 50%);</p> <p>Supported with writing, editing, reviewing and rebutting all parts of the paper, but the parts of the paper he had the major contributions were: Main Results (Section 4), Empirical Analysis (Section 5)</p>	<p>Signed by:</p>  <p>E18D86EC0C94416... 1/23/2025</p>

Jörg Franke	<p>Supported in reframing the paper; contributed by clarifying the narrative and enhancing the coherence of the paper;</p> <p>Supported with writing and reviewing all parts of the paper, but the parts of the paper he had major contributions were: Introduction and Conclusion (both jointly with Fabio);</p> <p>Supported in running long-run experiments on one of the Juwels clusters.</p>	<p>Signed by:  DC6598DF2302491... 1/24/2025</p>
Frank Hutter	<p>Helped conceptualize the problem;</p> <p>Co-led writing the paper, including contributions to all parts of the paper;</p> <p>Helped with reviewing, rebutting and editing the paper;</p> <p>Supervised the project and supervised Fabio Ferreira.</p>	<p>Signed by:  30DF1E88127C47F... 1/22/2025</p>

Appendices for On the Importance of Hyperparameters and Data Augmentation for Self-Supervised Learning

F.1 Paper Appendix

A. Search Spaces

Table 4. SimSiam data augmentation search space.

Hyperparameter	Type	Range	Log-Prior	Default
p_colorjitter	Float	[0, 1]	False	0.8
p_grayscale	Float	[0, 1]	False	0.2
p_horizontal_flip	Float	[0, 1]	False	0.5
p_solarize	Float	[0, 1]	False	0.2
brightness_strength	Float	[0, 1.5]	False	0.4
contrast_strength	Float	[0, 1.5]	False	0.4
saturation_strength	Float	[0, 1.5]	False	0.4
hue_strength	Float	[0, 0.5]	False	0.1
solarize_threshold	Integer	[0, 255]	False	127

Table 5. SimSiam training hyperparameters search space.

Hyperparameter	Type	Range	Log-Prior	Default
learning_rate	Float	[0.003, 0.3]	True	0.03
warmup_epochs	Integer	[0, 80]	False	0
warmup_multiplier	Float	[1.0, 3.0]	False	1.0
optimizer	Categorical	{AdamW, SGD, LARS}	False	SGD
weight_decay_start	Float	[$5 \cdot 10^{-6}$, $5 \cdot 10^{-2}$]	True	$5 \cdot 10^{-4}$
weight_decay_end	Float	[$5 \cdot 10^{-6}$, $5 \cdot 10^{-2}$]	True	$5 \cdot 10^{-4}$

Table 6. GroupAugment search space.

Hyperparameter	Type	Range	Log-Prior	Default
p_color_transformations	Float	[0, 1]	False	0.5
p_geometric_transformations	Float	[0, 1]	False	0.5
p_non_rigid_transformations	Float	[0, 1]	False	0.0
p_quality_transformations	Float	[0, 1]	False	0.0
p_exotic_transformations	Float	[0, 1]	False	0.0
num_color_transformations	Integer	[1, 5]	False	1
num_geometric_transformations	Integer	[1, 2]	False	1
num_non_rigid_transformations	Integer	[1, 3]	False	1
num_quality_transformations	Integer	[1, 2]	False	1
num_exotic_transformations	Integer	[1, 2]	False	1
num_total_group_samples	Integer	[1, 5]	False	1

Table 7. RandAugment search space.

Hyperparameter	Type	Range	Log-Prior	Default
num_ops	Integer	[1, 15]	False	3
magnitude	Integer	[0, 30]	False	4

Table 8. SmartAugment search space.

Hyperparameter	Type	Range	Log-Prior	Default
num_col_ops	Integer	[1, 9]	False	2
num_geo_ops	Integer	[1, 5]	False	1
col_magnitude	Integer	[0, 30]	False	4
geo_magnitude	Integer	[0, 30]	False	4
p_apply_ops	Float	[0, 1]	False	1

B. Experimental Details

B.1. Expert Priors

We use Bayesian optimization (BO) (Mockus et al., 1978) with expert priors (Hvarfner et al., 2021) as implemented in the NePS python package (Stoll et al., 2022). Therefore, we set expert priors to guide the search. The priors in NePS are, in the continuous case, Gaussian distributions centered at a default value with the standard deviation determined via a confidential setting. We always use a “medium” confidence and set the default value as described below.

Training Hyperparameters and Data Augmentation Strategy We set the defaults to the baseline for the training hyperparameters and data augmentation strategy. As no solarization is used in the SimSiam baseline and Chen & He (2021) shows that adding solarize might improve the performance, we add solarize to the search space and set the user prior default to the values reported by Chen & He (2021).

RandAugment For the RandAugment search space, we set the defaults according to the optimal data augmentation policy for CIFAR-10 following Cubuk et al. (2020).

SmartAugment As we are the first applying SmartAugment to classification, we set the user prior defaults based on the optimal data augmentation policy for CIFAR-10 following Cubuk et al. (2020).

GroupAugment For the GroupAugment config space, we set the default user priors to one augmentation per group. As only color and geometric augmentations occur in the baseline, we set the user prior defaults for these group probabilities to 0.5 and the other group probabilities user prior defaults to 0.

B.2. Resources and Compute Budget

For our Bayesian optimization runs, we allowed a budget of 50 evaluations. For CIFAR-10 and CIFAR-100, one configuration evaluation took ≈ 8 h with one GeForce RTX 2080 Ti GPU, for DermaMNIST ≈ 10 min with 1 GPU. We used 10 GPUs in parallel for CIFAR-10, 20 GPUs in parallel for CIFAR-100, and 5 GPUs in parallel for DermaMNIST. In order to take noise on the validation set during our HPO into account, we evaluate the best-performing configurations multiple times on the validation set.

B.3. GroupAugment Comparative Study: RandAugment Search Space

While SmartAugment and GroupAugment were designed with BO in mind, for RandAugment, which originally used Grid Search, we follow Negassi et al. (2022) and consider an extended search space for the number of operations between 1 and 15. Negassi et al. (2022) showed that a larger number of operations than 3 can be beneficial for the performance. See also Table 7.

B.4. Dataset Splits

Since CIFAR-10 and CIFAR-100 (Krizhevsky, 2009) do not provide a validation set, we split the training set and randomly sample a fixed validation set containing 10% of the training data for our hyperparameter optimization. We use the entire training set for training for our final test evaluations of the best-performing validation configurations. For DermaMNIST (Yang et al., 2021a;b), we have adopted the provided training, validation, and test split.

C. GroupAugment Details

Table 9. Details concerning the data augmentations from the groups. In our implementation, we use the data augmentations from the [albumentations library](#) (Buslaev et al., 2020).

Group	Augmentation
color	ColorJitter(brightness=0.4, contrast=0.4, saturation=0.4, hue=0.1) ToGray() Solarize() Equalize() ChannelShuffle()
geometric	ShiftScaleRotate(interpolation=cv2.INTER_CUBIC) HorizontalFlip()
non-rigid	ElasticTransform(alpha=0.5, sigma=10, alpha_affine=5, interpolation=cv2.INTER_CUBIC) GridDistortion(interpolation=cv2.INTER_CUBIC) OpticalDistortion(distort_limit=0.5, shift_limit=0.5, interpolation=cv2.INTER_CUBIC)
quality	GaussianBlur() GaussNoise()
exotic	RandomGridShuffle() Cutout(num_holes=4)

D. Individual Hyperparameter Analysis

Here, we individually analyze each hyperparameter and augmentation strategy parameter considered in Section 3. In particular, we plot density estimates for the values sampled in our search. We show density estimates for the best and worst-performing configurations (top and bad), all configurations (all), and configurations leading to collapsing. For categorical values, we show the sample distribution.

D.1. Tuned SimSiam Data Augmentation Strategy

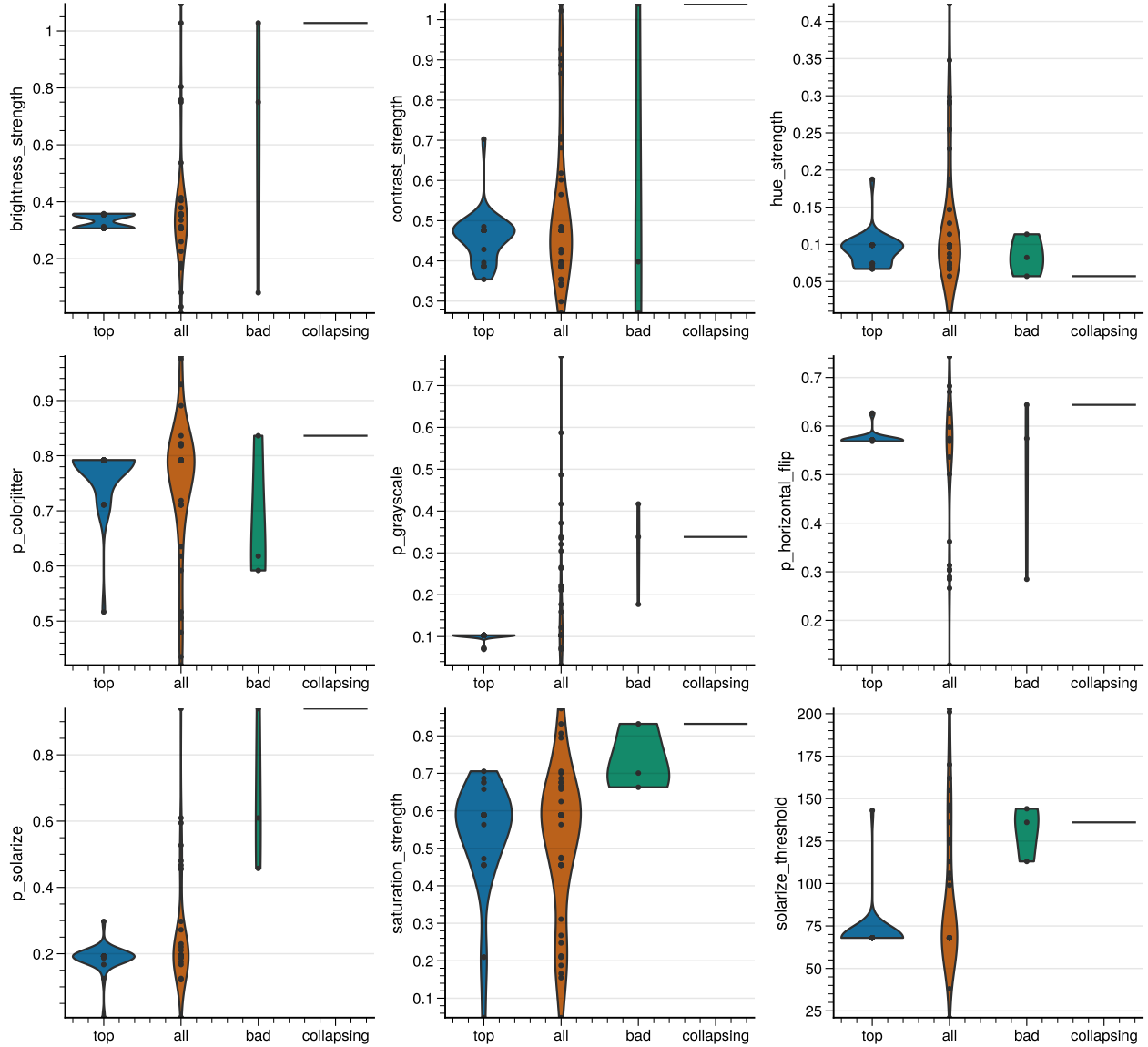


Figure 2. CIFAR-10 with SimSiam data augmentation search space.

On the Importance of Hyperparameters and Data Augmentation for SSL

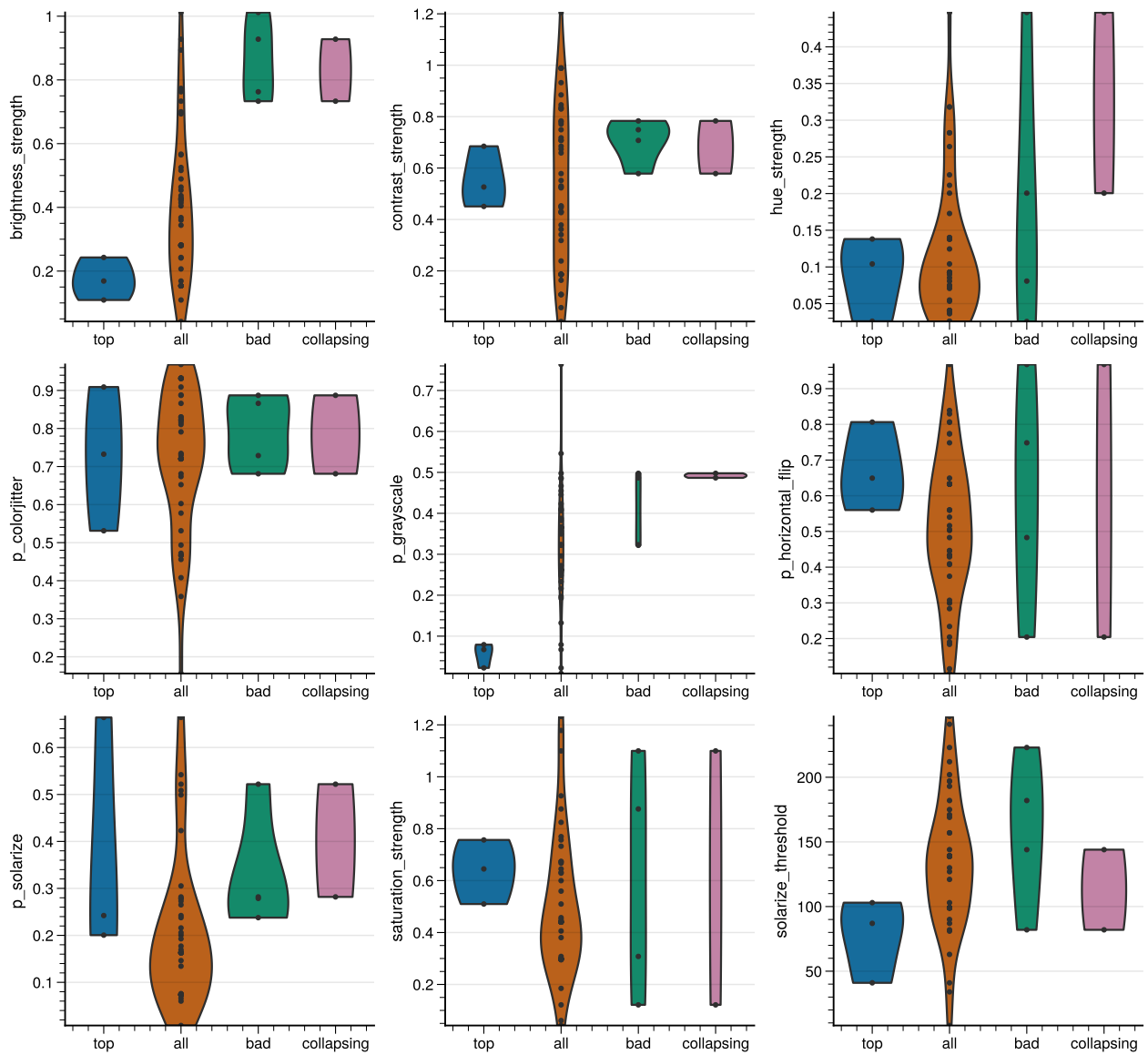


Figure 3. CIFAR-100 with SimSiam data augmentation search space.

On the Importance of Hyperparameters and Data Augmentation for SSL

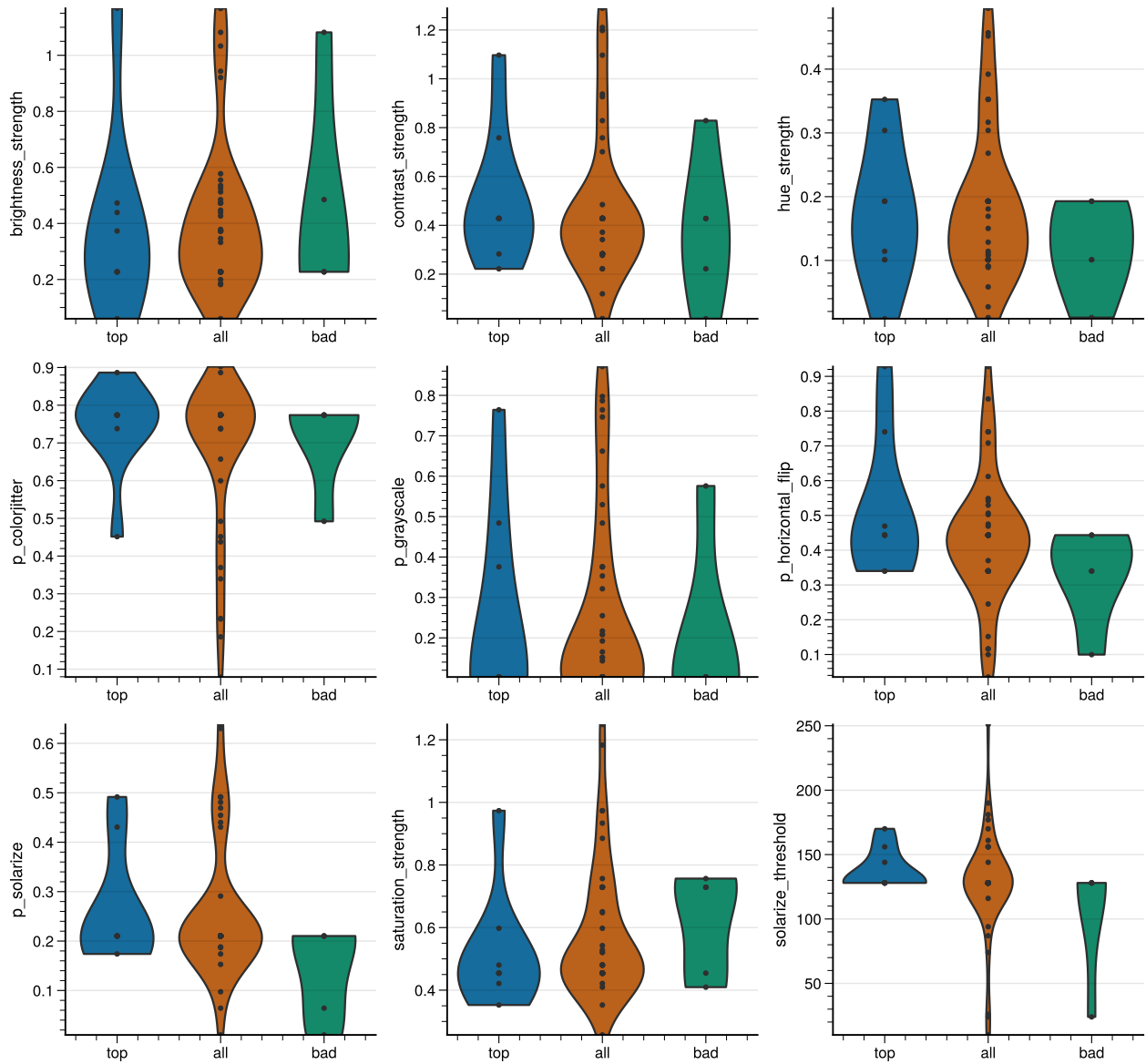


Figure 4. DermaMNIST with SimSiam data augmentation search space.

D.2. Tuned SimSiam Training Hyperparameters

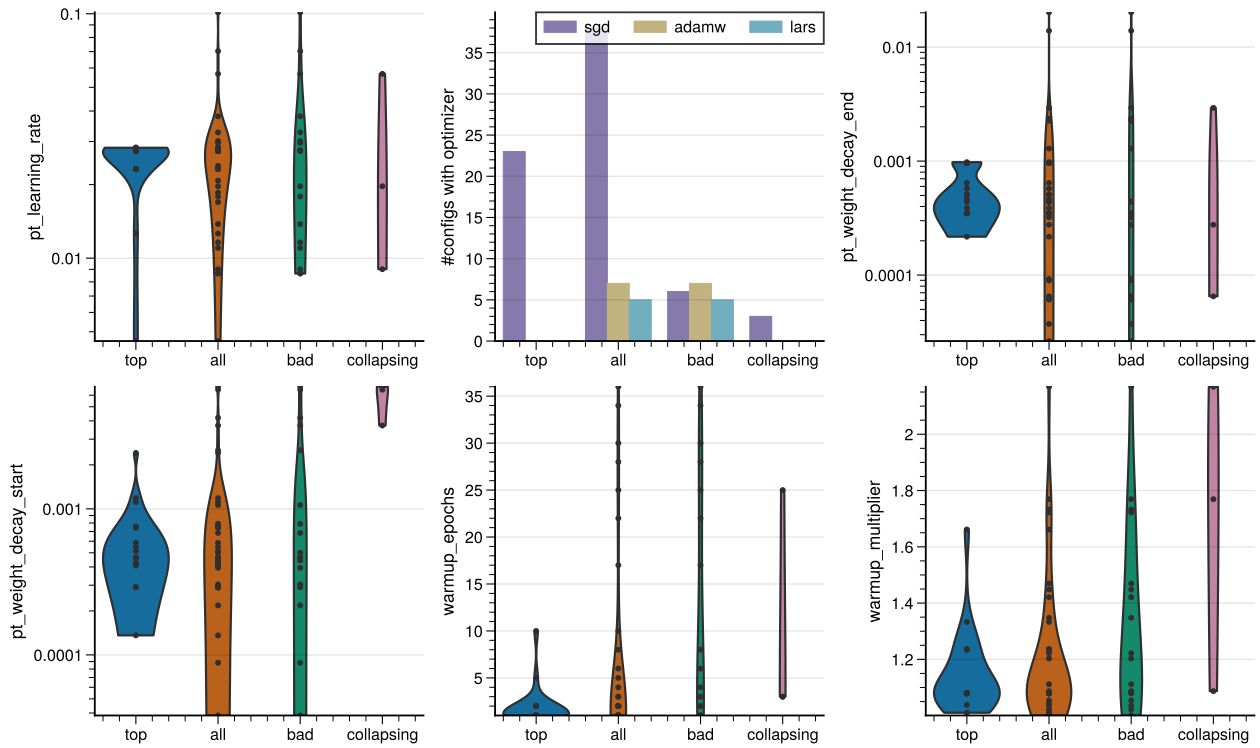


Figure 5. CIFAR-10 with SimSiam training hyperparameters search space.

On the Importance of Hyperparameters and Data Augmentation for SSL

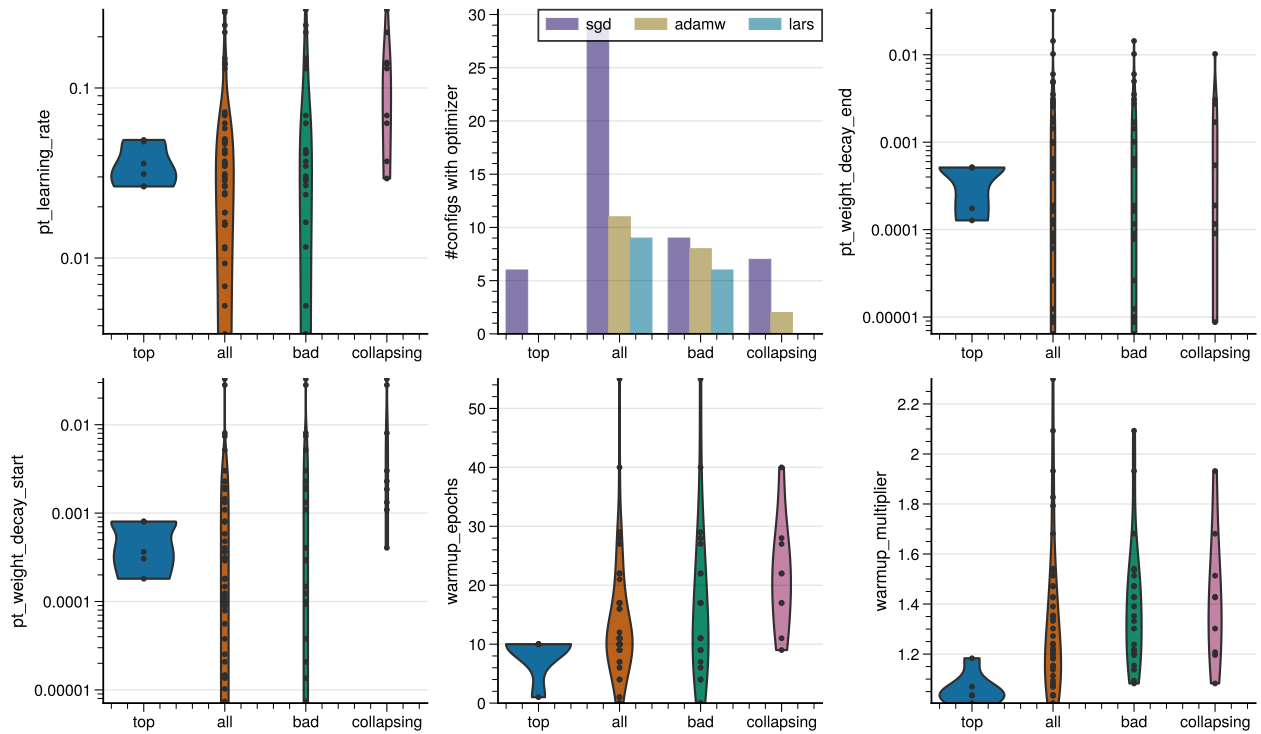


Figure 6. CIFAR-100 with SimSiam training hyperparameters search space.

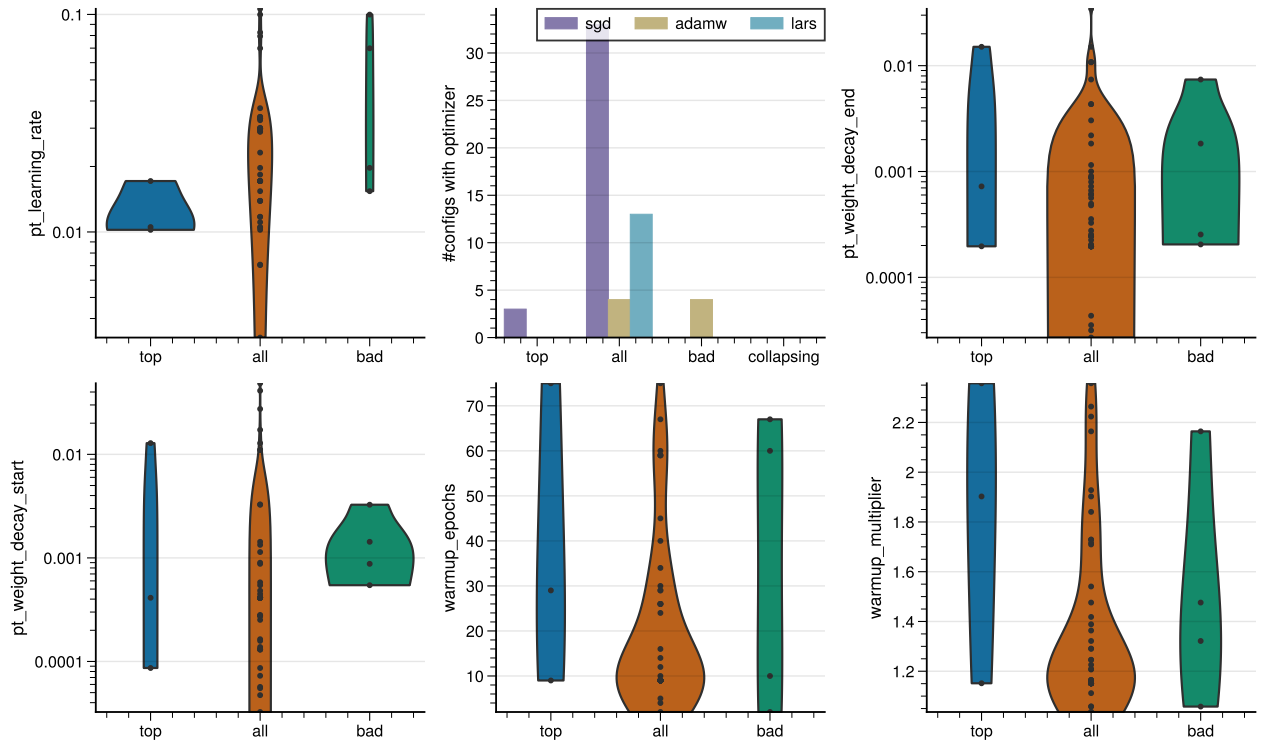


Figure 7. DermaMNIST with SimSiam training hyperparameters search space.

F.2 Statement of Contributions

Statement of Contributions for the following publication:

Title	On the Importance of Hyperparameters and Data Augmentation for Self-Supervised Learning
Link to Publication, DOI	https://arxiv.org/pdf/2207.07875.pdf https://openreview.net/forum?id=oBmAN382UL
Authors	Diane Wagner, Fabio Ferreira, Danny Stoll, Robin Tibor Schirrmeister, Samuel Müller, Frank Hutter
Publication Status	Accepted at the First Workshop of Pre-training: Perspectives, Pitfalls, and Paths Forward at ICML 2022
Publisher, Date	-
Peer-Review-Process	Yes
Rank	not ranked by CORE2023 (workshop)

Paper Summary

This paper investigates the influence of hyperparameters and data augmentation strategies on Self-Supervised Learning (SSL), using SimSiam with a ResNet-18 backbone across CIFAR-10, CIFAR-100, and DermaMNIST datasets. The study focuses on understanding the role of data augmentation in SSL, examining whether better augmentation strategies can significantly improve performance. It also explores which hyperparameters are most likely to cause model collapse when set incorrectly, and which hyperparameters should be prioritized to achieve high performance and outperform baselines in SSL.

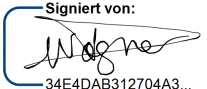
The results reveal that while hyperparameter optimization provides marginal improvements, data augmentation has a far more substantial impact on SSL performance. As an additional contribution, the authors introduce GroupAugment, a novel automated data augmentation algorithm that optimizes sampling across groups of augmentations. GroupAugment consistently delivers superior accuracy in linear evaluation protocols across all datasets, outperforming existing augmentation techniques.

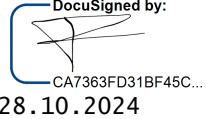
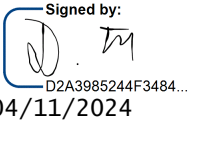
Additionally, the paper presents a detailed empirical analysis, offering insights into the importance of hyperparameter tuning and its effects on model stability and performance. This work highlights the often-underestimated role of data augmentation in SSL and provides practical insights for optimizing SSL pipelines through improved augmentation strategies. The key contributions of the paper are:

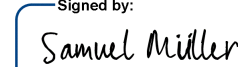
1. The paper investigates the role of hyperparameters and data augmentation in Self-Supervised Learning (SSL), identifying key factors that influence performance, including potential causes of model collapse.
2. The paper proposes GroupAugment, a novel automated data augmentation algorithm that optimizes sampling across groups of augmentations. It outperforms existing data augmentation strategies used in Supervised and Self-Supervised Learning across multiple datasets.

3. The paper provides insights into which hyperparameters are critical to optimize for achieving high SSL performance and avoiding model collapse.

Contributions Listing

Name	Contributions	Signature
Diane Wagner	<p>Proposed the idea to investigate hyperparameter and data augmentation in SSL, highlighting their key role in downstream task performance (jointly with Fabio)</p> <p>Owned and led all code implementations required for the paper;</p> <p>Owned, led, and carried out all experiments and created all figures and tables in the paper;</p> <p>Co-led the methodology of the project jointly with Fabio;</p> <p>Proposed, developed, evaluated, and analyzed GroupAugment (jointly with Danny);</p> <p>Contributed to shaping the project's vision and methodology in collaboration with the supervisory team.</p> <p>Lead the periodic code reviews;</p> <p>Co-wrote the paper and positioned the work in the research context together with Fabio and Danny.</p>	<p>Signiert von:</p>  <p>34E4DAB312704A3...</p> <p>31.10.2024</p>

Fabio Ferreira	<p>Proposed the idea to investigate hyperparameter and data augmentation in SSL, highlighting their key role in downstream task performance (jointly with Diane)</p> <p>Guided the project direction and co-led the methodology of the project jointly with Diane;</p> <p>Provided the initial code for training ResNet-18 with SimSiam, as well as the code for linear evaluation and support for CIFAR-10 and CIFAR-100;</p> <p>Co-designed the experimental setup jointly with Diane and Danny;</p> <p>Participated in the periodic code reviews (jointly with Diane);</p> <p>Contributed to shaping the project's vision and methodology in collaboration with the supervisory team.</p> <p>Owned and lead the paper writing, co-wrote the paper and positioned the work in the research context together with Diane and Danny.</p> <p>Lead the supervision of Diane.</p>	
Danny Stoll	<p>Co-supervised the project alongside Fabio, Robin, and Samuel;</p> <p>Contributed to shaping the project's vision and methodology;</p> <p>Proposed, developed, evaluated, and analyzed GroupAugment (jointly with Diane);</p> <p>Co-designed the experimental setup jointly with Diane and Fabio;</p>	

	<p>Co-wrote the paper and positioned the work in the research context with Diane and Fabio and contributed by clarifying the narrative and enhancing the coherence of the paper.</p>	
Robin Tibor Schirrmeister	<p>Co-supervised the project alongside Fabio, Danny, and Samuel;</p> <p>Offered insights on related work and helped refine the narrative within the broader context of medical machine learning;</p> <p>Assisted in writing the paper, particularly the introduction section;</p> <p>Supported with reviewing all parts of the paper.</p>	<p>Signed by:</p>  <p>9C5A138D83524AE... 10/28/2024</p>
Samuel Müller	<p>Co-supervised the project alongside Fabio, Danny, and Robin;</p> <p>Contributed to the initial code development and early experimental design, providing foundational assistance for the project;</p> <p>Supported with reviewing all parts of the paper.</p>	<p>Signed by:</p>  <p>Samuel Müller D963AEAD51FC4C0... 10/29/2024</p>
Frank Hutter	<p>Helped conceptualize the problem;</p> <p>Supported in writing, reviewing, and editing the paper;</p> <p>Supervised the project and supervised Fabio, Danny, Robin, Samuel.</p>	<p>Signed by:</p>  <p>3CDF1E88127C47F... 31/10/2024</p>

Appendices for Learning Synthetic Environments and Reward Networks for Reinforcement Learning

G.1 Paper Appendix

APPENDIX A SYNTHETIC ENVIRONMENTS

A.1 HEURISTICS FOR AGENT TRAINING AND EVALUATION

Determining the number of required training episodes n_e on an SE is challenging as the rewards of the SE may not provide information about the current agent’s performance on the real environment. Thus, we use a heuristic to early-stop training once the agent’s training performance on the SE converged. Specifically, let C_k be the cumulative reward of the k -th training episode. The two values \bar{C}_d and \bar{C}_{2d} maintain a non-overlapping moving average of the cumulative rewards over the last d and $2d$ episodes up to episode k . Now, if $\frac{|\bar{C}_d - \bar{C}_{2d}|}{|\bar{C}_{2d}|} \leq C_{diff}$ the training is stopped. In all SE experiments we choose $d = 10$ and $C_{diff} = 0.01$. Agent training on *real environments* is stopped when the average cumulative reward across the last d test episodes exceeds the solved reward threshold. In case no heuristic is triggered, we train for $n_e = 1000$ episodes at most on SEs and real environments. Independent of whether we train an agent on \mathcal{E}_{real} or \mathcal{E}_{syn} , the process to assess the actual agent performance is equivalent: we run the agent on 10 test episodes from \mathcal{E}_{real} for a fixed number of task-specific steps (200 on CartPole and 500 on Acrobot) and use the cumulative rewards as the performance.

A.2 DISCUSSION ON THE FEASIBILITY OF LEARNING SEs WITH OUR ALGORITHM

After identifying stable DDQN and NES hyperparameters (HPs), we ran Algorithm 1 in parallel with 16 workers for 200 NES outer loop iterations for both CartPole and Acrobot. Each worker had one Intel Xeon Gold 6242 CPU core at its disposal, resulting in an overall runtime of 6-7h on Acrobot and 5-6h on CartPole for 200 NES outer loop iterations. For reference, we note that (Salimans et al., 2017) used 80 workers each having access to 18 cores for solving the Humanoid task.

In Figure 6 it becomes evident that the proposed method with the given resources and used hyperparameters given by Table 3 allows identifying SEs that can teach agents to solve CartPole and Acrobot tasks respectively. Each thin line in the plot corresponds to the average of 16 worker evaluation scores given by *EvaluateAgent* in Algorithm 1 as a function of the NES outer loop iteration. We repeat this for 40 separate NES optimization runs and visualize the average across the thin lines as a thick line for each task. We note that we only show a random subset of the 40 thin lines for better visualization and randomly sample the seeds at all times in this work. We believe that the stochasticity introduced by this may lead to the variance visible in the plot when searching for good SEs.

Both the stochasticity of natural gradients and the sensitivity of RL agents to seeds and parameter initializations may additionally contribute to this effect. Notice, it is often sufficient to run approximately 50 NES outer loops to find SEs that solve a task. Besides early-stopping, other regularization techniques (e.g. regularizing the SE parameters) can be applied to address overfitting which we likely observe in the advanced training of the Acrobot task.

A.3 EVALUATION OF PERFORMANCE AND TRANSFERABILITY OF SEs ON THE ACROBOT TASK

Similar to Figure 3, we visualize the performance and transferability evaluation results of SEs for the Acrobot-v1 task. Again, the top row depicts the density functions of the average cumulative rewards collected by DDQN, Dueling DDQN and discrete TD3 agents based on 4k evaluations per density and DDQN-trained SEs. Like in the CartPole case, we show three different SE training settings: agents trained on real env. with varying agent HPs (blue), on DDQN-trained SEs when varying agent HPs during NES runs (orange), on DDQN-trained SEs where the agent HPs were fixed during training of the SEs (green). The bottom row visualizes the average reward, train steps, and episodes across the 4k evaluations and each bar correspond to one of the shown densities. We achieve on Dueling DDQN a $\sim 38\%$ (18376 vs. 29531 train steps) and on discrete TD3 a $\sim 82\%$ faster and more stable training compared to the baseline. However, we point out that many of the runs with discrete TD3 also fail (mean reward: -343). This is likely caused by the limited transferability already observed in the Cartpole case but may also due to sub-optimal hyperparameter selection since we reused the DDQN HPs found on Cartpole for Acrobot (as well as the HPs and ranges for

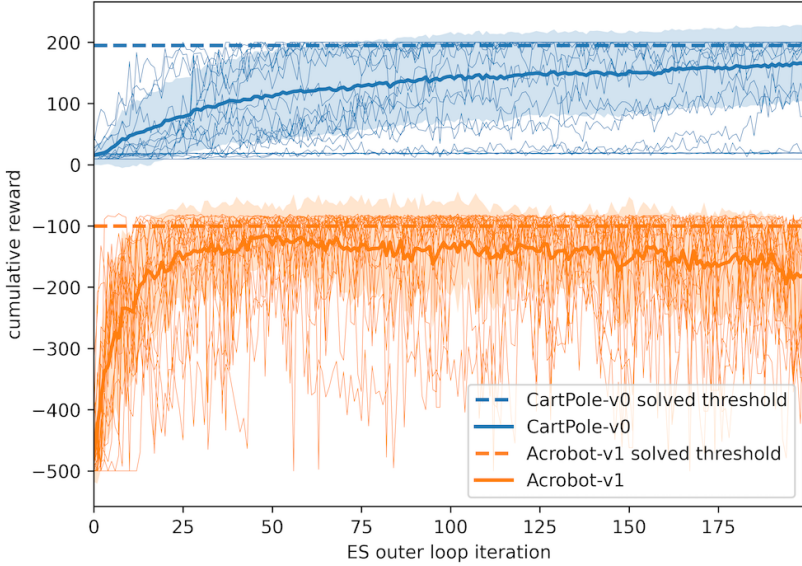


Figure 6: Results from 40 different NES runs with 16 workers each (using random seeds) show that our method is able to identify SEs that allow agents to solve the target tasks. Each thin line corresponds to the average of 16 worker evaluation scores returned by *EvaluateAgent* in our algorithm as a function of the NES outer loop iterations.

variation from Table 2). We further point out that training on SEs consistently yields a more stable training as can be seen in the standard deviations of the train steps and episodes bars.

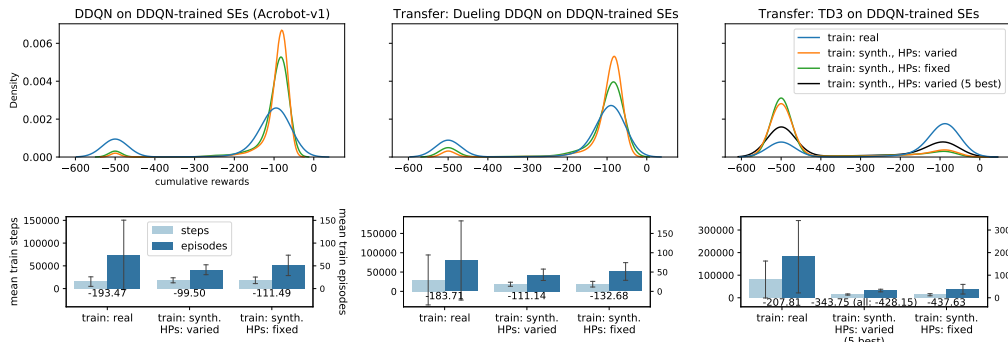


Figure 7: Evaluation of performance and transferability of SEs on the Acrobot-v1 task.

A.4 QUALITATIVE STUDY OF SYNTHETIC ENVIRONMENTS FOR THE CARTPOLE AND ACROBOT TASKS

To extend the qualitative analysis of SE behavior from Section 9, we depict in Figure 8 additional histograms for the approximate next state s' and reward r distributions produced by 10 agents with random seeds and default hyperparameters from Table 5 for each histogram plot. We here additionally show the behavior for Acrobot and also for Dueling DDQN and discrete TD3 agents. For the histograms with discrete TD3 we chose well-performing but arbitrary SE model according the individual model analysis, see Section F.1.1 and F.1.2. We chose a well-performing model in the case of discrete TD3 since we assumed that the significant number of failing runs would deteriorate the discrete TD3 performance and distort the comparison to the other (well-performing) DDQN and Dueling DDQN agents. For the DDQN and Dueling DDQN agents, we chose the SE model completely at random, independent of their performance. In summary, we see the same patterns that we

observed for CartPole and DDQN in Section 9 also with Dueling DDQN and discrete TD3 on both tasks: distribution shift, narrower synthetic distributions (and state-stabilizing or control behavior, meaning that the number of large positive and negative states are rarely encountered, for example, this can be seen in the cart velocity (CartPole) and the joint angular velocity (Acrobot) plots), and wider/dense reward distributions. The histograms in green show the SE responses when fed with real environment data based on the logged state-action the agents have seen during testing. Since the green distributions align better with the blue than the orange ones, we conclude it is more likely the shifts are generated by the SE than the agent. For CartPole we show all state dimensions and for Acrobot we show four of the six state dimensions due to brevity.

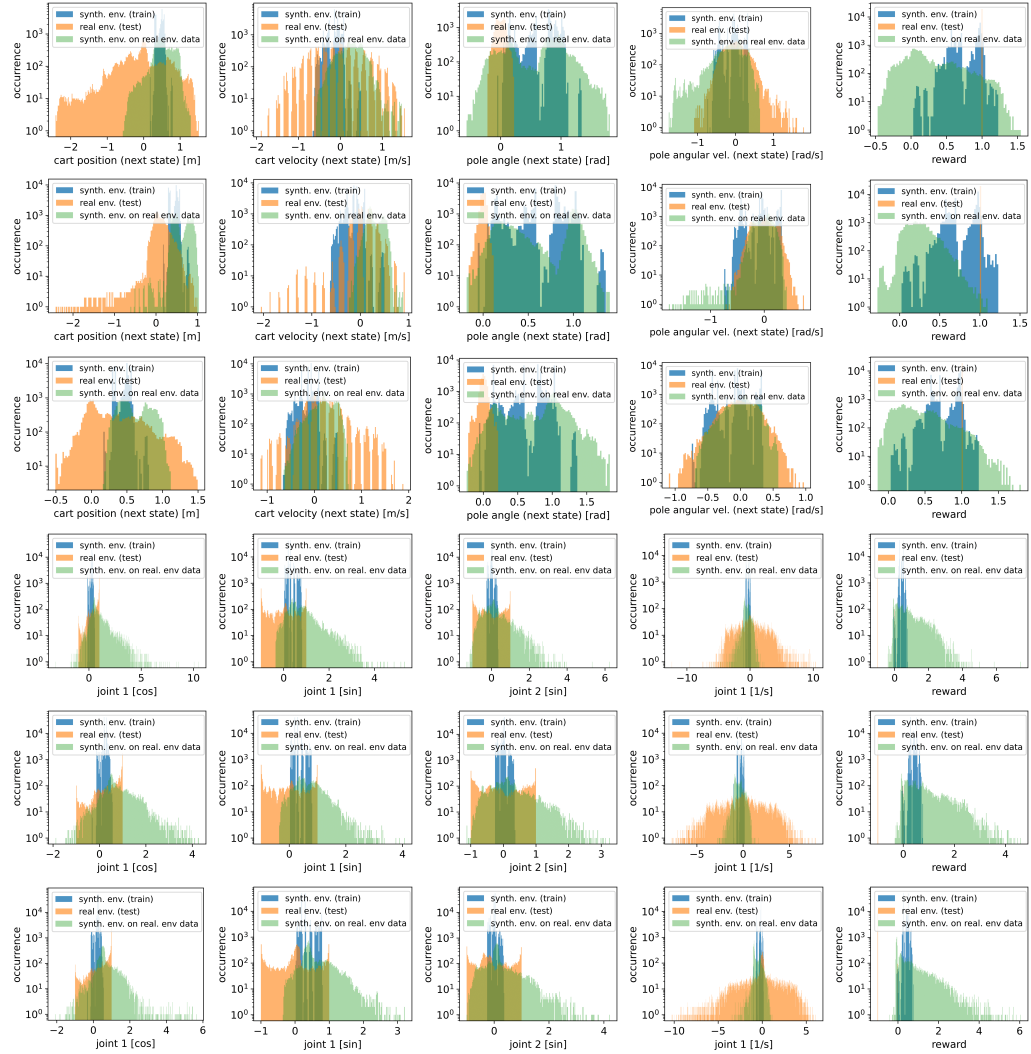


Figure 8: Histograms of approximate next state s' and reward r distributions produced by 10 DDQN or Dueling DDQN agents when trained on an SE (blue) and when afterwards tested for 10 episodes on a real environment (orange) for each task. **1st row:** CartPole and DDQN, **2nd row:** CartPole and Dueling DDQN, **3rd row:** CartPole and discrete TD3, **4th row:** Acrobot and DDQN, **5th row:** Acrobot and Dueling DDQN, **6th row:** Acrobot and discrete TD3

The average cumulative rewards across the 10 runs for each agent variant and task are:

- CartPole and DDQN (1st row): 199.3
- CartPole and Dueling DDQN (2nd row): 193.75
- CartPole and discrete TD3 (3rd row): 197.26

- Acrobot and DDQN (4th row): -91.62
- Acrobot and Dueling DDQN (5th row): -88.56
- Acrobot and discrete TD3 (6th row): -93.17

A.5 SYNTHETIC ENVIRONMENT HYPERPARAMETERS

The following table provides an overview of the agent and NES hyperparameter (HP) ranges that we optimized in an additional outer loop of our algorithm. The HPs in the 2nd and 3rd columns represent the results of this optimization and which we used for learning SEs. Note that in experiments where we sampled agent HPs from ranges given by Table 2 we overwrite a small subset (namely DDQN learning rate, batch size, DDQN no. of hidden layers, and DDQN hidden layer size) of the listed HPs below (runs denoted by "HPs: varied").

Table 3: Hyperparameter configuration spaces optimized for learning SEs.

Hyperparameter	CartPole-v0	Acrobot-v1	Optimization value range	log. scale
NES step size (α)	0.148	0.727	0.1 – 1	True
NES noise std. dev. (σ)	0.0124	0.0114	0.01 – 1	True
NES mirrored sampling	True	True	False/True	-
NES score transformation	All Better 2	All Better 2	see Appendix Section E.1	-
NES SE no. of hidden layers	1	1	1 – 2	False
NES SE hidden layer size	83	167	48 – 192	True
NES SE activation function	LReLU	PReLU	Tanh/ReLU/LReLU/PReLU	-
DDQN initial episodes	1	20	1 – 20	True
DDQN batch size	199	149	64 – 256	False
DDQN learning rate	0.000304	0.00222	0.0001 – 0.005	True
DDQN target net update rate	0.00848	0.0209	0.005 – 0.05	True
DDQN discount factor	0.988	0.991	0.9 – 0.999	True (inv.)
DDQN initial epsilon	0.809	0.904	0.8 – 1	True
DDQN minimal epsilon	0.0371	0.0471	0.005 – 0.05	True
DDQN epsilon decay factor	0.961	0.899	0.8 – 0.99	True (inv.)
DDQN no. of hidden layers	1	1	1 – 2	False
DDQN hidden layer size	57	112	48 – 192	True
DDQN activation function	Tanh	LReLU	Tanh/ReLU/LReLU/PReLU	-

The following table lists the hyperparameters that we always kept fixed and which were never optimized:

Table 4: Subset of the hyperparameter configuration spaces that we kept fixed (not optimized) for learning SEs.

Hyperparameter	Symbol	CartPole-v0	Acrobot-v1
NES number of outer loops	n_o	200	200
NES max. number of train episodes	n_e	1000	1000
NES number of test episodes	n_{te}	10	10
NES population size	n_p	16	16
DDQN replay buffer size	-	100000	100000
DDQN early out number	d	10	10
DDQN early out difference	C_{diff}	0.01	0.01
env. max. episode length	-	200	500
env. solved reward	-	195	-100

The table below lists the agent hyperparameters (HPs) that we chose as default. We used these HPs in all experiments after SEs were found, i.e. for evaluations in Figures 3, 4, and 7. Note that in some cases we sampled agent HPs from ranges given by Table 2. In these cases (runs denoted by "HPs: varied", "HPs: fixed", and also the individual SE models plots below) the HPs of the table are overwritten by the sampled ones.

Table 5: Default agent hyperparameters for the evaluations depicted in Figure 3, 4, and 7. *DDQN early out number* and *DDQN early out difference* are equivalent to Table 4.

Agent hyperparameter	Default value
initial episodes	10
batch size	128
learning rate (DDQN & D.DDQN / TD3)	0.001 / 0.0005
target network update rate	0.01
discount factor	0.99
epsilon decay factor	0.9
number of hidden layers	2
hidden layer size	128
activation function (DDQN & D. DDQN / TD3)	ReLU / Tanh
replay buffer size	100000
max. train episodes	1000
Gumbel Softmax start temperature / one-hot-encoded actions (TD3)	1 / False

APPENDIX B REWARD NETWORKS

B.1 HALFCHEETAH RNs PLOTS

For HalfCheetah, we see that *additive non-potential RN* (and also *exclusive non-potential RN*) trains well-performing agents the fastest but saturates at a cumulative reward of $\sim 3k$ which corresponds to the used solved reward threshold. This may be due to the used objective function since its term $\max(0, C_{sol} - C_{fin})$ does not incentivize RNs to improve after reaching the threshold.

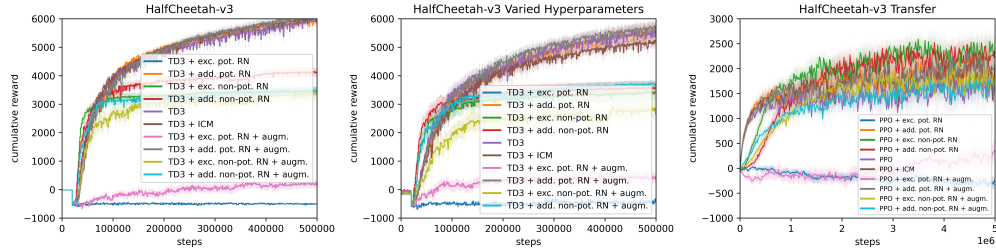


Figure 9: Performance of different RN variants for the HalfCheetah-v3 environment. Left: performance of RNs that train the known TD3 agent with default hyperparameters. Center: performance of RNs when the hyperparameters of known agents are varied. Right: Transfer performance to the unseen PPO agents with default hyperparameters. All curves denote the mean cumulative reward across 25 runs (5 agents \times 5 RNs). Shaded areas show the standard error of the mean and the flat curves in TD3 stem from a fixed number of episodes that are used to fill the replay buffer before training. Notice that using the observation vector v in the RN variants (denoted by “+augm.”) only marginally yields a higher train efficiency.

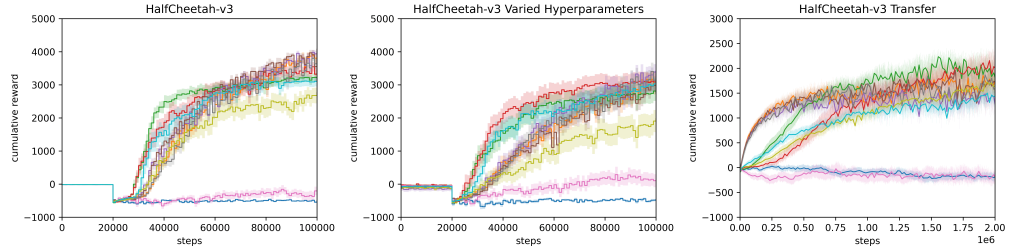


Figure 10: This is the zoomed in version of Figure 9.

B.2 QUALITATIVE STUDY OF REWARD NETWORKS ON THE CLIFF WALKING TASK

Like in Section A.4, we again make use of the small state and action space and analyze the learned augmented rewards of the proposed different RN variants across 50 generated RN models on our Cliff Walking environment (Sutton et al., 2020). Cliff Walking consists of a two-dimensional grid with 4×12 states in which the agent, starting at the start state (S), has to reach the goal state (G) by moving up, down, left, or right to adjacent states. 10 of the states in the lower row are cliffs. The agent receives a reward of -1 for every action it takes and a reward of -100 if it enters a cliff state. The episode terminates if the agent enters either the goal state or a cliff state. The environment is further bounded by walls, e.g. if the agent moves left when being in the state (S), it stays in the state (S).

In Figure 11 we depict a visual representation of the learned rewards for different RN variants averaged across 50 RN models taken from the RN experiment in Section 6 (i.e. trained with a Q-Learning agent with non-varying HPs, no early stopping criterion in the outer loop, 50 outer loop iterations). To do this, we color-coded the rewards we received from the RNs for all possible state-action pairs. To visualize the rewards corresponding to each of the four actions, every state is split up into four triangles corresponding to the different actions (move up, down, left, right) that the agent can perform when being in this state. We show small, average, and high rewards in red, yellow, and green, respectively. The left column of Figure 11 shows the grids with all rewards

where we can observe that the negative rewards of -100 of the additive RNs distort the color plot such that the fine-grained reward structure learned by the RNs becomes invisible. To address this, the right column features the same plots while ignoring any rewards ≤ -50 . This implies for the additive RN variants, that the rewards in the cliff states are ignored (white color) since the additive RN variants produce large negative rewards and lead to the described distortion of fine-grained rewards. For the goal state we further note that, although actions were never executed in this terminal state, the (neural network of the) RNs still compute rewards in this case which we did not ignore in the plot simply because it did not lead to distortions.

Matching the performances shown in Figure 5 (top row, left), the reward structure learned by the exclusive potential RN is sub-optimal as the high rewards are nearly randomly distributed. In contrast, the additive potential RNs clearly assign low rewards to any state-action pair that lets the agent enter a cliff state. The RNs further output a low reward for transitions that go from the third row up to the second row and a high reward for the contrarily directed transitions. This keeps the agents close to the cliff and reduces the exploration space which results in faster training. The exclusive non-potential RNs assign useful rewards around the start and goal states but fail to adequately shape the reward along the shortest path from the start to the goal state. Lastly, the additive non-potential RNs clearly assign high rewards that guide the agent along the shortest path towards the goal state while avoiding cliff states. As expected, the well-performing RN variants seem to learn informed reward representations of the task that guide the agent towards relevant states for completing the task like in the SE case.

B.3 REWARD NETWORK HYPERPARAMETERS

B.3.1 GENERAL NES AND ENVIRONMENT HYPERPARAMETERS

The below table lists all HPs for learning RNs that we kept fixed (not optimized) and which are identical across all RN experiments:

Table 6: Hyperparameters that we kept fixed (not optimized) for learning RNs.

Hyperparameter	Symbol	Value
NES number of outer loops	n_o	50
NES number of test episodes	n_{te}	1
NES population size	n_p	16
NES unsolved weight	w_{sol}	100

Below table lists all HPs for learning RNs that we optimized and which are identical across all experiments. The NES score transformations are described in detail in Appendix Section E.1 and we also report the results for the BOHB hyperparameter optimization of different score transformation variants in Appendix Section E.2.

Table 7: Hyperparameters that we optimized and which are identical across all RN experiments

Hyperparameter	Symbol	Optimized value
NES mirrored sampling	-	True
NES score transformation	-	All Better 2 (see Appendix Section E.1)
NES step size	α	0.5
NES noise std. dev.	σ_G	0.1

Below table lists the environment-specific HPs:

Table 8: Environment-specific hyperparameters

Hyperparameter	Cliff Walking	CartPole-v0	MountainCarContinuous-v0	HalfCheetah-v3
max. episode length	50	200	999	1000
solved reward	-20	195	90	3000
NES max. number of train episodes	100	100	100 (TD3) 1000 (PPO)	100 (TD3) 1000 (PPO)

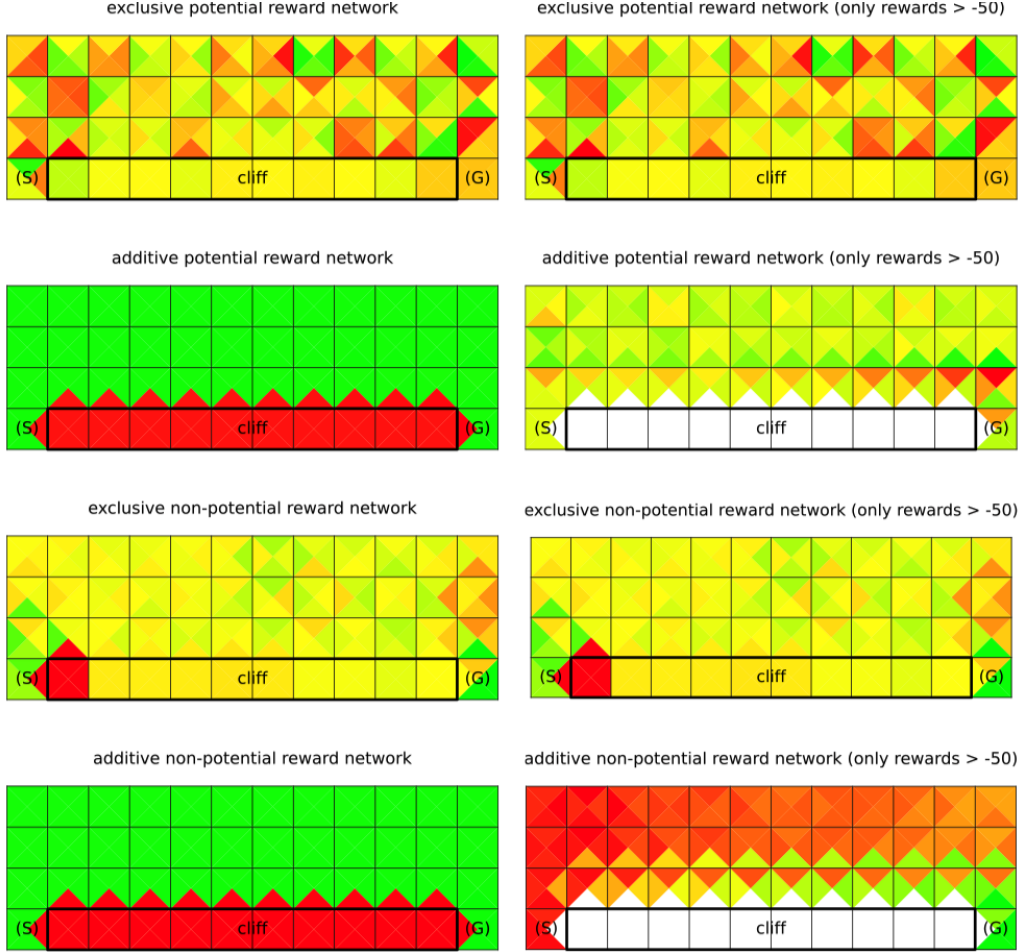


Figure 11: Learned Cliff Walking reward for different reward network types. Shown is the start state (S), goal state (G), all cliff states in the lower row and the learned reward of each state-action pair (red: low reward, yellow: medium reward, green: high reward). The plots on the left side show averaged values across 50 reward networks when considering all rewards, the plots on the right side ignore all rewards that are ≤ -50 . Values have been normalized to be in a [0,1] range in both cases (left with full reward range, right without ignored rewards range).

B.3.2 VARIED AGENT HYPERPARAMETERS

The following tables list the for Q-Learning, DDQN and TD3 agent hyperparameter ranges from which we sampled in the HP variation experiment.

Table 9: Hyperparameter sampling ranges for the reward networks HP variation experiment

QL hyperparameter	Value Range	log. scale
learning rate	0.1 - 1	False
discount factor	0.1 - 1	False

DDQN hyperparameter	Value range	log. scale
learning rate	$8.3 \cdot 10^{-5} - 7.5 \cdot 10^{-4}$	True
batch size	11 - 96	True
hidden size	21 - 192	True
hidden layer	1 - 2	False

TD3 hyperparameter	Value range	log. scale
learning rate	$10^{-4} - 9 \cdot 10^{-4}$	True
batch size	85 - 768	True
hidden size	42 - 384	True
hidden layer	1 - 3	False

B.3.3 AGENT AND NES HYPERPARAMETERS FOR CLIFF WALKING

In Table 10 we list the NES and Q-Learning hyperparameter configuration spaces that we optimized for learning RNs on Cliff Walking. In Table 11 we list the default Q-Learning and SARSA (transfer) hyperparameters that we used once RNs have been learned. In Table 12 we list the hyperparameter configuration spaces that we used (and optimized over) for the count-based Q-Learning baseline.

Table 10: Hyperparameter configuration spaces optimized for learning RNs on Cliff Walking.

Hyperparameter	Optimized value	Value range	log. scale
NES RN number of hidden layers	1	1 – 2	False
NES RN hidden layer size	32	32 – 192	True
NES RN activation function	PReLU	Tanh/ReLU/LReLU/PRelu	-
Q-Learning learning rate	1	0.001 – 1	True
Q-Learning discount factor	0.8	0.001 – 1	True (inv.)
Q-Learning initial epsilon	0.01	0.01 – 1	True
Q-Learning minimal epsilon	0.01	0.01 – 1	True
Q-Learning epsilon decay factor	0.0	0.001 – 1	True (inv.)

Table 11: Default Q-Learning and SARSA hyperparameters that we used after learning RNs.

Hyperparameter	Default value
Q-Learning & SARSA learning rate	1
Q-Learning & SARSA discount factor	0.8
Q-Learning & SARSA initial epsilon	0.1
Q-Learning & SARSA minimal epsilon	0.1
Q-Learning & SARSA epsilon decay factor	0.0

Table 12: Used baseline hyperparameter configuration spaces

Hyperparameter	Optimized value	Value range	log. scale
Count-based Q-Learning β	0.1	0.0001 – 2	False

B.3.4 AGENT AND NES HYPERPARAMETERS FOR CARTPOLE-V0

In Table 13 we list the NES and DDQN hyperparameter configuration spaces that we optimized for learning RNs on CartPole. We do not list the optimization value range in this table since they are equivalent as in the learning SE case described in Table 3. In Table 14 we list the default DDQN and Dueling DDQN (transfer) hyperparameters that we used once RNs have been learned. In Table 13 we list the hyperparameter configuration spaces that we used (and optimized over) for the ICM baseline (Pathak et al., 2017). We note that, despite optimizing the ICM HPs, we did not find that the optimized ICM HPs yielded better results than the default ones which is why we use the default ICM HPs in all experiments that involve ICM.

Table 13: Optimized hyperparameters for learning RNs on CartPole. The value ranges are the same as in Table 3. Hyperparameters not listed were not optimized.

Hyperparameter	Optimized value
NES RN number of hidden layers	1
NES RN hidden layer size	64
NES RN activation function	PReLU
DDQN initial episodes	1
DDQN batch size	192
DDQN learning rate	0.003
DDQN target network update rate	0.01
DDQN discount factor	0.99
DDQN initial epsilon	0.8
DDQN minimal epsilon	0.03
DDQN epsilon decay factor	0.95
DDQN number of hidden layers	1
DDQN hidden layer size	64
DDQN activation function	LReLU
DDQN replay buffer size	1000000

Table 14: Default DDQN and Dueling DDQN hyperparameters that we used after learning RNs.

Hyperparameter	Default value
DDQN & Dueling DDQN initial episodes	1
DDQN & Dueling DDQN batch size	32
DDQN & Dueling DDQN learning rate	0.00025
DDQN & Dueling DDQN target network update rate	0.01
DDQN & Dueling DDQN discount factor	0.99
DDQN & Dueling DDQN initial epsilon	1.0
DDQN & Dueling DDQN minimal epsilon	0.1
DDQN & Dueling DDQN epsilon decay factor	0.9
DDQN & Dueling DDQN number of hidden layers	1
DDQN & Dueling DDQN hidden layer size	64
DDQN & Dueling DDQN activation function	ReLU
DDQN & Dueling DDQN replay buffer size	1000000
Dueling DDQN feature dimension	128
Dueling DDQN value and adv. stream no. hidden layers	1
Dueling DDQN value and adv. stream hidden layer size	128

B.3.5 AGENT AND NES HYPERPARAMETERS FOR MOUNTAINCARCONTINUOUS-V0 AND HALFCHEETAH-V3

In Table 16 we list the NES and TD3 hyperparameter configuration spaces that we optimized for learning RNs on MountainCarContinuous (CMC) and HalfCheetah (HC). In Table 17 we list the default TD3 hyperparameters that we used once RNs have been learned. Table 18 shows the PPO agent hyperparameters we used for showing transfer of RNs to train PPO agents. In Table 19 we list the hyperparameter configuration spaces that we used (and optimized over) for the ICM baseline (Pathak et al., 2017). We note that, despite optimizing the ICM HPs, we did not find that the optimized ICM HPs yielded better results than the default ones which is why we use the default ICM HPs in all experiments that involve ICM.

Table 15: Used ICM (Pathak et al., 2017) baseline hyperparameter configuration spaces optimized with CartPole and DDQN. We additionally report the default values taken from the ICM reference implementation.

Hyperparameter	Default value	Optimized value	Value range	log. scale
ICM learning rate	0.0001	0.00001	0.00001 – 0.001	True
ICM β	0.2	0.05	0.001 – 1	True
ICM η	0.5	0.03	0.001 – 1	True
ICM feature dimension	64	32	16-256	True
ICM hidden layer size (forward, feature and inverse model)	128	128	16-256	True
ICM number of hidden layers (forward, feature and inverse model)	2	-	not optimized	-
ICM activation function	LReLU	-	not optimized	-
ICM number of residual blocks	4	-	not optimized	-

Table 16: Optimized hyperparameters for learning RNs on MountainCarContinuous-v0 (short "CMC") and HalfCheetah-v3 (short "HC"). Hyperparameters not listed were not optimized.

Hyperparameter	Optimized value	Value range	log. scale
NES RN number of hidden layers	1	1-2	False
NES RN hidden layer size	128	48-192	True
NES RN activation function	PReLU	Tanh/ReLU/LReLU/PReLU	-
TD3 initial episodes (CMC/HC)	50 / 20	1-50	True
TD3 batch size	192	64 - 256	False
TD3 learning rate	0.003	0.0001 - 0.005	True
TD3 target network update rate	0.01	0.005 - 0.05	True
TD3 discount factor (CMC/HC)	0.99 / 0.98	0.9 - 0.99	True
TD3 policy update delay factor	1	1-3	False
TD3 number of action repeats (CMC/HC)	2 / 1	1-3	False
TD3 action noise std. dev.	0.05	0.05 - 0.2	True
TD3 policy noise std. dev.	0.2	0.1 - 0.4	True
TD3 policy noise std. dev. clipping	0.5	0.25 - 1	True
TD3 number of hidden layers	2	1-2	False
TD3 hidden layer size	128	48 - 192	True
TD3 activation function (CMC/HC)	LReLU / ReLU	Tanh/ReLU/LReLU/PReLU	-
TD3 replay buffer size	100000	not optimized	-

Table 17: Default TD3 hyperparameters that we used after learning RNs on MountainCarContinuous-v0 (short "CMC") and HalfCheetah-v3 (short "HC").

Hyperparameter	Default value
TD3 initial episodes (CMC/HC)	50 / 20
TD3 batch size	256
TD3 learning rate	0.0003
TD3 target network update rate	0.005
TD3 discount factor	0.99
TD3 policy update delay factor	2
TD3 number of action repeats (CMC/HC)	2 / 1
TD3 action noise std. dev.	0.1
TD3 policy noise std. dev.	0.2
TD3 policy noise std. dev. clipping	0.5
TD3 number of hidden layers	2
TD3 hidden layer size	128
TD3 activation function	ReLU
TD3 replay buffer size	100000

Table 18: PPO (clip) hyperparameters that we used for showing the transfer of RNs on MountainCarContinuous-v0 (short "CMC") and HalfCheetah-v3 (short "HC").

Hyperparameter	Default value
PPO epochs (CMC/HC)	80 / 10
PPO learning rate	0.0003 / 0.00001
PPO number of episode updates (CMC/HC)	10 / 1
PPO discount factor	0.99
PPO policy update delay factor	2
PPO number of action repeats (CMC/HC)	5 / 1
PPO value function coefficient	1
PPO entropy coefficient (CMC/HC)	0.01 / 0.001
PPO clip ratio	0.2
PPO number of hidden layers	2
PPO hidden layer size (CMC/HC)	64 / 128
PPO activation function (CMC/HC)	ReLU / tanh

Table 19: Used ICM (Pathak et al., 2017) baseline hyperparameter configuration spaces optimized on MountainCarContinuous-v0 (short "CMC") and HalfCheetah-v3 (short "HC") with TD3. We additionally report the default values taken from the ICM reference implementation.

Hyperparameter	Default value	Optimized value	Value range	log scale
ICM learning rate (CMC/HC)	0.0001	0.0005 / 0.00001	0.00001 – 0.001	True
ICM β (CMC/HC)	0.2	0.1 / 0.001	0.001 – 1	True
ICM η (CMC/HC)	0.5	0.01 / 0.1	0.001 – 1	True
ICM feature dimension	64	32	16-256	True
ICM hidden layer size (forward, feature and inverse model)	128	128	16-256	True
ICM number of hidden layers (forward, feature and inverse model)	2	-	not optimized	-
ICM activation function	LReLU	-	not optimized	-
ICM number of residual blocks	4	-	not optimized	-

B.4 STUDYING THE INFLUENCE OF DIFFERENT REWARD NETWORK OPTIMIZATION OBJECTIVES

After we noticed the efficiency improvements of SEs, we tested whether RNs could also yield such improvements by directly optimizing for efficiency. Another reason for optimizing for efficiency directly was that the real environment is involved in the RN case and we pursued the goal to reduce real environment interactions. Based on this, we developed the RN objective reported in the paper in Section 4 which we refer to as the *Reward Threshold* objective. However, to analyse whether different objectives would yield similar results, we conducted a small study on the environments to assess the influence of different objectives.

For this, we considered the area-under-the-curve of the cumulative returns objective (*AUC*) as well as the cumulative reward maximization objective (*max reward*) which is the reward threshold objective with just the C_{fin} term.

The overall conclusion from these results is that an AUC objective generally yields similar results as for the reward threshold objective, but in some cases it seems to minorly reduce the efficiency. However, the overall significant efficiency gains remain. Moreover, in contrast to SEs, efficiency improvements in the RN case seem to arise more often when explicitly optimized for it (compare AUC vs. reward threshold below) while maximizing reward (only tested for CartPole and Cliff environments) leads to efficiency improvements only in the CartPole but not in the Cliff environment.

B.4.1 CLIFF

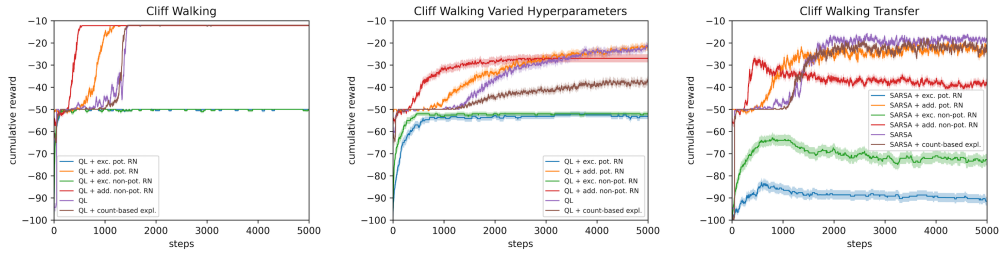


Figure 12: The Cliff environment RNs optimized with the AUC objective.

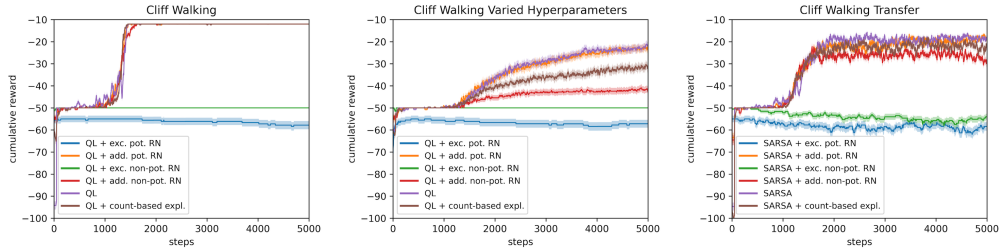


Figure 13: The Cliff environment RNs optimized with the max reward objective.

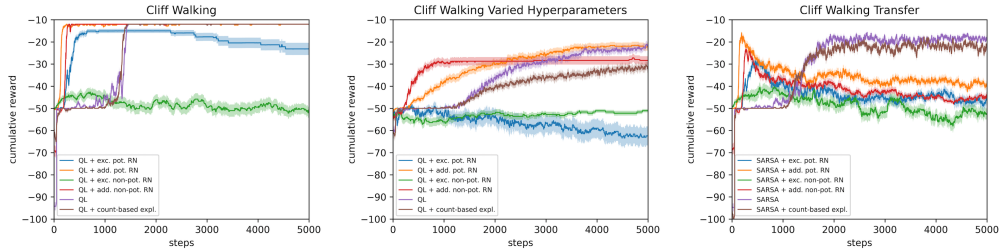


Figure 14: The Cliff environment RNs optimized with the reward threshold objective (similar to the results reported in Section 6).

B.4.2 CARTPOLE

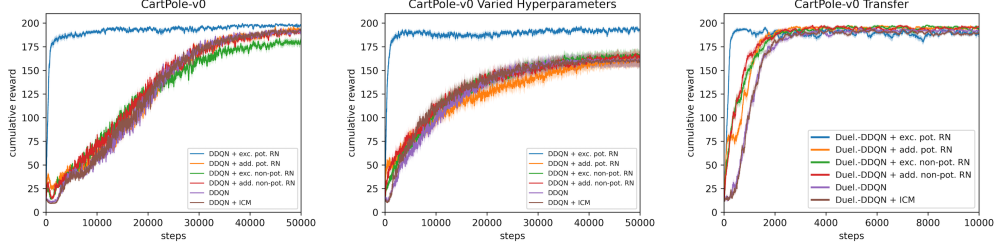


Figure 15: The CartPole environment RNs optimized with the AUC objective.

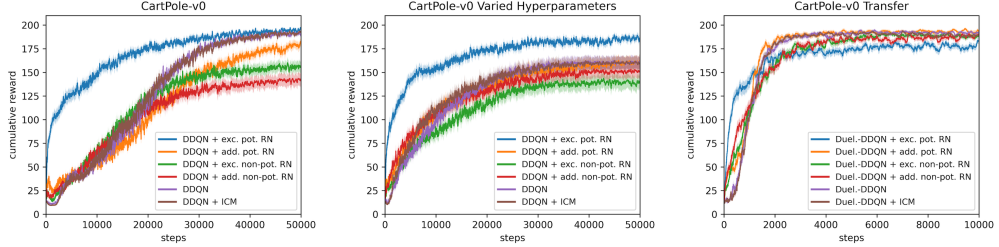


Figure 16: The CartPole environment RNs optimized with the max reward objective.

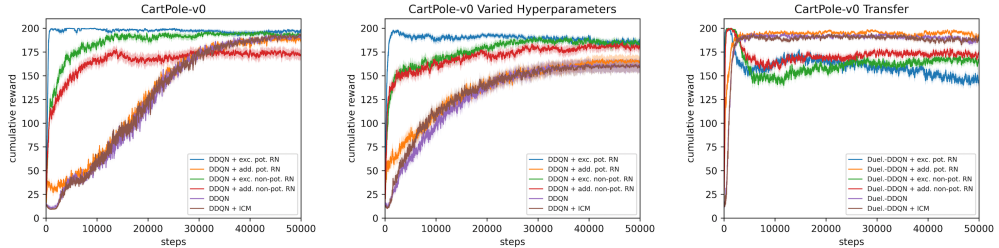


Figure 17: The CartPole environment RNs optimized with the reward threshold objective (similar to the results reported in Section 6).

B.4.3 MOUNTAINCARCONTINUOUS

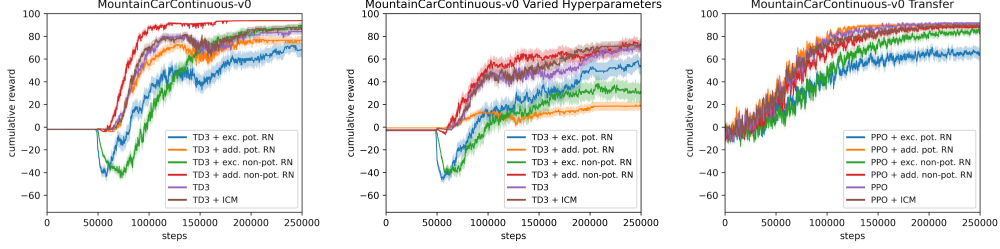


Figure 18: The MountainCarContinuous environment RNs optimized with the AUC objective.

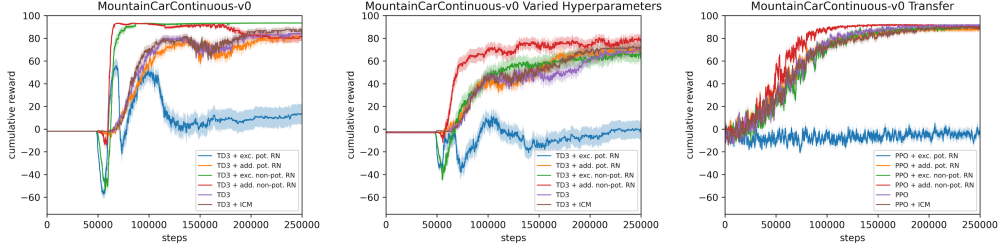


Figure 19: The MountainCarContinuous environment RNs optimized with the reward threshold objective (similar to the results reported in Section 6).

B.5 HALFCHEETAH

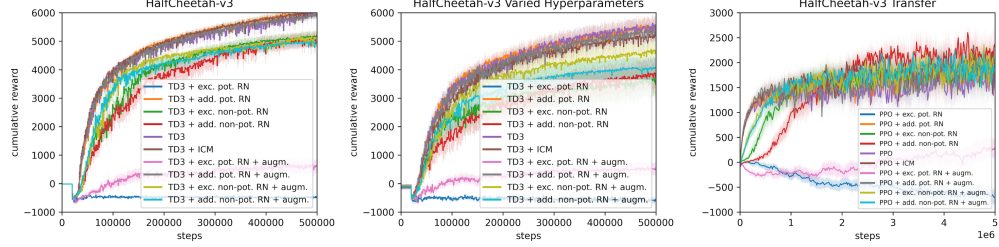


Figure 20: The HalfCheetah environment RNs optimized with the AUC objective.

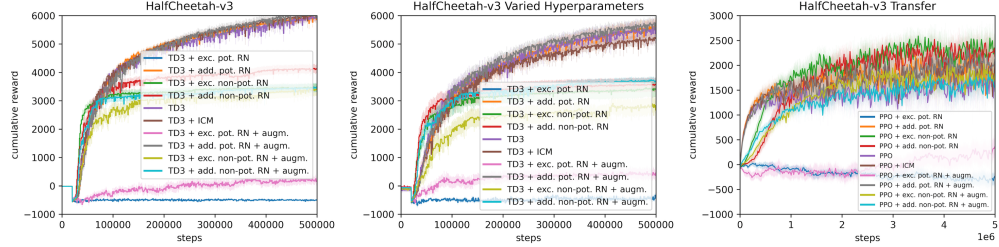


Figure 21: The HalfCheetah environment RNs optimized with the reward threshold objective (similar to the results reported in Appendix Section B.1).

APPENDIX C COMPUTATIONAL COMPLEXITY FOR TRAINING SYNTHETIC ENVIRONMENTS AND REWARD NETWORKS

Training both SEs and RNs can be computationally demanding, depending on the environment complexity and the available resources per worker. Table 20 lists approximate timings for a single NES outer loop iteration based on our log files. Every population member had one Intel Xeon Gold 6242 CPU core at its disposal.

Table 20: Approximate timings for one NES outer loop for SEs and RNs

Environment	Synthetic Environment	Reward Network
Cliff Walking	-	10s
Acrobot-v1	100s	-
CartPole-v0	100s	100s
MountainCarContinuous-v0	-	500s
HalfCheetah-v3	-	2000s

Given 200 NES outer loop iterations in the SE case and 50 steps in the RN case, these timings result in the following overall runtime for finding one SE or RN, respectively:

SEs:

- Acrobot: \sim 6-7 hours
- CartPole: \sim 5-6 hours

RNs:

- Cliff Walking: \sim 8 minutes
- CartPole: \sim 7 hours
- MountainCarContinuous: \sim 7 hours
- HalfCheetah: \sim 28 hours

We note that the required time can vary by more than a magnitude, depending on how quickly the RL agent can solve the environment in the inner loop.

APPENDIX D SUPERVISED LEARNING AND SYNTHETIC ENVIRONMENTS

One might ask how our proposed way of learning synthetic environments relates and compares to purely learning a synthetic environment model through a supervised learning (or model-based RL (MBRL)) objective. In this Section, we discuss the differences from our view point and show results of a small experiment that aimed at giving some answers to this question.

D.1 CONTRASTING BOTH APPROACHES

First, our interpretation can be summarized with the following table:

We now elaborate in more detail what we believe are the core differences between both concepts and their resulting effects.

In the case of the supervised learning of the model as a jointly learned mapping from (state, action) pairs to the next state and the reward, we are limited by the human prior in regards to what is beneficial and informative to achieve a certain given task. This prior typically is encoded in the reward. Whereas the states of a problem almost always arise from a physical (e.g. Cartpole) or a logical/rule based (e.g. board games) foundation, the reward is to a much higher degree based on a human perspective. This limits the supervised approach to almost only a replication of the problem designer’s choices. Now, it might be argued that therefore it is a pure approach for modeling a world or an environment, but by shifting the perspective towards the artificial nature of a reward signal,

Table 21: Comparing attributes between supervised learning and SE learning.

	Synthetic Environments	Supervised Learning
Learning Objective	Mapping $(S, A) \rightarrow (S, R_{defined})$	Mapping $(S, A) \rightarrow (S, R_{beneficial})$
Signal of Information	Error in mapping like MSE, MLE	Performance of agent on given real environment
Learned Function	mapping defined by environment; quality in terms of closeness	A functional mapping of same input-output dimensionality as in the supervised case but defined to increase agents performance; Quality is in terms of reward on a given real environment
Potential	Imitate/replicate the given environment	Can imitate state transitions but is not restricted to this and can learn a very different environment that nevertheless helps to quickly train agents to do well on the real environment

the choice of reward might as well be a source of misguidance or at least a potential hindrance to learning in a effective / efficient, and more unbiased fashion.

We believe that our approach reduces the potential shortcomings of human bias and choice of design to some degree by taking a more “task-aware” perspective. In our approach, the feedback signal for the model training comes from the given environment (similar to supervised model learning), but does not constrict the model to explicitly learn an approximate duplicate mapping. Rather, by using the performance of the agent as the only information, the model gains the ability to construct a mapping of states actions to the next states and a reward signal of which the sole purpose is to improve the future performance of the agent (task-awareness). With this, we allow the model to converge to a different kind of distribution (mapping) and potentially one that might squeeze or extend either or both state and rewards. This could be seen as a compression of information on the one hand and (by having a larger space) also as storing and extending additional information explicitly. Of course, our approach is not completely unbiased by the choice of reward because here as well the human-designed reward influences the performance signal on which the model is trained.

D.2 COMPARING SUPERVISED LEARNING WITH SYNTHETIC ENVIRONMENTS ON CARTPOLE

We have conducted an experiment on the CartPole environment to compare SEs to models trained purely with supervised learning. Before we show results, we will explain our setup:

Setup: To train such a supervised learning model and also to maintain comparability to SEs, we used the data coming from SE runs (i.e. executing Alg. 1). More precisely, we recorded all the real environment data from each outer loop step on which agents are evaluated (10 test episodes), across 5 populations with each 16 workers/agents over 25-50 outer loop steps. The (s, a, s', r) tuples coming from each population run were used to fit a supervised model, yielding in total 5 models. We note that the amount of data that each supervised model has been trained with corresponds to the same amount that we would use to learn an SE. The models have the identical architecture as the SEs and we used an MSE loss to optimize the error between predicted (s', r) and ground truth (s', r) pairs given (s, a) as input. We trained the models for 100 epochs with Adam and a batch size of 1024, finally yielding an average error of 5e-07.

After fitting the supervised baseline models, we executed the same train and evaluation pipeline for SEs that we describe in Section 5. First, we trained agents with randomly sampled hyperparameters on the supervised model. Second, we evaluated them on the real environment and used the resulting rewards to fit the density plot curves. We hereby ensured the same number of reward data points (4000) as for the curves given in the paper by sampling more agent configurations. To also show transfer performance of the supervised baseline models, we executed the same procedure for unseen agents (Dueling DDQN & discrete TD3).

Result: In Figure 22 we can observe that the supervised baseline underperforms the other models significantly in terms of the reward distribution and the average cumulative reward (15.01 vs. 190.7 for SEs). In terms of training efficiency we can see a low number of steps and episodes but this

stems from inferior policies that cause an early termination. We also ran an experiment where we only considered two of the “best” models which we depict in Figure 23. Hereby “best” means that the majority of samples in the dataset come from high-quality trajectories achieving rewards ≥ 190 (i.e. which effectively solve the environment). However, in this case, we can only observe a slight increase in performance compared to using all five models (15.01 vs 17.73 average cumulative reward).

The reasons for underperformance can be manifold and their analysis were not part of this experiment. Potential explanations for this are (but are not limited to):

- The supervised baseline models may be subject to overfitting, resulting in inaccurate dynamics models and rendering policy learning a difficult task (it also may increase agent hyperparameter sensitivity).
- Catastrophic forgetting / sensitivity to the order of seen trajectories during baseline training may not allow to recover accurate dynamics at, for example, early stages of policy learning.
- The supervised baseline models may entail other sources of inaccuracies, for example, smoothness or noise, resulting in an inferior approximation of the real environment that may also hinder policy learning.
- In the case of SEs, the task-aware meta-loss (and the meta-learning itself) may be a good regularizer for preventing the above failure cases.

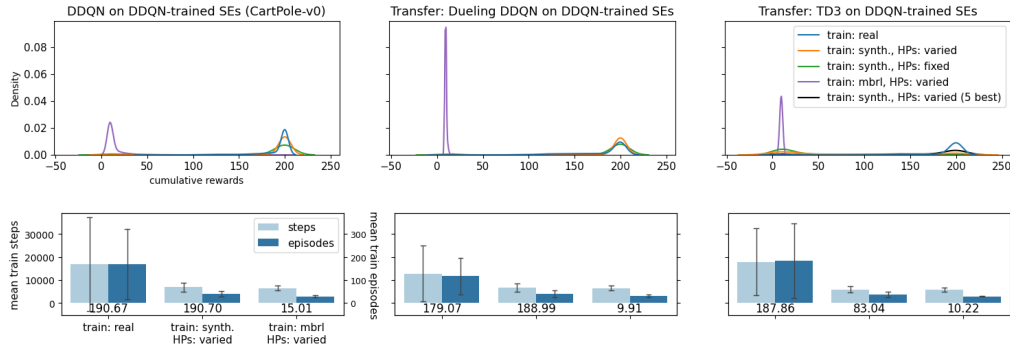


Figure 22: **Top:** Comparing the cumulative test reward densities of agents trained on SEs (green and orange), supervised baseline (purple), and baseline on real environment (blue). Agents trained on the supervised model underperform the SE models and the real baseline. **Bottom:** Comparing the needed number of test steps and test episodes to achieve above cumulative rewards. Left: real baseline, center: SEs, right: supervised (MBRL) baseline.

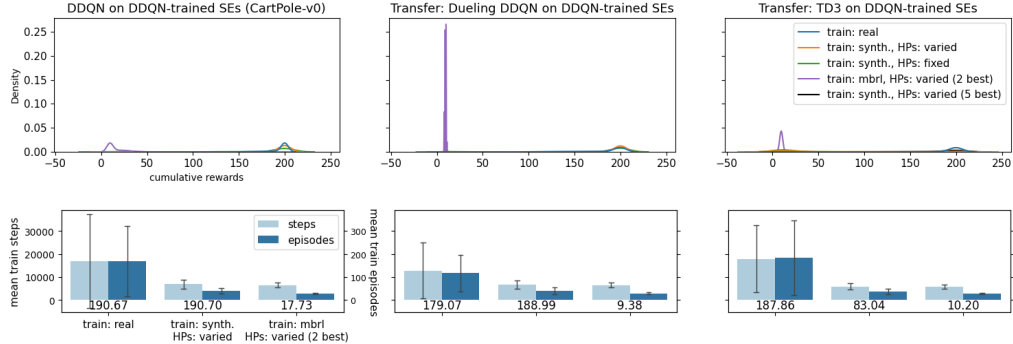


Figure 23: **Top:** Comparing the cumulative test reward densities of agents trained on SEs (green and orange), supervised baseline (purple), and baseline on real environment (blue). Agents trained on the supervised model underperform the SE models and the real baseline and using only the best two supervised models (purple) does not seem to change this. **Bottom:** Comparing the needed number of test steps and test episodes to achieve above cumulative rewards only using the best two of the five models. Left: real baseline, center: SEs, right: supervised (MBRL) baseline

APPENDIX E NES SCORE TRANSFORMATION

E.1 SCORE TRANSFORMATION VARIANTS

The following overview lists eight score transformations for calculating F_i based on the expected cumulative reward (ECR) K_i or the associated rank R_i . These score transformations were also used in the hyperparameter optimization configuration space for finding SEs and RNs (e.g., in Tables 3 and 7). The rank R_i is defined as the number of population members that have a lower ECR than the i -th member, i.e. the rank associated with the lowest ECR is 0, the one with the highest ECR $n_p - 1$ (the population size minus 1). We denote the ECR associated with the current SE or RN incumbent as K_ψ .

- **Linear Transformation:** The linear transformation maps all fitness values to the $[0; 1]$ range as

$$F_i = \frac{K_i - \min_i(K_i)}{\max_i(K_i) - \min_i(K_i)}, \quad (2)$$

with $\min_i(K_i)$ as the lowest of all ECRs and $\max_i(K_i)$ as the highest of all ECRs.

- **Rank Transformation:** For the rank transform the individual rewards are first ranked with respect to each other, resulting in R_i . The ranks are then linearly mapped to the $[0; 1]$ range as

$$F_i = \frac{R_i - \min_i(R_i)}{\max_i(R_i) - \min_i(R_i)}, \quad (3)$$

with $\min_i(R_i)$ as the lowest rank and $\max_i(R_i)$ as the highest rank.

- **NES:** Originally published in (Wierstra et al., 2008) and hence named after the paper “Natural Evolution Strategies” (NES), this method first transforms the rewards to their ranks R_i in a similar manner as the rank transformation. In the next step, the fitness values are calculated from the individual ranks as

$$\hat{F}_i = \frac{\max(0, \log(\frac{n_p}{2} + 1) - \log(R_i))}{\sum_{j=1}^{n_p} \max(0, \log(\frac{n_p}{2} + 1) - \log(R_j))} - \frac{1}{n_p}, \quad (4)$$

$$F_i = \frac{\hat{F}_i}{\max_i(|\hat{F}_i|)}, \quad (5)$$

with n_p as the size of the population. Whereas Eq. (4) constitutes the essential transformation, Eq. (5) acts solely as a scaling to the range $[x; 1]_{x < 0}$ and is used for convenience. The NES transformation also allows negative fitness values F_i through the $-\frac{1}{n_p}$ term in Eq. (4).

- **NES unnormalized:** We also consider an unnormalized NES score transformation variant. Eq. (4) and Eq. (5) here become

$$\hat{F}_i = \frac{\max(0, \log(\frac{n_p}{2} + 1) - \log(R_i))}{\sum_{j=1}^{n_p} \max(0, \log(\frac{n_p}{2} + 1) - \log(R_j))}, \quad (6)$$

$$F_i = \frac{\hat{F}_i}{\max_i(|\hat{F}_i|)}. \quad (7)$$

Although not directly visible from the equations above, the worse half of all fitness values becomes 0.

- **Single Best:** We can induce a strong bias towards the best performing population member by only assigning a nonzero weight to the incumbent of the current ES iteration. The corresponding transformation scheme can be expressed by

$$F_i = \begin{cases} 1 & \text{if } R_i = \max_i(R_i), \\ 0 & \text{else,} \end{cases} \quad (8)$$

with $\max_i(R_i)$ as the best rank.

- **Single Better:** It might be advantageous to update the SE and RN parameters only if their performance is supposed to improve. By calculating the ECR K_ψ associated with the parameters, the adapted “single best” transformation becomes

$$F_i = \begin{cases} 1 & \text{if } K_i > K_\psi \text{ and } K_i = \max_i(K_i), \\ 0 & \text{else.} \end{cases} \quad (9)$$

- **All Better 1:** The “single best” transformation relies at most on a single population member to update the SE or RN parameters in each ES iteration. A more regularized version considers all population members whose ECR K_i is better than the ECR K_ψ of the current SE or RN parameters. In a more mathematical notation, this can be expressed as

$$\hat{F}_i = \begin{cases} \frac{K_i - K_\psi}{\max_i(K_i) - K_\psi} & \text{if } K_i > K_\psi, \\ 0 & \text{else,} \end{cases} \quad (10)$$

$$F_i = \frac{\hat{F}_i}{\max_i \hat{F}_i}, \quad (11)$$

with K_ψ being evaluated similarly as the individual ECRs K_i .

- **All Better 2:** This transformation is almost identical to the “all better 1” transformation, except that we divide by the sum of all \hat{F}_i values when calculating the F_i values and not by the maximum \hat{F}_i value:

$$\hat{F}_i = \begin{cases} \frac{K_i - K_\psi}{\max_i(K_i) - K_\psi} & \text{if } K_i > K_\psi, \\ 0 & \text{else,} \end{cases} \quad (12)$$

$$F_i = \frac{\hat{F}_i}{\sum_i \hat{F}_i}, \quad (13)$$

E.2 EVALUATION OF SCORE TRANSFORMATION VARIANTS

Below we visualize the BOHB hyperparameter optimization results of different score transformation variants for SEs and plot these as a function of the NES step size with (left) and without (right)

mirrored sampling. The colors indicate the number of outer loop iterations of Algorithm 1 required to solve the target task (here: 2x2 grid world environment). Green signifies 0, yellow 25, and red 50 outer loop iterations. Each of the roughly 3500 dots corresponds to a single evaluation. We can observe multiple things:

- none of the rank transformations fails completely for the given simple environment
- mirrored sampling is only marginally better (if at all) while doubling the computational load (at least in this simple 2x2 grid world environment)
- noise: good performing samples in regions with bad performing samples and vice versa
- the "all better " score transformation seems to perform best

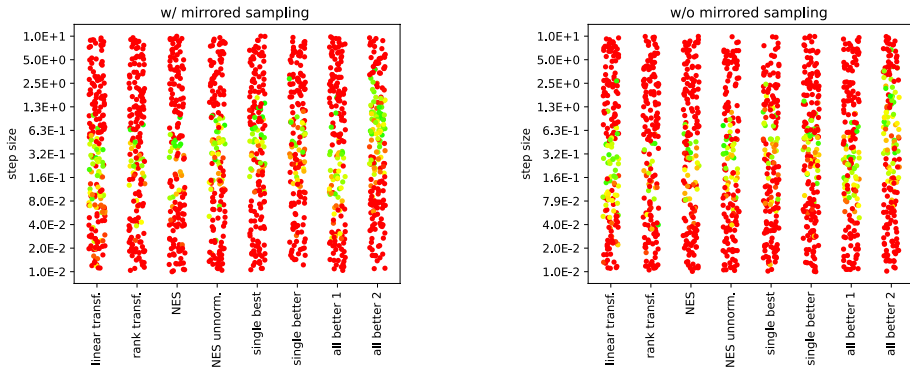


Figure 24: Evaluation of different score transformation schemes for synthetic environments: Shown is the required number of NES outer loop iterations (green: 0, yellow: 25, red: 50) for different hyperparameter configurations until an SE is found that solves the real environment (here: a 2x2 grid world environment).

APPENDIX F ADDITIONAL PLOTS

F.1 SYNTHETIC ENVIRONMENTS

F.1.1 EVALUATION OF INDIVIDUAL SE MODELS (CARTPOLE)

Below we show the individual or model-based violin plots for the 40 SE models which we calculated based on the cumulative rewards of 1000 randomly sampled agents that were each evaluated across 10 test episodes. For agent sampling we again chose the hyperparameters ranges denoted in Table 2. As the best five models for discrete TD3 (Figure 3) we chose the models `CartPole-v0_25_4I271D`, `CartPole-v0_22_CW9CSH`, `CartPole-v0_21_DRWNIK`, `CartPole-v0_8_QGN9IF`, and `CartPole-v0_17_WPWK3R`.

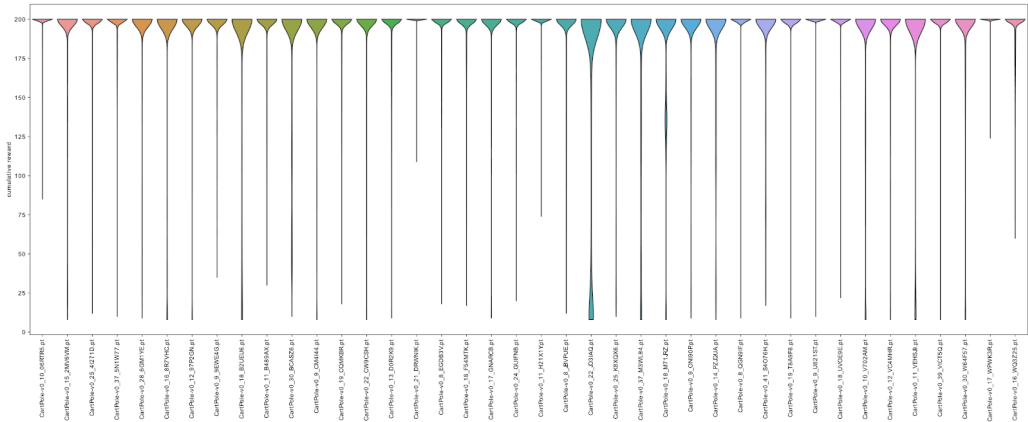


Figure 25: Model-wise evaluation: 1000 randomly sampled **DDQN** agents à 10 test episodes per SE model.

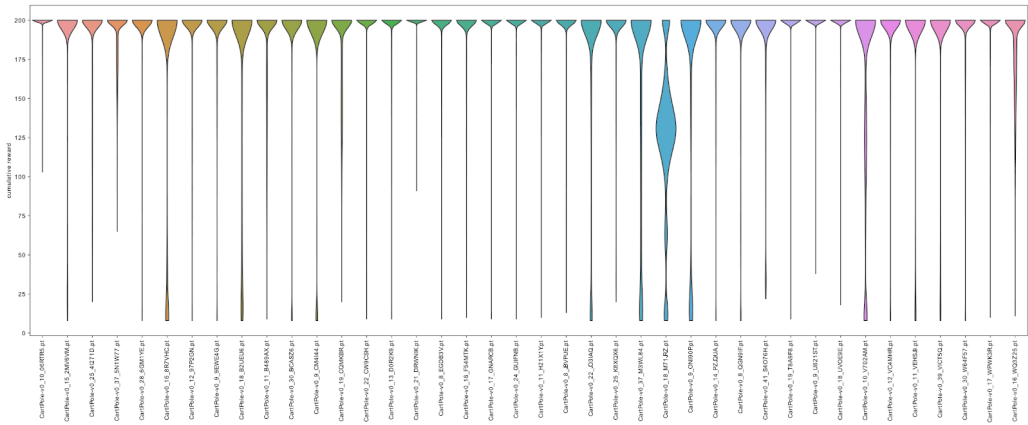


Figure 26: Model-wise evaluation based on the cumulative rewards of 1000 randomly sampled **Dueling DDQN** agents à 10 test episodes per SE model.

F.1.2 EVALUATION OF INDIVIDUAL SE MODELS (ACROBOT)

Below we show the individual or model-based violin plots for the 40 SE models which we calculated based on the cumulative rewards of 1000 randomly sampled agents that were each evaluated across 10 test episodes. For agent sampling we again chose the hyperparameters ranges denoted in Table 2. As the best five models for discrete TD3 (Figure 7) we chose the models Acrobot-v1_223R5W, Acrobot-v1_2XMO40, Acrobot-v1_7DQP5Z, Acrobot-v1_9MA9G8 and Acrobot-v1_8MYN67.

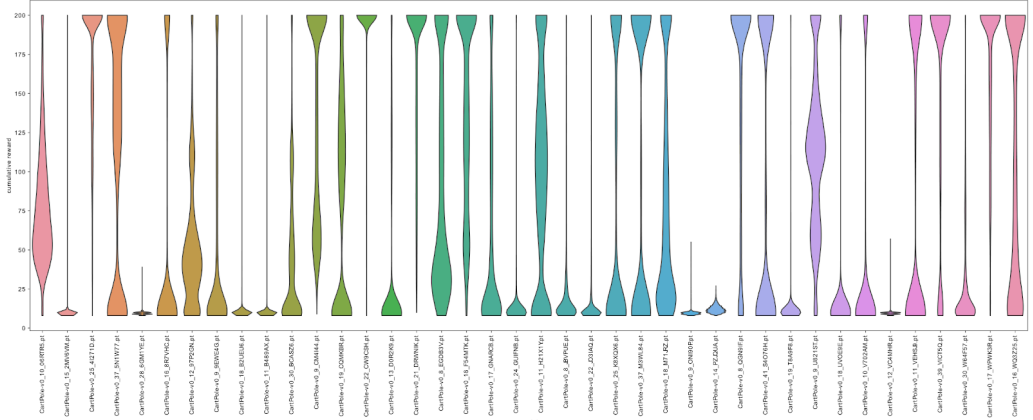


Figure 27: Model-wise evaluation based on the cumulative rewards of 1000 randomly sampled **discrete TD3 agents** à 10 test episodes per SE model.

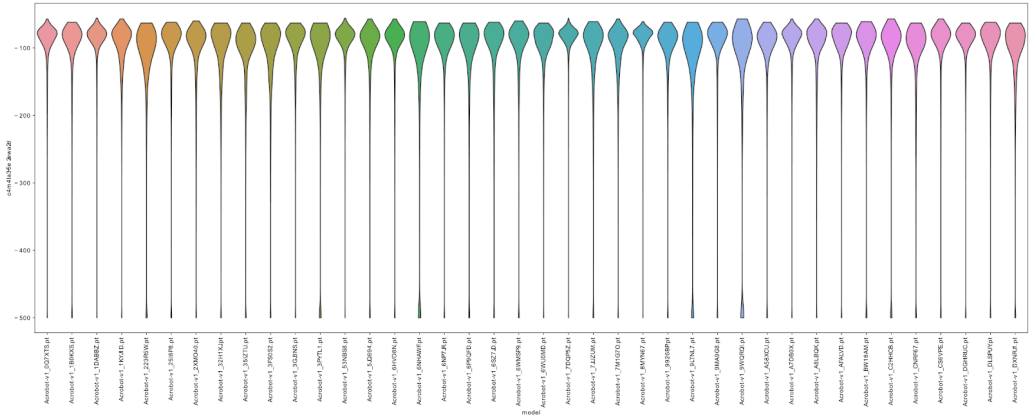


Figure 28: Model-wise evaluation based on the cumulative rewards of 1000 randomly sampled **DDQN agents** à 10 test episodes per SE model.

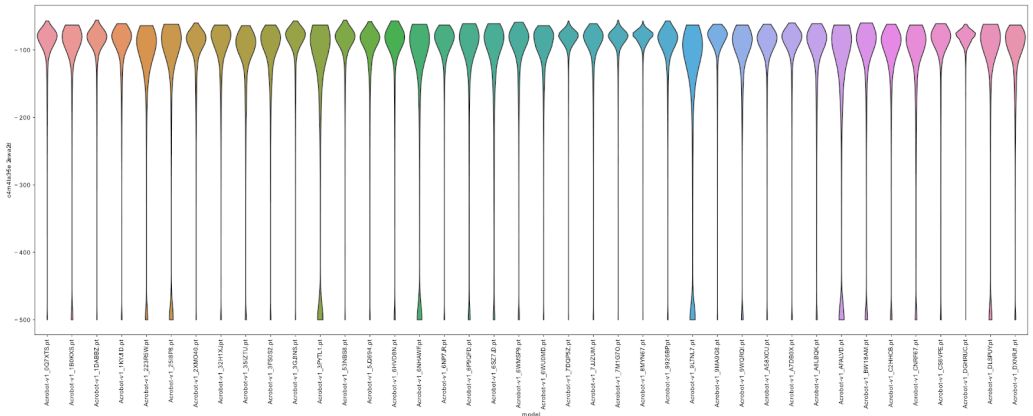


Figure 29: Model-wise evaluation based on the cumulative rewards of 1000 randomly sampled **Dueling DDQN agents** à 10 test episodes per SE model.

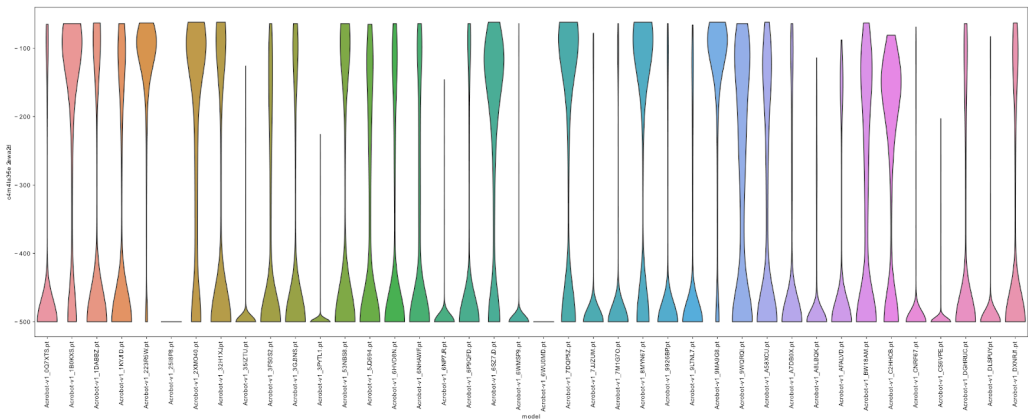


Figure 30: Model-wise evaluation based on the cumulative rewards of 1000 randomly sampled **discrete TD3 agents** à 10 test episodes per SE model.

G.2 Statement of Contributions

Statement of Contributions for the following publication:

Title	Learning Synthetic Environments and Reward Networks for Reinforcement Learning
Link to Publication, DOI	https://iclr.cc/virtual/2022/poster/6495 https://openreview.net/forum?id=C1_esHN6AVn
Authors	Fabio Ferreira, Thomas Nierhoff, Andreas Sälinger and Frank Hutter
Publication Status	Accepted and published
Publisher, Date	Proceedings of the 10th International Conference on Learning Representations (ICLR), 2022
Peer-Review-Process	Yes
Rank	Ranked A* by the CORE2023 ranking

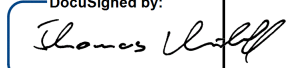
Paper Summary

This paper introduces a novel approach for training reinforcement learning (RL) agents using synthetic environments (SEs) and reward networks (RNs). These environment models serve as proxies for real environment models that simulate state dynamics and rewards (SEs) or rewards only (RNs) and ultimately allow for a more efficient agent training with fewer interactions than compared to training on the real environments after SE and RN generation. The paper proposes to use a bi-level evolutionary optimization for generating SEs and RNs: the inner loop trains the RL agent and the outer loop trains the parameters of the SE or RN conditional on the performance of the RL agent in the inner loop. The key contributions of the paper are:

1. The paper introduces the novel concept of learning Synthetic Environments and Reward Networks with a bi-level optimization scheme that is guided by the agent performance. The concept allows generating full proxy models that incorporate state dynamics and rewards of real environments that enable training RL agents without any interaction with the actual environments after SE generation.
2. The efficacy of SEs and RNs is demonstrated across several classic control environments such as CartPole, Acrobot (SEs), as well as Cliff Walking, CartPole, MountainCarContinuous, and HalfCheetah (RNs). The study confirms that these proxies can train RL agents effectively while requiring up to 60% fewer training steps.
3. The study shows that these proxies are robust against variations in hyperparameters and capable of transferring learned policies to new, unseen agents, demonstrating their general applicability across different environments and hyperparameter settings.
4. The paper presents empirical evidence showing that SEs and RNs achieve their efficiency gains for training new agents through condensed and informed state and reward representations.

Contributions Listing

Name	Contributions	Signature
Fabio Ferreira	<p>Proposed the original idea of Synthetic Environments (SEs) and extending the methodology of Generative Teaching Networks to RL for learning SEs;</p> <p>Proposed using the efficiency improvements in training agents on SEs (and Reward Networks (RNs)) and their transferability to other agents as the central novelties of the paper, highlighting a significant gap in the existing related work;</p> <p>Co-led the methodology of the project, in particular showed that SEs trained with DDQN agents are able to transfer and generalize to other agents; proposed, implemented, and carried out studies to show that agents require up to 60% fewer training steps when trained on SEs;</p> <p>Extended Thomas' code framework by adding baseline agents such as Dueling DDQN, discrete TD3, and improved potential reward shaping functions for RNs, implemented baselines for RNs, e.g., the Intrinsic Curiosity Module (ICM), and together with Thomas, Fabio also worked on hyperparameter optimization and the extension of plotting scripts;</p> <p>Owned and was responsible for the code development for assessing efficiency improvements (Fig. 3), gradient flow analysis, and integrating support for running multiple seeds;</p> <p>Participated in the periodic code reviews (jointly with Thomas);</p>	<p>DocuSigned by:</p>  <p>CA7363FD31BF45C... 15.05.2024</p>

	<p>Co-carried out approximately 50% of all the experiments (Thomas carried out the other approx. 50%);</p> <p>Owned, led and wrote the majority of the paper, including contributions to all parts of the paper. Created the visualizations of the final paper version (except Fig. 2 which was entirely created by Thomas; code for generating Fig. 4 and 5 also was initially created by Thomas and extended by Fabio). Led and contributed significantly to the rebuttal process;</p> <p>Created the repository with the final version of the code;</p> <p>Supervised Thomas and Andreas.</p>	
Thomas Nierhoff	<p>Proposed the idea of using Natural Evolution Strategies (NES) for solving the bi-level optimization necessary to learn synthetic environments and reward networks;</p> <p>Discovered the efficiency improvements in training agents on SEs (and Reward Networks (RNs)) and their transferability to other agents.</p> <p>Co-led the methodology of the project (showed that SEs trained with DDQN agents are robust towards hyperparameter changes by varying hyperparameters dynamically during training; proposed, implemented, and executed the qualitative studies to shed light on what the agents learn from SEs);</p> <p>Co-owned the core implementation, more specifically: implementing the core NES/bi-level optimization framework, the majority of baseline agents (DQN, DDQN, Q-Learning, PPO, SARSA, continuous</p>	<p>DocuSigned by:</p>  <p>04591023C1B749A... 16.05.2024</p>

	<p>TD3), the whole logic for SE generation (early stopping and evaluation), hyperparameter optimization (jointly with Fabio), parallelization, plotting scripts (jointly with Fabio);</p> <p>Co-carried out approximately 50% of all the experiments (Fabio carried out the other approx. 50%);</p> <p>Led the periodic code reviews;</p> <p>Supported with writing, reviewing and rebutting all parts of the paper but the parts of the paper he had the major contributions were: Related Work (Section 2), Feasibility (Section 5), Analyzing SE Behavior (Section 5), Appendix</p>	
Andreas Sälinger	<p>Had a key role in reframing the paper after the prior conference submission (NeurIPS 2021); contributed by clarifying the narrative and enhancing the coherence of the paper;</p> <p>Supported with writing, reviewing and rebutting all parts of the paper, but the parts of the paper he had major contributions were: Introduction and Conclusion (both jointly with Fabio);</p> <p>Contributed to the rebuttal process (together with Fabio, Thomas and Frank).</p>	<p>DocuSigned by:</p>  <p>AADA8541F55A4D6... 23/05/2024</p>
Frank Hutter	<p>Helped conceptualize the problem;</p> <p>Co-led writing the paper, including contributions to all parts of the paper;</p> <p>Helped with reviewing, rebutting and editing the paper;</p> <p>Supervised the project and supervised Fabio.</p>	<p>DocuSigned by:</p>  <p>3CDF1E88127C47F... 6/28/2024</p>

Appendices for One-shot World Models Using a Transformer Trained on a Synthetic Prior

H.1 Paper Appendix

A Studying the Momentum Prior

Unlike the Neural Network prior, the Momentum prior is based on physics-driven dynamics, modeling velocity and positional updates to simulate environments with simple physical laws.

To analyze the behavior of the Momentum prior, we generate histograms in the same manner as with the NN prior, sampling batches of data and calculating the minimum and maximum values for each dimension. These dimensions reflect aspects like velocity and position, which are updated according to basic physical interactions such as gravity or action forces. The range of each dimension is then divided into 100 equal bins, and the occurrences in each bin are counted to visualize the distribution of values.

The Momentum prior produces a variety of distributions across dimensions, as shown in Figure 5. In some cases, we observe broad distributions with values spread uniformly across the range (Fig. 5a). This often occurs in environments with elastic reflections or angular motion without gravity. In other cases, the distribution is multi-modal, featuring multiple peaks (Fig. 5b), which can arise from non-elastic reflections or angular dynamics with insufficient torque to overcome gravity. Finally, some dimensions exhibit sparse distributions (Fig. 5c), where values cluster into a few discrete states. This pattern typically results from environments lacking friction or other forces that would normally smooth out the motion.

These distribution patterns reflect the diversity of physical interactions captured by the Momentum prior. Compared to the NN prior, the behavior here is more interpretable, as it directly corresponds to simplified physical models of motion and interaction.

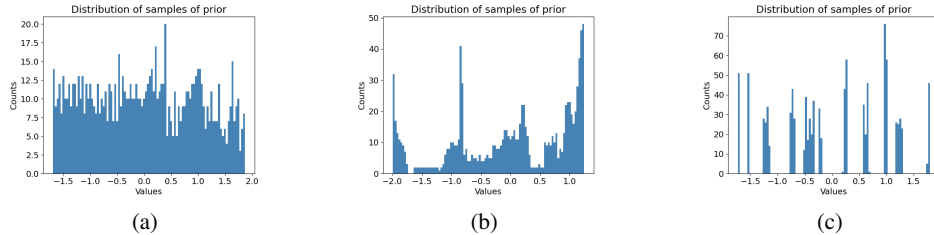


Figure 5: Typical distribution patterns generated by the Momentum prior: (a) broad, (b) multi-modal, and (c) sparse distributions.

B Context Generation Evaluation

To further investigate the effect of different context-generation strategies, we performed an evaluation using a proxy loss for full OSWM training and RL agent evaluation. The proxy set was constructed by generating transitions from a PPO agent trained on each specific environment. These transitions included state-action pairs, next states, and rewards.

We simulated different levels of randomness to capture a range of behaviors. Specifically, we generated rollouts with 0% randomness (only expert actions), 50% randomness (half expert, half random), and 100% randomness (only random actions). For each level of randomness, we collected 5000 transitions across multiple episodes and randomly subsampled 500 transitions per level, resulting in a total of 1500 transitions per environment. This proxy set was used to compute the mean squared error (MSE) between the predicted dynamics from OSWM and the actual transitions.

The intuition behind why we believe the proxy set is effective lies in its ability to cover a wide range of environment dynamics. Certain environments, like MountainCar-v0, require exploration using both efficient, expert-like actions to solve the task, and suboptimal actions to discover diverse states in the environment. Similarly, for environments like CartPole, non-goal-oriented actions—such as those where the pole is not upright or the cart velocity is high—allow the model to observe critical states not typically encountered by an expert agent alone. By including random actions in the proxy set, we aim to capture these middle-ground dynamics, such as a scenario in MountainCar where a fast-moving car decelerates, a behavior not covered by either purely expert or random actions. Additionally, this

strategy helps represent the trajectory from suboptimal to successful actions, enhancing OSWM’s capacity to generalize across different levels of agent performance.

The results for each context-generation strategy (random, repeat, expert, p-expert, and mixture) across the various environments are shown in Table 3. This table provides a detailed view of how the different strategies affect the proxy loss, which serves as a reliable proxy for predictive performance.

Environment	Random	Repeat	Expert	p-expert	Mixture
GridWorld	0.468	0.413	NaN	0.218	0.203
CartPole-v0	0.0048	0.0054	0.0138	0.00079	0.00186
MountainCar-v0	0.00065	0.00025	5e-05	1.19e-05	8.5e-06
SimpleEnv	0.38	0.701	9.614	0.103	0.139
Pendulum-v1	0.025	0.03173	0.0779	0.0578	0.018
Reacher-v4	0.312	0.552	1.456	0.347	0.322

Table 3: Proxy loss with respect to the different context generation techniques. Mean squared error loss for 1500 validation transitions in the corresponding environment. The best performance per environment is in bold.

C Hyperparameters

The hyperparameters for the OSWM can be found in table 4. For training the OSWM, the hyperparameters can be found in 5.

Hyperparameter	Value
Embedding size	512
Number of Attention Heads	4
Hidden size	1024
Number of layers	6
Embedding size	512

Table 4: Hyperparameters defining the OSWM transformer architecture.

Hyperparameter	Value
Optimizer	AdamW
β_1, β_2	0.9, 0.999
ϵ	$1e^{-8}$
Weight decay	0.0
Initial Learning Rate	$5e^{-5}$
Batch size	8
Epochs	50
Steps per epoch	100
Warm-up epochs	12
Sequence length	1001
Maximum eval position	1000
Minimum eval position	500
Eval position sampling function	$p_i = \frac{1}{((\max - \min) - i)^q}$
q for eval function	0.4

Table 5: Hyperparameters that define the training pipeline of the OSWM training.

D Custom Environment Details

This following section will describe the details of the custom environment used to evaluate the OSWM. First, the GridWorld environment will be described, afterward the SimpleEnv.

D.1 Custom GridWorld

The GridWorld environment is designed as a simple environment with discrete states and actions. It is deliberately easy to solve, as its main goal is to test the modeling capabilities of the OSWM in an easy base case. This is further helped by the fact that for discrete spaces, the OSWM predictions are rounded to the next integer value. This allows us to use the same condition for termination. And give the agent the same interface as the real environment.

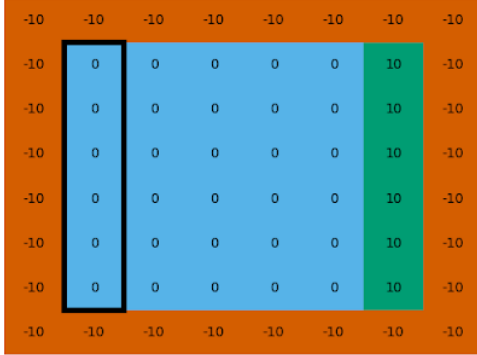


Figure 6: Visualization of the custom GridWorld environment. Terminal states are in red, goal states are in green, and initial states are highlighted in black. Immediate reward in the cells.

The GridWorld consists of an 8x8 grid. Observations are the x-position and y-position. Actions are 4 discrete moves (up, down, left, and right). With the outer ring of cells being terminal states with a negative ten reward. The goal states give a positive ten reward and are located in the second last column to the right. They span from the second row to the second last row. Each step gives a negative one reward and a small positive ($0.01 * x_{pos}$) for being further to the right. Episodes are truncated after exceeding 25 episode steps. The agent starts the episode at $x_{pos} = 1$ and with a y_{pos} between 1 and 6. A visualization of the GridWorld can be found in fig. 6.

D.2 Custom SimpleEnv

The SimpleEnv serves to provide a first intuition for continuous action and state space environments, while using simplistic dynamics. Similar to the GridWorld, it is designed to be easily solved by RL agents with smooth and dense goal-oriented rewards.

It has 1-dimensional continuous action space ($a \in [-10., 10.]$) and a 1-dimensional continuous state space ($s \in [-30., 30.]$). The immediate reward is the negative absolute state, $r = -1 \cdot \text{abs}(s)$. Episodes have a fixed length of 20 steps. The dynamics of the environment are defined by the action being added to the state, $s_t = s_{t-1} + a_t$. The initial state of the environment is sampled uniformly between -5 and 5.

D.3 Solved Reward for Custom Environments

To establish the solved threshold for custom environments, a relative score is determined based on a comparison between expert performance and random actions. This approach allows for the definition of a consistent threshold across various environments. The solved reward is calculated using the following equation:

$$R_{solved} = R_{max} - (R_{max} - R_{random}) \times 0.03 \quad (1)$$

In this equation, R_{max} represents the expert-level performance, while R_{random} is the expected reward when taking random actions. The coefficient of 0.03 is chosen as it aligns with the solved

threshold established for the CartPole-v0 environment, providing a standard for evaluating other environments.

E Additional Reward Function Analysis

Here, we conduct the reward function analysis for the Pendulum environment, shown in Figure 7. The original environment’s reward function is already dense, and OSWM generally preserves this dense structure. However, OSWM introduces more discrete rewards, especially in states where the pendulum is near upright, offering higher rewards compared to the real environment. In some extreme states, where penalties should be applied, OSWM rewards the agent instead. This smoothing may reduce the model’s ability to capture more precise control at the edges of the pendulum’s motion range, which could explain the model’s inferior performance in this task. For both the Cartpole and Pendulum environments, the reward depends solely on the angular position. To assess whether the OSWM can accurately model this relationship, we plot the results based on this dimension, although the observation space for both environments has higher dimensionality. We aggregate the results as follows.

We sample 1000 observation-action pairs and predict the dynamics using OSWM. For Pendulum, the entire observation space is sampled, while for Cartpole, the velocity components of the observation space are capped at a magnitude of 5. The angular position is discretized into 100 bins for Pendulum and 20 bins for Cartpole. For each bin, we compute the mean over all observations that fall within that bin to represent the relationship between angular position and the predicted reward.

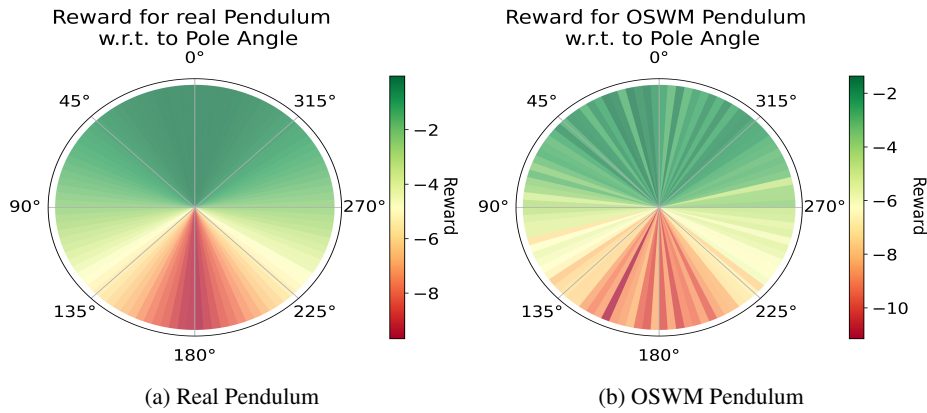


Figure 7: Reward distributions for the real and OSWM Pendulum environments.

F BO for Prior and Model Hyperparameter

In order to determine the ideal hyperparameter for both the OSWM model and the underlying prior, an automatic optimization was performed. For the prior, especially, the architecture of the neural networks in NN prior play a crucial role in its performance. The library used for this optimization is HpBandSter. The model is trained for a fixed 50 epochs, we omit using Hyperband, as it is unclear how the different complexity of priors plays into the reliance of the low-cost proxy for the OSWM. The optimization was performed for 45 iterations with 3 workers. The configuration space and results can be found in 6. The target function, being optimized, is the same validation loss used for evaluating the context generation types in Sec. 4.3.

For the optimization of the encoder and decoder models of the OSWM, the same optimization was performed. The baseline is a linear encoder and decoder, for more complex data, a more expressive encoder and decoder might aid in representation. Additionally, it allows us to separately encode action and state, and separately decode the next state and reward. The choices for encoding and decoding are a standard MLP or a model with separate MLPs concatenating both outputs, denoted with *Cat*. An overview of the entire configuration space and the results are given in table 7.

Hyperparameter	Type	Range/Choices	Final
Number hidden layer	integer	[1, 6]	1
Width hidden layers	integer	[8, 64]	16
Use bias	bool	[True, False]	False
Use dropout	bool	[True, False]	False
Dropout probability	cond. float	[0.1, 0.9]	-
Activation Functions	bool (each)	[relu, sin, sigmoid, tanh]	(sin, tanh)
Initial state scale	float	[1., 20.]	18.14
Initial state offset	float	[1., 5.]	3.28
Use layer norm	bool	[True, False]	True
Use residual connection	bool	[True, False]	True

Table 6: Hyperparameters of the NN Prior optimized using BO. Each hyperparameter, with its type, the range or choices, and final best performing value.

Hyperparameter	Type	Range/Choices	Final
Encoder type	categoric	[MLP, Cat]	Cat
Encoder width	categoric	[16, 64, 256, 512]	512
Encoder depth	Integer	[1,6]	3
Encoder activation	categoric	[ReLU, sigmoid, GeLU]	GeLU
Encoder use bias	bool	[True, False]	True
Encoder use res connection	bool	[True, False]	True
Decoder type	categoric	[MLP, Cat]	Cat
Decoder width	categoric	[16, 64, 256, 512]	64
Decoder depth	Integer	[1,6]	2
Decoder activation	categoric	[ReLU, sigmoid, GeLU]	sigmoid
Decoder use bias	bool	[True, False]	False
Decoder use res connection	bool	[True, False]	True

Table 7: The hyperparameters of the encoder and decoder of the OSWM optimized using BO. Each hyperparameter, with its type, the range or choices, and final best-performing value.

H.2 Statement of Contributions

Statement of Contributions for the following publication:

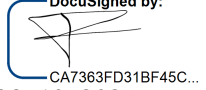
Title	One-shot World Models Using a Transformer Trained on a Synthetic Prior
Link to Publication, DOI	https://arxiv.org/abs/2409.14084
Authors	Fabio Ferreira*, Moreno Schlageter*, Raghu Rajan, André Biedenkapp and Frank Hutter (*: joint first author)
Publication Status	Accepted at the NeurIPS 2024 Workshop on Open-World Agents
Publisher, Date	-
Peer-Review-Process	Yes
Rank	not ranked by CORE2023 (workshop)

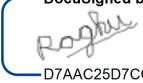
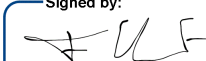
Paper Summary

This paper introduces One-Shot World Models (OSWM), a novel transformer-based approach for building world models entirely from synthetic data. OSWM is trained using a synthetic prior composed of randomly initialized and untrained neural networks, which simulate the state dynamics and reward functions of target environments. By leveraging in-context learning, the model adapts to new environments with minimal real-world interactions. Specifically, OSWM can rapidly adapt using only 1,000 sampled transition steps as context, allowing it to train agents for various simple reinforcement learning tasks. The method has been shown to solve tasks in environments such as GridWorld, CartPole, and a custom control environment, demonstrating its effectiveness in learning policies for different simple environments. However, performance was less consistent in the more complex Reacher environment, where the model achieved only mediocre results. Despite this, the use of synthetic priors to generate diverse environment dynamics presents a promising direction for efficient world model training without needing extensive real-world data. The key contributions of the paper are:

1. Introduction of OSWM, a transformer-based world model trained on synthetic data from a prior of randomly initialized and untrained neural networks simulating environment dynamics and rewards.
2. Rapid Adaptation via In-Context Learning: After training on synthetic prior data, OSWM adapts to new environments and serves as a proxy using only 1,000 sampled interaction steps from the target environment during inference.
3. The paper shows that OSWM effectively trains agents for GridWorld, CartPole, and a custom control environment.
4. The paper provides an empirical analysis that assesses the importance of context sampling and include an ablation study on the design of the synthetic prior.

Contributions Listing

Name	Contributions	Signature
Fabio Ferreira	<p>Proposed the original idea of One-Shot World Models (OSWM) using synthetic priors;</p> <p>Developed the overall methodology of the project and guided its direction;</p> <p>Owned, led, and wrote the majority of paper and created Figure 1;</p> <p>Provided critical insights for positioning the paper within the context of related work and framed the key contributions;</p> <p>Lead the supervision of Moreno.</p>	 <p>DocuSigned by: CA7363FD31BF45C... 28.10.2024</p>
Moreno Schlageter	<p>Owned and led the implementation and experimentation for OSWM and developed the code for training OSWM;</p> <p>Ran all experiments and created the majority of figures (excluding Figure 1);</p> <p>Proposed the logic for the NN and Momentum prior, worked on the core OSWM architecture and implemented the synthetic prior mechanism;</p> <p>Led and executed all experimental evaluations across various environments, including all experiments on sampling context, as well as on analyzing and ablating the prior;</p> <p>Contributed to shaping the project's vision and methodology in collaboration with the supervisory team;</p> <p>Supported with writing and reviewing all parts of the paper.</p>	 <p>Signiert von: Moreno Schlageter 6E9AEE629B124B3... 28.10.2024</p>

Raghu Rajan	<p>Co-supervised the project alongside Fabio and André;</p> <p>Contributed to shaping the project's vision and methodology;</p> <p>Supported in framing and writing of the paper, contributed by clarifying the narrative and enhancing the coherence of the paper;</p> <p>Offered insights on related work and helped refine the narrative within the broader context of reinforcement learning research.</p>	<p>DocuSigned by:</p>  <p>D7AAC25D7CCF49D... 10/28/2024</p>
André Biedenkapp	<p>Co-supervised the project alongside Fabio and Raghu;</p> <p>Contributed to shaping the project's vision and methodology;</p> <p>Supported in framing and writing of the paper, contributed by clarifying the narrative and enhancing the coherence of the paper;</p> <p>Offered insights on related work and helped refine the narrative within the broader context of reinforcement learning research.</p>	<p>DocuSigned by:</p>  <p>B57C612393B6408... 10/28/2024</p>
Frank Hutter	<p>Helped conceptualize the problem;</p> <p>Supported in reviewing, and editing the paper;</p> <p>Supervised the project and supervised Fabio, Raghu, and André.</p>	<p>Signed by:</p>  <p>3CDF1E88127C47F... 31/10/2024</p>

Bibliography

Abramson, J., J. Adler, J. Dunger, R. Evans, T. Green, A. Pritzel, O. Ronneberger, L. Willmore, A. J. Ballard, J. Bambrick, et al. (2024). “Accurate structure prediction of biomolecular interactions with AlphaFold 3”. In: *Nature*, pp. 1–3 (cit. on p. 3).

Achiam, J., S. Adler, S. Agarwal, L. Ahmad, I. Akkaya, F. L. Aleman, D. Almeida, J. Altenschmidt, S. Altman, S. Anadkat, et al. (2023). “Gpt-4 technical report”. In: *arXiv preprint arXiv:2303.08774* (cit. on p. 3).

Achille, A., M. Lam, R. Tewari, A. Ravichandran, S. Maji, C. C. Fowlkes, S. Soatto, and P. Perona (2019). “Task2Vec: Task Embedding for Meta-Learning”. In: *Proceedings of the 22nd IEEE/CVF International Conference on Computer Vision (ICCV’19)*. Computer Vision Foundation and IEEE Computer Society. IEEE, pp. 6429–6438 (cit. on pp. 22, 134).

Alayrac, J.-B., J. Donahue, P. Luc, A. Miech, and et al. (2022). “Flamingo: a Visual Language Model for Few-Shot Learning”. In: *Proceedings of the 36th International Conference on Advances in Neural Information Processing Systems (NeurIPS’22)*. Ed. by S. Koyejo, S. Mohamed, A. Agarwal, D. Belgrave, K. Cho, and A. Oh. Curran Associates (cit. on p. 3).

Andrychowicz, M., M. Denil, S. Colmenarejo, M. Hoffman, D. Pfau, T. Schaul, and N. de Freitas (2016). “Learning to learn by gradient descent by gradient descent”. In: *Proceedings of the 30th International Conference on Advances in Neural Information Processing Systems (NeurIPS’16)*. Ed. by D. Lee, M. Sugiyama, U. von Luxburg, I. Guyon, and R. Garnett. Curran Associates, pp. 3981–3989 (cit. on pp. 5, 23).

Anil, R., S. Borgeaud, J.-B. Alayrac, J. Yu, R. Soricut, J. Schalkwyk, A. M. Dai, A. Hauth, K. Millican, et al. (2023). “Gemini: a family of highly capable multimodal models”. In: *arXiv preprint arXiv:2312.11805* (cit. on p. 3).

Antoniou, A (2017). “Data Augmentation Generative Adversarial Networks”. In: *arXiv preprint arXiv:1711.04340* (cit. on p. 26).

Arango, S. Pineda, F. Ferreira, A. Kadra, F. Hutter, and J. Grabocka (2024). “Quick-Tune: Quickly Learning Which Pretrained Model to Finetune and How”. In: *Proceedings of the International Conference on Learning Representations (ICLR’24)*. Published online: iclr.cc. ICLR. URL: <https://iclr.cc/virtual/2024/oral/19719> (cit. on pp. 4, 19, 45).

Bengio, S., Y. Bengio, J. Cloutier, and J. Gecsei (1997). *On the Optimization of a Synaptic Learning Rule* (cit. on p. 21).

Bengio, Y. (2011). “Deep Learning of Representations for Unsupervised and Transfer Learning”. In: *Proceedings of the 28th International Conference on Machine Learning (ICML’11)*. Ed. by L. Getoor and T. Scheffer. Omnipress, pp. 17–36 (cit. on p. 23).

Bengio, Y., A. C. Courville, and P. Vincent (2013). “Representation Learning: A Review and New Perspectives”. In: *IEEE Trans. Pattern Anal. Mach. Intell.* 35.8, pp. 1798–1828 (cit. on p. 22).

Bengio, Y., J. Louradour, R. Collobert, and J. Weston (2009). “Curriculum learning”. In: *Proceedings of the 26th annual international conference on machine learning*, pp. 41–48 (cit. on p. 134).

Bilalli, B., A. Abelló, and T. Aluja-Banet (2017). “On the predictive power of meta-features in OpenML”. In: *Int. J. Appl. Math. Comput. Sci.* 27.4, pp. 697–712 (cit. on p. 22).

Bischl, B., P. Kerschke, L. Kotthoff, M. Lindauer, Y. Malitsky, A. Frechétte, H. Hoos, F. Hutter, K. Leyton-Brown, K. Tierney, and J. Vanschoren (2016). "ASlib: A Benchmark Library for Algorithm Selection". In: *Artificial Intelligence* 237, pp. 41–58 (cit. on p. 23).

Bourlard, Hervé and Yves Kamp (1988). "Auto-association by multilayer perceptrons and singular value decomposition". In: *Biological cybernetics* 59.4, pp. 291–294 (cit. on p. 26).

Brown, T., B. Mann, N. Ryder, M. Subbiah, J. Kaplan, P. Dhariwal, A. Neelakantan, P. Shyam, G. Sastry, A. Askell, S. Agarwal, A. Herbert-Voss, G. Krueger, T. Henighan, R. Child, A. Ramesh, D. Ziegler, J. Wu, C. Winter, C. Hesse, M. Chen, E. Sigler, M. Litwin, S. Gray, B. Chess, J. Clark, C. Berner, S. McCandlish, A. Radford, I. Sutskever, and D. Amodei (2020). "Language Models are Few-Shot Learners". In: *Proceedings of the 34th International Conference on Advances in Neural Information Processing Systems (NeurIPS'20)*. Ed. by H. Larochelle, M. Ranzato, R. Hadsell, M.-F. Balcan, and H. Lin. Curran Associates, pp. 1877–1901 (cit. on p. 3).

Caron, M., H. Touvron, I. Misra, H. Jégou, J. Mairal, P. Bojanowski, and A. Joulin (2021). "Emerging Properties in Self-Supervised Vision Transformers". In: *Proceedings of the 24nd IEEE/CVF International Conference on Computer Vision (ICCV'21)*. Computer Vision Foundation and IEEE Computer Society. IEEE, pp. 9630–9640 (cit. on p. 26).

Caruana, R. (1998). "Multitask Learning". In: *Learning to Learn*. Ed. by S.n Thrun and L. Y. Pratt. Springer, pp. 95–133 (cit. on p. 22).

Chawla, N., K. Bowyer, L. Hall, and W. Kegelmeyer (2002). "SMOTE: Synthetic Minority over-Sampling Technique". In: *Journal of Artificial Intelligence Research* 16.1, pp. 321–357 (cit. on p. 6).

Chen, A. S., S. Nair, and C. Finn (2021). "Learning Generalizable Robotic Reward Functions from "In-The-Wild" Human Videos". In: *Robotics: Science and Systems XVII, Virtual Event, July 12-16, 2021*. Ed. by D. A. Shell, M. Toussaint, and M. Ani Hsieh (cit. on p. 10).

Chen, T., S. Kornblith, M. Norouzi, and G. E. Hinton (2020). "A Simple Framework for Contrastive Learning of Visual Representations". In: *Proceedings of the 37th International Conference on Machine Learning (ICML'20)*. Ed. by H. Daume III and A. Singh. Vol. 98. Proceedings of Machine Learning Research, pp. 1597–1607 (cit. on pp. 10, 26).

Chen, X. and K. He (2021). "Exploring Simple Siamese Representation Learning". In: *Proceedings of the International Conference on Computer Vision and Pattern Recognition (CVPR'21)*. Computer Vision Foundation and IEEE Computer Society. IEEE, pp. 15750–15758 (cit. on p. 26).

Cubuk, E., B. Zoph, D. Mane, V. Vasudevan, and Q. Le (2019). "Autoaugment: Learning augmentation strategies from data". In: *Proceedings of the International Conference on Computer Vision and Pattern Recognition (CVPR'19)*. Computer Vision Foundation and IEEE Computer Society. IEEE, pp. 113–123 (cit. on pp. 6, 15, 25).

Cubuk, E., B. Zoph, J. Shlens, and Q. Le (2020). "RandAugment: Practical automated data augmentation with a reduced search space". In: *Proceedings of the International Conference on Computer Vision and Pattern Recognition (CVPR'20)*. Computer Vision Foundation and IEEE Computer Society. IEEE, pp. 702–703 (cit. on pp. 15, 26).

DeVries, T. and G. Taylor (2017). "Improved Regularization of Convolutional Neural Networks with Cutout". In: *arXiv:1708.04552 [cs.CV]* (cit. on p. 6).

Doersch, C., A. Gupta, and A. A. Efros (2015). "Unsupervised Visual Representation Learning by Context Prediction". In: *Proceedings of the 18th International Conference on*

Computer Vision (ICCV'15). Computer Vision Foundation and IEEE Computer Society. IEEE, pp. 1422–1430 (cit. on p. 26).

Dubey, A., A. Jauhri, A. Pandey, A. Kadian, A. Al-Dahle, A. Letman, A. Mathur, A. Schelten, A. Yang, A. Fan, et al. (2024). “The llama 3 herd of models”. In: *arXiv preprint arXiv:2407.21783* (cit. on p. 3).

El Baz, A., I. Ullah, E. Alcobaça, A. C. P. L. F. Carvalho, H. Chen, F. Ferreira, H. Gouk, C. Guan, I. Guyon, T. Hospedales, S. Hu, M. Huisman, F. Hutter, Z. Liu, F. Mohr, E. Öztürk, J. N. van Rijn, H. Sun, X. Wang, and W. Zhu (2021). “Lessons learned from the NeurIPS 2021 MetaDL challenge: Backbone fine-tuning without episodic meta-learning dominates for few-shot learning image classification”. In: *Proceedings of the Neural Information Processing Systems Track on Datasets and Benchmarks*. Ed. by J. Vanschoren and S. Yeung. Curran Associates, pp. 80–96 (cit. on p. 19).

Esser, P., S. Kulal, A. Blattmann, R. Entezari, J. Müller, H. Saini, Y. Levi, D. Lorenz, A. Sauer, F. Boesel, et al. (2024). “Scaling rectified flow transformers for high-resolution image synthesis”. In: *Proceedings of the 41st International Conference on Machine Learning (ICML'24)*. Ed. by R. Salakhutdinov, Z. Kolter, K. Heller, A. Weller, N. Oliver, J. Scarlett, and F. Berkenkamp. Vol. 251. Proceedings of Machine Learning Research. PMLR (cit. on p. 3).

Ferreira, F., T. Nierhoff, A. Sälinger, and F. Hutter (2022). “Learning Synthetic Environments and Reward Networks for Reinforcement Learning”. In: *Proceedings of the International Conference on Learning Representations (ICLR'22)*. Published online: [iclr.cc](https://iclr.cc/virtual/2022/poster/6495). ICLR. URL: <https://iclr.cc/virtual/2022/poster/6495> (cit. on p. 103).

Ferreira, F., I. Rapant, J. K.H. Franke, and F. Hutter (2025). “Beyond Random Augmentations: Pretraining with Hard Views”. In: *Proceedings of the International Conference on Learning Representations (ICLR'25)*. Published online: [iclr.cc](https://iclr.cc/virtual/2025/poster/6495). ICLR. URL: <https://openreview.net/forum?id=AK1C55o4r7> (cit. on pp. 26, 27, 89).

Ferreira, F., M. Schlageter, R. Rajan, A. Biedenkapp, and F. Hutter (2024). “One-shot World Models Using a Transformer Trained on a Synthetic Prior”. In: *NeurIPS 2024 Workshop on Open-World Agents* (cit. on p. 117).

Feurer, M., K. Eggensperger, S. Falkner, M. Lindauer, and F. Hutter (2022). “Auto-Sklearn 2.0: Hands-free AutoML via Meta-Learning”. In: *Journal of Machine Learning Research* 23.261. Ed. by M. Schoenauer, pp. 1–61 (cit. on p. 24).

Feurer, M., A. Klein, K. Eggensperger, J. Springenberg, M. Blum, and F. Hutter (2015). “Efficient and Robust Automated Machine Learning”. In: *Proceedings of the 29th International Conference on Advances in Neural Information Processing Systems (NeurIPS'15)*. Ed. by C. Cortes, N. Lawrence, D. Lee, M. Sugiyama, and R. Garnett. Curran Associates, pp. 2962–2970 (cit. on p. 134).

Feurer, M., A. Klein, K. Eggensperger, J. Springenberg, M. Blum, and F. Hutter (2019). “Auto-sklearn: Efficient and Robust Automated Machine Learning”. In: *Automated Machine Learning: Methods, Systems, Challenges*. Ed. by F. Hutter, L. Kotthoff, and J. Vanschoren. Available for free at <http://automl.org/book>. Springer. Chap. 6, pp. 113–134 (cit. on p. 9).

Finn, C., P. Abbeel, and S. Levine (2017). “Model-Agnostic Meta-Learning for Fast Adaptation of Deep Networks”. In: *Proceedings of the 34th International Conference on Machine Learning (ICML'17)*. Ed. by D. Precup and Y. Teh. Vol. 70. Proceedings of Machine Learning Research, pp. 1126–1135 (cit. on pp. 5, 23).

Giradis, S., P. Singh, and N. Komodakis (2018). “Unsupervised Representation Learning by Predicting Image Rotations”. In: *Proceedings of the International Conference on Learning Representations (ICLR’18)*. Published online: iclr.cc. ICLR (cit. on pp. 25, 26).

Goodfellow, I., Y. Bengio, and A. Courville (2016). *Deep Learning*. MIT Press (cit. on p. 3).

Goodfellow, I., J. Pouget-Abadie, M. Mirza, B. Xu, D. Warde-Farley, A. Courville S. Ozair, and Y. Bengio (2014). “Generative Adversarial Nets”. In: *Proceedings of the 28th International Conference on Advances in Neural Information Processing Systems (NeurIPS’14)*. Ed. by Z. Ghahramani, M. Welling, C. Cortes, N. Lawrence, and K. Weinberger. Curran Associates, pp. 2672–2680 (cit. on pp. 6, 27).

Grill, J., F. Strub, F. Altché, C. Tallec, P. H. Richemond, E. Buchatskaya, C. Doersch, B. Ávila Pires, Z. Daniel Guo, M. G. Azar, B. Piot, K. Kavukcuoglu, R. Munos, and M. Valko (2020). “Bootstrap Your Own Latent: A New Approach to Self-Supervised Learning”. In: *Proceedings of the 34th International Conference on Advances in Neural Information Processing Systems (NeurIPS’20)*. Ed. by H. Larochelle, M. Ranzato, R. Hadsell, M.-F. Balcan, and H. Lin. Curran Associates (cit. on pp. 6, 10, 26).

Guo, D., D. Yang, H. Zhang, J. Song, R. Zhang, R. Xu, Q. Zhu, S. Ma, P. Wang, X. Bi, et al. (2025). “DeepSeek-R1: Incentivizing Reasoning Capability in LLMs via Reinforcement Learning”. In: *arXiv preprint arXiv:2501.12948* (cit. on pp. 3, 135).

Hinton, Geoffrey E and Richard Zemel (1993). “Autoencoders, minimum description length and Helmholtz free energy”. In: *Advances in neural information processing systems 6* (cit. on p. 26).

Ho, D., E. Liang, X. Chen, I. Stoica, and P. Abbeel (2019). “Population Based Augmentation: Efficient Learning of Augmentation Policy Schedules”. In: *Proceedings of the 36th International Conference on Machine Learning, ICML 2019, 9-15 June 2019, Long Beach, California, USA*. Ed. by K. Chaudhuri and R. Salakhutdinov. Vol. 97. Proceedings of Machine Learning Research, pp. 2731–2741 (cit. on p. 25).

Ho, J., A. Jain, and P. Abbeel (2020). “Denoising diffusion probabilistic models”. In: *Proceedings of the 34th International Conference on Advances in Neural Information Processing Systems (NeurIPS’20)*. Ed. by H. Larochelle, M. Ranzato, R. Hadsell, M.-F. Balcan, and H. Lin. Curran Associates, pp. 6840–6851 (cit. on p. 6).

Hochreiter, S., A. Younger, and P. Conwell (2001). “Learning to Learn Using Gradient Descent”. In: *Proceedings of the 11th International Conference on Artificial Neural Networks (ICANN’01)*. Ed. by G. Dorffner, H. Bischof, and K. Hornik. Springer, pp. 87–94 (cit. on p. 21).

Hoffmann, J., S. Borgeaud, A. Mensch, E. Buchatskaya, T. Cai, E. Rutherford, D. d. L. Casas, L. A. Hendricks, J. Welbl, A. Clark, et al. (2022). “Training compute-optimal large language models”. In: *arXiv preprint arXiv:2203.15556* (cit. on p. 4).

Hollmann, N., S. Müller, K. Eggensperger, and F. Hutter (2023). “TabPFN: A Transformer That Solves Small Tabular Classification Problems in a Second”. In: *Proceedings of the International Conference on Learning Representations (ICLR’23)*. Published online: iclr.cc. ICLR (cit. on p. 28).

Hospedales, T., A. Antoniou, P. Micaelli, and A. Storkey (2021). “Meta-Learning in Neural Networks: A Survey”. In: *IEEE Transactions on Pattern Analysis and Machine Intelligence’21*. Ed. by K. M. Lee. IEEE Computer Society (cit. on p. 5).

Hu, E. J., Y. Shen, P. Wallis, Z. Allen-Zhu, Y. Li, S. Wang, and W. Chen (2021). “LoRA: Low-Rank Adaptation of Large Language Models”. In: *CoRR* abs/2106.09685. URL: <https://arxiv.org/abs/2106.09685> (cit. on p. 133).

Hugging Face, Inc. (2024). *Hugging Face Model Hub*. <https://huggingface.co/models>. Accessed: 6 November 2024 (cit. on pp. 3, 9).

Hutter, F., L. Kotthoff, and J. Vanschoren, eds. (2019). *Automated Machine Learning: Methods, Systems, Challenges*. Available for free at <http://automl.org/book>. Springer (cit. on pp. 5, 6, 23, 24).

Jakobi, N., P. Husbands, and I. Harvey (1995). “Noise and the reality gap: The use of simulation in evolutionary robotics”. In: *Advances in Artificial Life: Third European Conference on Artificial Life Granada, Spain, June 4–6, 1995 Proceedings 3*. Springer, pp. 704–720 (cit. on p. 6).

Jiang, A. Q., A. Sablayrolles, A. Roux, A. Mensch, B. Savary, C. Bamford, D. S. Chaplot, D. d. l. Casas, E. B. Hanna, F. Bressand, et al. (2024). “Mixtral of experts”. In: *arXiv preprint arXiv:2401.04088* (cit. on p. 3).

Jomaa, H., L. Schmidth-Thieme, and J. Grabocka (2021). “Dataset2vec: Learning dataset meta-features”. In: *Data Mining and Knowledge Discovery* 35 (3), pp. 964–985 (cit. on p. 22).

Kadioglu, S., Y. Malitsky, M. Sellmann, and K. Tierney (2010). “ISAC - Instance-Specific Algorithm Configuration”. In: *Proceedings of the Nineteenth European Conference on Artificial Intelligence (ECAI'10)*. Ed. by H. Coelho, R. Studer, and M. Wooldridge. IOS Press, pp. 751–756 (cit. on p. 5).

Kaplan, J., S. McCandlish, T. Henighan, T. Brown, B. Chess, R. Child, S. Gray, A. Radford, J. Wu, and D. Amodei (2020). “Scaling Laws for Neural Language Models”. In: *arXiv:2001.08361 [cs.LG]* (cit. on p. 3).

Kingma, D. and M. Welling (2014). “Auto-Encoding Variational Bayes”. In: *Proceedings of the International Conference on Learning Representations (ICLR'14)*. CBLS (cit. on p. 6).

Koçyigit, M. Taha, T. M. Hospedales, and H. Bilen (2023). “Accelerating Self-Supervised Learning via Efficient Training Strategies”. In: *Proc. of WACV*. IEEE, pp. 5643–5653 (cit. on p. 27).

Kotthoff, L., I. Gent, and I. Miguel (2012). “An evaluation of machine learning in algorithm selection for search problems”. In: *AI Communications* 25.3, pp. 257–270 (cit. on p. 23).

Kotthoff, L., C. Thornton, H. Hoos, F. Hutter, and K. Leyton-Brown (2017). “Auto-WEKA 2.0: Automatic model selection and hyperparameter optimization in WEKA”. In: *jmlr* 18, 25:1–25:5 (cit. on p. 9).

Krizhevsky, A., I. Sutskever, and G. Hinton (2012). “ImageNet Classification with Deep Convolutional Neural Networks”. In: *Proceedings of the 26th International Conference on Advances in Neural Information Processing Systems (NeurIPS'12)*. Ed. by P. Bartlett, F. Pereira, C. Burges, L. Bottou, and K. Weinberger. Curran Associates, pp. 1097–1105 (cit. on p. 3).

LeCun, Y., B. Boser, J. Denker, D. Henderson, R. Howard, W. Hubbard, and L. Jackel (1989). “Backpropagation Applied to Handwritten Zip Code Recognition”. In: *Neural Comput.* 1.4, pp. 541–551 (cit. on p. 3).

Li, K. and J. Malik (2017). “Learning to Optimize”. In: *Proceedings of the International Conference on Learning Representations (ICLR’17)*. Published online: iclr.cc. ICLR (cit. on p. 23).

Lalin, V., V. Deshpande, and A. Rumshisky (2023). “Scaling Down to Scale Up: A Guide to Parameter-Efficient Fine-Tuning”. In: *arXiv:2303.15647 [cs.CL]* (cit. on p. 133).

Lim, S., I. Kim, T. Kim, C. Kim, and S. Kim (2019a). “Fast AutoAugment”. In: *Proceedings of the 33rd International Conference on Advances in Neural Information Processing Systems (NeurIPS’19)*. Ed. by H. Wallach, H. Larochelle, A. Beygelzimer, F. d’Alche-Buc, E. Fox, and R. Garnett. Curran Associates (cit. on pp. 15, 25).

Lim, S., I. Kim, T. Kim, C. Kim, and S. Kim (2019b). “Fast AutoAugment”. In: *Proceedings of the 33rd International Conference on Advances in Neural Information Processing Systems (NeurIPS’19)*. Ed. by H. Wallach, H. Larochelle, A. Beygelzimer, F. d’Alche-Buc, E. Fox, and R. Garnett. Curran Associates (cit. on p. 15).

Liu, T., N. Astorga, N. Seedat, and M. van der Schaar (2024). “Large Language Models to Enhance Bayesian Optimization”. In: *Proceedings of the International Conference on Learning Representations (ICLR’24)*. Published online: iclr.cc. ICLR (cit. on p. 134).

Maclaurin, D., D. Duvenaud, and R. Adams (2015). “Gradient-based Hyperparameter Optimization through Reversible Learning”. In: *Proceedings of the 32nd International Conference on Machine Learning (ICML’15)*. Ed. by F. Bach and D. Blei. Vol. 37. Omnipress, pp. 2113–2122 (cit. on p. 28).

Maslej, N., L. Fattorini, R. Perrault, et al. (2024a). “Chapter Title (e.g., Trends in AI Development)”. In: *The AI Index 2024 Annual Report*. Stanford, CA: Institute for Human-Centered AI, Stanford University. Chap. Chapter 1: Research and Development, pp. 52–55 (cit. on pp. 4, 10).

Maslej, N., L. Fattorini, R. Perrault, V. Parli, A. Reuel, E. Brynjolfsson, J. Etchemendy, K. Ligett, T. Lyons, J. Manyika, J. C. Niebles, Y. Shoham, R. Wald, and J. Clark (Apr. 2024b). *The AI Index 2024 Annual Report*. Tech. rep. Stanford, CA: AI Index Steering Committee, Institute for Human-Centered AI, Stanford University (cit. on pp. 3, 4).

Meta (2024). *Llama 3.3 Model Card*. Accessed: 12 December 2024. URL: https://github.com/meta-llama/llama-models/blob/main/models/llama3_3/MODEL_CARD.md (cit. on pp. 4, 134).

Müller, S., N. Hollmann, S. Arango, J. Grabocka, and F. Hutter (2022). “Transformers Can Do Bayesian Inference”. In: *Proceedings of the International Conference on Learning Representations (ICLR’22)*. Published online: iclr.cc. ICLR (cit. on p. 28).

Müller, S. and F. Hutter (2021). “TrivialAugment: Tuning-Free Yet State-of-the-Art Data Augmentation”. In: *Proceedings of the 24nd IEEE/CVF International Conference on Computer Vision (ICCV’21)*. Computer Vision Foundation and IEEE Computer Society. IEEE, pp. 774–782 (cit. on pp. 15, 26).

Noroozi, M. and P. Favaro (2016). “Unsupervised learning of visual representations by solving jigsaw puzzles”. In: *ECCV*, pp. 69–84 (cit. on p. 26).

Öztürk, E., F. Ferreira, H. S. Jomaa, L. Schmidth-Thieme, J. Grabocka, and F. Hutter (2022). “Zero-Shot AutoML with Pretrained Models”. In: *Proceedings of the 39th International Conference on Machine Learning (ICML’22)*. Ed. by K. Chaudhuri, S. Jegelka, L. Song, C. Szepesvári, G. Niu, and S. Sabato. Vol. 162. Proceedings of Machine Learning Research. PMLR, pp. 1128–1135. URL: <https://icml.cc/virtual/2022/spotlight/18008> (cit. on pp. 19, 31).

Pan, S. J. and Q. Yang (2010). “A Survey on Transfer Learning”. In: *IEEE Trans. Knowl. Data Eng.* 22.10, pp. 1345–1359 (cit. on p. 22).

Parker-Holder, J., P. Ball, J. Bruce, V. Dasagi, K. Holsheimer, C. Kaplanis, A. Moufarek, G. Scully, J. Shar, J. Shi, S. Spencer, J. Yung, M. Dennis, S. Kenjeyev, S. Long, V. Mnih, H. Chan, M. Gazeau, B. Li, F. Pardo, L. Wang, L. Zhang, F. Besse, T. Harley, A. Mitenkova, J. Wang, J. Clune, D. Hassabis, R. Hadsell, A. Bolton, S. Singh, and T. Rocktäschel (2024). *Genie 2: A Large-Scale Foundation World Model*. Accessed: 12 December 2024. URL: <https://deepmind.google/discover/blog/genie-2-a-large-scale-foundation-world-model/> (cit. on p. 136).

Parker-Holder, J., R. Rajan, X. Song, A. Biedenkapp, Y. Miao, T. Eimer, B. Zhang, V. Nguyen, R. Calandra, A. Faust, F. Hutter, and M. Lindauer (2022). “Automated Reinforcement Learning (AutoRL): A Survey and Open Problems”. In: *Journal of Artificial Intelligence Research (JAIR)* 74, pp. 517–568 (cit. on p. 135).

Physical Intelligence (2024). *Pi0: Our First Generalist Policy*. <https://www.physicalintelligence.company/blog/pi0>. Accessed: 6 November 2024 (cit. on p. 10).

Pineau, J., P. Vincent-Lamarre, K. Sinha, V. Larivière, A. Beygelzimer, F. d’Alché-Buc, E. B. Fox, and H. Larochelle (2021). “Improving Reproducibility in Machine Learning Research(A Report from the NeurIPS 2019 Reproducibility Program)”. In: *JMLR* 22, 164:1–164:20 (cit. on p. 10).

Pratt, L. Y. (1992). “Discriminability-Based Transfer between Neural Networks”. In: *Advances in Neural Information Processing Systems (NIPS)* 5. Ed. by S. J. Hanson, J. D. Cowan, and C. Lee Giles. M. Kaufmann, pp. 204–211 (cit. on p. 23).

Radford, A., J. W. Kim, C. Hallacy, A. Ramesh, G. Goh, S. Agarwal, G. Sastry, A. Askell, P. Mishkin, and J. Clark (2021). “Learning transferable visual models from natural language supervision”. In: *Proceedings of the 38th International Conference on Machine Learning (ICML’21)*. Ed. by M. Meila and T. Zhang. Vol. 139. Proceedings of Machine Learning Research. PMLR, pp. 8748–8763 (cit. on pp. 3, 135).

Radford, A., J. W. Kim, T. Xu, G. Brockman, C. McLeavey, and I. Sutskever (2023). “Robust Speech Recognition via Large-Scale Weak Supervision”. In: *Proceedings of the 40th International Conference on Machine Learning (ICML’23)*. Ed. by A. Krause, E. Brunskill, K. Cho, B. Engelhardt, S. Sabato, and J. Scarlett. Vol. 202. Proceedings of Machine Learning Research. PMLR (cit. on p. 3).

Radford, A., J. Wu, R. Child, D. Luan, D. Amodei, and I. Sutskever (2019). “Language models are unsupervised multitask learners”. In: *OpenAI blog* 1.8, p. 9 (cit. on p. 3).

Rapant, I., L. Purucker, F. Ferreira, S. P. Arango, A. Kadra, J. Grabocka, and F. Hutter (2024). “Quick-Tune-Tool: A Practical Tool and its User Guide for Automatically Finetuning Pretrained Models”. In: *Third International Conference on Automated Machine Learning - Workshop Track*. Ed. by M. Lindauer, K. Eggensperger, R. Garnett, J. Vanschoren, and J. Gardner. URL: <https://openreview.net/forum?id=d0Hapti3Uc> (cit. on p. 61).

Ravi, N., V. Gabeur, Y.-T. Hu, R. Hu, C. Ryali, T. Ma, H. Khedr, R. Rädle, C. Rolland, L. Gustafson, et al. (2024). “Sam 2: Segment anything in images and videos”. In: *arXiv preprint arXiv:2408.00714* (cit. on p. 3).

Ravi, S. and H. Larochelle (2017). “Optimization as a Model for Few-Shot Learning”. In: *ICLR*. Published online: iclr.cc. ICLR (cit. on p. 23).

Reed, C. J., S. Metzger, A. Srinivas, T. Darrell, and K. Keutzer (2021). “Selfaugment: Automatic augmentation policies for self-supervised learning”. In: *Proceedings of the In-*

ternational Conference on Computer Vision and Pattern Recognition (CVPR'21). Computer Vision Foundation and IEEE Computer Society. IEEE, pp. 2674–2683 (cit. on p. 15).

Rice, J. (1976). “The Algorithm Selection Problem”. In: *Advances in Computers* 15, pp. 65–118 (cit. on pp. 5, 23).

Rumelhart, D., G. Hinton, and R. Williams (1985). “Learning internal representations by error propagation”. In: *Parallel Distributed Processing*. Vol. 1. MIT Press. Chap. 8, pp. 318–362 (cit. on p. 3).

Sankaranarayanan, S., Y. Balaji, A. Jain, S. N. Lim, and R. Chellappa (2018). “Learning from synthetic data: Addressing domain shift for semantic segmentation”. In: *Proceedings of the International Conference on Computer Vision and Pattern Recognition (CVPR'18)*. Computer Vision Foundation and IEEE Computer Society. IEEE, pp. 3752–3761 (cit. on p. 6).

Santoro, A., S. Bartunov, M. Botvinick, D. Wierstra, and T. Lillicrap (2016). “Meta-Learning with Memory-Augmented Neural Networks”. In: *Proceedings of the 33rd International Conference on Machine Learning (ICML'17)*. Ed. by M. Balcan and K. Weinberger. Vol. 48. Proceedings of Machine Learning Research (cit. on p. 23).

Schmidhuber, J. (May 1987). “Evolutionary Principles in Self-Referential Learning. On Learning now to Learn: The Meta-Meta-Meta...-Hook”. Diploma Thesis. Technische Universität München, Germany. URL: <http://www.idsia.ch/~juergen/diploma.htm> 1 (cit. on pp. 5, 21).

Schmidhuber, J. (1992). *Learning To Control Fast-Weight Memories: An Alternative To Dynamic Recurrent Networks* (cit. on p. 23).

Sener, O. and S. Savarese (2018). “Active Learning for Convolutional Neural Networks: A Core-Set Approach”. In: *Proceedings of the International Conference on Learning Representations (ICLR'18)*. Published online: iclr.cc. ICLR (cit. on p. 28).

Shi, Y., N. Siddharth, P. H. S. Torr, and A. R. Kosiorek (2022). “Adversarial Masking for Self-Supervised Learning”. In: *Proceedings of the 39th International Conference on Machine Learning (ICML'22)*. Ed. by K. Chaudhuri, S. Jegelka, L. Song, C. Szepesvári, G. Niu, and S. Sabato. Vol. 162. Proceedings of Machine Learning Research. PMLR, pp. 20026–20040 (cit. on p. 27).

Shorten, C. and T. M. Khoshgoftaar (2019). “A survey on image data augmentation for deep learning”. In: *Journal of big data* 6.1, pp. 1–48 (cit. on pp. 6, 25).

Simard, P., D. Steinkraus, and J. Platt (2003). “Best practices for convolutional neural networks applied to visual document analysis”. In: *Proceedings of the Seventh International Conference on Document Analysis and Recognition ICDAR'03*, pp. 958–963 (cit. on p. 6).

Smith-Miles, K. (2008). “Cross-disciplinary perspectives on meta-learning for algorithm selection”. In: *ACM Computing Surveys* 41.1 (cit. on p. 23).

Snell, J., K. Swersky, and R. S. Zemel (2017). “Prototypical Networks for Few-shot Learning”. In: *Proceedings of the 31st International Conference on Advances in Neural Information Processing Systems (NeurIPS'17)*. Ed. by I. Guyon, U. von Luxburg, S. Bengio, H. Wallach, R. Fergus, S. Vishwanathan, and R. Garnett. Curran Associates, pp. 4077–4087 (cit. on p. 22).

Strangmann, T., L. Purucker, J. K.H. Franke, I. Rapant, F. Ferreira, and F. Hutter (2024). “Transfer Learning for Finetuning Large Language Models”. In: *NeurIPS 2024 Workshop on Adaptive Foundation Models* (cit. on p. 71).

Such, F. P., A. Rawal, J. Lehman, K. O. Stanley, and J. Clune (2020). “Generative Teaching Networks: Accelerating Neural Architecture Search by Learning to Generate Synthetic Training Data”. In: *Proceedings of the 37th International Conference on Machine Learning (ICML’20)*. Ed. by H. Daume III and A. Singh. Vol. 98. Proceedings of Machine Learning Research (cit. on pp. 4, 6, 27).

Tamkin, A., M. Wu, and N. D. Goodman (2021). “Viewmaker Networks: Learning Views for Unsupervised Representation Learning”. In: *Proceedings of the International Conference on Learning Representations (ICLR’21)*. Published online: iclr.cc. ICLR (cit. on p. 27).

Thornton, C., F. Hutter, H. Hoos, and K. Leyton-Brown (2013). “Auto-WEKA: combined selection and Hyperparameter Optimization of classification algorithms”. In: *The 19th ACM SIGKDD International Conference on Knowledge Discovery and Data Mining (KDD’13)*. Ed. by I. Dhillon, Y. Koren, R. Ghani, T. Senator, P. Bradley, R. Parekh, J. He, R. Grossman, and R. Uthurusamy. ACM Press, pp. 847–855 (cit. on pp. 5, 9, 23, 24).

Thrun, S. (1995). “Is Learning The n-th Thing Any Easier Than Learning The First?” In: *Advances in Neural Information Processing Systems (NIPS) 8*. Ed. by D. S. Touretzky, M. Mozer, and M. E. Hasselmo. MIT Press, pp. 640–646 (cit. on p. 23).

Thrun, S. and T. M. Mitchell (1995). “Learning One More Thing”. In: *Proceedings of the 14th International Joint Conference on Artificial Intelligence (IJCAI’95)*. Ed. by C. Mellish. Morgan Kaufmann Publishers, pp. 1217–1225 (cit. on p. 23).

Thrun, S. and L. Pratt (2012). *Learning to learn*. Springer Science & Business Media (cit. on pp. 21, 22).

Tian, Y., C. Sun, B. Poole, D. Krishnan, C. Schmid, and P. Isola (2020). “What Makes for Good Views for Contrastive Learning?” In: *Proceedings of the 34th International Conference on Advances in Neural Information Processing Systems (NeurIPS’20)*. Ed. by H. Larochelle, M. Ranzato, R. Hadsell, M.-F. Balcan, and H. Lin. Curran Associates (cit. on p. 27).

Tobin, J., R. Fong, A. Ray, J. Schneider, W. Zaremba, and P. Abbeel (2017). “Domain randomization for transferring deep neural networks from simulation to the real world”. In: *2017 IEEE/RSJ international conference on intelligent robots and systems (IROS)*. IEEE, pp. 23–30 (cit. on p. 6).

Tremblay, J., A. Prakash, D. Acuna, M. Brophy, V. Jampani, C. Anil, T. To, E. Cameracci, S. Boochoon, and S. Birchfield (2018). “Training deep networks with synthetic data: Bridging the reality gap by domain randomization”. In: *Proceedings of the IEEE conference on computer vision and pattern recognition workshops*, pp. 969–977 (cit. on p. 6).

Tsang, I. W., J. T. Kwok, Pak-Ming Cheung, and N. Cristianini (2005). “Core vector machines: Fast SVM training on very large data sets.” In: ed. by L. Raedt and S. Wrobel (cit. on p. 28).

Uesato, J., N. Kushman, R. Kumar, F. Song, N. Siegel, L. Wang, A. Creswell, G. Irving, and I. Higgins (2022). “Solving math word problems with process-and outcome-based feedback”. In: *arXiv preprint arXiv:2211.14275* (cit. on p. 135).

Vanschoren, J. (2019). “Meta-Learning”. In: *Automated Machine Learning: Methods, Systems, Challenges*. Ed. by F. Hutter, L. Kotthoff, and J. Vanschoren. Available for free at <http://automl.org/book>. Springer. Chap. 2, pp. 35–61 (cit. on pp. 5, 21–23).

Vilalta, R. and Y. Drissi (Oct. 2002). “A perspective view and survey of meta-learning”. In: *Artificial intelligence review* 18.2, pp. 77–95 (cit. on p. 21).

Wagner, D., F. Ferreira, D. Stoll, R. T. Schirrmeister, S. Müller, and F. Hutter (2022). “On the importance of hyperparameters and data augmentation for self-supervised learning”. In: *Pre-Training Workshop at the International Conference for Machine Learning (ICML)*. Ed. by K. Chaudhuri, S. Jegelka, L. Song, C. Szepesvári, G. Niu, and S. Sabato. Vol. 162. Proceedings of Machine Learning Research. PMLR. URL: <https://icml.cc/virtual/2022/20697> (cit. on p. 81).

Wang, R., J. Lehman, J. Clune, and K. O. Stanley (2019). “Paired open-ended trailblazer (poet): Endlessly generating increasingly complex and diverse learning environments and their solutions”. In: *arXiv preprint arXiv:1901.01753* (cit. on p. 136).

Wang, T., J. Zhu, A. Torralba, and A. A. Efros (2018). “Dataset distillation”. In: *arXiv:1811.10959 [cs.LG]* (cit. on p. 28).

Wei, J., X. Wang, D. Schuurmans, M. Bosma, F. Xia, E. Chi, Q. V Le, D. Zhou, et al. (2022). “Chain-of-thought prompting elicits reasoning in large language models”. In: *Proceedings of the 36th International Conference on Advances in Neural Information Processing Systems (NeurIPS’22)*. Ed. by S. Koyejo, S. Mohamed, A. Agarwal, D. Belgrave, K. Cho, and A. Oh. Curran Associates, pp. 24824–24837 (cit. on p. 134).

Wightman, Ross (2019). *PyTorch Image Models*. <https://github.com/rwightman/pytorch-image-models>. DOI: 10.5281/zenodo.4414861 (cit. on p. 3).

Wikipedia contributors (2025). *Jevons paradox* — Wikipedia, The Free Encyclopedia. https://en.wikipedia.org/wiki/Jevons_paradox. Accessed: 2025-01-28 (cit. on p. 3).

Xu, L., F. Hutter, H. Hoos, and K. Leyton-Brown (2008). “SATzilla: Portfolio-based Algorithm Selection for SAT”. In: *Journal of Artificial Intelligence Research* 32, pp. 565–606 (cit. on p. 5).

Xu, L., F. Hutter, H. Hoos, and K. Leyton-Brown (2012). “Evaluating Component Solver Contributions to Portfolio-Based Algorithm Selectors”. In: *Proceedings of the Fifteenth International Conference on Theory and Applications of Satisfiability Testing (SAT’12)*. Ed. by A. Cimatti and R. Sebastiani. Vol. 7317. Lecture Notes in Computer Science. Springer, pp. 228–241 (cit. on p. 5).

Xu, L., H. Xie, S.-Z. J. Qin, X. Tao, and F. L. Wang (2023). “Parameter-Efficient Fine-Tuning Methods for Pretrained Language Models: A Critical Review and Assessment”. In: *arXiv:2312.12148 [cs.CL]* (cit. on p. 133).

Zhou, J., C. Wei, H. Wang, W. Shen, C. Xie, A. L. Yuille, and T. Kong (2021). “iBOT: Image BERT Pre-Training with Online Tokenizer”. In: *Proceedings of the 39th International Conference on Machine Learning (ICML’22)*. Ed. by K. Chaudhuri, S. Jegelka, L. Song, C. Szepesvári, G. Niu, and S. Sabato. Vol. 162. Proceedings of Machine Learning Research. PMLR (cit. on p. 26).